Stanford Geothermal Program
Interdisciplinary Research in
Engineering and Earth Sciences
STANFORD UNIVERSITY
Stanford, California

SGP-TR-64

EFFECT OF TEMPERATURE ON OIL-WATER RELATIVE PERMEABILITIES OF UNCONSOLIDATED AND CONSOLIDATED SANDS

By

Mark A. Miller

June 1983

Financial support was provided through the Stanford Geothermal Program under Department of Energy Contract No. DE-AT-03-80SF11459 and by the Department of Petroleum Engineering, Stanford University.

Dedicated to my son, Curtis.

He arrived in the middle of it all,

providing joy with his presence, but

sadness because he received so little

of my time.

AKNOWLEDGEMENTS

This work could not have been completed without the help of a great number of people.

My wife, Carla, had to tolerate more than anyone should, but she was always there to help in every possible way. Without her, I never would have made it.

Dr. H. J. Ramey, Jr., my faculty advisor, provided the inspiration for this work and the necessary direction to get it accomplished. The other members of my committee, Drs. W. E. Brigham, S. S. Marsden, Jr., K. Aziz, and R. N. Horne, also kept me on the right path with their helpful suggestions.

Above all, I would like to express sincere appreciation to the many friends and colleagues who provided help, feedback, criticism, encouragement, and advice: Paul Pettit for his invaluable assistance in the lab, Peter Gordon who did most of the machining 'work, Jean Cook who managed to keep the paperwork straight and out of my hair, and my colleagues Avrami Sageev, Arshad Sufi, and Luis Macias-Chapa -- they were the sounding boards for many ideas, both good and bad.

This work, of course, could not have been accomplished without financial support provided under the Stanford Geothermal Program, Department of Energy contract DE-AT03-80SF11459. Sincere appreciation also goes to the AMOCO Foundation for their very generous support of my studies.

ABSTRACT

Over the last 20 years, a number of studies have reported temperature effects on two-phase relative permeabilities in porous media. However, some of the reported results have been contradictory. Also, the observed effects have not been explained in terms of fundamental properties known to govern two-phase flow. The purpose of this study was to attempt to isolate the fundamental properties affecting two-phase relative permeabilities at elevated temperature, either: a) to determine what phenomena caused observed effects, or b) to show that relative permeabilities in simple systems were not affected by temperature, as consideration of fundamental flow properties would predict.

Laboratory dynamic displacement relative permeability measurements were made on both unconsolidated and consolidated sand cores, using water and a refined white mineral oil. Experiments were run on 2 in. diameter, 20 in. long cores from room temperature to 300°F.

Unlike the results of previous researchers, essentially no change with temperature was observed in either residual saturations or relative permeability relationships. It was concluded that previous results may have been affected by viscous instabilities, capillary end-effects, and/or difficulties in maintaining material balance determinations.

TABLE OF CONTENTS

LIST OF TABLES

LIST OF FIGURES

1. INTRODUCTION

Engineering design and analysis of many mineral fluid production processes require the use of multi-phase flow characteristics of porous earth materials. Engineering for geothermal energy production and a variety of thermal oil recovery processes require an understanding of multi-phase flow at elevated and changing temperatures. Early thermal oil recovery field operations (well heaters, steam injection, in situ-combustion) indicated oil flowrate increases far in excess of what would be predicted by viscosity reductions due to heating. This suggested an effect of temperature on relative permeabilities.

Over the past 20 years, a number of studies have presented results on the effect of temperature on two-phase relative permeabilities of a number of porous media and fluids. Unfortunately, these studies have tended to pose more questions than they have answered. Observed changes with temperature have not been explained in terms of fundamental properties known to affect relative permeabilities. Some of the results have been contradictory. Without fundamental explanations, the lingering question is whether observed temperature effects were real.

The approach for this research was to use simple, well-known porous media and fluid systems to determine which fundamental properties affected relative permeabilities at elevated temperatures. The objective was to perform laboratory measurements carefully, so as to: a) minimize laboratory-scale effects, and b) minimize the number of factors that could be causing changes with temperature. Hopefully, further understanding of the phenomena would thus be achieved.

2. LITERATURE REVIEW

Flow characteristics of porous media cannot be directly computed because of the complex nature of the microscopic flow paths. It is common to use an empirical approach to determine both single and multi-phase flow properties of a porous medium. The absolute permeability derived from Darcy's law is an empirical constant of proportionality relating the volumetric flowrate (q) to the pressure gradient (dp/dx), cross-sectional area (A), and fluid viscosity (μ).

$$q = - \frac{kA}{\mu} \frac{dp}{dx} \tag{2.1}$$

Multi-phase flow is usually treated empirically by deriving the effective permeability of each phase (k_i) from the individual phase volumetric flowrates, pressure gradients, and viscosities.

$$q_i = \frac{k_i A}{\mu_i} \frac{dp_i}{dx} \tag{2.2}$$

This concept has proven useful because for most situations, the effective permeabilities can be considered to be Single-valued functions of fluid saturations only. By normalizing effective permeabilities to some base permeability, curves of relative permeability vs. saturation can be presented.

One of *two* basic methods is usually used to measure relative permeabilities in the laboratory. The steady-state method is the most direct. Individual phases are flowed simultaneously through a short section of porous medium until flowrates and pressure gradients stabilize. Effective permeabilities may be calculated using Eq. 2.2, knowing the individual flowrates, viscosities, and pressure gradients.

The main drawback to this method is the amount of time required (often several hours) to generate a single point on a relative permeability vs. saturation curve.

The dynamic displacement (sometimes referred to as unsteady-state) method is less time-consuming. Complete relative permeability curves can be generated in a single experiment, requiring only a few hours. In dynamic displacement experiments, one fluid displaces another from the porous medium. By measuring the effluent production of both phases, and the differential pressure across the core, relative permeability curves can be calculated.

Welge (1952) presented a technique for calculating two-phase relative permeability ratio vs. saturation from dynamic displacement experiments. by assuming that relative permeabilities were single-valued functions of saturation, and using Eq. 2.2 combined with a mass balance equation, Welge derived (shown here for water displacing oil):

$$\bar{S}_w - S_{w2} = f_o W_i \tag{2.3}$$

$$\frac{k_{rw}}{k_{ro}} \frac{\mu_o}{\mu_w} = \frac{1}{f_o} - 1 \tag{2.4}$$

where:

$\bar{S}_w$ = average water saturation in core

S_{w2} = water saturation at core outlet

f_o = fractional volume of oil flowing from core outlet

k_{rw}, k_{ro} = relative permeabilities of water and oil

μ_w, μ_o = viscosities of water and oil

W_i = cumulative pore volumes of water injected

The importance of this method is that the saturation at the outlet face can be calculated from the average core saturation. Since average saturations can be determined from material balance, and f_o can be measured directly from the effluent production, Eqs. *2.3* and *2.4* provide an easy and convenient method of calculating relative permeability ratio curves.

Theory necessary to determine individual relative permeabilities was later presented by Johnson, Bossler, and Naumann (1959). By integrating Eq. **2.2** along the length of the core, the following was derived:

$$\frac{f_o}{k_{ro}} = \frac{d\left[\frac{1}{W_i I_r}\right]}{d\left[\frac{1}{W_i}\right]} \qquad (2.5)$$

where:

I_r = relative injectivity, $(q/\Delta p)/(q/\Delta p)_{initial}$

q = total volumetric flowrate

Ap = differential pressure across the core

Thus, by measuring the differential pressure across the core throughout the experiment, individual relative permeability curves could be determined.

Jones and Roszelle (1978) presented a graphical approach based on the Welge, and Johnson, Bossler, and Naumann techniques that is direct and provides insight into interpretation of the data. The Jones and Roszelle technique is based on two graphs -- pore volumes of oil recovered (for a water displacement experiment) vs. pore volumes of water injected, and relative injectivity vs. pore volumes injected. The oil fractional flow, f_o, is determined from the slope of a tangent to the oil recovery curve. The corresponding $(\bar{S}_w - S_{w2})$ is calculated as the

recovery intercept at $W_i=0$ minus the initial water saturation, S_{wi}. At a corresponding W_i on the relative injectivity curve, another tangent is drawn, and f_o/k_{ro} is found as the intercept at $W_i=0$. A complete discussion of this technique based on class notes by Brigham (1979) is presented in the U.S. Department of Energy report by Sufi et al. (1982).

Several authors [Osoba et al. (1951), Richardson et al. (1952), Owens et al. (1956), and Richardson (1957)] have compared relative permeabilities determined from dynamic displacement experiments to those obtained by steady-state methods. Although slight differences were sometimes experienced, it has generally been concluded that comparable results are obtained from both types of experiments.

The usefulness of the concept of relative permeability lies in the fact that for many processes, relative permeability for a given porous medium can be considered to be a function of fluid saturation only. However, in recent years, research in enhanced oil recovery techniques has indicated conditions where this may no longer be a valid assumption. One parameter that has been presented as having a large effect on relative permeabilities is temperature.

Interest in the measurement of relative permeabilities at elevated temperatures corresponded with strong petroleum industry interest in thermal oil recovery beginning in the 1960's. Continued interest in thermal oil recovery and in geothermal energy production make this topic one of current importance.

One of the early studies of temperature effects on relative permeabilities was presented by Edmondson (1965), who reported the results of dynamic displacement measurements in Berea sandstone cores.

Distilled water was used with two different white mineral oils and two crude oils. Two different cores were used, measuring 9 and 26 in. long, and 1.6 and 2.0 in. diameter, respectively. Runs were made from room temperature to 500°F with the white oils, and to 300°F with the crude oils.

Edmondson reported that residual oil saturations (at the end of 10 pore volumes of water injected) decreased with increasing temperature. Relative permeability ratios decreased with temperature at high water saturations, but increased with temperature at low water saturations. Interestingly, the curves measured with crude oil were significantly different from the white oil curves, even at room temperature (see Fig. 2.1).

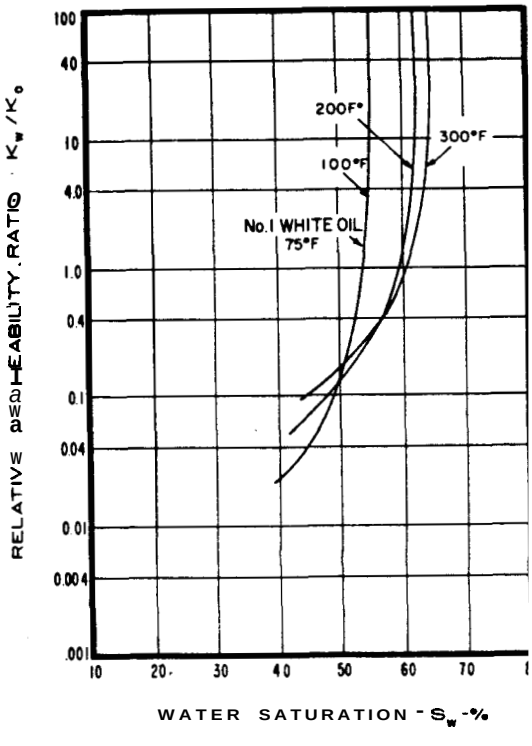

Figure 10.—k_w/k_o versus S_w at Various Temperatures.
Core No. 2—No. 15 White Oil

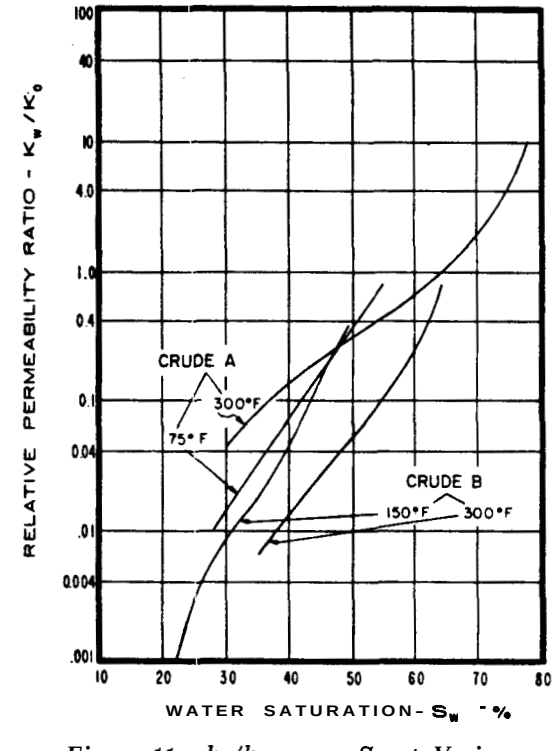

Figure 11.—k_w/k_o versus S_w at Various Temperatures.
Core No. 2—with Crude Oils

Fig. 2.1 Relative Permeability Ratios vs. Temperature Reported by Edmondson (1965)

Edmondson attributed this behavior to differences in interfacial tension. Differences in curves between the two white oils at elevated temperatures were attributed to viscosity differences. Since Irreducible water saturations were established at room temperature, no temperature effects on this end-point were measured.

A series of elevated temperature, dynamic displacement relative permeability measurements on unconsolidated sands made at Texas A&M University were reported by Poston et al. (1970). These measurements were made on both a clean quartz sand and a "natural" sand from the Midway-Sunset field in California. Distilled water and refined oils were used in the experiments. Room temperature oil viscosities were 80-, 99-, and 600-cp. Figure 2.2 summarizes the findings of Poston et al.

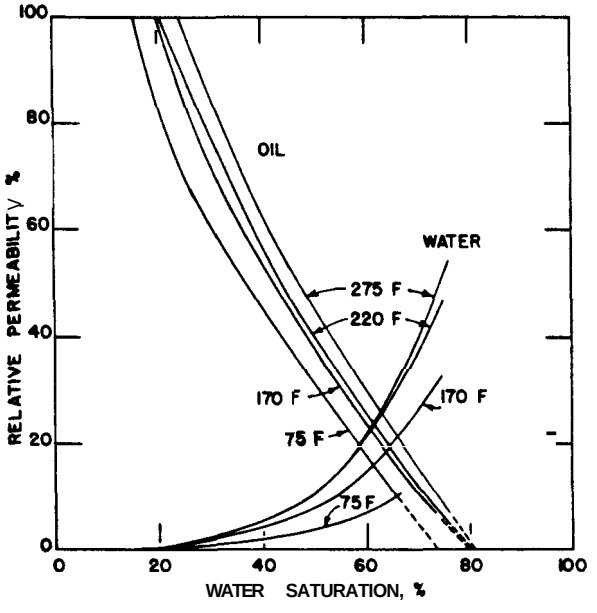

FIG. 10 — WATER AND OIL RELATIVE PERMEABILITIES VS WATER SATURATION, HOUSTON SAND, 80-CP OIL.

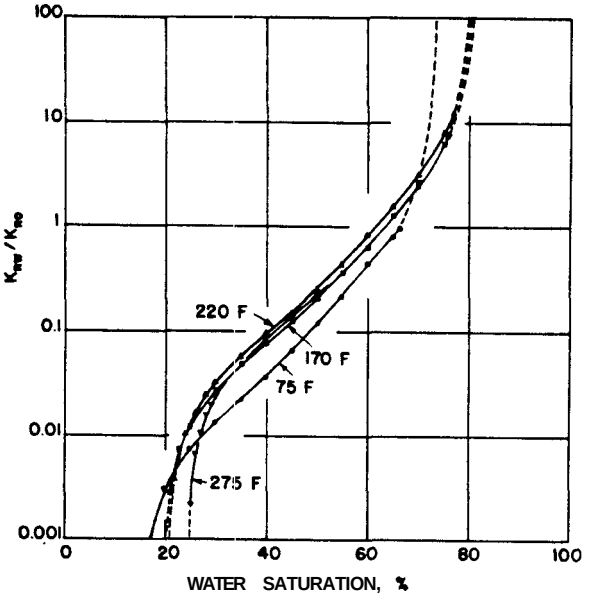

FIG. 11 — RELATIVE PERMEABILITY RATIO VS WATER SATURATION, HOUSTON SAND, 80-CP OIL.

Fig. 2.2 Relative Permeabilites vs. Temperature Reported by Poston et al. (1970)

Like Edmondson, Poston et al. reported a decrease in the practical residual oil saturation (at less than 1% oil cut) with temperature. Poston et al. also reported an increase in irreducible water saturation with temperature. Both oil and water relative permeabilities increased with temperature. The relative permeability ratio curves did not exhibit the same behavior at elevated temperatures reported by Edmondson. Above 170°F, Poston et al.'s relative permeability ratio curves were nearly the same, especially in the middle range of water saturations.

Poston et al. postulated that the cores were becoming increasingly water-wet with temperature and also with successive runs. Evidence for this was the fact that the increase in irreducible water saturation with temperature was not completely reversible. Although irreducible water saturations decreased with temperature, they did not. revert to the original room temperature values. Measured quartz plate contact angles did, in fact, decrease with temperature, from 35°-37° at room temperature to 22"-25" at 190°F. Oil-water interfacial tensions were also measured as a function of temperature. Interfacial tensions were found to decrease from 20-25 dyne/cm at room temperature to approximately 15-23 dyne/cm at 170 °F.

Amaefule and Handy (1982) measured water-oil relative permeabilities of Berea sandstone cores at a variety of interfacial tensions. They found that for interfacial tensions above 0.1 dynes/cm, relative permeabilities were independent of interfacial tension. Amaefule and Handy also reported measurements of end-point saturations as functions of capillary number. The capillary number is usually defined as:

$$N_c = \frac{v\mu}{\sigma \cos\theta} \qquad (2.6)$$

where :

N_c = capillary number (dimensionless)

v = darcy velocity, q/A

μ = displacing fluid viscosity

σ = interfacial tension

θ = contact angle

The contact angle is often not included in the al ulation f capillary number, for circumstances where the contact angle is believed to be nearly constant.

Amaefule and Handy's measurements of residual oil saturations vs. capillary number confirmed observations reported by Abrams (1975), i.e., that residual oil saturations varied little below a certain value of capillary number. Above this "breakover" value of capillary number, residual oil saturations decreased markedly with increasing capillary number. Amaefule and Handy reported a breakover point at a capillary number around 10^{-4}. Abrams also modified the capillary number by the factor $(\mu_w/\mu_o)^{0.4}$, and was better able to correlate his results.

Data regarding the effect of capillary number on irreducible water saturations were also reported by Amaefule and Handy. The results were similar to those for residual oil saturations. Irreducible water saturation remained constant to a capillary number around 10^{-4} and then decreased markedly as capillary number increased. Data presented by Dombrowski and Brownell (1954) appear to confirm this conclusion. They presented results of fluid drainage experiments from a variety of unconsolidated porous media. Irreducible water saturations were shown

to remain constant with capillary number to around 10^{-2} before beginning to decrease. Some limited data by Gupta and Truchenski (1979) also exhibited a breakover capillary number around 10^{-4} for Berea sandstone. Lefebvre duPrey (1973), however, presented results showing residual wetting phase saturations decreasing continually with increasing capillary number. The differences between these studies have not been explained.

Most studies on changes of relative permeability with wettability (or contact angle) have usually focused on differences between oil-wet and water-wet porous media. However, Owens and Archer (1971) presented relative permeability measurements over a wide range of contact angles, including two for water-wet systems, having contact angles of 47" and 0°. Oil relative permeabilities were presented, which increased with decreasing contact angle, while water relative permeabilities decreased with increasing contact angle. The point where oil and water relative permeabilities crossed, shifted toward high water sstturations (as expected) as contact angle decreased. However, the relative permeability value at the cross-over point remained nearly constant. Poston et al.'s (1970) results exhibited different behavior with temperature. The cross-over point remained at a constant saturation, but moved to higher relative permeability values.

The findings of Owens and Archer tend to support the idea of increasing water-wetness with temperature. However, the magnitude of the changes that might occur with relatively small contact angle changes were not defined.

The capillary pressure across an interface in a small circular tube can be shown to be [Amyx, Bass, and Whiting (1960, p.137)]:

$$p_c = \frac{2\,\sigma\,\cos\theta}{r} \qquad (2.7)$$

where:

p_c = capillary pressure

r = tube radius

Since a porous medium can be visualized as a randomly-connected network of capillary flow paths, it would be expected that contact angle and interfacial tension together should affect relative permeability behavior in relation to ($\sigma \cos\theta$). Most displacement experiments (except those at ultra-low interfacial tensions) occur in a range of capillary number that is well below the point where results depend on capillary number. Thus, in this range, relatively small changes in contact angle might be expected to have little effect.

Another study of temperature effects on relative permeabilities of unconsolidated sands was presented by Davidson (1969). Davidson measured dynamic displacement relative permeability ratios for a 47-63 mesh sand and aquarium gravel core, 3 ft long by 3.15 in. diameter. Chevron No. 15 white oil [same as the No. 15 white oil used by Edmondson (1965)] was displaced by distilled water, nitrogen and super-heated steam at temperatures to 540°F. Chevron No. 15 white oil has a viscosity of approximately 200 cp at room temperature. Davidson was careful to correct for oil-water solubility effects, which became significant above 300°F.

Davidson performed water displacement runs starting both with irreducible water in the core and from 100% oil saturation. From irreducible water saturation, relative permeability ratio curves (Fig. 2.3) were similar to Edmondson's (1965). Water-oil permeability ratios

increased with temperature at low water saturations, but decreased with temperature at high water saturations. However, starting from 100% oil saturated cores, the curves changed little with temperature, except at low water saturations. Davidson attributed this behavior to changes in interfacial tension with temperature and postulated that such changes would have the most effect at low water saturations.

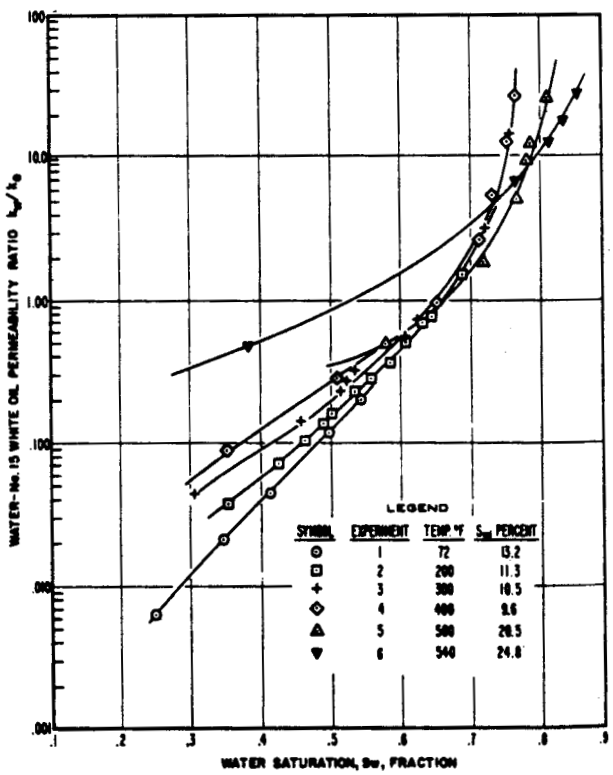

Fig. 9 — Water-No. 15 white oil imbibition permeability ratios using initial water and oil viscosities adjusted for dissolved water.

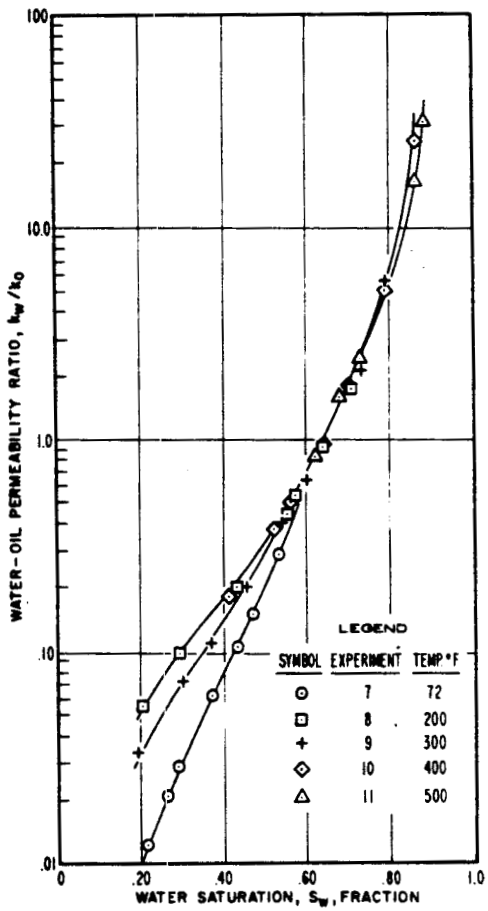

Fig. II — Water-No. 15 white oil imbibition permeability ratios using viscosities adjusted for dissolved water and using no initial water.

Fig. 2.3 Relative Permeability Ratios vs. Temperature Reported by Davidson (1969).

Irreducible water saturations in Davidson's study were established at room temperature. These saturations are presented in Table 2.1.

Table 2.1 Measured Irreducible Water Saturations from Davidson (1969)

Experiment	Temperature (°F)	Irreducible Water Saturation (%)
1	72	13.2
2	200	11.3
3	300	10.5
4	400	9.6
5	500	20.5
6	540	24.8

Since these saturations were measured at elevated temperature (although established at room temperature), the slight decrease from 72°F to 400°F may be attributed to differences in thermal expansion between oil and water. However, the increase in irreducible water saturation to over 20% for the runs above 500°F appears significant. These runs exhibited the most temperature effect. If these runs are disregarded, the results starting from irreducible water saturation would be similar to the runs starting from 100% oil saturation.

Another troublesome aspect of Davidson's work was the core cleaning procedure. A hydrocarbon solvent, isopropyl alcohol, water, steam, and air (in that order) were used to clean and then dry the core between experiments. No mention was made of consideration of wettability changes. However, wettability changes could explain the large change in irreducible water saturation.

Internal pressures in Davidson's runs were increased with temperature in order to maintain water as a liquid. Room temperature runs were made at atmospheric downstream pressure, while 540°F runs were

made with a downstream pressure over 1200 psig. It is impossible to ascertain what effect these large internal pressure changes might have had on flow properties. Stress effects may have been considerable. Gobran (1981) reported significant absolute permeability changes *(3%)* over similar changes of pore pressure for unconsolidated sands.

Davidson found that nitrogen-oil relative permeability ratios increased with temperature over the entire saturation range, yet steam-oil curves exhibited effects only at low water saturations. Temperature effects on the gas-fluid curves were attributed to Klinkenberg gas slippage. However, no explanation was offered why the steam-oil system changed less with temperature than the nitrogen-oil system.

Poston et al. (1970) postulated that if increasing temperature caused increasing water-wetness, this should be evident from capillary pressure measurements. Sinnokrot et al. (1971) followed this suggestion and performed capillary pressure measurements on consolidated sandstone and limestone cores from room temperature to 325°F. Distilled water and Chevron No. 15 white oil were used as fluids. Sinnokrot et al. confirmed that for sandstones, the practical irreducible water saturation appeared to increase with temperature. Correspondingly, capillary pressure curves increased with temperature at all saturations. Also, the hysteresis between drainage and imbibition curves reduced to essentially zero at 300°F. The results are presented in Fig. 2.4.

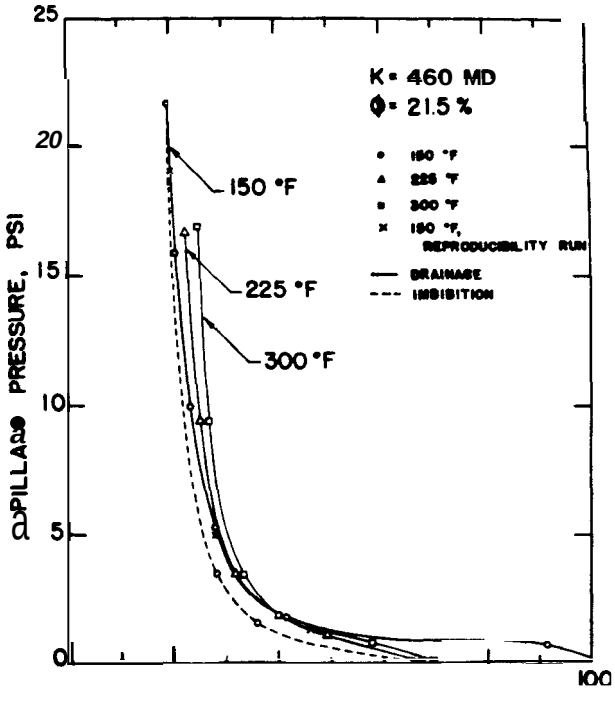

FIG. 4 — CAPILLARY PRESSURE VS WATER SATURATION FOR BEREA SANDSTONE CORE B.

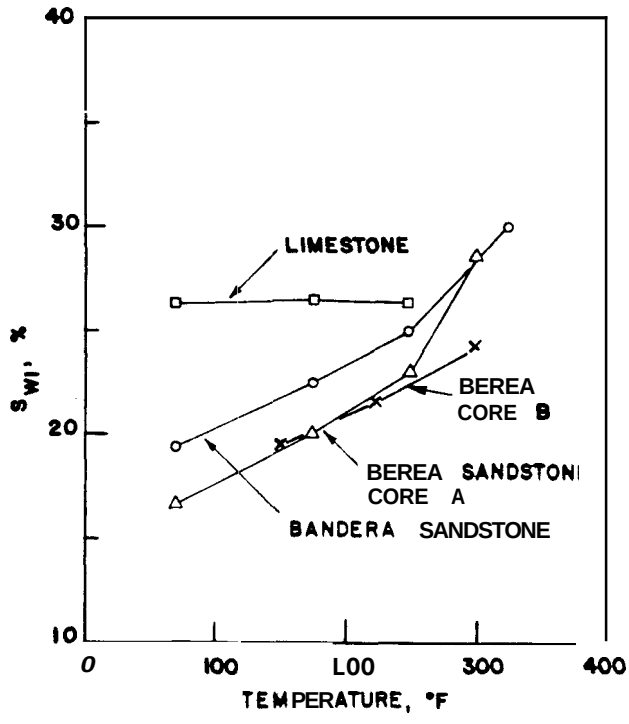

FIG. 6 — IRREDUCIBLE WATER SATURATION VS TEMPERATURE.

Fig. 2.4 Capillary Pressures vs. Temperature Reported by Sinnokrot et al. (1971)

The limestone core exhibited different behavior. Irreducible water saturations remained constant with temperature as did capillary pressure curves. Sinnokrot et al. did not determine why limestone behaved differently from sandstone. They postulated differences in wettability characteristics.

Weinbrandt et al. (1975) performed dynamic displacement experiments on consolidated Boise sandstone cores to 175°F. Relative permeability ratios and individual relative permeabilities were determined using distilled water and Chevron No. 15 white oil on cores 1.3 to 2.1 in. long by 1 in. diameter. Core pore volumes were approximately 4-8 cc. Figure 2.5 summarizes the results of Weinbrandt et al.'s experiments.

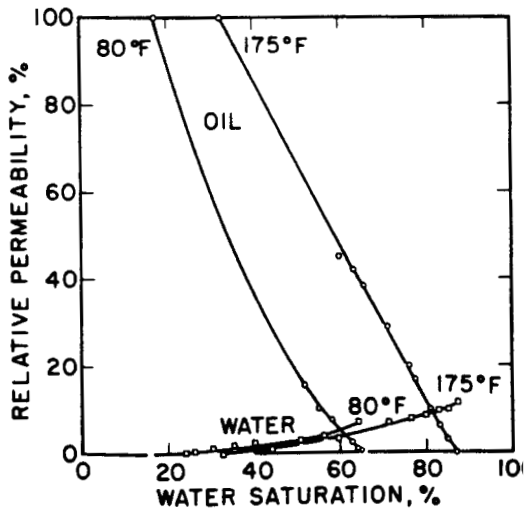

FIG. 3 — INDIVIDUAL RELATIVE PERMEABILITIES AS A FUNCTION OF TEMPERATURE: CORE 4, BOISE SANDSTONE.

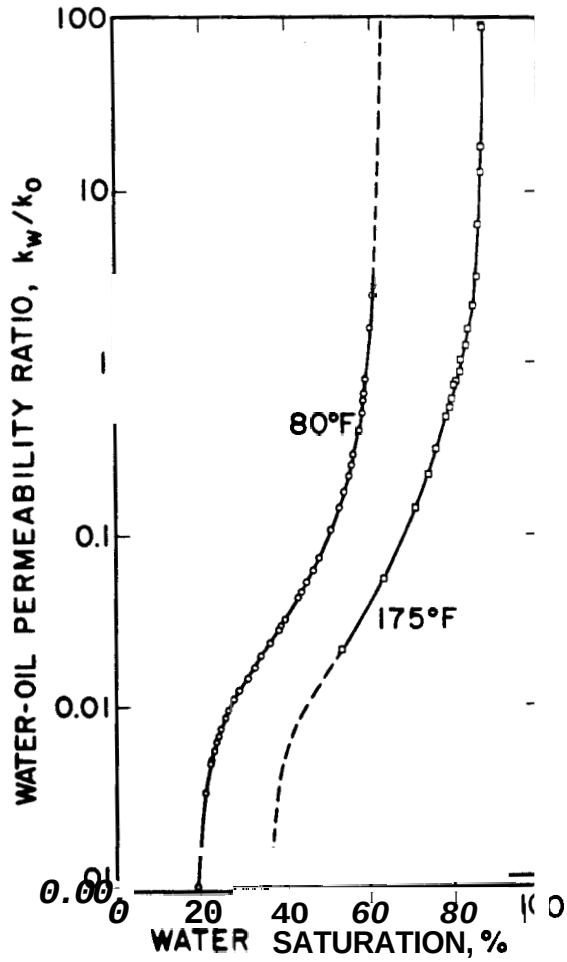

FIG. 4 — EFFECT OF TEMPERATURE ON RELATIVE PERMEABILITY RATIO: CORE 4, BOISE SANDSTONE.

Fig. 2.5 Relative Permeabilities vs. Temperature Reported by Weinbrandt et al (1975)

Oil relative permeabilities shifted toward high, water saturations with increasing temperature, while the water relative permeabilities exhibited little change with temperature. Relative permeability ratios thus decreased with increasing temperature. Weinbrandt et al. confirmed previous studies' findings of increasing irreducible water saturation and decreasing residual oil saturation with increasing temperature.

A surprising observation made in the course of these experiments was a significant decrease of absolute permeability with temperature. Absolute permeabilities at 175°F were reported to be approximately half the values at room temperature. This result was unexpected and was left unexplained. Some type of water/silica interaction at high temperatures was postulated to affect both absolute and relative permeabilities. This would also explain the lack of temperature effects on limestone capillary pressures reported by Sinnokrot et al. (1971).

Temperature effects on absolute permeability to distilled water were also measured by Cassé and Ramey (1979) on several sandstones, including fired Berea. They presented approximately the same magnitude of temperature effect as reported by Weinbrandt et al. (1975). Sydansk (1980), replying to the Cas& and Kamey study, presented results indicating that distilled water caused progressive plugging of Berea cores due to clay particle migration. Sydansk presented data that showed temperature effects disappeared when a 3% sodium chloride solution was used instead of distilled water.

Sageev (1980) and Gobran (1981) further investigated temperature effects on absolute permeabilities and found that for pure unconsolidated quartz sand and distilled water, there was no temperature effect on absolute permeability. In personal discussions, Sageev indicated that he also attempted to measure distilled water absolute permeabilites on consolidated Boise cores at elevated temperatures. Like Sydansk, he reported severe clay plugging problems that were aggravated by interrupting injection and by changing; temperatures. Sageev was unable to stabilize permeabilities sufficiently to make any conclusions.

Clay migration problems with distilled water casts some doubt on the studies reported by Edmondson (1965), Sinnokrot et al. (1971), and Weinbrandt et al. (1975). However, the Poston et al. (1970) and Davidson (1969) studies on clean unconsolidated sands should not have been affected by the use of distilled water, because of the absence of clays.

The only steady-state relative permeabilities measured at elevated temperature known to the author were reported by Lo and Mungan (1973). Measurements were made on both Berea (water-wet) and Teflon (oil-wet) consolidated cores using a 3% sodium chloride brine and three different oils: Kaydol, Protol, and tetradecane. Kaydol is essentially the same as Chevron No. 15, having a room temperature viscosity around 200 cp. Protol has a room temperature viscosity of approximately 80 cp. Tetradecane viscosity is around 2 cp. Berea cores were 3 in. diamater by 12 in. long. Teflon cores were 1.6 in. diameter by 3.4 to 5.3 in. long.

Lo and Mungan found for both the water-wet and oil-wet systems, temperature affected relative permeabilities using Kaydol and Protol. However, with tetradecane, no temperature effect was observed. Since the oil-water viscosity ratio decreased substantially for Kaydol and Protol, but changed little for tetradecane, Lo and Mungan concluded that viscosity ratio effects were responsible for changes with temperature.

Interfacial tensions and contact angles were measured for all systems and confirmed Poston et al.'s (1970) findings that changes were not enough to explain observed effects. This was believed true especially because both Teflon and Berea exhibited the same type of behavior with temperature.

The trend of relative permeability curves with temperature using Kaydol (Fig. 2.6) was similar to that reported by Weinbrandt et al. (1975) (Fig. 2.5). Along with higher irreducible water saturations and lower residual oil saturations, oil relative permealbilities shifted toward high water saturations. This shift, however, was less than Weinbrant et al.'s, even though temperatures were higher. Lo and Mungan did not comment on why viscosity ratio should affect irreducible water saturations.

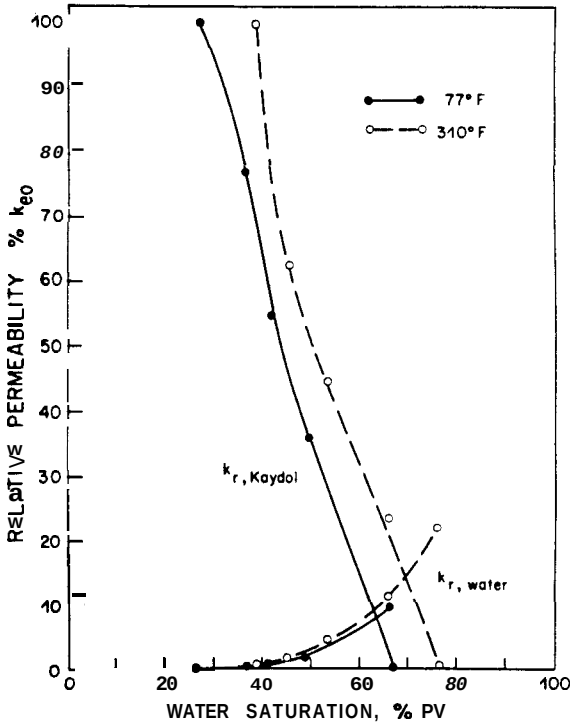

Fig. 7 - Relative permeability curves in Berea sandstone core.

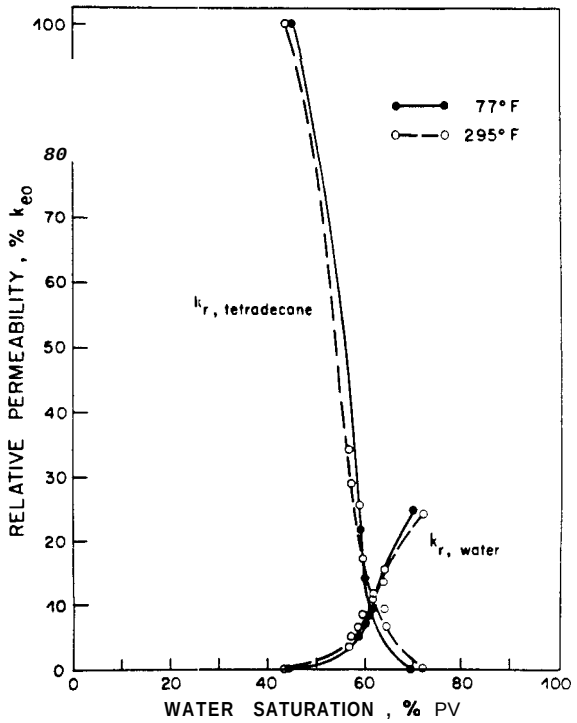

Fig 9 - Relative permeability curves in Bereo sandstone core

Fig. 2.6 Relative Permeabilities vs. Temperature Reported by Lo and Mungan (1973)

Viscosity ratio is generally believed not to affect relative permeability measurements. Leverett (1939) measured steady-state

relative permeabilities in a 100–200 mesh sand pack at oil–water viscosity ratios from 0.057 to 90.0, and found no effect on relative permeability due to viscosity ratio. Richardson (1957) presented results of relative permeability ratios calculated from dynamic displacement experiments for 1.8 and 151 cp. oils. both results agreed with steady–state measurements on the same unconsolidated sand core.

A study by Odeh (1959), based on both experimental data and theoretical considerations, presented arguments that viscosity ratio does affect relative permeabilities on cores having less than 1 darcy absolute permeability. No viscosity ratio effect was observed on the single measured core above 1 darcy. Replies to Odeh's study [Baker (1960), Downie and Crane (1961)] presented theoretical and experimental arguments contrary to Odeh's conclusions. Since oil relative permeabilities at irreducible water saturation measured by Odeh were as high as 240% greater than 100% brine permeabilities, arguments centered on clay–water interactions, end–effects, etc.

Another aspect of Lo and Mungan's results, was the dependence of the curves on the oil used. This would support their hypothesis of viscosity dependence, although it does not appear that identical results would be obtained with two different oils at the same viscosity ratio, but different temperature. Differences in surface tension and wettability might also be considered, but should have minor effect as discussed earlier in this section.

In his studies of steam–water relative permeabilities, Counsil (1979) also measured nitrogen–water relative permeabilities at elevated temperatures. Counsil used a 2 ft long by 2 in. diameter, synthetically–consolidated quartz sand (using calcium cement). Counsil

noted no temperature effect on the curves. It has been suggested that Counsil's system may have behaved more like a limestone than a sandstone because of the artificial cementing process. This would be in agreement with the lack of temperature effects on capillary pressure curves of limestones reported by Sinnokrot et al. (1971).

A recent study by Sufi et al. (1982) began to indicate some of the difficulties with relative permeability measurements at elevated temperatures. Dynamic displacement relative permeabilities were measured on clean unconsolidated quartz sand packs, 1 in. diameter by 7 in. long. Distilled water was used to displace Kaydol white oil (similar to Chevron No. 15). Major findings were related to temperature effects on residual saturations. However, Sufi et al. also discussed measurement difficulties relating to temperature effects on relative permeability curves.

Material-balance-measured irreducible water saturations were found to depend on what was termed a "viscous force", $q\mu_o$. Irreducible water saturations were found to decrease with increasing flowrate and/or increasing oil viscosity. If interfacial tension, cross-sectional area, and porosity are included in Sufi et al.'s parameter, the results can be presented in terms of a more universal parameter, the capillary number. Converting the results to capillary number, irreducible water saturations decreased from around 11% at a capillary number of 2×10^{-5} to approximately 6% at a capillary number of 3×10^{-3}. The importance of this result was that changes in either flowrate or oil viscosity with temperature followed the same relationship. Since immediate additional water production was observed upon increasing the oil injection rate (at the end of a displacement run), it was concluded that changes in the

measured irreducible water saturation were probably a result of the capillary end-effect and did not represent reductions in the true value. The results presented earlier in this section by Dombrowski and Brownell (1954), Amaefule and Handy (1982), and Gupta and Truchenski (1979) support this conclusion, although the higher capillary numbers used by Sufi et al. may be in a range which affects the true irreducible water saturation as well.

Hadley and Handy (1956), in a theoretical study of the capillary end-effect, concluded that the size of the end-effect decreases with both increasing flowrate and increasing displacing fluid viscosity. This is in agreement with Sufi et al.'s findings, arid provides further indication that results such as Weinbrandt et al.'s (1975) regarding temperature effects on irreducible water saturations may have been due primarily to end-effects. Lo and Mungan's (1972) results may also have been affected by end-effects. White oil viscosities, were more temperature-dependent than those for tetradecane. Also, the white oils displaced water to lower irreducible water saturations than tetradecane, which was of much lower viscosity. Although Lo and Mungan used internal taps to measure differential pressures, saturations were measured by material balance. Thus, end-effects could have affected saturation determinations.

Poston et al.'s (1970) experiments, however, were run on cores nearly 3 ft long. Saturation measurement errors due to the end-effect would be expected to be small in such cores. Using sand material that was similar to that used by Sufi et al., Poston et al. indicated changes in irreducible water saturation from 10%to around 22%. Sufi et al.'s results do not explain such a high irreducible water saturation, nor do

they explain Poston et al.'s observation of increasing irreducible water saturation with successive runs.

Temperature effects on residual oil saturations were also discussed by Sufi et al. It was found that residual oil saturations were difficult to compare at different temperatures because of viscosity ratio effects. Picking a "practical" residual oil saturation at a fixed oil fractional flow or a fixed number of pore volumes injected may result in very different values, because of changes in the fractional flow function, even when relative permeabilities remain constant. Even after several hundred pore volumes injected, Sufi et al. were unable to eliminate this effect completely.

This finding, however, does not totally explain the changes in residual oil saturation with temperature experienced by most previous studies. Sufi et al.'s discussion was based on effects caused when relative permeabilities are constant. In previous studies, entire oil relative permeability curves shifted toward higher water saturation. If temperature affected only the viscosity ratio, the result would have been curves that were comparable, but which ended at different points. The oil relative permeability curves of other studies discussed in this section could generally not be extrapolated to the same residual oil saturations at all temperatures. In fact, many of Sufi et al.'s relative permeability curves could not be extrapolated to the same residual oil saturation. Apparently some effect was occuring other than simply viscosity ratio changes.

In measuring relative permeabilities, Sufi et al. reported experimental difficulties from two well-known causes. First, dynamic displacement experiments must be measured at "stabilized" conditions.

Rapoport and Leas (1953) concluded that dynamic displacement experiments must be run at conditions so that the scaling coefficient, Lvp (L=core length, v=velocity, μ=viscosity of displacing phase), is sufficiently large to avoid premature breakthrough caused by smearing of the "shock" front from capillary pressure. Rapoport and Leas found, for the system they measured, the scaling coefficient must be greater than approximately 5 cm^2-cp/min. Although this cut-off value is widely used, it was only claimed to be specific to a particular system. Also, the experiments on which the scaling coefficient was based were made with a non-wetting phase displacing a wetting phase -- the opposite of the flow process usually of interest.

Kyte and Rapoport (1958) extended the work of Rapoport and Leas to experiments where the wetting phase displaced the non-wetting phase. Although the same type of behavior was found, Kyte and Rapoport reported that true breakthrough was difficult to establish, because the first wetting fluid to arrive at the outlet end of the core is retained by capillary forces (end-effect) until a sufficient saturation builds to allow production. This problem, however, would not exist in experiments starting from an initial water saturation (Kyte and Rapoport started experiments from 100%non-wetting phase saturation). In this case, the end-effect is already in place and the first wetting phase to arrive at the outlet face would be produced. Thus, the Rapoport and Leas criterion should still be valid for displacements from irreducible water saturation, but not valid for runs from 100%oil Saturation.

Since most of Sufi et al.'s results were based on runs from 100% oil saturation, a different criterion for selecting stabilized flow was used. Instead of comparing breakthrough recoveries, relative

permeability curves were used. Stabilized flow was selected as the point when relative permeability curves were independent of the scaling parameter. For runs at room temperature and 150°F, Sufi *et al* determined that stabilized flow was achieved above a scaling parameter of *6* cm^2-cp/min. This is surprisingly consistent with the systems measured by both Rapoport and Leas and Kyte and Rapoport. Based on this criterion, a flowrate of *400* cc/hr was selected for all runs.

The second difficulty discussed by Sufi *et al* was the problem of viscous fingering. Since a less viscous fluid (water) is used to displace a more viscous fluid (oil), water has a tendency not to displace as a sharp front, but to form instabilities that finger ahead. Although several studies have analyzed the problem of viscous instabilities, some of the most recent and useful results were presented by Peters and Flock (1981). Using theoretical considerations, results were presented showing that the onset of viscous instabilities could be predicted by a dimensionless number defined as (for water displacing oil):

$$I_{sc} = \left[\frac{\mu_o}{\mu_w} - 1\right] \frac{v\,\mu_w\,d^2}{C^*\,\sigma\,k} \qquad (2.8)$$

where:

I_{sc} = viscous instability number, dimensionless

d = core diameter

C^* = empirical wettability number, dimensionless

An empirical approach must be used to determine actual values for the viscous instability number (because of the wettability number). However, the results can still be used to judge the effects of various parameters. Peters and Flock recommended using a wettability number of

302.5 for water-wet systems and cylindrical cores. Using this value, their experimental results and others in the literature experienced the onset of viscous instabilities and the theoretically predicted viscous instability number 13.56.

Graphing breakthrough recoveries vs. flowrate, Sufi et al., found a relationship indicative of viscous fingering as predicted by Peters and Flock. That is, as flowrate increased, breakthrough recoveries remained constant, and then decreased with the onset of viscous fingering. At sufficiently high rates, breakthrough recoveries again become constant, but at a lower value. The onset of the lower plateau corresponds approximately to the same rate required to achieve stabilized relative permeability curves. Sufi et al. did not comment on this fact. However, the coincidence is difficult to ignore. Relative permeability runs were made at 400 cc/hr, recognizing that viscous fingering would probably affect the results.

The onset of viscous fingering predicted by breakthrough recoveries may be too harsh a criterion. Small instabilities formed just ahead of a displacement front would cause early breakthrough, but would disappear as soon as the main front reached the core outlet. Thus Sufi et al.'s relative permeabilities may have been less affected by viscous instabilities than the Peters and Flock criterion would suggest. Some results from this study which tend to confirm this hypothesis are discussed in Section 4.

Although Sufi et al. presented many results regarding end-point saturation changes with temperature, only a few measurements of relative permeability curves were presented. The only comparison of elevated temperature relative permeabilities was made between a room temperature

run and another at 122°F. Both of these runs were made starting at 100% oil saturation, although a run starting from 6% irreducible water saturation also compared favorably. A review of other runs at temperatures to 150°F revealed that temperature effects were not eliminated completely. Figure 2.7 presents some of the relative permeability data reported by Sufi et al.

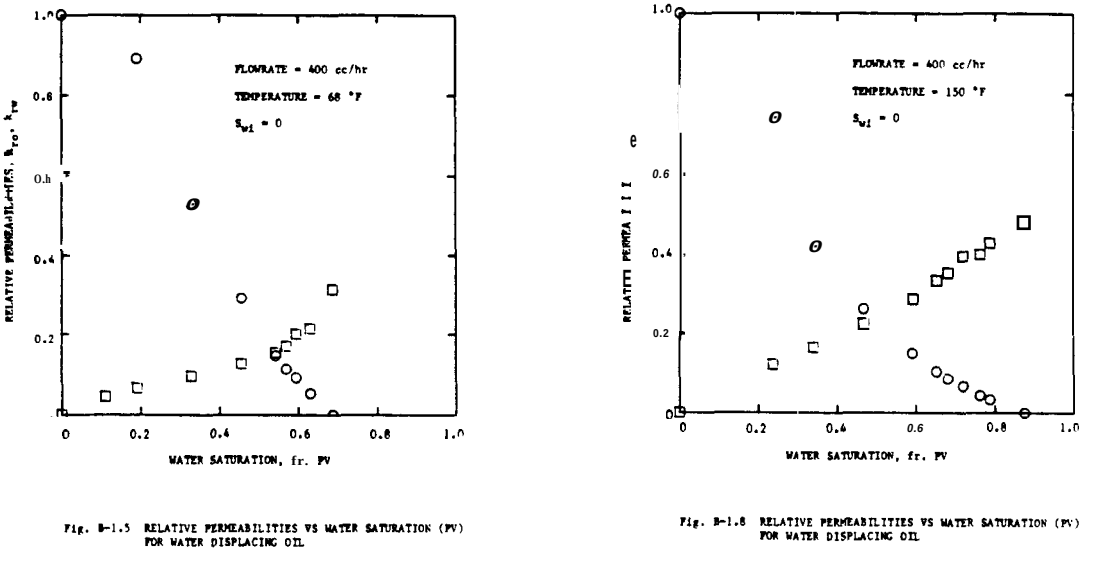

Fig. B-1.5 RELATIVE PERMEABILITIES VS WATER SATURATION (PV) FOR WATER DISPLACING OIL

Fig. B-1.8 RELATIVE PERMEABILITIES VS WATER SATURATION (PV) FOR WATER DISPLACING OIL

Fig. 2.7 Relative Permeabilities vs. Temperature Reported by Sufi et al. (1982)

This result is not surprising, since changes in measured irreducible water saturation with temperature, although explained, were not eliminated. Also, Sufi et al, like Davidson (1969), used a core cleaning procedure between runs that utilized hydrocarbon solvents to remove oil from the core. Some of Sufi et al.'s reported results at elevated temperatures showed a cross-over point of the oil and water curves at a water saturation less than 0.5. Shifts of the cross-over

point to lower water saturations is usually indicative of increasing oil-wetness. This possibility was not discussed.

In all of the studies known to the author on temperature effects on relative permeabilities, measurements with only one fluid pair were shown to be independent of temperature [tetradecane/water, measured by Lo and Mungan (1972)]. However, other fluid pairs under comparable wettability and interfacial tension conditions exhibited different behavior at room temperature and also a different temperature effect. This is contrary to other results discussed at length in this section. Sufi et al. (1982) made progress in attempting to isolate some of the factors causing temperature effects. These results indicated that temperature effects on relative permeabilities, at least in simple systems, might be due primarily to laboratory phenomena. Sufi et al. were unable to eliminate temperature effects above 122°F and were thus unable to confirm this conclusion.

The next section describes the goals of this research to investigate the existence of temperature effects and to isolate fundamental factors controlling such effects.

3. PROBLEM STATEMENT

Almost all studies discussed in Section 2 presented substantial effects of temperature on relative permeabilities. However, the results of Lo and Mungan (1972) and Sufi et al. (1982) suggest that temperature effects may be more a result of measurement difficulties and laboratory-scale phenomena than actual porous media flow behavior.

The goal of this study was first to attempt to minimize both measurement difficulties and laboratory-scale phenomena to determine whether temperature effects on relative permeabilities do, in fact, exist. It was believed that because of the vastly different results in the literature, the first step should be to use as simple a system as possible to focus on the most fundamental properties that might cause temperature effects. The system initially selected consisted of pure unconsolidated quartz sand, distilled water, and a refined white mineral oil. Unconsolidated quartz sand was selected to eliminate clay migration difficulties. Distilled water and white oil were used as fluids because of the high degree of immiscibility, ease of handling, and well-known or easily-determined properties. Distilled water also causes minimal corrosion problems at elevated temperatures. Blandol was the oil selected for the experiments. Blandol has a room temperature viscosity around 30 cp. The results of Sufi et al. suggested the possibility of viscous fingering problems. It was hoped that a less viscous oil than used by previous researchers would minimize this problem.

Both to minimize capillary end-effects and to provide a large pore volume, it was decided to use a core holder that would allow core

lengths to approach 2 ft. A 2 in. core diameter could be used in the available core holder, which resulted in unconsolidated sand pack pore volumes around 400 cc.

Dynamic displacement was chosen as the method to measure relative permeabilities. This type of experiment is the least difficult and time consuming to perform. Also, most previous studies were performed by dynamic displacement. It was believed that the results of this study should thus be more closely comparable to previous studies.

Should temperature effects not be found in unconsolidated sand systems, it was anticipated that other more complex systems might also be run. Consolidated sandstones and limestones would be the next logical choices.

4. EXPERIMENTAL EQUIPMENT, PROCEDURES AND ANALYSIS

Dynamic displacement experiments were conducted with distilled and salt water, a white mineral oil, and both unconsolidated and consolidated core materials. This section describes the apparatus, the fluids used, the procedures for core preparation and displacement experiments, and the methods used for data analysis.

4.1 Apparatus

The apparatus used in this study was designed to perform dynamic displacement relative permeability measurements at elevated temperatures using two immiscible fluids (oil and water). The apparatus was modified from the original design and construction by Jeffers (1981). Much of the equipment used for the apparatus was previously used by Counsil (1979) in his studies of steam–water relative permeabilities. A schematic of the main flow system is shown in Fig. 4.1. Details of the apparatus are given in Appendix A.

The main features of the apparatus are:

1. Ability to inject both oil and water.
2. Isothermal temperature control to 300+°F.
3. Measurement of the following parameters vs. time:
    a) cumulative injection volumes
    b) cumulative displaced fluid production volumes
    c) differential pressure across the core
    d) total volumetric flowrate

A single controlled–volume diaphragm pump was used to inject both water and oil. For the distilled water runs, water was injected directly from the pump, while oil was displaced by water from a pressure

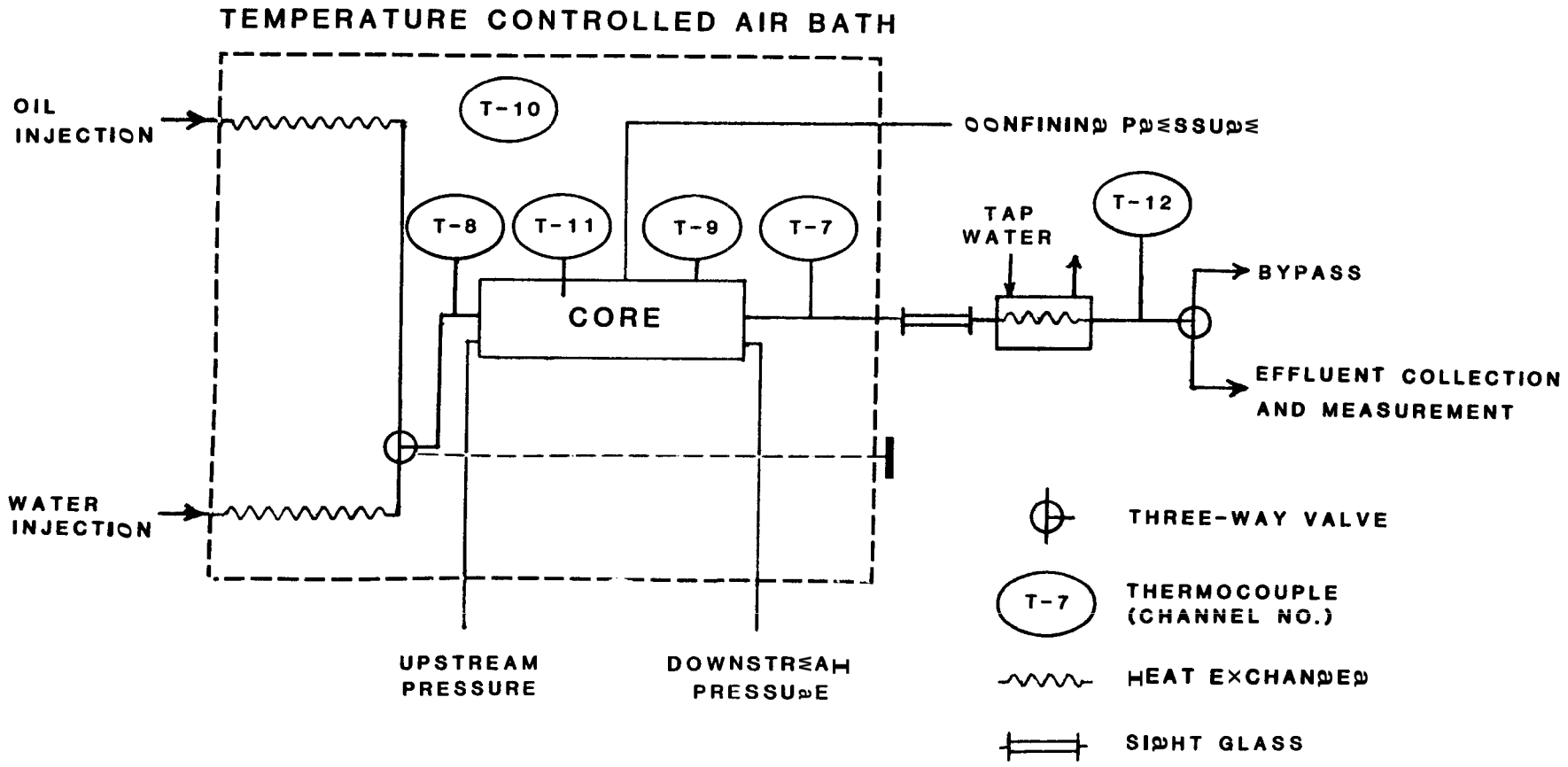

Fig. 4.1 Schematic of the Main Flow System of Dynamic Displacement Relative Permeability Apparatus

vessel in an alternate flow loop. This arrangement was reversed when salt water was used, i.e., oil was pumped directly and salt water was displaced from a pressure vessel. A nitrogen-charged accumulator and a rate-adjusting needle valve eliminated pumping pressure pulsations. The needle valve and an excess flow loop were used to approach constant-rate injection. The average volumetric flowrate between measurement points was determined with graduated cylinders and a stopwatch (see Appendix B). Instantaneous flowrates were determined from a capillary tube flowmeter using a differential pressure transducer with output recorded on a strip-chart recorder. The average flowrate measurements provided continual calibration of the flowmeter throughout a run.

A graduated scale on a 1 in. I.D. high-pressure glass tube separator was used to measure cumulative displaced fluid volumes. Cumulative injection volumes were determined by measuring separator overflow in graduated cylinders downstream of a pressure regulator set at 100 psig (to maintain system pressure above steam saturation pressure at elevated temperatures).

A bank of three pressure transducers was used to measure differential pressures across the core. Output from any two of the transducers could be recorded simultaneously on a strip-chart recorder. Bourdon tube pressure gauges both upstream and downstream of the core gave a visual reading of internal core pressures.

A schematic of the core holder used for unconsolidated sands is shown in Fig. 4.2. Core material was packed in a 2 in. I.D, 1/8 in. wall thickness stainless steel tube. The core was confined by a free-traveling end plug forced against the core by 500 psig confining pressure. Core lengths were approximately 20 inches. Unconsolidated

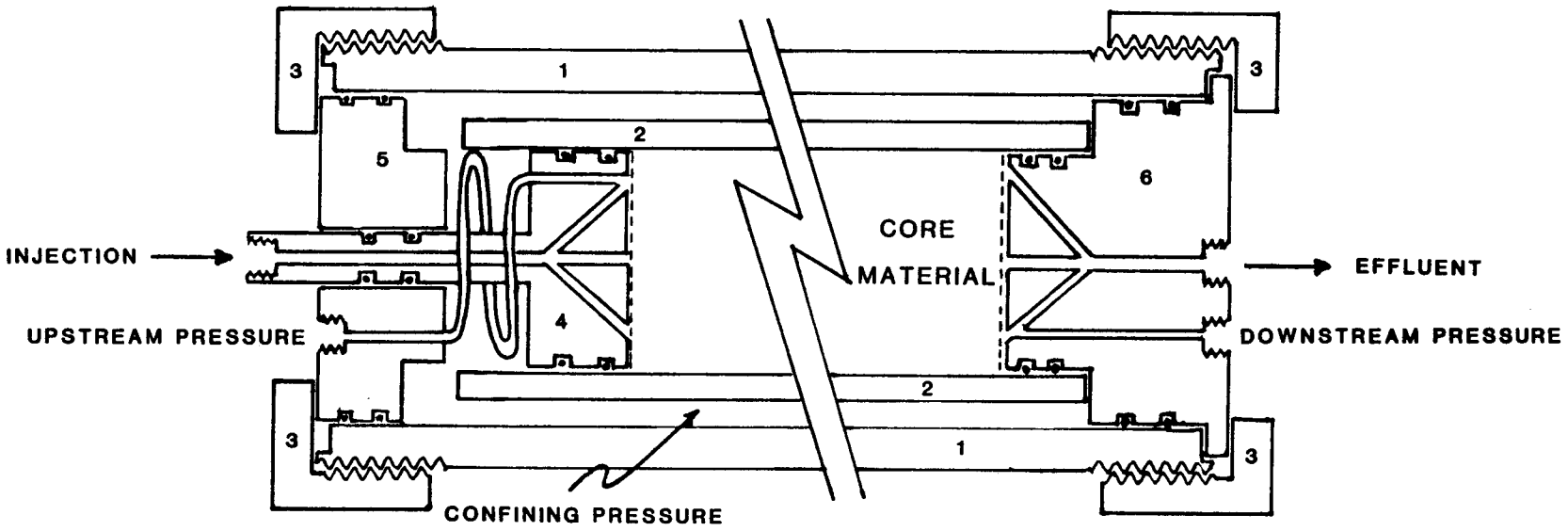

1 - OUTER SLEEVE

2 - INNER SLEEVE

3 - SCREW-ON RETAINER

4 - TRAVELING END PLUG

5 - TAPERING END PLUG GUIDE

6 - FIXED END PLUG

• O-RING

STAINLESS STEEL SCREEN
270 MESH

Fig. 4.2 Schematic of Core Holder Used for Unconsolidated Sands

sands consisted of a 100–200 mesh mixture (see Appendix B.l) of Ottawa silica sand. Porosities were approximately 38% and permeabilities were around 7 darcies.

Berea sandstone was used for the consolidated sand runs. Cores were 2 in. diameter and just over 20 in. long. Heat-shrinking FEP Teflon was used as a confining sleeve in place of the steel sleeve used for unconsolidated sands. Slight modifications required in the upstream pressure tap arrangement for consolidated cores are discussed in Appendix A. 6.

Distilled water was used for the confining fluid. Pressure was applied from a high–pressure nitrogen cylinder through a sealed pressure vessel partially filled with water. This system provided sufficient compressibility during heating and cooling of the core to avoid rapid changes in confining pressure. Once the system was at isothermal conditions, closing a valve leading to the core reduced the system compressibility to that of water alone. This allowed rapid detection of even minor confining pressure leaks.

4.2 Fluids

Distilled water and Blandol, a refined white mineral oil, were used for the unconsolidated sand runs. Blandol has a viscosity of 30 cp at 70°F. For the consolidated sand runs, a 2% sodium chloride solution was used in place of distilled water to prevent clay migration.

Distilled water viscosity and density vs. temperature at 100 psig were determined from ASME Steam Tables (1979) and curve fit with correlating equations (see Appendixes D.l and D.2). The viscosity and density of the salt water solution were obtained from the International Critical Tables (1927). The correlating equations for distilled water

properties were modified slightly for salt water (see Appendixes D.3 and D.4).

Oil viscosity and density were measured at temperatures to 175°F at atmospheric pressure. For extrapolation purposes, measured oil density vs. temperature data were curve fit assuming a constant oil thermal expansion coefficient. The equation matched the oil density data to within ±0.05%. Oil viscosity vs. temperature data were also extrapolated using a curve fit based on the equation used for ASTM Standard Viscosity–Temperature charts [Wright (1969)]. The equation matched the measured data to within ±0.7%. Further details on the measured data and equations are given in Appendixes D.5 and D.6. A graph of Blandol and distilled water viscosities is given in Fig. *4.3*.

4.3 Procedures

Procedures for core preparation and the displacement runs are summarized in the following sections. Additional details are given in Appendix B.

4.3.1 Core Preparation

Unconsolidated sand was dry packed in the inner sleeve of the core holder. A pneumatic vibrator strapped to the sleeve was used while the sand was being poured, to aid in settling of the pack. The weight of packed sand was carefully measured to determine the core pore volume (see Appendix B.l). Berea cores were furnace–fired at 500°C for five hours to remove organic materials. Heat–shrinking Teflon tubing was applied to the Berea cores with end plugs in place.

After assembling end plugs and the outer sleeve, the entire core holder was mounted in the air bath and confining pressure applied. The

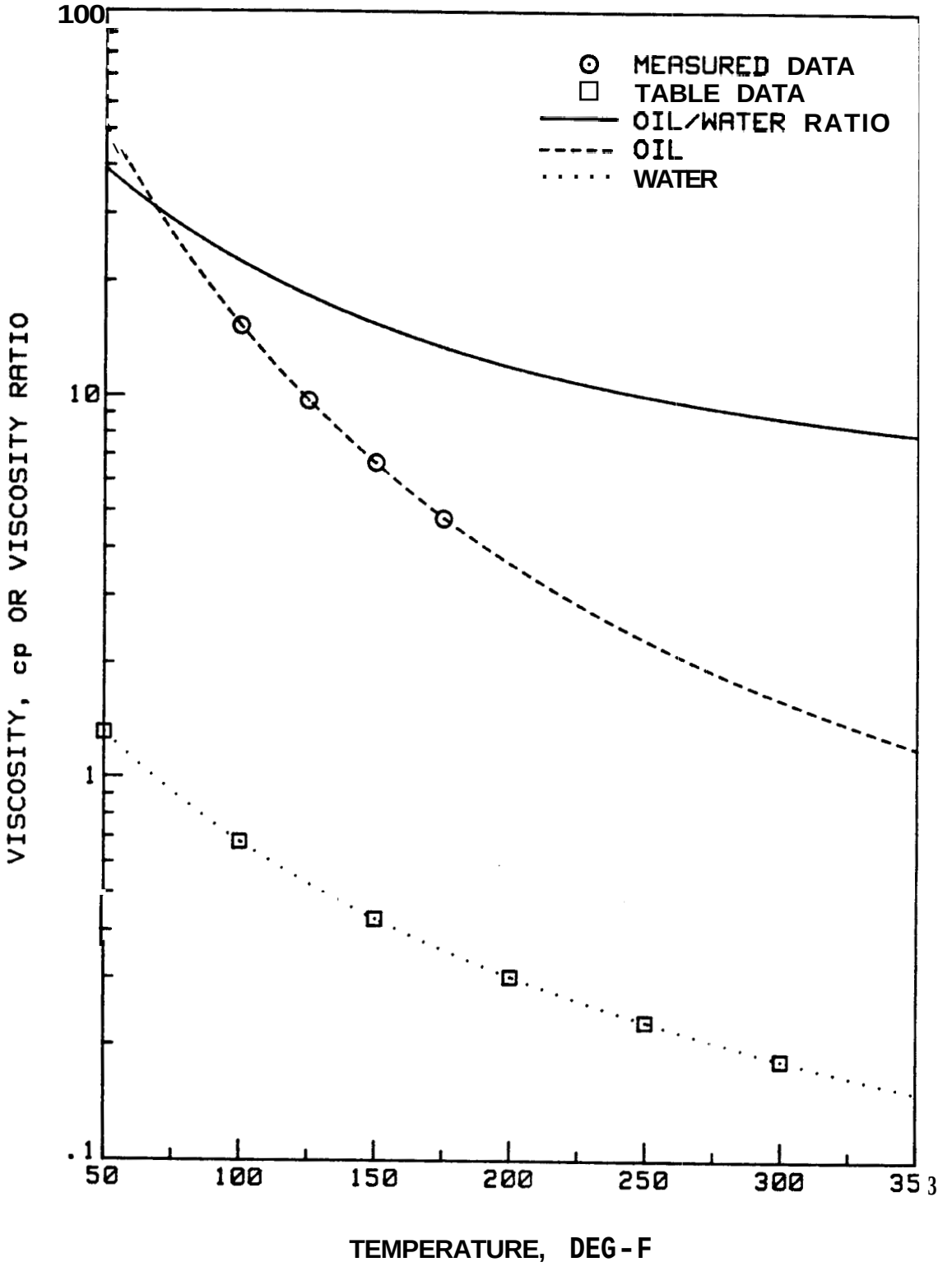

Fig. *4.3* Viscosity of Distilled Water and Blandol. vs. Temperature

core was then evacuated to less than 50 μTorr vacuum and filled with water. The amount of water required to fill the consolidated cores was measured to determine the core pore volume. System connections were made and lines bled of air in preparation for displacement runs.

4.3.2 Displacement Runs

Before starting the runs, absolute permeability of the pack to water was determined in the usual manner by measurement of flowrate and differential pressure. The length and diameter of unconsolidated cores were determined from core holder dimensions (see Appendix A.*6)*. Consolidated core dimensions were measured before loading into the core holder. Flowrates were measured with a graduated cylinder and a stopwatch. Several permeability measurements were made, usually being repeatable to within ±0.5%. Absolute permeabilities of all cores are given in Appendix C.

The absolute permeability of an unconsolidated core not used for displacement experiments was checked to be certain negligible temperature effects were seen. At 200°F, the permeability was only 2% higher than at room temperature.

Next, irreducible water saturation was establis'hed by displacing the core with approximately two pore volumes of oil. Measurements of water recovery and core injectivity were taken throughout the oil displacement run (procedural details are given in Appendix *B.4)*. At the end of two pore volumes, changes in water recovery (and thus irreducible water saturation) were undetectable. Further oil injection was not felt to be warranted.

After measuring the total amount of water produced into the effluent separator (see Appendix B.6), a water displacement run was then

initiated. The pump was first started with the injection system injecting oil. After reaching a stable rate and differential pressure, water injection was started. Measurements made throughout the run included cumulative water injected, cumulative oil produced, total volumetric flowrate, and differential pressure. Details of the measurement procedures are given in Appendix B.5. At room temperature, most experiments were run to approximately 10 pore volumes injected. Higher temperature runs were often terminated sooner, because of extremely low oil fractional flows. For example, at the end of 7 pore volumes injected in Run 2/6 at 297°F, the fractional flow of oil was only 0.0006. After calibrating the separator to get an accurate measurement of total oil produced (see Appendix B.6), the system was ready for another run.

The injection rate originally selected for the unconsolidated sand runs was 20 cc/min, the same as that used by Poston et al. (1970) for similar core material of almost identical dimensions. The rate used by Poston et al. was chosen by the method recommended by Kapoport and Leas (1953), i.e., to increase the injection rate (or the scaling parameter $Lv\mu_w$) on successive runs until no change is experienced in breakthrough recovery (stabilized flow). Sufi et al. (1982) recommended an alternative procedure for determining stabilized flow as the point at which relative permeability curves cease to change with rate. For this study, a room temperature run was made at a rate of approximately 30 cc/min (on Core 2) to check for stabilized flow. Both the breakthrough recovery and the relative permeability curves confirmed stabilized flow. The scaling parameter, $Lv\mu_w$, for high temperature runs was much lower than that for the room temperature runs because of the reduced

water viscosity. As will be seen in Section 5, these runs also gave essentially the same relative permeabilities. The injection rate used for consolidated core runs ranged from 4 to 16 cc/min. As high a rate as possible was used, keeping the pressure drop across the core less than 200 psi.

Temperature changes were made after water displacement runs with the core near residual oil saturation. For heating from room temperature, the system was first brought to an internal pressure of 100 psig, and then isolated with an upstream valve and the separator pressure regulator. During heating, core fluids expanded into the separator. Overflow from the separator through the pressure regulator was measured in a graduated cylinder. Thus the amounts of both oil and water that expanded from the core were measured. The same procedure was followed in cooling to room temperature, except that water was used to make up fluid volume contraction within the core. Further details on procedures for changing temperature are given in Appendix B.7.

Measurements of fluid expansion volumes indicate that the core pore volume changed very little, if at all, with temperature. Rough calculations considering thermal expansion of quartz sand grains and the steel sleeve indicate a maximum increase in pore volume of around 2 cc *(0.5%)*. This assumes that none of the thermal stress is taken up as mechanical stress between the grains (i.e. the grains are perfectly free to move). Since the 2 cc change is small and is a high estimate, it was assumed that the core pore volume did not change with temperature.

Repeat runs to re-establish irreducible water saturation were made after the preceeding water displacement run with the core near residual oil saturation. This procedure was followed by Poston et al. (1970) and

Weinbrandt et al. (1975). Davidson (1969) and Sufi et al. (1982) re-established 100% water or oil saturation by staged care cleaning procedures before making another run. Because these procedures utilized hydrocarbon solvents, there was concern about possible wettability changes. The major difficulty with starting from the end-point of the previous run was the necessity of keeping accurate material balances. Core 2, for example, had over 27,000 cc (70 pore volumes) of total fluid injected over six oil displacement runs and six water displacement runs. The material-balance-determined final oil saturation at the end of the final run was only 62 cc (16% of pore volume). The material balance problem was compounded by the necessity of accounting for fluid expansion during heating and contraction during cooling. As will be seen in Section 5, reproducibility of successive runs in the same pack at room temperature indicate that in most cases, accurate material balances were successfully maintained.

4.4 Data Analysis

In the Section 2 of this report, it was discussed that relative permeability vs. saturation curves could be determined from displacement experiments based on the techniques of Welge (1952) and Johnson, Bossler, and Naumann (1959). In summary, these techniques are based on the following three equations:

$$f_o = \frac{1}{1 + \frac{k_{rw}}{k_{ro}} \frac{\mu_o}{\mu_w}} = - \frac{d(N_p)}{d(W_i)} \tag{4.1}$$

$$S_{w2} - S_{wi} = N_p - W_i f_o \tag{4.2}$$

$$\frac{f_o}{k_{ro}} = \frac{d\left[\frac{1}{W_i I_r}\right]}{d\left[\frac{1}{W_i}\right]} \qquad (4.3)$$

where :

f_o = fractional flow of oil from core outlet

S_{wi} = irreducible (initial) water saturation

S_{w2} = water saturation at core outlet

k_{rw}, k_{ro} = relative permeabilities of water and oil

μ_w, μ_o = viscosities of water and oil

N_p = cumulative pore volumes of oil recovered

W_i = cumulative pore volumes of water injected

I_r = relative injectivity, $(q/\Delta p)/(q/\Delta p)_{initial}$

q = flowrate

Δp = core differential pressure

Jones and Roszelle *(1978)* derived a graphical approach which determined f_o by drawing tangents to the experimental N_p vs. W_i curve and finding $(S_{w2}-S_{wi})$ as the corresponding intercept at $W_i=0$. They also used the following modified form of Eq. *4.3* to determine f_o/k_{ro} as the intercept on an experimental $1/I_r$ vs. W_i curve:

$$\frac{f_o}{k_{ro}} = -W_i \frac{d(1/I_r)}{d(W_i)} + \frac{1}{I_r} \qquad (4.4)$$

Differentiating experimental data graphically is an inaccurate process, particularly if there is much scatter in the data. The technique derived from Eqs. *4.1* through *4.4* calls for taking two slopes on two separate curves at the same W_i value. Even with smoothing, analyzing the data graphically sometimes leads to strangely shaped relative permeability curves.

For this study, curve-fit equations of the recovery and injectivity data were used to determine relative permeability relationships. Derivatives of these curves were used in place of graphical slopes in the calculations. Three requirements were used in selecting equational forms for this purpose:

1. The equations should fit the data visually as well as might be done by hand.
2. The equations should be smooth and monotonic, since the data should behave in this manner.
3. The resulting relative permeability curves should be smooth and look like conventional relative permeability curves.

The equational forms originally used were suggested by Chris MacAskill of Petrophysical Services, Inc.:

$$N_p = a_0 + a_1[\ln(Wi)] + a_2[\ln(Wi)]^2 + a_3[\ln(Wi)]^3 + \ldots\ldots \quad (4.5)$$

$$I_r = b_0 + b_1[\ln(Wi)] + b_2[\ln(Wi)]^2 + b_3[\ln(Wi)]^3 + \ldots\ldots \quad (4.6)$$

Second and third order forms of both equations were tried. Although third order matches were a little better, with some data the resulting relative permeability curves had unusual shapes (due to changes in curvature of the equations). The second order match of recovery worked very well for all runs at all temperatures. However, for some of the elevated temperature runs, the second order injectivity equation was not satisfactory and the resulting relative permeability curves were unacceptable.

Since f_o/k_{ro} is directly the slope on a $1/(W_i I_r)$ vs. $1/W_i$ curve, fitting of $(W_i I_r)$ vs. W_i was next tried. The equation finally selected was:

$$\ln(W_i I_r) = b_0 + b_1[\ln(W_i)] + b_2[\ln(W_i)]^2 \qquad (4.7)$$

This form gave excellent matches of the $(W_i I_r)$ data at all temperatures, and with the second order N_p vs. $\ln(W_i)$ data match, yielded well-behaved relative permeability curves at **all** temperatures (see Appendix H). Because relative permeability calculations were based on functional relationships, the resulting curves were smooth. The usual scatter was removed by curve matching the raw data.

Data were, of course, limited to those taken after breakthrough. However, the first recovery and injectivity points immediately after breakthrough were disregarded. Rapid changes in both saturation and flowing volume fractions occur at water breakthrough. Also, capillary pressure, gravity effects, and viscous fingering cause the saturation front not to be as "sharp" as assumed in Buckley-Leverett (1942) displacement theory. The first post-breakthrough point was thus not felt to be representative. The first post-breakthrough point almost never matched the trend of the rest of the data.

Figure 4.4 shows an example of the results. The recovery data in this example has a maximum deviation from the equation of ±0.2% and an average absolute deviation of 0.1%. The $(W_i I_r)$ curve match has a maximum deviation of ±2.9% and an average absolute deviation of 0.9%. The important thing is that visually, the smoothing of the data with the equation is what might have been done by hand. Similar matches were achieved for all runs (see Appendix J for detailed data).

An "inferred" breakthrough point is shown in Fig. 4.4. This point is where the recovery equation crosses the pre-breakthrough relationship, $N_p = W_i$. On the $(W_i I_r)$ graph prior to breakthrough, a curve is drawn from the inferred breakthrough W_i, assuming that $1/I_r$ is linear

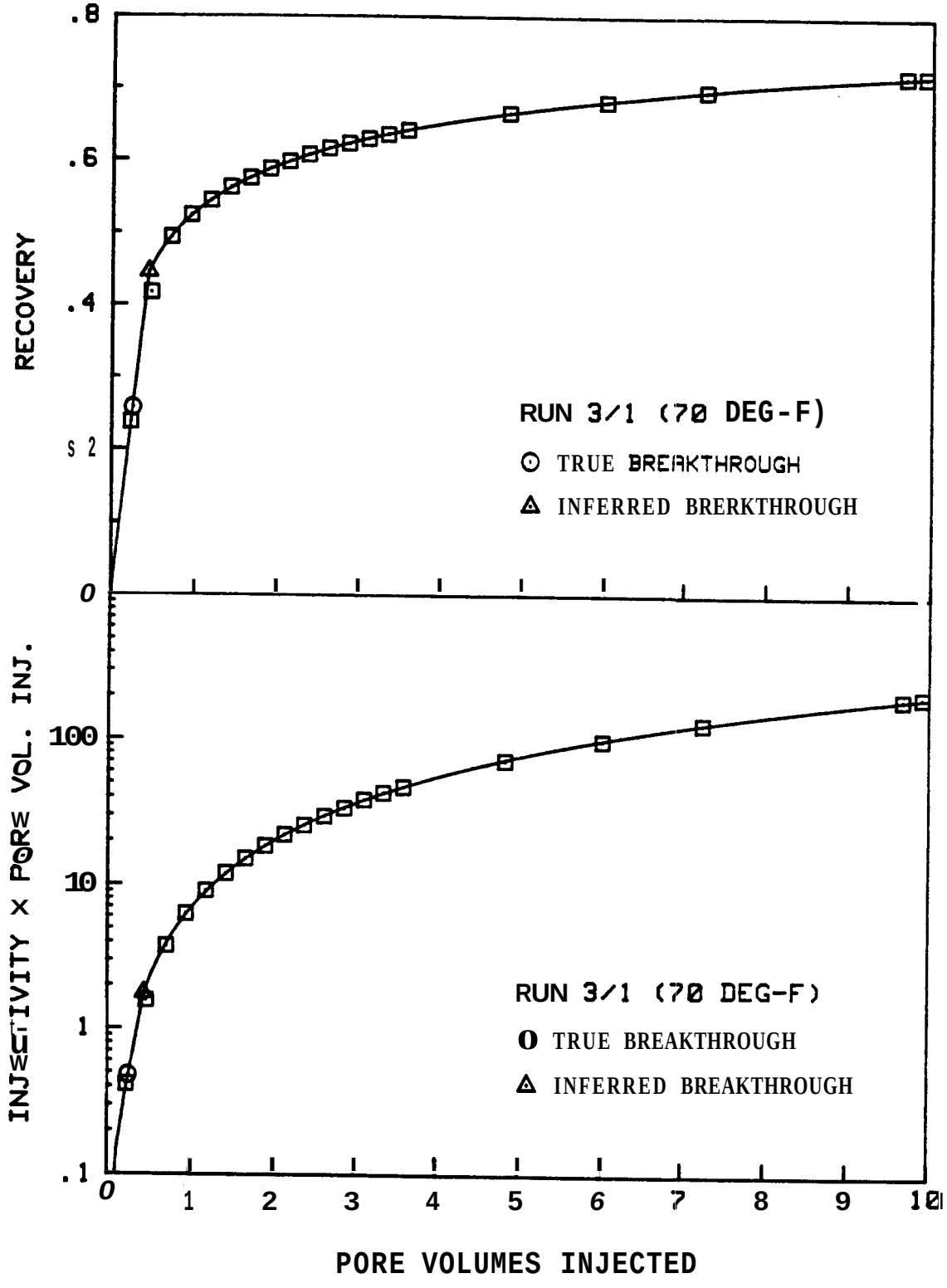

Fig. *4.4* Example Recovery and Injectivity **Curve** Fits

with W_i (as it theoretically is). The true breakthrough point was always prior to "inferred" breakthrough. The primary reason for this is believed to be small viscous instabilities just ahead of the water front. In Fig. 4.4, the first post-breakthrough recovery point is closer to the $N_P=W_i$ curve than to the post-breakthrough equation. The inferred breakthrough point was not used in any calculations.

Figure 4.5 shows further evidence that the first: post-breakthrough point should not be used. In this figure, recovery is shown graphed against the logarithm of pore volumes injected. After breakthrough, the curvature of the data is gentle -- except for the first post-breakthrough point. This figure also shows that the equational form used for the recovery curve match works well.

An analysis of water fractional flow ($f_w=1-f_o$) vs. water saturation was made with the data from Run 3/1. Figure 4.6 compares the curve calculated by the analysis technique described previously, with a curve calculated utilizing the true breakthrough point arid all post-breakthrough data. The analysis technique used in this study appears to yield more reasonable fractional flow behavior, than if all post-breakthrough data is used.

Jones and Roszelle (1978) recommended using graphs of recovery and injectivity vs. the reciprocal of pore volumes injected at large values of pore volumes injected. This procedure allows more accurate tangents to be drawn, since at large injected volumes, both recovery and injectivity tend to flatten. Appendix J presents graphs of recovery and injectivy times pore volumes injected vs. the reciprocal of pore volumes injected for all runs in this study. An example is given in Fig. 4.7. The curve match equations are shown to work just as well for this type of graph.

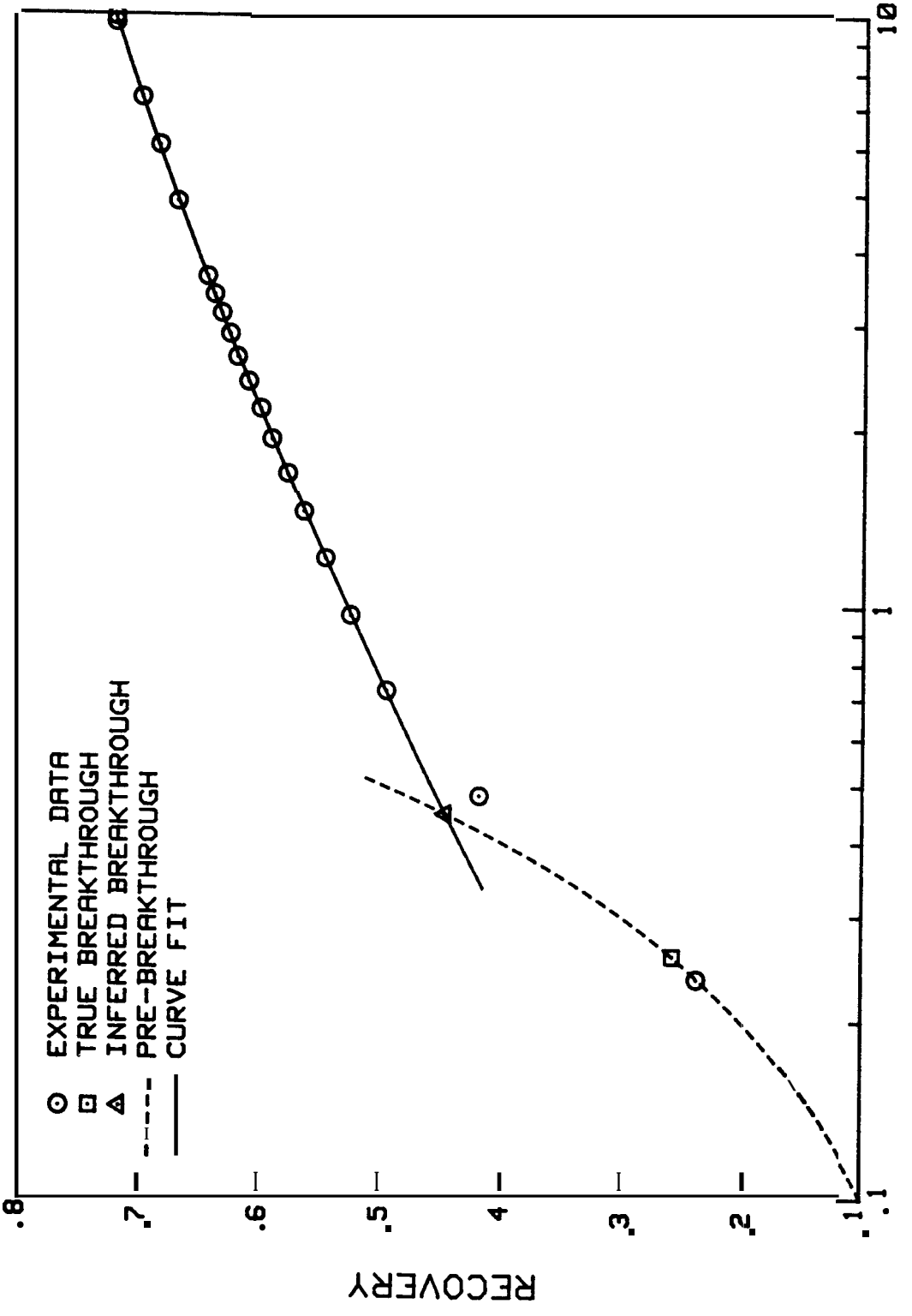

Fig. 5 Recovery vs. Logarithm of Pore Volumes Injected for Run 3/1

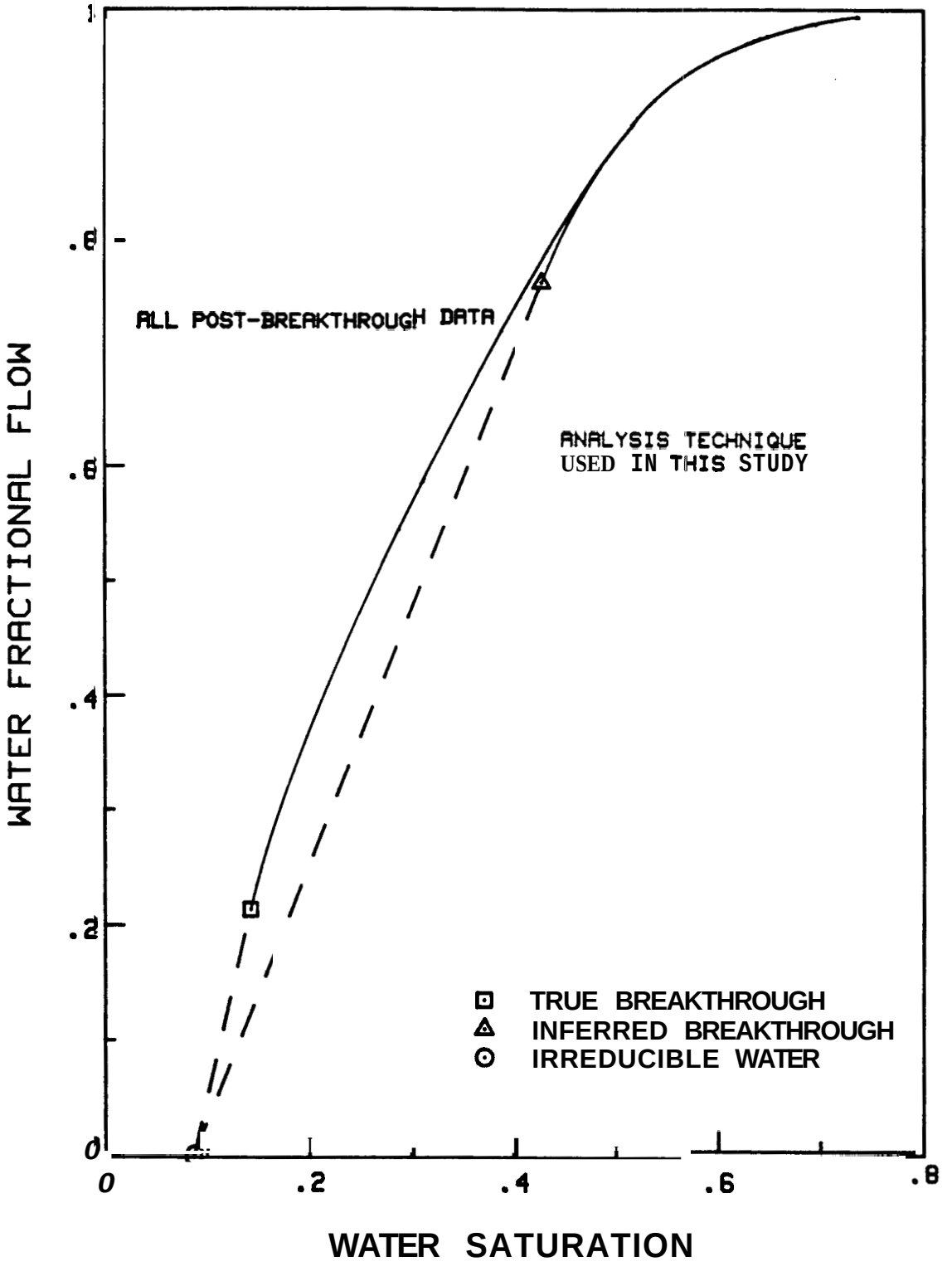

Fig. *4.6* Water Fractional **Flow vs.** Water Saturation for Run **3/1**

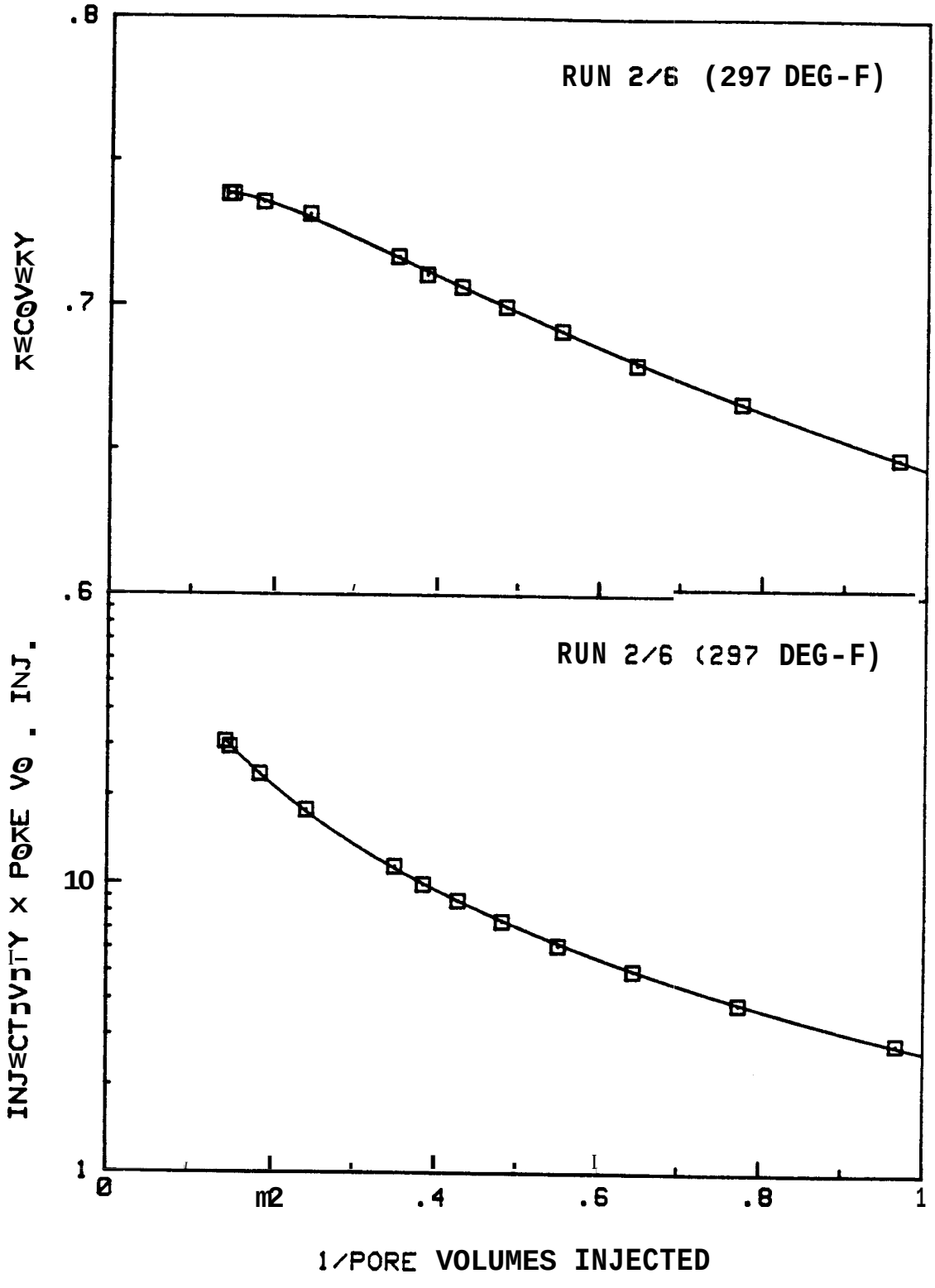

Fig. 4.7 Example Graph of Recovery and Injectivity x Pore Volumes Injected vs. 1/Pore Volumes Injected (Run 2/6)

Jones and Roszelle also recommended using the graph of recovery vs. the reciprocal of pore volumes injected to extrapolate to residual oil saturation. Figure 4.7 provides an indication that this procedure may not be appropriate. At high injected volumes, the curve recovery vs. the reciprocal of pore volumes injected begins to flatten instead of proceeding along the trend of previous data. Since Run 2/6 was taken to a relative permeability to oil of 0.003, the last point was nearly at residual oil saturation. This is confirmed by the flattening of the curve. Had the experiment been terminated sooner, the extrapolated residual oil saturation would have been too low. No attempts were made to extrapolate to residual oil saturations in this study.

In the early stages of this study, attempts were made to include the actual breakthrough point in the curve match. This usually required a third-degree equation to obtain reasonable results. Also, calculations were performed using the Jones and Roszelle (1978) technique on curves drawn by hand. In both cases, the resulting relative permeabilities were not acceptable. Using the breakthrough point tended to make the oil relative permeability curve flatten or even increase slightly with increasing water saturation. This was not believed to be reasonable behavior for a homogeneous sand pack.

Relative permeabilities were calculated in this study using the absolute permeability of the core to water as a base. With the Johnson, Bossler, and Naumann method, relative permeability curves are usually calculated using oil permeability at irreducible water saturation as a base. The reason this was believed to be inappropriate was because of the capillary end-effect. Prior to water breakthrough, the end-effect is at a maximum. Water saturation must rise from irreducible to a

maximum value at the outlet core face. This creates an additional pressure drop. After breakthrough, the end-effect pressure drop is greatly reduced because of the high water saturation in the core. At large pore volumes injected, the end-effect is reduced to nearly zero as the water saturation along the core is essentially uniform. Because of the additional pressure drop caused by the end-effect, the computed permeability to oil just before the start of water injection must be less than the true oil permeability at irreducible water saturation.

By presenting results using absolute permeability as a base, the additional end-effect pressure drop before breakthrough is excluded. Errors arising from post-breakthrough end-effects are believed to be small, expecially considering the length of the core. Sections 5 and 6 present further evidence that relative permeabilites should be graphed in this manner.

Appendix G describes a computer program written to analyze the displacement data. The program is written in **BASIC** for the Hewlett-Packard 9845B desk-top minicomputer. In addition to performing the calculations, the program utilizes the plotting capabilities of the minicomputer to generate graphs of:

a) recovery and injectivity times pore volumes injected vs. pore volumes injected and vs. the reciprocal of volumes injected

b) logarithm of water-oil permeability ratio vs. water saturation

c) individual water and oil relative permeabilities vs. water saturation

Results of the displacement experiments are discussed in the next section.

5. RESULTS

Elevated temperature runs were made on three unconsolidated sand packs (cores) and one consolidated (Berea) core. The following sections describe the residual saturation and relative permeability measurements on these cores.

5.1 Residual Saturations — Unconsolidated Cores

Table 5.1 presents the results of the oil displacement runs to establish irreducible water saturation in the unconsolidated sand cores.

Table 5.1 Irreducible Water Saturations - Unconsolidated Cores

Core	Run	Temperature (°F)	Irreducible Water Saturation (%)
2	1	71	7.3
	2	69	8.2
	3	197	9.3
	4	70	10.1
	5	67	8.4
	6	298	10.3
3	1	70	8.7
	2	200	10.4
	3	295	9.7
	4	202	8.1
4	1	67	9.4
	2	295	10.9
	3	67	8.0

Unlike the reported results of previous researchers [Poston et al. (1970), Weinbrandt et al. (1975), and Sinnokrot et al. (1971)], these

experiments failed to show an increase in irreducible water saturation with temperature. In some cases, a slight increase with temperature appears. However, this small effect may be attributed to reduced oil viscosity at elevated temperatures, and thus less efficient displacement at a given number of pore volumes injected. The results of Sufi et al. (1982) also suggest changes in the capillary end-effect with temperature.

No attempt was made to evaluate changes in residual oil saturation with temperature. Sufi et al. (1982) discussed the problem of comparing residual oil saturations of runs with different viscosity ratios (because of temperature changes). This problem was caused by the large injected volumes required to approach the true residual oil saturation. Fractional flow changes with viscosity ratio may have an appreciable effect on what is called the "practical" residual oil saturation. Even after several hundred pore volumes injected, Sufi et al. were not able to eliminate this problem completely. For this study, it was believed that changes in residual oil saturation should be evident from changes in relative permeability curves.

5.2 Relative Permeabilities -- Unconsolidated Cores

Reproducibility of relative permeability measurements in unconsolidated sand cores and the results at elevated temperatures are discussed in the following sections.

5.2.1 Reproducibility

Two important aspects relating to run reproduci'bility were investigated. First, it was believed that there should be reasonable reproducibility in sand pack preparation to be certain that an adequate

packing procedure was being used, and more importantly, to be confident of displacement run measurements and calculational techniques.

Another important point was to determine whether multiple room-temperature runs in the same pack would be reproducible, or would show hysteresis effects. Poston et al (1970) reported that increases in irreducible water saturation with temperature were not entirely reversible. Water saturation appeared to increase measurably with successive runs, although there was a decrease with temperature decrease.

Reproducibility of relative permeability curves for the three different sand packs is shown in Figs. 5.1 and 5.2. In spite of the scatter in the oil relative permeabilities at irreduci'ble water saturation (Fig. 5.2), the relative permeability curves are remarkably similar. These results indicate reproducible packing and measurement techniques.

Figures 5.3 through 5.6 show good reproducibility of runs in the same sand pack. These results and the irreducible water saturation measurements indicate stability of the sand packs and no sequential change in wettability. The comparisons also indicate the accuracy of material balances possible in these experiments. Figure 5.4 again shows a scatter in the oil relative permeabilities at irreducible water saturation.

For Core 3, the two relative permeability curves at room temperature are practically identical (Figs. 5.5 and 5.6). The displacement measurements on Core 3 are believed to have been more accurate than for Core 2. Core 2 was the first experiment with repeated high temperature runs. Many procedural problems were discovered and solved in making these first runs.

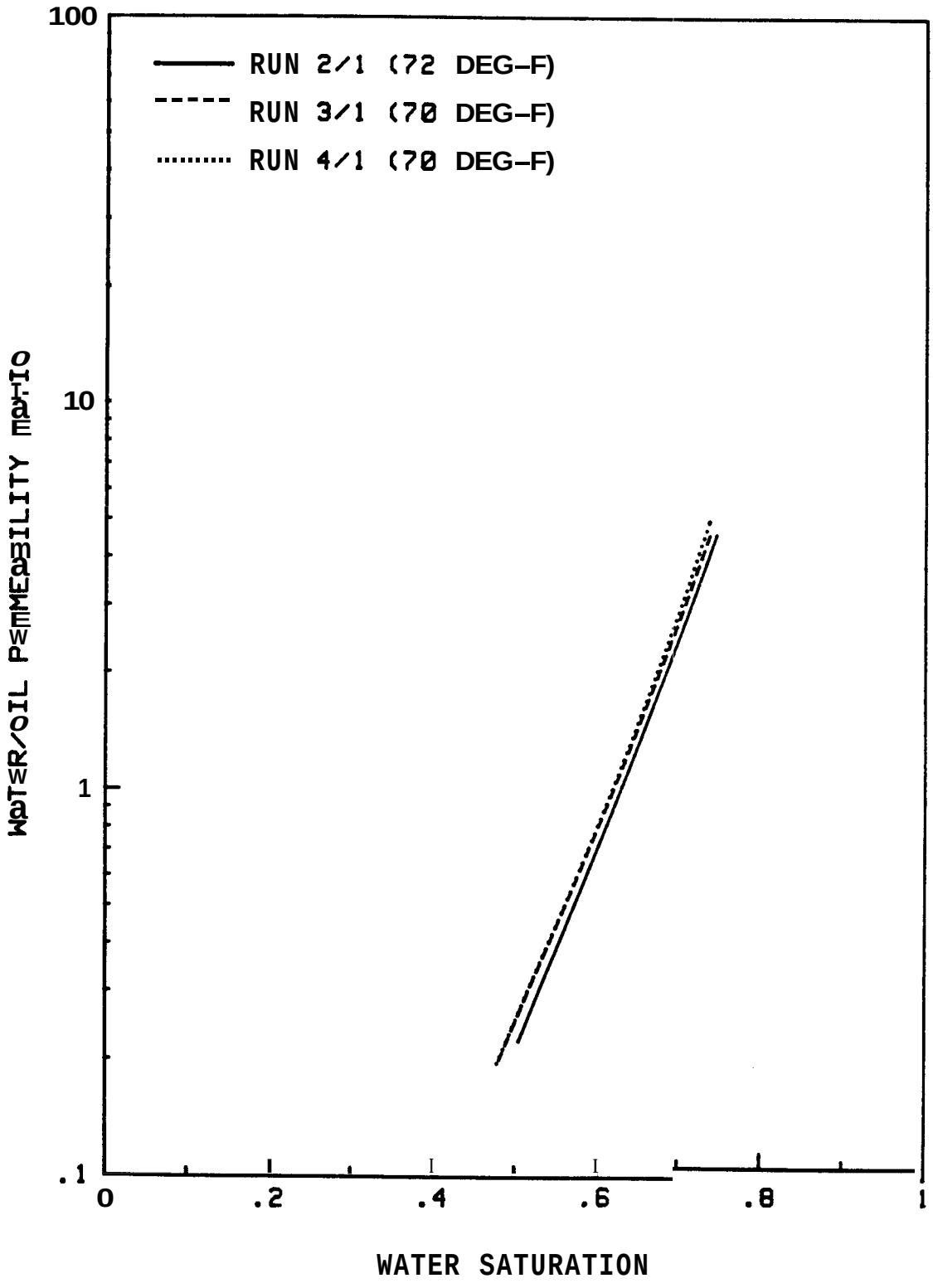

Fig. 5.1 Relative Permeability Ratios of First (Room Temperature) Runs on Unconsolidated Cores

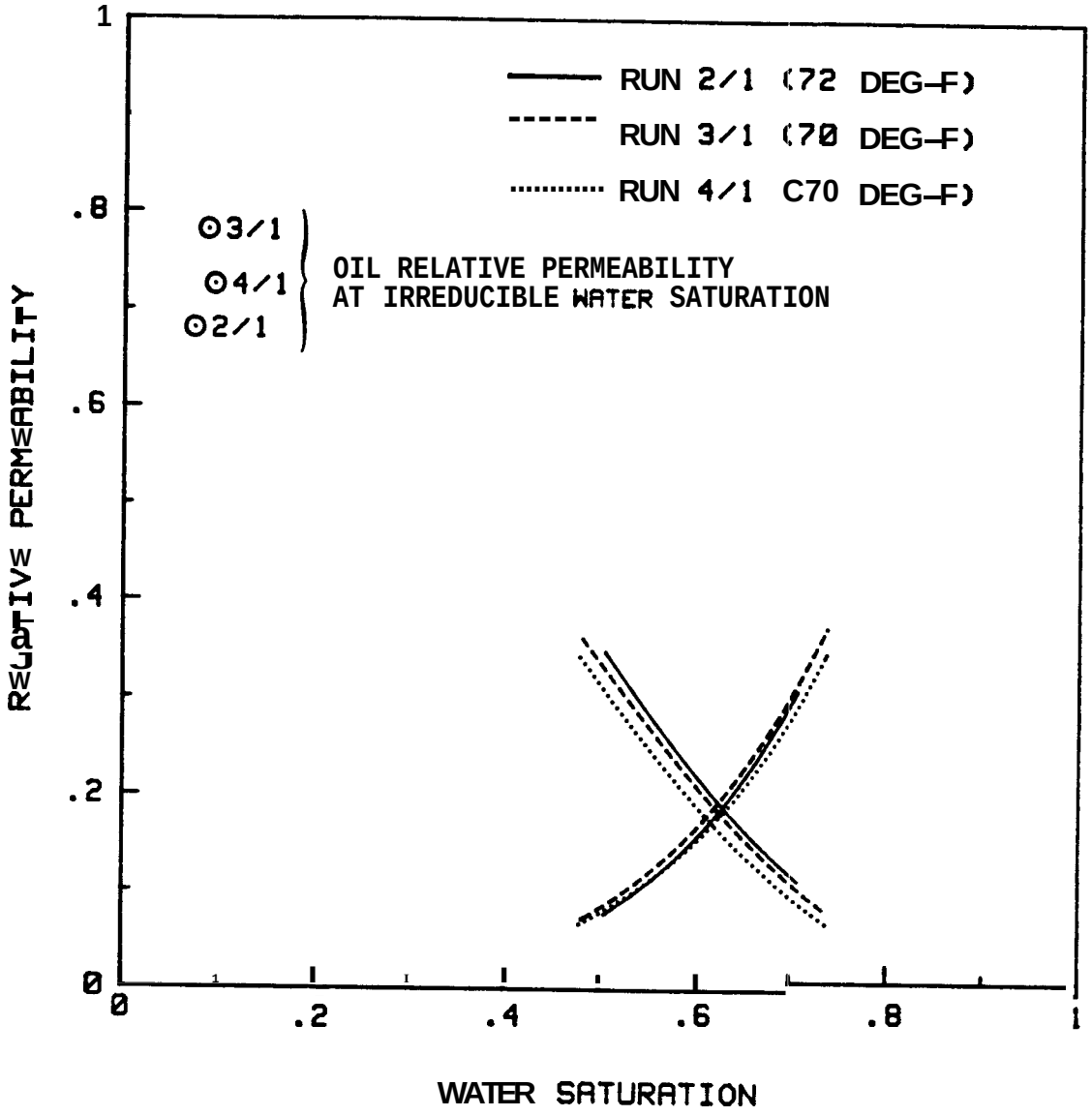

Fig. 5.2 Relative Permeabilities of First (Room Temperature) Runs on Unconsolidated Cores

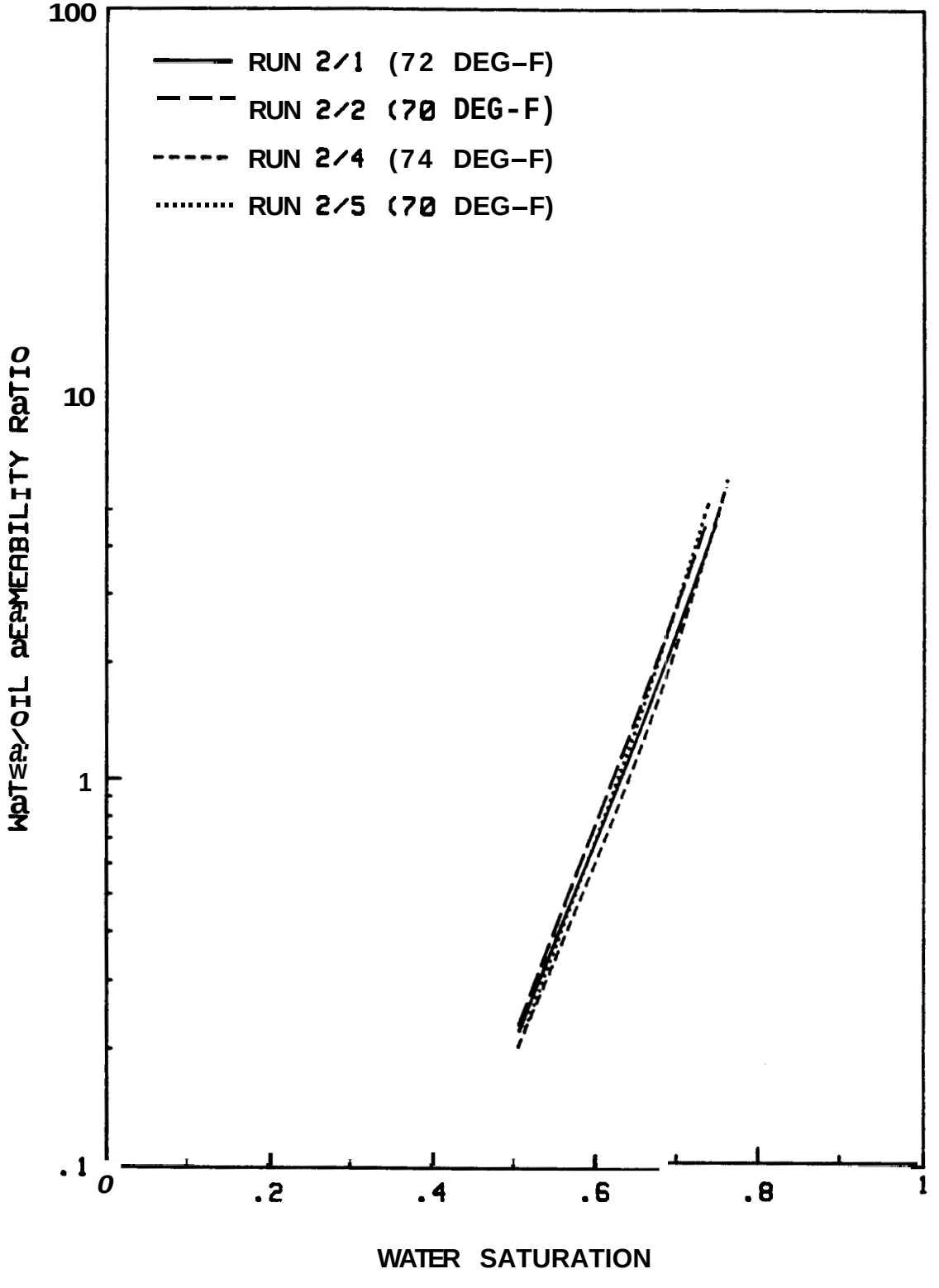

Fig. 5.3 Room Temperature Relative Permeability Ratios for Core 2

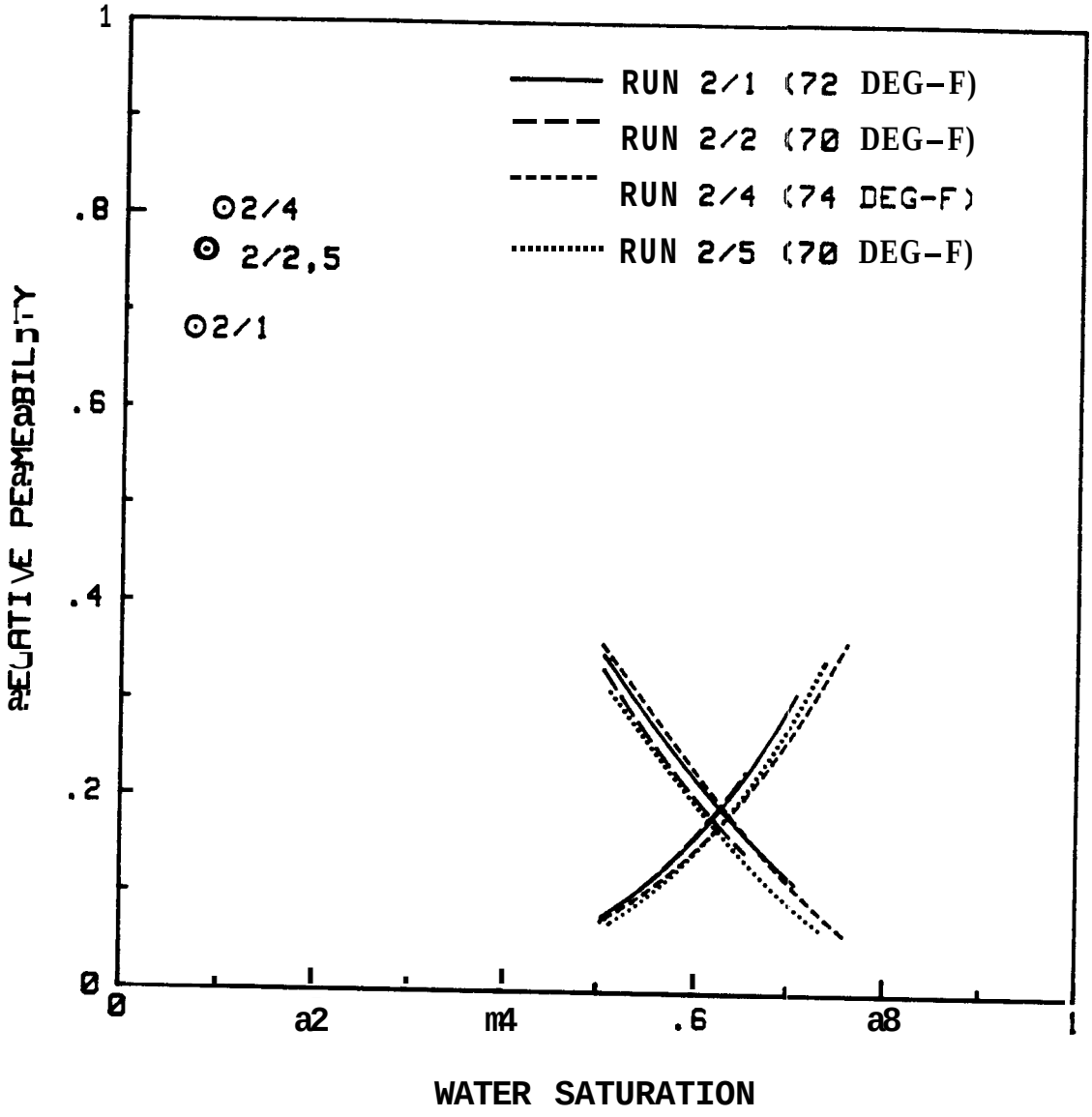

Fig. 5.4 Room Temperature Relative Permeabilities for Core 2

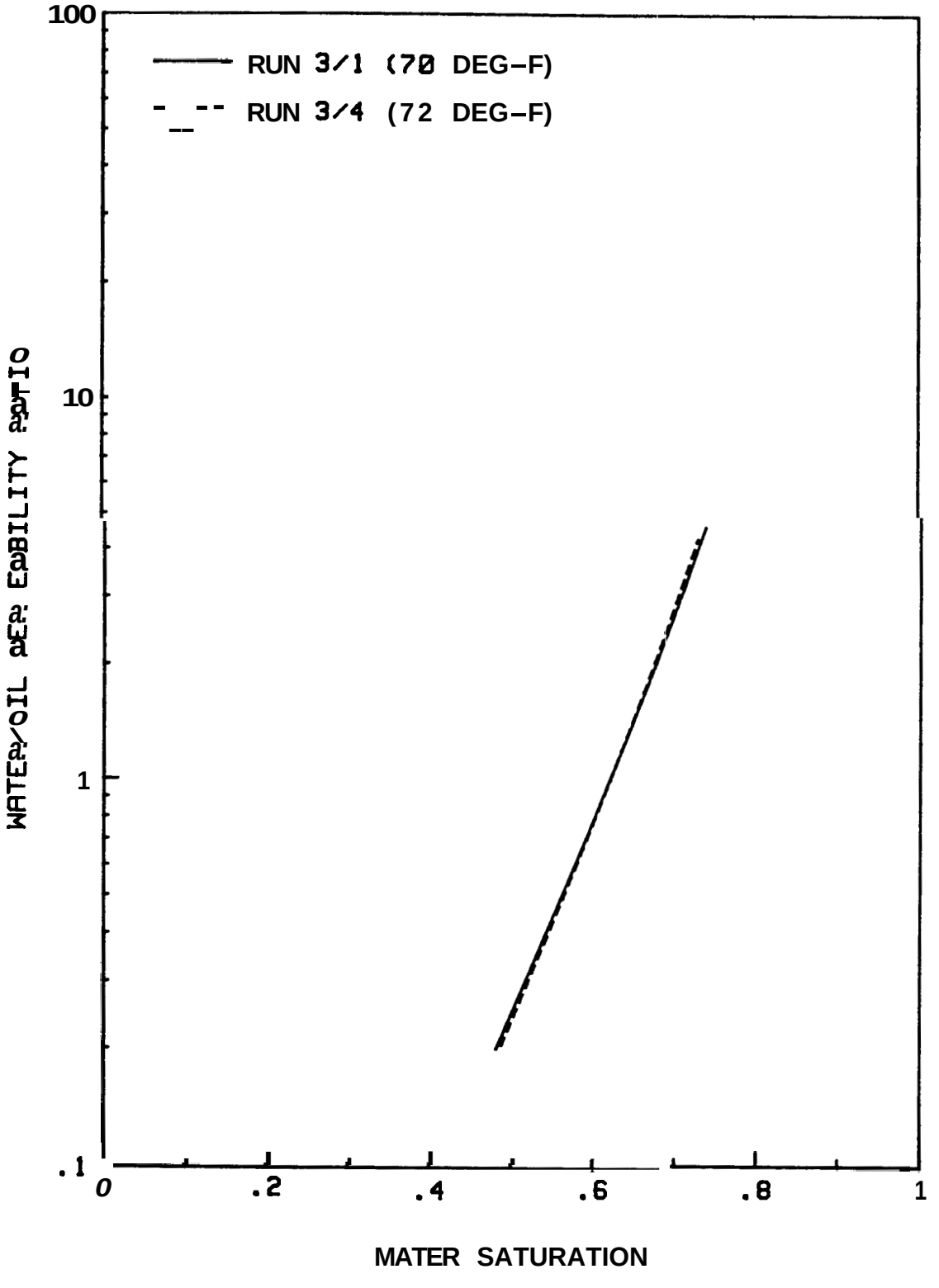

Fig. 5.5 Room Temperature Relative Permeability Ratios for Core 3

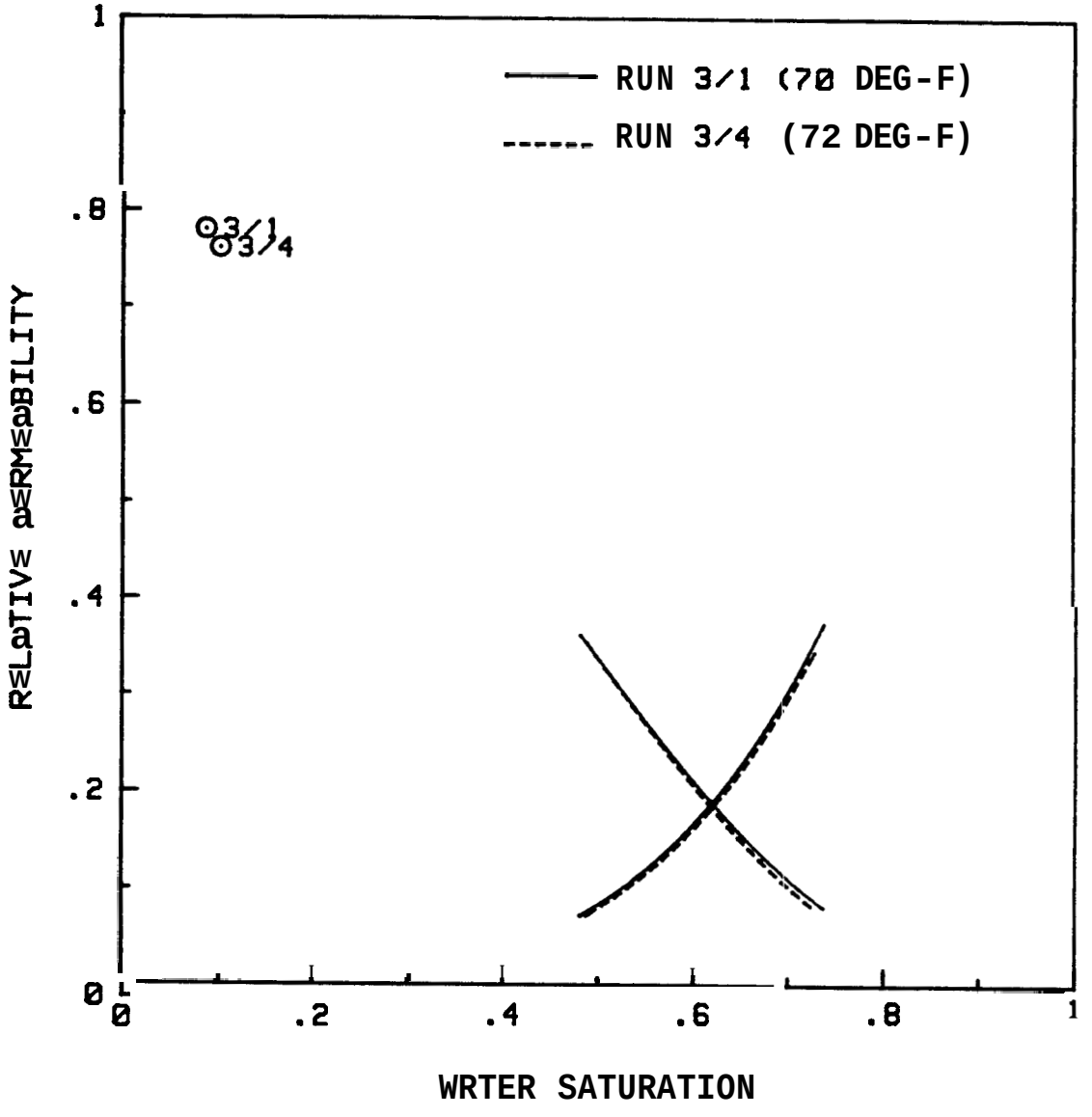

Fig. 5.6 Room Temperature Relative Permeabilities for Core 3

The relative permeability curves measured in this study on unconsolidated sands were compared to the steady-state measurements on similar sands by Leverett (1939). The curves compared favorably and provided further evidence that measurements were accurate. The room temperature curves of Sufi et al. (1982) and Poston et al. (1980) did not compare favorably with the Leverett curves. Poston et al.'s curves were, however, similar to the Leverett curves at elevated temperatures.

The results of the relative permeability measurements at elevated temperatures are presented in the next section.

5.2.2 Elevated Temperatures

Figures 5.7 and 5.8 present the elevated temperature runs on Core 2. The 197°F curves (Run 2/3) are, for practical purposes, identical to the room temperature curves (Run 2/4), both in terms of relative permeability ratios and the individual relative permeabilities. The 297°F curves (Run 2/6), however, are shifted slightly to the right in both figures. Because the 297°F permeability ratio curve is exactly parallel to the 197°F curve, it is believed that small material balance measurement errors caused a saturation shift of the 297°F curve. The indicated saturation shift is only 1.5% of pore volume -- a discrepancy which is entirely feasible, considering that by the time Run 2/6 was initiated, the core had over 60 pore volumes of total throughput and had gone through three temperature changes.

The elevated temperature runs for Core 3 are shown in Figs. 5.9 and 5.10. The permeability ratio curves show little change with temperature. However, the individual relative permeabilities do show a small change at 294°F. Although there is no concrete evidence, this

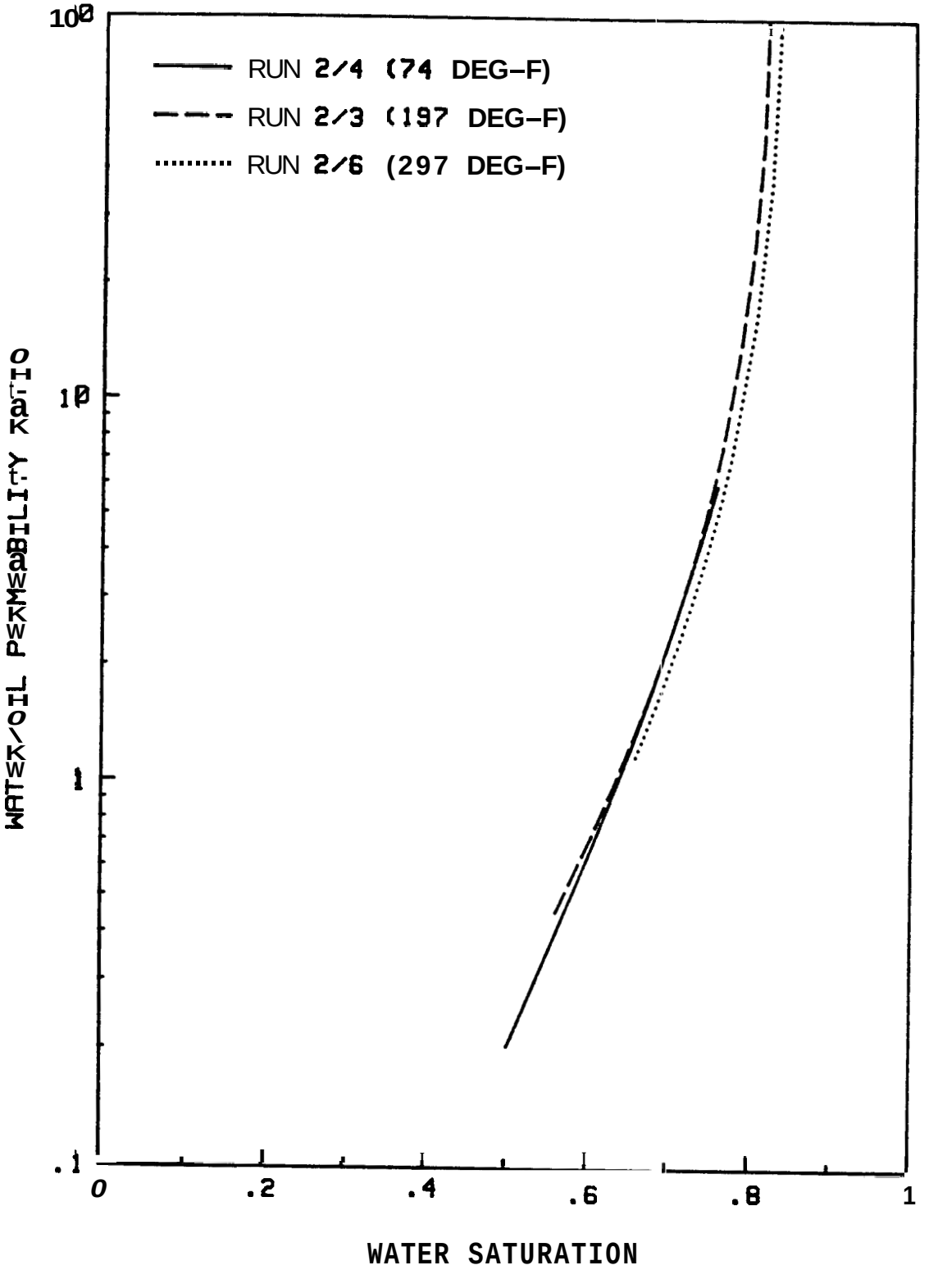

Fig. 5.7 Elevated Temperature Relative Permeability Ratios for Core 2

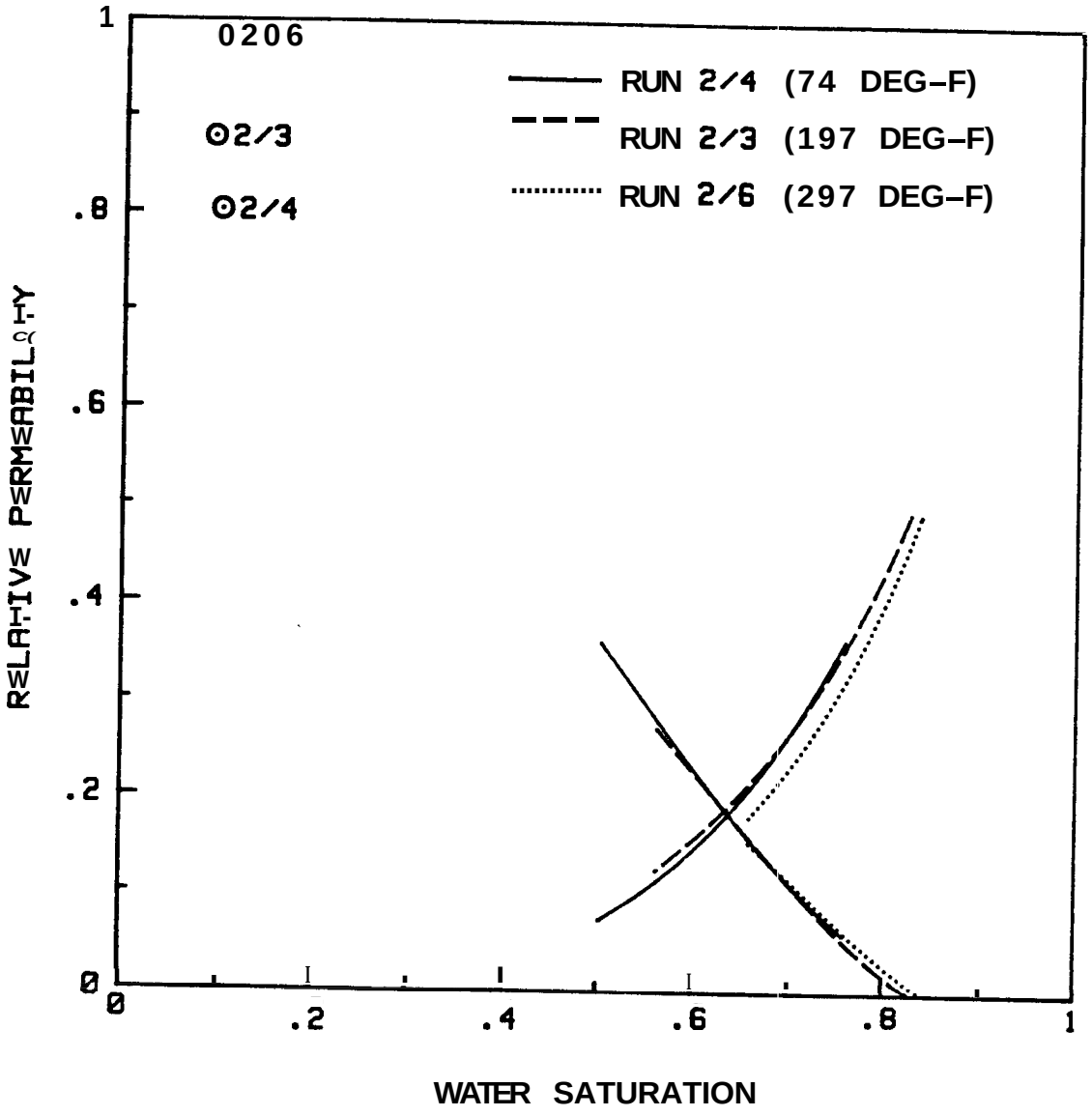

Fig. 5.8 Elevated Temperature Relative Permeabilities for Core 2

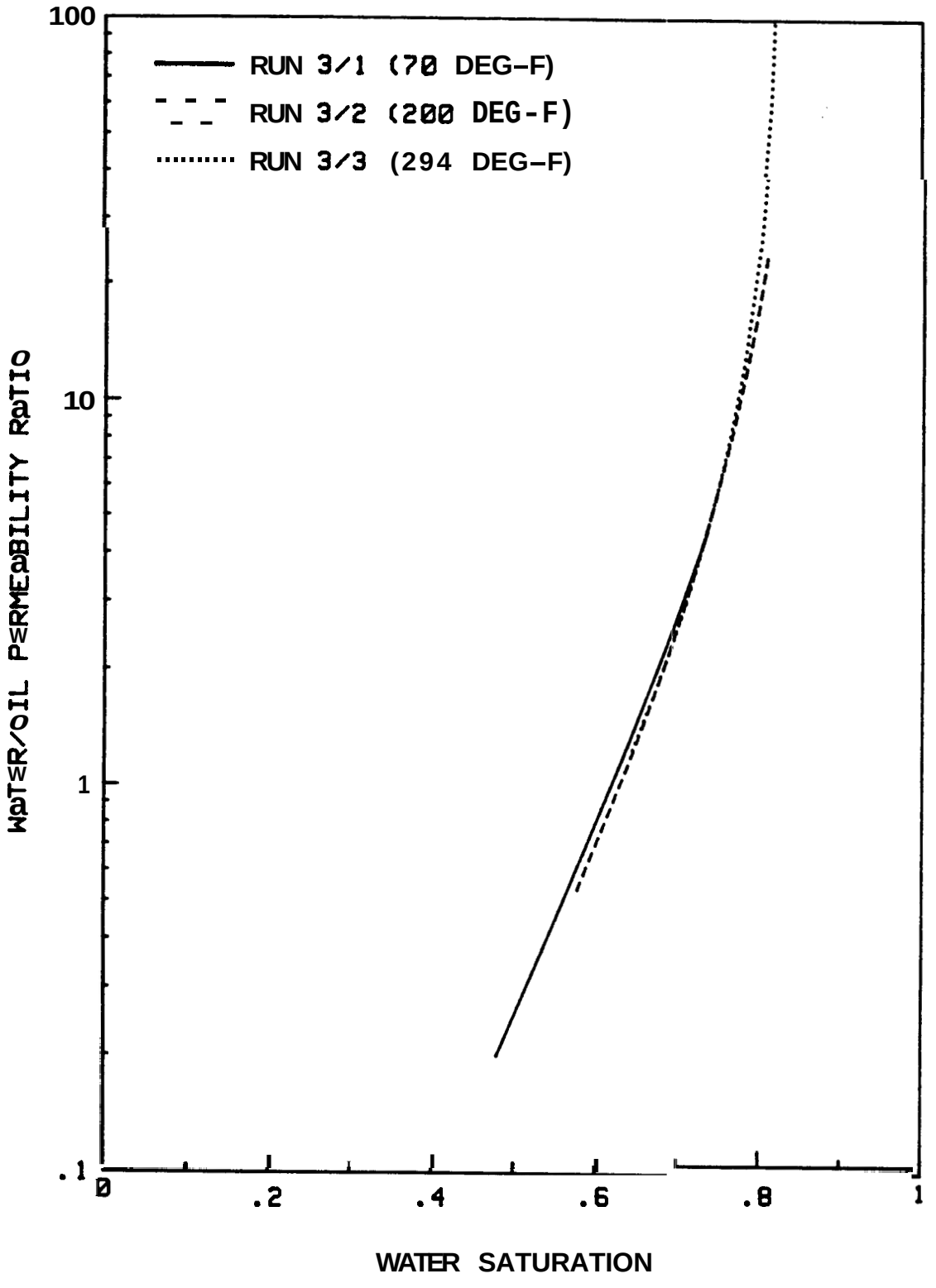

Fig. 5.9 Elevated Temperature Relative Permeability Ratios for Core 3

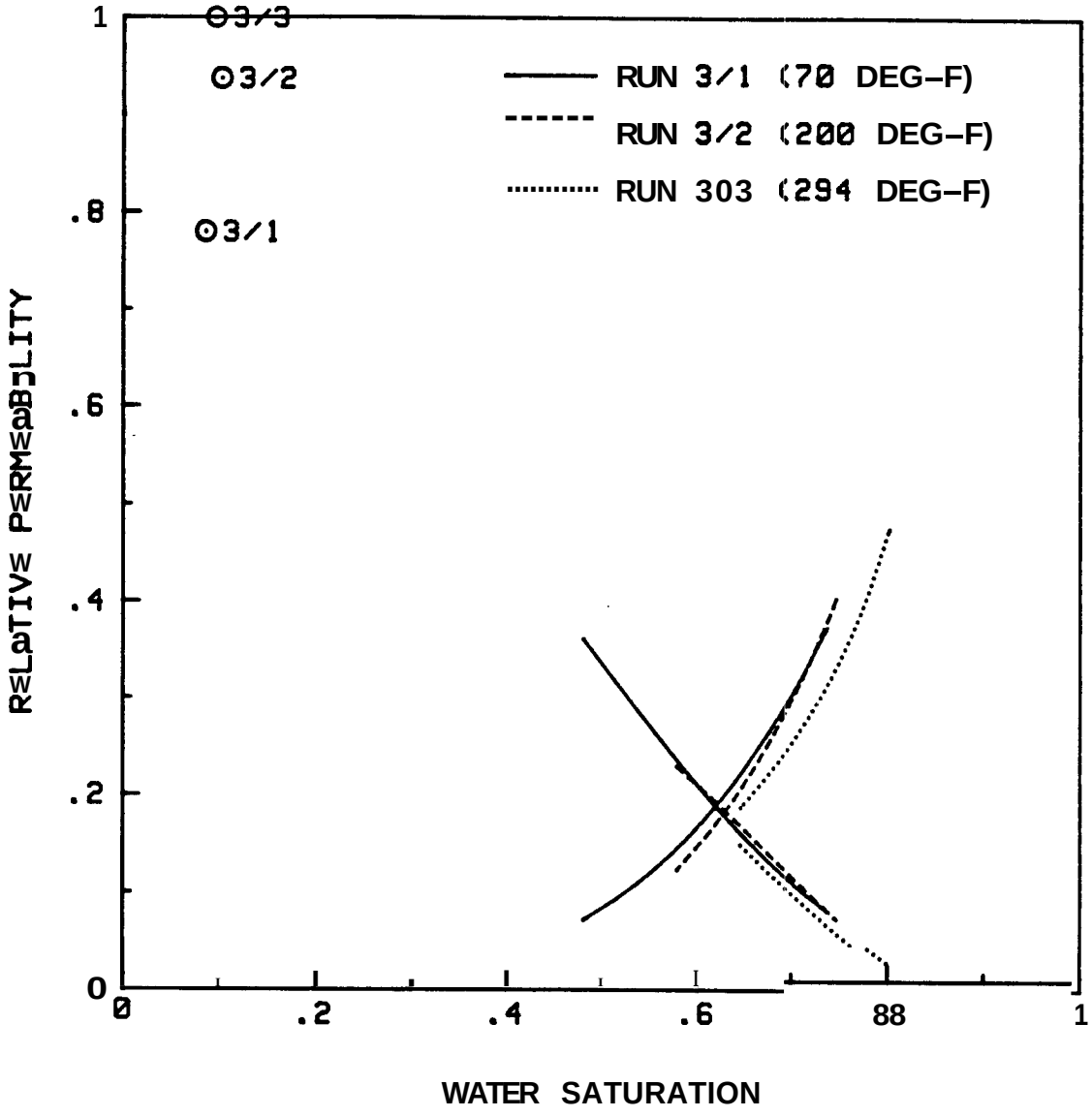

Fig. 5.10 Elevated Temperature Relative Permeabilities for Core 3

change is believed a result of experimental errors in the differential pressure measurements. Both the oil and water relative permeabilities curves lie below those at room temperature and at 200°F. Both are low by almost exactly the same ratio. Post-breakthrough differential pressures for this run were 0.6 to 1.0 psi. At these low differential pressures, transducer accuracy is reduced. Also, small capillary effects at the entrance to the pressure taps could cause the differential pressures to be inaccurate. The stainless steel retaining screen, which is between the tap entrance and the sand pack, aggravates this problem. There was experimental evidence to support this conjecture. Run 3/2 at 200°F had two unexplained sudden jumps (plus and minus) in differential pressure of approximately 0.5 psi, probably caused by capillary effects. The small change in the 294°F curve is still within the range of experienced reproducibility. Also, the change is much smaller than reported by either Poston et al. (1970) or Weinbrandt et al. (1975).

Figures 5.11 and 5.12 show the single high-temperature run made on Core 4. The 292°F run is shifted slightly to the right of the room temperature run in terms of both relative permeability ratio and individual relative permeabilities. Runs on Core 4 were terminated because of a suspected slow leak in confining pressure. This may have caused the small shift in the curves.

The reproducibility of the relative permeability ratios at elevated temperatures was evidence that viscosity ratios had been correctly determined. Incorrect viscosity ratios would have caused the relative permeability ratio curves to show a constant vertical displacement (constant multiplier effect on a logarithmic scale). This did not

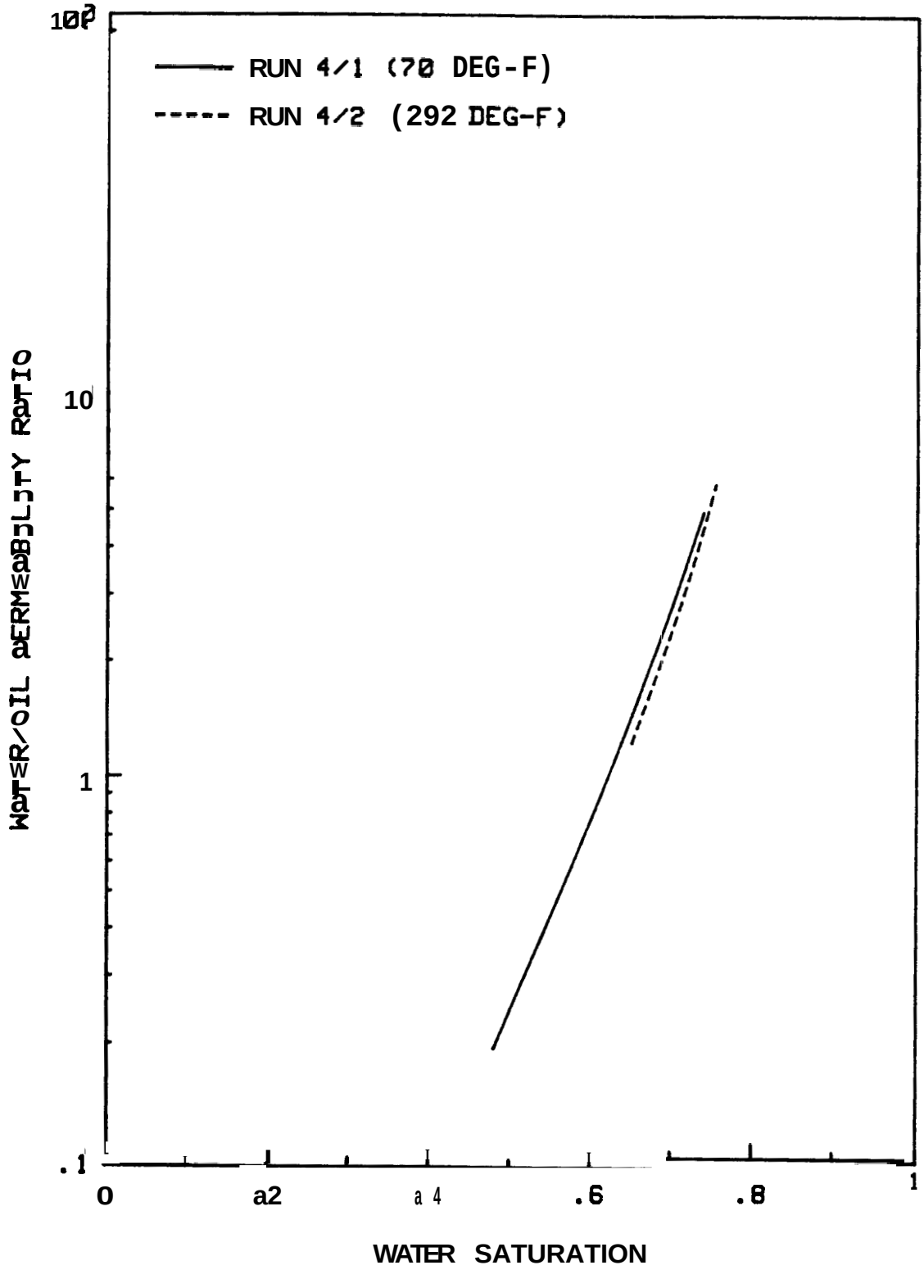

Fig. 5.11 Elevated Temperature Relative Permeability Ratios for Core *4*

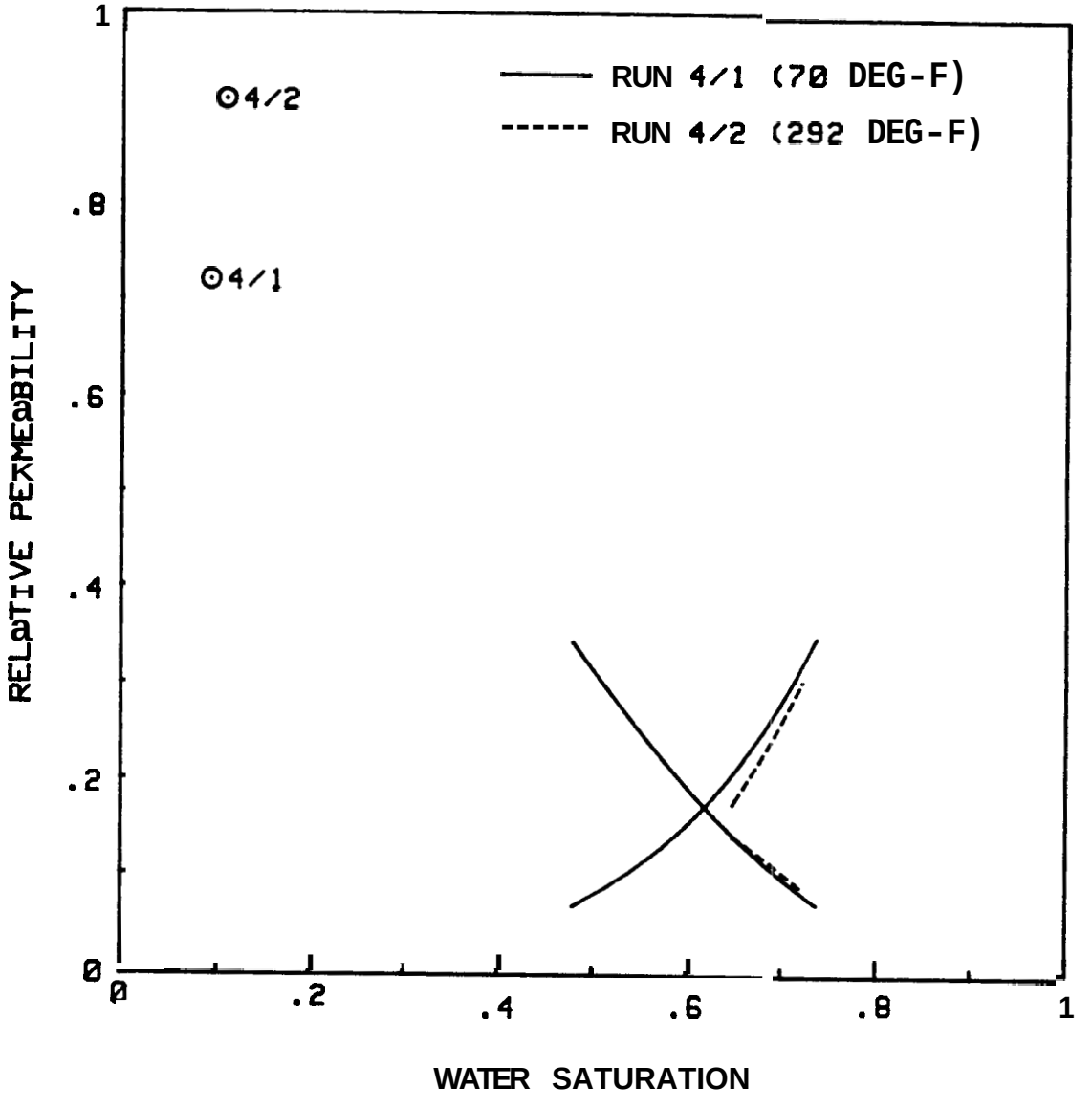

Fig. 5.12 Elevated Temperature Relative Permeabilities for Core *4*

occur. At elevated temperatures, the produced oil appeared milky white instead of the usual clear color. The viscosity of this milky oil was re-measured to determine if dissolved water or emulsification had caused a change in properties. The viscosity was found to be identical to that of the injected oil at all measured temperatures (up to 175°F). The milkiness was believed to be due to minute amounts of water dissolved in the oil at high temperatures that precipitated when the oil was cooled to room temperature. The milkiness disappeared when the oil was reheated during the viscosity measurements.

For all three cores, the oil relative permeability at irreducible water saturation increased substantially with temperature, starting from roughly 0.8 at room temperature and increasing to essentially unity at 300°F. Runs were made on a fourth unconsolidated sand pack (Core 5) with a pressure tap inserted approximately 3 in. from the core outlet to attempt to determine the cause of this effect. In a room temperature oil displacement run, the additional end-effect pressure drop was found to be only 1.3 psi, less than 2% of the total pressure drop of 68 psi. Exclusion of the additional pressure drop changed the oil relative permeability at irreducible water saturation from 0.837 to 0.853. The same determination was made after heating the core to 295°F. At this temperature, the end-effect pressure drop was approximately 0.2 psi, approximately 4% of the total pressure drop of 4.85 psi. As with other runs, oil permeability at irreducible water saturation was essentially equal to the absolute permeability. A discussion of possible causes for changes in oil permeabilities at irreducible water saturation is given in Section 6.

5.3 Consolidated Core

Prior to performing relative permeability runs on the Berea core, absolute permeability to water was measured. At room temperature, absolute permeability was stable (over several pore volumes injected) at 310 md. At 199°F, however, permeability decreased to 193 md. After cooling, room temperature absolute permeability was re-measured at 220 md. In spite of the use of salt water, a permanent change in absolute permeability appeared to have occurred, either due to increased temperature, or perhaps simply due to stopping and re-starting injection (injection was not re-started prior to raising the temperature). Because the change in permeability appeared permanent, it was believed that relative permeability measurements could now be made on a core with a stable absolute permeability.

Because of the nature of Berea relative permeabilities, use of the 30 cp. oil resulted in nearly piston-like displacement by both water and oil. Thus, only end-point relative permeabilities and saturations could be measured. Also, because a confining pressure leak developed at 300°F, temperature comparisons were made only to 200°F. The "room temperature" run was made at 97°F to keep the pressure drop across the core at an acceptable level with a reasonable injection rate (by reducing oil viscosity). Results of the runs are summarized in Table 5.2 Because displacement was very piston-like, good residual oil saturation values could be determined in these experiments. After only 4-5 pore volumes of water injected, no detectable oil was produced.

Table 5.2 End-Point Relative Permeabilities and Saturations -- Berea Core

Temperature (°F)	Irreducible Water Saturation (%)	Residual Oil Saturation (%)	Oil Relative Permeability at Irreducible Water Saturation	Water Relative Permeability at Residual Oil Saturation
97	32.3	38.0	0.943	0.117
199	32.6	37.1	0.982	0.105

These results confirm the lack of temperature effects observed for unconsolidated sands. Even though relative permeability curves could not be measured, there were essentially no changes in either residual saturations or end-point relative permeabilities with temperature.

The temperature effect on oil relative permeability at irreducible water saturation for the Berea core was reduced, compared to the unconsolidated sands. However, oil permeability at irreducible saturation for the Berea core still increased during the time oil injection was halted, as with the unconsolidated sands. At 97°F, oil permeability at irreducible water saturation rose from 0.869 to 0.943, while at 197°F, the change was from 0.960 to 0.982.

The next section compares the results of this study with those of previous researchers, and attempts to explain why temperature effects may have been observed in their studies.

6. DISCUSSION

The absence of temperature effects on relative permeabilities found in this study is contrary to nearly all reported findings in the literature. Although it is impossible to explain adequately why previous researchers found temperature effects, it is possible to speculate why, based on some of the findings of this study.

Table 6.1 presents a summary of reported elevated temperature dynamic displacement relative permeability measurements. The physical characteristics of cores and fluids are presented, as well as values for the Rapoport and Leas (1953) scaling coefficient ($Lv\mu_w$) and the Peters and Flock (1981) viscous instability number, I_{sc}, (based on a wettability number, C*, of 302.5). The Abrams (1975) modified capillary number was also estimated for all reported experiments. This number was found to vary only from $1x10^{-6}$ to $6x10^{-6}$, except for Weinbrandt et al. (1975), who ran experiments with a modified capillary number as high as $4x10^{-5}$. These values are below those where significant effects on residual oil saturation would be expected.

The most obvious difference between this study and others in Table 6.1 is oil viscosity. Corresponding to the lower oil viscosity used in this study, lower values were found for the Peters and Flock viscous instability number.

Table 6.1 Summary of Dynamic Displacement Relative Permeability Measurements Reported in the Literature

	Sand	Perm. (darcies)	Length (cm)	Diameter (cm)	Oil Visc. @ Room T (cp)	Max. Temp. (°F)	Flux Velocfty (cm/min)	$L v \mu_w$ (cm^2-cp/sec)	I_{sc}
Edmondson (1965)-white oils	Berea	*0.5*	23-66	4.1-5.1	35-200	500	.52	1-12	20-87.000
-crude oils					80-3000	300	.34-.52	2-22	23-6,400
Poston et al. (1970)	Unconsol.	15	84	5.4	80-600	280	.87	15-67	57-28,000
Davidson (1969)	Unconsol.	5.9	91	8.0	*200*	*540*	?	>10	>14-443
Welnbrsndt et al. (1972)	Boise	0.8-2.6	3.3-5.5	2.5	200	175	1.4-5.3	6-24	880-56,000
Sufi et al. (1982)	Unconsol.	5.3	18	2.5	*200*	150	1.3	10-23	44-440
This study	Unconsol.	7.0	51	5.0	30	300	1.0	9-50	10-200

Sufi et al. (1982) reported the onset of viscous instabilities at a viscous instability number equal to approximately 110. This is different from the theoretical number of 13.56 reported by Peters and Flock, however, a different wettability number may apply to the system studied by Sufi et al. The highest value of I_{sc} achieved in the runs reported in Section 5 was approximately 200, while runs made by Edmondson (1965), Poston et al. (1970), and Weinbrandt et al. (1975) had viscous instability numbers as high as 87,000. Davidson (1969) did not explicitly report flowrates, although it was implied that rates were used that were just high enough to exceed a Rapoport and Leas scaling coefficient of 10 cm^2-cp/min. This would imply that the viscous instability numbers in Davidson's experiments were below 450.

In Section 2, it was discussed that the Peters and Flock criteria may be too restrictive in judging the effects of viscous instabilities on relative permeability measurements. Some results from this study

appear to confirm this hypothesis. A case was made in Section 4 that the "inferred" breakthrough point may be a more representative breakthrough value than true water breakthrough, because of the trend of the post-breakthrough data. At room temperature, where viscous fingering should be the most pronounced, true water breakthrough was usually well before inferred breakthrough (especially in Cores 3 and 4). At high temperatures, true and inferred breakthroughs were much closer together, suggesting a reduction in viscous fingering. Relative permeability curves, however, were unaffected by temperature. This may explain why in Davidson's runs, relative permeability ratios only experienced temperature effects at low water saturations -- those measured just after breakthrough. This argument: may not apply to runs by Edmondson, Poston et al., and Weinbrandt et al., which achieved very high values of the Peters and Flock viscous instability number.

Temperature effects on irreducible water saturation were reported by both Poston et al. and Weinbrandt et al. Capillary end-effects may have at least been partially responsible for Weinbrandt et al.'s results, although there should have been minimal effects with Poston et al.'s much longer cores. Difficulties may have arisen in maintaining good material balances in these two studies. Weinbrandt et al. used cores with pore volumes on the order of 7 cc. Accurate material balance measurements were likely quite difficult. Also, the resulting relative permeability ratio curves were nearly parallel, appearing to have merely been shifted toward higher water saturations at elevated temperatures. Material balance saturation errors could account for this shift.

Poston et al.'s result of increasing irreducible water saturation with successive runs was not reproduced in this study. Errors in their

material balance would also explain this result. Poston et al used graduated cylinders to measure produced volumes. At the ends of displacement runs, small amounts of oil or water in each cylinder might be difficult to measure accurately. The use of a separator for the runs in the current study eliminated this problem and may account for the reproducibility of irreducible water saturation determinations.

As discussed in Section 2, Lo and Mungan's (1973) apparent increase in irreducible water saturation may at least partially be explained by core end-effects. A correlation between oil viscosity and irreducible water saturation is apparent. However, oil relative permeability curves in Lo and Mungan's study, like Weinbrandt et al.'s, tended to be parallel and shifted toward higher water saturations at elevated temperatures. That is, the increase in irreducible water saturation with temperature was almost exactly matched by a decrease in residual oil saturation. This type of behavior is suspicious. Also, different oils produced not only different end-point saturations, but differently shaped relative permeability curves as well. Teflon, especially, should not have been strongly affected by the different oils because of Teflon's distinct and constant wettability characteristics. Differences in interfacial tension were also not significant enough to explain the differences between oils. It is not known why Lo and Mungan should have experienced different results with different oils.

The absence of temperature effects found in this study is strong evidence that the results of previous researchers were not representative of actual flow characteristics. Although definite reasons for this are not obtainable, it does suggest the necessity of careful consideration of laboratory-scale phenomena.

The only temperature effect observed in this study was an apparent increase in oil relative permeabilities at irreducible water saturation. This result was, at first, believed to be related to end-effects. However, runs using the internal pressure tap reported in Section 5 indicated that this is not the case. The end-effect pressure drop was insignificant at both room temperature and near 300°F.

An interesting phenomenon noted from the runs suggests a possible explanation for the end-point change with temperature. At the end of each oil displacement run (to establish irreducible water saturation), the apparatus was shut down while the effluent separator was calibrated. This usually required about an hour. Oil injection was then re-initiated and the flowrate and differential pressure allowed to stabilize before switching to water injection. Figure 6.1 compares oil relative permeabilities at the end of the oil displacement runs (beginning of arrow) to oil permeabilities just prior to starting water injection (end of arrow). For nearly every run, oil relative permeability at irreducible water saturation increased during the time oil injection was halted. The amount of increase was greater at elevated temperatures, particularly around 300°F. Oil relative permeabilities at the end of oil displacement at 300°F were not much greater than for the room temperature runs. However, upon re-starting injection, oil relative permeabilities at 300°F increased to essentially 1.0. At room temperature, oil relative permeabilities remained near 0.8. It is interesting that the oil relative permeabilities at irreducible water saturation reported by both Amaefule and Handy (1982) for Berea cores, and Leverett (1939) for unconsolidated cores, were also around 0.8 (they too graphed curves using absolute permeability as a base).

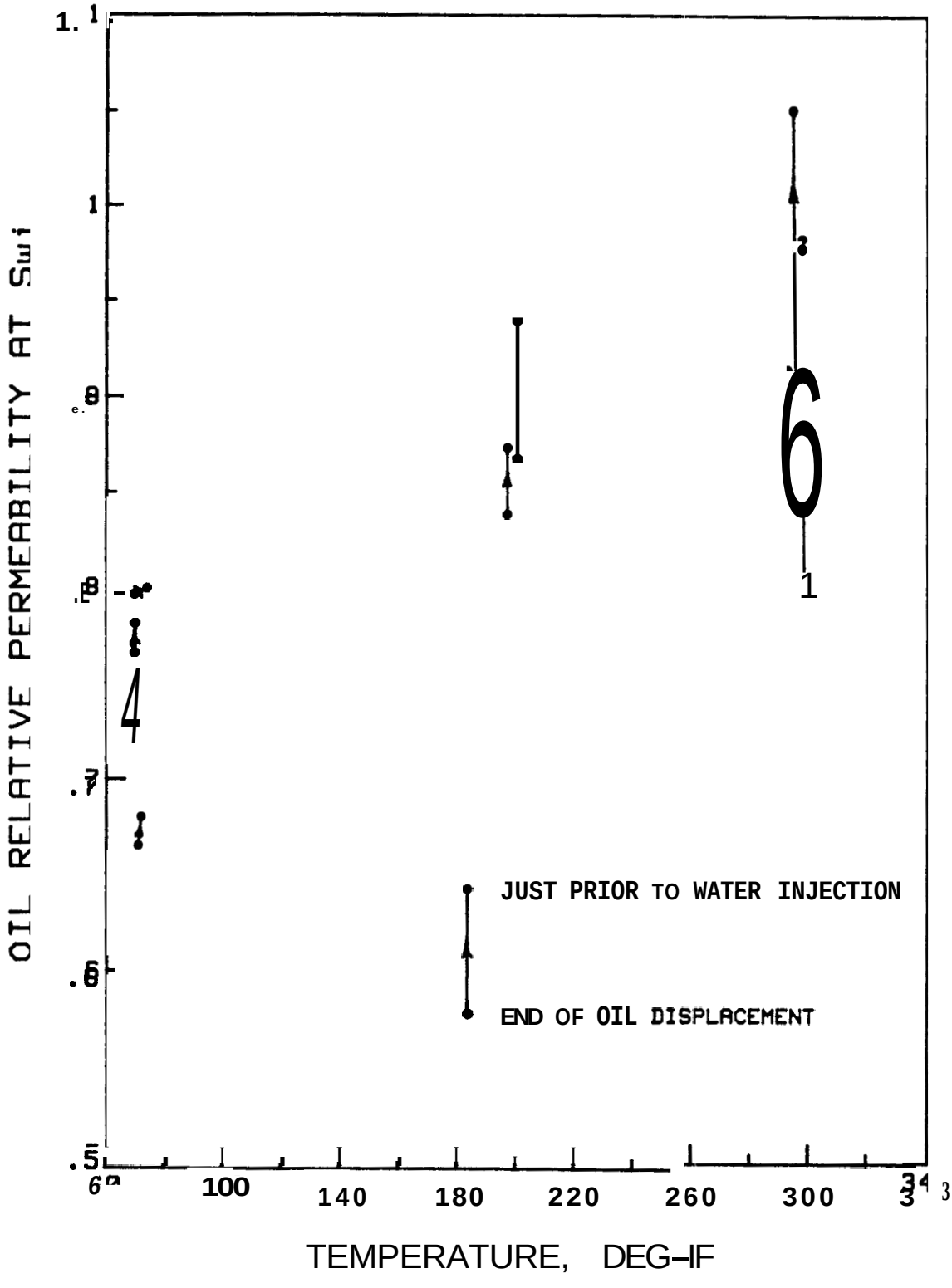

Fig. 6.1 Oil Relative Permeabilities at Irreducible Water Saturation -- Showing Changes from End of Oil Displacement to Initiation of Water Displacement

This phenomenon may be related to fluid re-distribution within the core when flowing pressure gradients are removed. One possible process is the movement of water from bypassed pores to more stable pendular ring locations around sand grain contacts. Reductions in fluid viscosities and interfacial tension with temperature may enhance this process. Water located in pendular rings and smaller pores would reduce oil permeability the least.

Another observation lends some credence to the hypothesis of fluid re-distribution. At the end of oil displacement runs (around two pore volumes injected), small water droplets could still be seen being produced periodically. However, when oil injection was re-started, no water droplets were observed. Similar effects occurred at the end of water displacement runs. An argument against this hypothesis is that even after sitting for as long as 20 hours, room temperature relative permeabilites at irreducible water saturation did not increase any more than they had when sitting for only one hour.

Owens and Archer (1971), in their study of wettability effects on relative permeabilities, presented data that showed effective oil permeability at irreducible water saturation increasing with decreasing contact angle. Between a contact angle of 47" and 0", the effective oil permeability of a consolidated sandstone increased by approximately 20%. At 0° contact angle, the effective oil permeability was 98% of the air permeability. Owens and Archer attributed this behavior to changes in the initial distribution of the irreducible water saturation.

It is believed that this may be correct. Reductions in interfacial tension and contact angles with temperature, may cause changes in the location of the initially established irreducible water saturation

(again, perhaps the difference is between bypassed pores and pendular rings). This effect, however, seems to disappear when water displaces oil from the core. Relative permeability curves at all temperatures are nearly identical in spite of the 20% change in oil permeabilities at irreducible water saturation.

These results point to the necessity of calculating the curves using absolute permeability as a base, instead of using oil permeability at irreducible water saturation. Figures 6.2 and 6.3 show the elevated temperature relative permeabilities for Cores 2 and 3 calculated using oil permeability at irreducible water saturation as a base. Although essentially no temperature effect was observed when relative permeabilities were calculated based on absolute permeability (Figs. 5.8 and 5.10), distinct temperature effects are indicated in Figs. 6.2 and 6.3. This effect is to reduce both apparent oil and water permeabilities at elevated temperatures -- the opposite to the effect observed by both Poston et al. (1970) and Weinbrandt et al. (1972).

An attempt was made to determine if the change in oil permeability at irreducible water saturation was evident in the displacement data reported in Poston's PhD dissertation (1967). Oil permeability at irreducible water saturation was found to vary much more than the data from this study. No discernable pattern with temperature was observed.

Changes in oil permeabilities at irreducible water saturation with temperature are still unexplained. However, this effect is not reflected in either residual saturations or water-oil relative permeability curves. It is possible that elevated temperatures may have more of an effect on drainage processes than for imbibition. This might

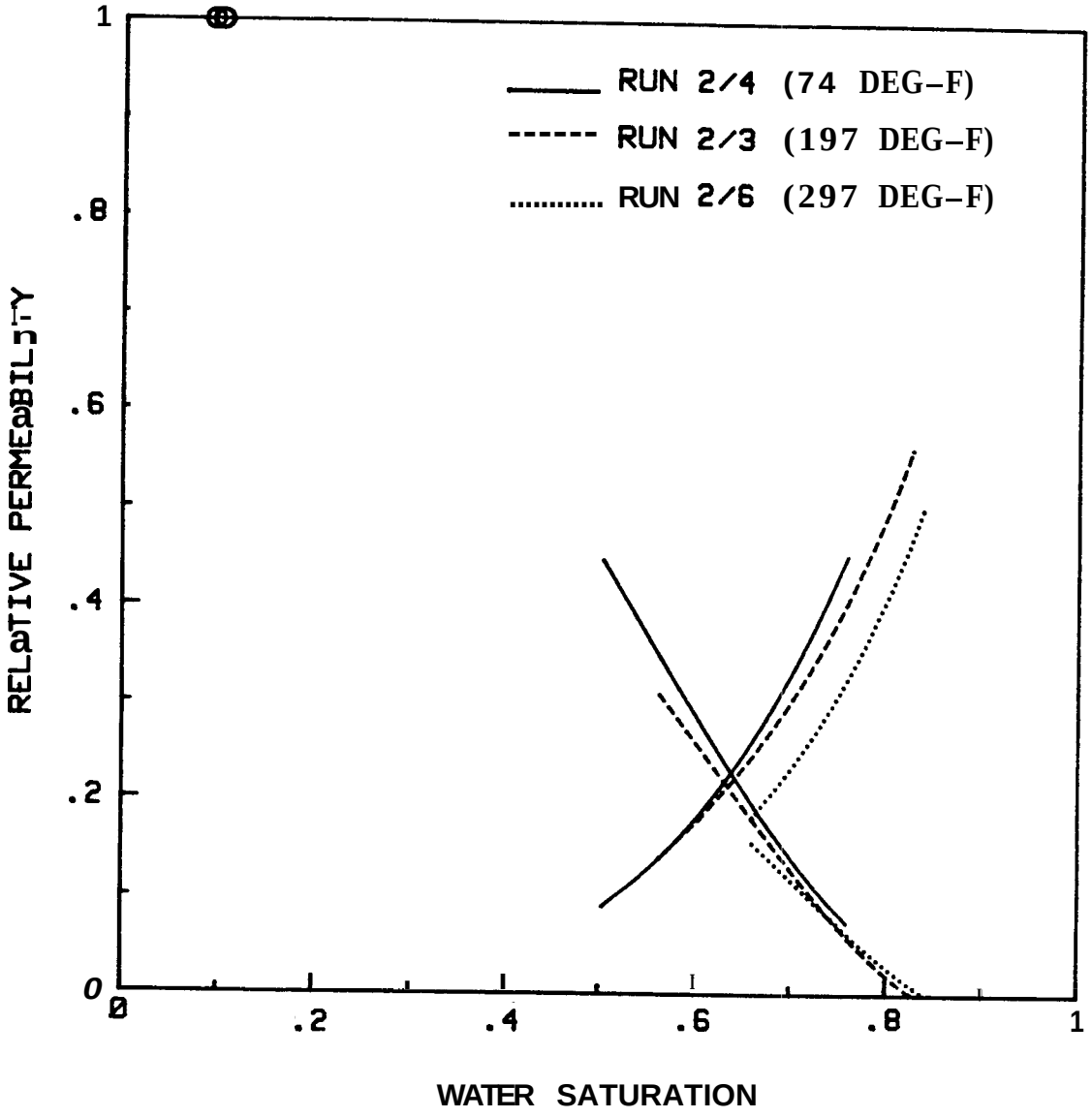

Fig. 6.2 Elevated Temperature Relative Permeabilities for Core 2 — Calculated Relative to **Oil** Permeability at Irreducible Water Saturation

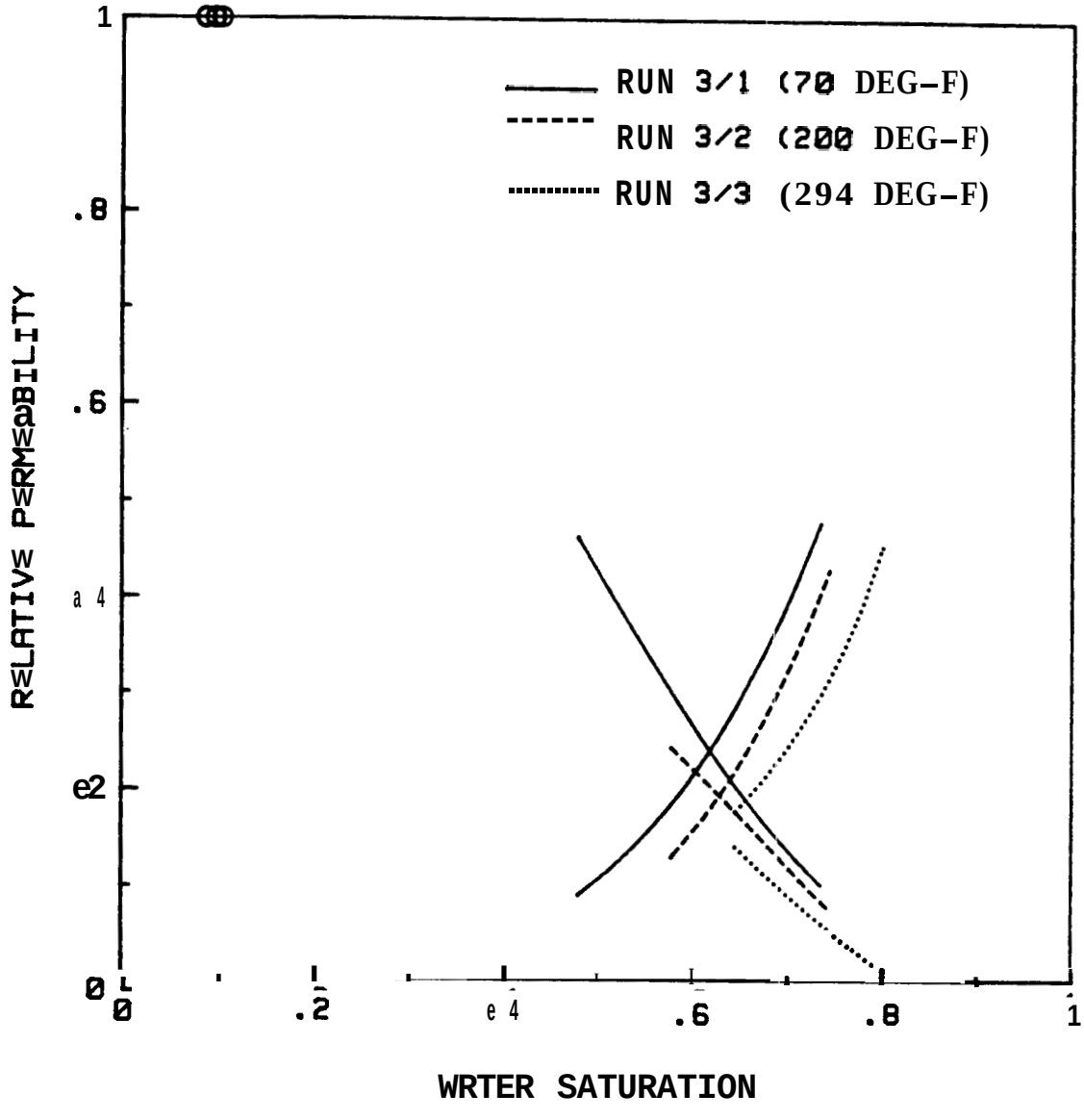

Fig. *6.3* Elevated Temperature Relative Permeabilities for Core 3 — Calculated Relative to Oil Permeability at Irreducible Water Saturation

also explain the capillary pressure behavior reported by Sinnokrot et al. (1971).

The temperature effect on oil permeabilities at irreducible water saturation might be a factor in the productivity increases seen from steam stimulation. However, generally, the end-point oil permeability is of limited practical significance.

7. CONCLUSIONS AND KECOMMENDATIONS

The following conclusions and recommendations are made from this study.

Conclusions

1. Distilled water–white oil relative permeabilities and residual saturations in pure unconsolidated quartz sands are unaffected by temperature to 300°F, for relative permeabilities referenced to single–phase absolute permeability.

2. End–point relative permeabilities and saturations in Berea cores were unaffected by temperature to 200°F.

3. A temperature effect was noted on oil relative permeability at irreducible water saturation. However, the effect was believed to be related to fluid re–distribution. This parameter is of minor importance in predicting two–phase flow behavior.

4. Previous results for unconsolidated sands are believed to have been affected by viscous instabilities, end–effects, and material balance measurement difficulties. However, since there is no way to evalute such problems in others' research, this conclusion is highly speculative.

5. This study does not prove that temperature effects do not exist with real reservoir fluids and rocks. However, it does imply that such effects are probably not related to fundamental flow properties. Rather, changes in such factors as clay interactions, pore structure, etc., would need to be investigated to explain changes in these more complex systems.

6. Comparing the results of this study with previous studies suggests that care must be taken to achieve accurate measurements of porous media flow behavior. Consideration of fundamental properties known

to govern flow through porous media suggest that in simple systems (such as used in this study), temperature should not affect relative permeabilities. Use of appropriate fluids, core dimensions, measurement techniques, etc. have proven this to be true.

Recommendations

1. Measurement of relative permeabilities using high viscosity oils should be attempted with the apparatus used in this study. This would provide further insight into whether previous studies (most used an oil with 200 cp viscosity at room temperature) were indeed affected by viscous instabilities. Also, these measurements would indicate whether such heavy oils can be used with accuracy. Use of higher viscosity oils will be necessary to measure relative permeability curves in consolidated cores.

2. Runs at temperatures above 300°F should also be attempted. Most geothermal reservoirs and thermal oil recovery processes operate above *400°F.* Fluid-rock interactions may be more pronounced at these temperatures. A revision of the effluent measurement system will be required to operate at these high temperatures.

3. Temperature effects on capillary pressures have not been explained. This should be investigated further, initially using cores and fluids similar to those used in this study. In Section *6*, it was pointed out that capillary pressure may be more affected by temperature than relative permeabilities.

4. Because of the differences in capillary pressure behavior between limestone and sandstone, high temperature relative permeability runs should be made with limestone materials. This may not be a simple process, because limestone will likely be more susceptible to dissolution at high temperature than would be expected with silica sands.

5. Investigation of the measurement of relative permeabilities with smaller, short cores should be made to determine procedures, conditions, etc. where short core data can be made to match the behavior of larger, longer cores, such as used in this study. Only in this way, can assurances be achieved that measurements on real reservoir materials (usually limited to small cores) are representative of reservoir flow behavior.

6. Work should proceed eventually to the measurement of relative permeabilities for real reservoir rocks and fluids. The use of crude oils with distilled water or synthetic brines and pure quartz sand might be a reasonable first step. Eventually, attempts should be made to prove whether relative permeabilities in natural systems are affected by temperature, whether gas-oil or boiling brine systems.

7. The behavior of gas-liquid systems at elevated temperatures would be of interest to geothermal energy production. Of particular interest might be Klinkenberg gas-slippage effects mentioned by Davidson (1969), or investigation of non-Darcy two-phase flow.

NOMENCLATURE

A = cross-sectional area, cm^2

calib = separator calibration, cc/cm

C^* = wettability number, dimensionless

cSt = kinematic viscosity, cSt

dp/dx = pressure gradient, atm/cm

d = core diameter, cm

D = downstream dead volume, cc

ΣDv = cumulative volume of displacing fluid produced from separator, cc

k = absolute permeability, darcies

k_i = effective permeability to phase i, darcies

k_{ro} = relative permeability to oil, dimensionless

k_{rw} = relative permeability to water, dimensionless

f_d = fractional flow of displaced phase, dimensionless

f_o = fractional flow of oil, dimensionless

f_w = fractional flow of water, dimensionless

h_d = initial dynamic separator level, cm

h_o = level of outlet tube in separator, cm

Δh = difference between initial static and dynamic separator levels, cm

I_r = relative injectivity, $(q/\Delta p)/(q/\Delta p)_{initial}$

I_{sc} = viscous instability number, dimensionless

L = length of core, cm

L_m = measured length of traveling end plug extending from end plug guide, cm

N_c = capillary number, dimensionless

N_p = cumulative pore volumes of oil recovered, dimensionless

Δp = differential pressure across core, psi

p_c = capillary pressure, dynes/cm

Pv = core pore volume, cc

q = total volumetric flowrate, cc/min

q_i = volumetric flowrate of phase i, cc/sec

r = radius, cm

Sep = cumulative separator (produced) volume, cc

$\bar{S}_{o1}$ = average oil saturation before temperature change, dimensionless

$\bar{S}_{o2}$ = average oil saturation after temperature change, dimensionless

$\bar{S}_{w2}$ = average water saturation after temperature change, dimensionless

S_{w2} = water saturation at core outlet, dimensionless

$\bar{S}_w$ = average water saturation, dimensionless

S_{wi} = irreducible water saturation, dimensionless

$\bar{S}_{wf}$ = average water saturation after oil displacement, dimensionless

t = time, min

T = temperature, °F

U = upstream dead volume, cc

v = flux velocity (q/A), cm/min

v_b = average separator bubble velocity, cm/min

V_e = volume of oil expanded from core by heating, cc

V_p = total displaced fluid produced, cc

μ_i = viscosity of phase i, cp

μ_o = oil viscosity, cp

μ_w = water viscosity, cp

η = ratio of 2% NaCl solution viscosity to distilled water viscosity, dimensionless

ρ_{wc} = water density at core temperature, g/cc

ρ_{oc} = oil density at core temperature, g/cc

ρ_{we} = water density at effluent temperature, g/cc

ρ_{oe} = oil density at effluent temperature, g/cc

ρ_{oc1} = oil density before core heating, g/cc

ρ_{oc2} = oil density after core heating, g/cc

σ = interfacial tension, dynes/cm

θ = contact angle, degrees

REFERENCES

Abrams, A.: "The Influence of Fluid Viscosity, Interfacial Tension, and Flow Velocity on Residual Oil Saturation Left by Waterflood", Soc. Pet. Eng. J. (October 1975) 437.

Amaefule, J. O. and Handy, L. L.: "The Effect of Interfacial Tensions on Relative Oil/Water Relative Permeabilities of Consolidated Porous Media", Soc. Pet. Eng. J. (June 1982) 371.

Amyx, J. W., Bass, D. M., Jr., and Whiting, R. L.: Petroleum Reservoir Engineering - Physical Properties", McGraw-Hill Book Co., New York City (1960).

ASME Steam Tables, Fourth Edition, American Society of Mechanical Engineers, New York City (1979).

Barnea, G. M.: "Calculator Program Finds Petroleum. Fraction Viscosities Over Wide Temperature Range", Oil & Gas J. (May 10, 1982) 148.

Baker, P. E.: "Discussion of Effect of Viscosity on Relative Permeability'", Trans., AIME (1960) 219, 404.

Brigham, W. E.: "Another Method to Calculate Relative Permeability -- And Some Far-Reaching Implications", course notes, Heriot-Watt U. (1979).

Buckley, S. E. and Leverett, M. C.: "Mechanism of Fluid Displacement in Sands", Trans., AIME (1942) 146, 107.

Cassé, F. J. and Ramey, H. J., Jr.: "The Effect of Temperature and Confining Pressure on Single-phase Flow in Consolidated Rocks", J. Pet. Tech. (August 1979) 1051.

Chu, P. S. Y. and Cameron, A.: "Compressibility and Thermal Expansion of Oils", J. Inst. Pet. (May 1963) 49, 140.

Counsil, J. R.: "Steam-Water Relative Permeability", PhD dissertation, Stanford U., Stanford, CA (1979).

Craig, F. F., Jr.: The Reservoir Engineering Aspects of Waterflooding, Monograph Series, SPE, Dallas (1971) 3.

Davidson, L. B.: "The Effect of Temperature on the Relative Permeability Ratio of Different Fluid Pairs in Two Phase System!;", J. Pet. Tech. (August 1969) 1037.

Dombrowski, H. S. and Brownell, L. E.: "Residual Equilibrium Saturation of Porous Media", Ind. and Eng. Chem. (June 1954) 46, No. 6, 1207.

Downie, J. and Crane, F. E.: "Effect of Viscosity on Relative Permeability", Soc. Pet. Eng. J. (June 1961) 59.

Edmondson, T. A.: "Effect of Temperature on Waterflooding", J. Can. Pet. Tech. (Oct.-Dec. 1965) 236.

Frick, T.C. (ed.): Petroleum Production Handbook, SPE (1962) 1.

Geffen, T. M., Owens, W. W., Parish, D. R., and Morse, R. A.: "Experimental Investigations of Factors Affecting Laboratory Relative Permeability Measurements", Trans., AIME (1951) 192, 99.

&bran, B. D., Brigham, W. E., and Ramey, H. J., Jr.: "Absolute Permeability as a Function of Confining Pressure, Pore Pressure and Temperature", paper SPE 10156 presented at the SPE 56th Annual Fall Technical Conference and Exhibition, San Antonio, Oct. 5–7, 1981.

Gobran, B. D.: "The Effects of Confining Pressure, Pore Pressure and Temperature on Absolute Permeability", PhD dissertation, Stanford U., Stanford, CA (1981).

Gupta, S. P. and Truchenski, S. P.: "Micellar Flooding - Compositional Effects on Oil Displacement", Soc. Pet. Eng. J. (April 1979) 116; Trans., AIME, 267.

Hadley, G. F., and Handy, L. L.: "A Theoretical and Experimental Study of the Steady State Capillary End Effect", paper SPE 707-G presented at the SPE 31st Annual Meeting, Los Angeles, Oct. 14–1.7, 1956.

Hossain, A. K. M. S.: "The Displacement of Oil From Unconsolidated Sands by High Temperature Fluid Injection", MS thesis, Texas A&M U., College Station, TX, (1965).

International Critical Tables, McGraw Hill Book Co., New York City (1927).

Jeffers, M. K., Jr.: "The Design and Construction of a Reservoir Conditioned Relative Permeameter", MS report, Stanford U., Stanford, CA (1981).

Jones, S. C. and Roszelle, W. O.: "Graphical Techniques for Determining Relative Permeability from Displacement Experiments", J. Pet. Tech. (May 1978) 807; Trans., AIME, 265.

Johnson, E. F., Bossler, D. P., and Naumann, V. O.: "Calculation of Relative Permeability from Displacement Experiments", Trans., AIME (1959) 216, 370.

Kyte, J. R. and Rapoport, L. A.; "Linear Waterflood Behavior and End Effects in Water-Wet Porous Medium, Trans., AIME (1958) 213, 423.

Lefebvre duPrey, E. J.: "Factors Affecting Liquid-Liquid Relative Permeabilities of a Consolidated Medium", Soc. Pet. Eng. J. (January 1973) 39.

Leverett, M. C.: "Flow of Oil-Water Mixtures Through Unconsolidated Sands", Trans., AIME (1939) 132, 149.

Lo, H. Y. and Mungan, N.: "Effect of Temperature on Water-Oil Relative Permeabilities in Oil-Wet and Water-Wet Systems", paper SPE 4505 presented at the SPE 48th Annual Meeting, Las Vegas, Sept. 30-Oct. 3, 1973.

Montgomery, E. F., III: "The Effect of Temperature Level on Displacement of Oil by Fluid Injection", MS thesis, Texas A&M U., College Station, TX (1966).

Odeh, A. S.: "Effect of Viscosity Ratio on Relative Permeability", Trans., AIME (1959) 216, 346.

Osoba, J. S., Richardson, J. G., Kerver, J. K., Hafford, J. A., and Blair, P. M.: "Laboratory Measurements of Relative Permeability", Trans., AIME (1951) 192, 47.

Owens, W. W. and Archer, D. L.: "The Effect of Rock Wettability on Oil-Water Relative Permeability Relationships", J. Pet,, Tech. (July 1971) 873.

Owens, W. W., Parrish, D. R., and Lamoreaux, W. E.:: "An Evaluation of a Gas Drive Method for Determining Relative Permeability Relationships", Trans., AIME (1956) 207, 275.

Paulsen, W. L. : "Review of Test Procedures", Proceedings: Workshop Toward an Oxygen Transfer Standard, U.S. Environmental Protection Agency Report EPA-600/9-78-021 (1979), 42.

Peters, E. J. and Flock, D. L.: "The Onset of Instability During Two-Phase Immiscible Displacement in Porous Media", Soc. Pet. Eng. J. (April 1981) 249; Trans., AIME, 271.

Poston, S. W., Ysrael, S., Hossain, A. K. M. S., Montgomery, E. F., III, and Ramey, H. J., Jr.: "The Effect of Temperature on Irreducible Water Saturation and Relative Permeability of Unconsolidated Sands", Soc. Pet. Eng. J. (June 1970) 171.

Poston, S. W.: "Effect of Temperature on Relative Permeability of Unconsolidated Sands", PhD dissertation, Texas A&M U., College Station, TX (1967).

Rapoport, L. A., and Leas, W. J.: "Properties of Linear Waterfloods", Trans., AIME (1953) 198, 139.

Richardson, J. G., Kerver, J. K., Hafford, J. A., and Osoba, J. S.: "Laboratory Determination of Relative Permeability", Trans., AIME (1952) 195, 187.

Richardson, J. G. : " The Calculation of Waterflood Recovery from Steady-State Relative Permeability Data", Trans. AIME (1957) 210, 373.

Sageev, A. : "The Design and Construction of an Absolute Permeameter to Measure the Effect of Elevated Temperature on the Absolute Permeability to Distilled Water of Unconsolidated Sand Cores", MS report, Stanford U., Stanford, CA (1980).

Sageev, A., Gobran, B. D., Brigham, W. E., and Ramey, H. J., Jr.: "The Effect of Temperature on the Absolute Permeability to Distilled Water of Unconsolidated Sand Cores", Proceedings, 6th Workshop on Geothermal Reservoir Engineering, Dec. 16-18, 1980, Stanford U., 297.

Sinnokrot, A. A., Ramey, H. J., Jr., and Marsden, S. S., Jr.: "Effect of Temperature Level upon Capillary Pressure Curves", Soc. Pet. Eng. J. (March 1971) 13.

Sufi, A. S., Ramey, H. J., Jr., and Brigham, W. E.: "Temperature Effects on Oil-Water Relative Permeabilities for Unconsolidated Sands", U.S. Department of Energy Report DOE/ET/12056-35 (December 1982).

Sufi, A. S., Ramey, H. J., Jr., and Brigham, W. E.: "Temperature Effects on Relative Permeabilities of Oil-Water Systems", paper SPE 11071 presented at the SPE 57th Annual Technical Conference and Exhibition, New Orleans, Sept. 26-29, 1982.

Sydansk, R. D.: "Discussion of the Effect of Temperature and Confining Pressure on Single-phase Flow in Consolidated Rock:;", J. Pet. Tech. (August 1980) 1329.

Welge, H. J.: "A Simplified Method for Computing Oil Recovery by Gas or Water Drive", Trans., AIME (1952) 195, 91.

Weinbrandt, R. M., Ramey, H. J., Jr., and Cassé, F. J.: "The Effect of Temperature on Relative and Absolute Permeability of Sandstones", Soc. Pet. Eng. J. (October 1975) 376.

Weinbrandt, R. M.: "The Effect of Temperature on Relative Permeability", PhD dissertation, Stanford U., Stanford, CA (1972).

Wright, W. A.: "An Improved Viscosity-Temperature Chart for Hydrocarbons", J. of Materials, JMLSA (March 1969) 4, No. 1, 19.

Ysrael, S.: "The Effect of Temperature on Relative Permeability of Unconsolidated Sand", MS thesis, Texas A&M U., College Station, TX (1965).

APPENDIX A - APPARATUS DETAILS

The following sections give detailed descriptions of the apparatus used for the dynamic displacement experiments.

A.1 Main Flow System

A schematic of the main flow system of the apparatus is shown in Fig. A.1. A photograph of the apparatus is presented in Fig. A.2. The core holder was mounted in a Napco Model 430 temperature-controlled air bath, capable of uniform temperature control of ±5°F to approximately 400°F. Coiled 1/8 in. 316-stainless steel tubing was used to heat injected fluids to air bath temperature prior to injection into the core. Approximately 40 ft of tubing was used for the water line and 30 ft for the oil line. Temperature measurements of injected fluid just upstream of the core confirmed that these lengths were sufficient. A 10 in. diameter fan at one end of the air bath provided air circulation.

A Valco Model 3P three-way valve was used to switch between oil and water injection. The valve was rated to 400 psig at 175°C (350°F). A handle extension provided valve control outside the air bath near the apparatus control panel.

Five Type J iron-constantan thermocouples were placed at various points in the air bath to measure bath temperature,, A sixth thermocouple was placed in the flowline downstream of a cooling heat exchanger, to be certain that effluent fluids were sufficiently near room temperature. Thermocouples were connected to a Leeds and Northrup Speedomax W 24-point temperature recorder as follows:

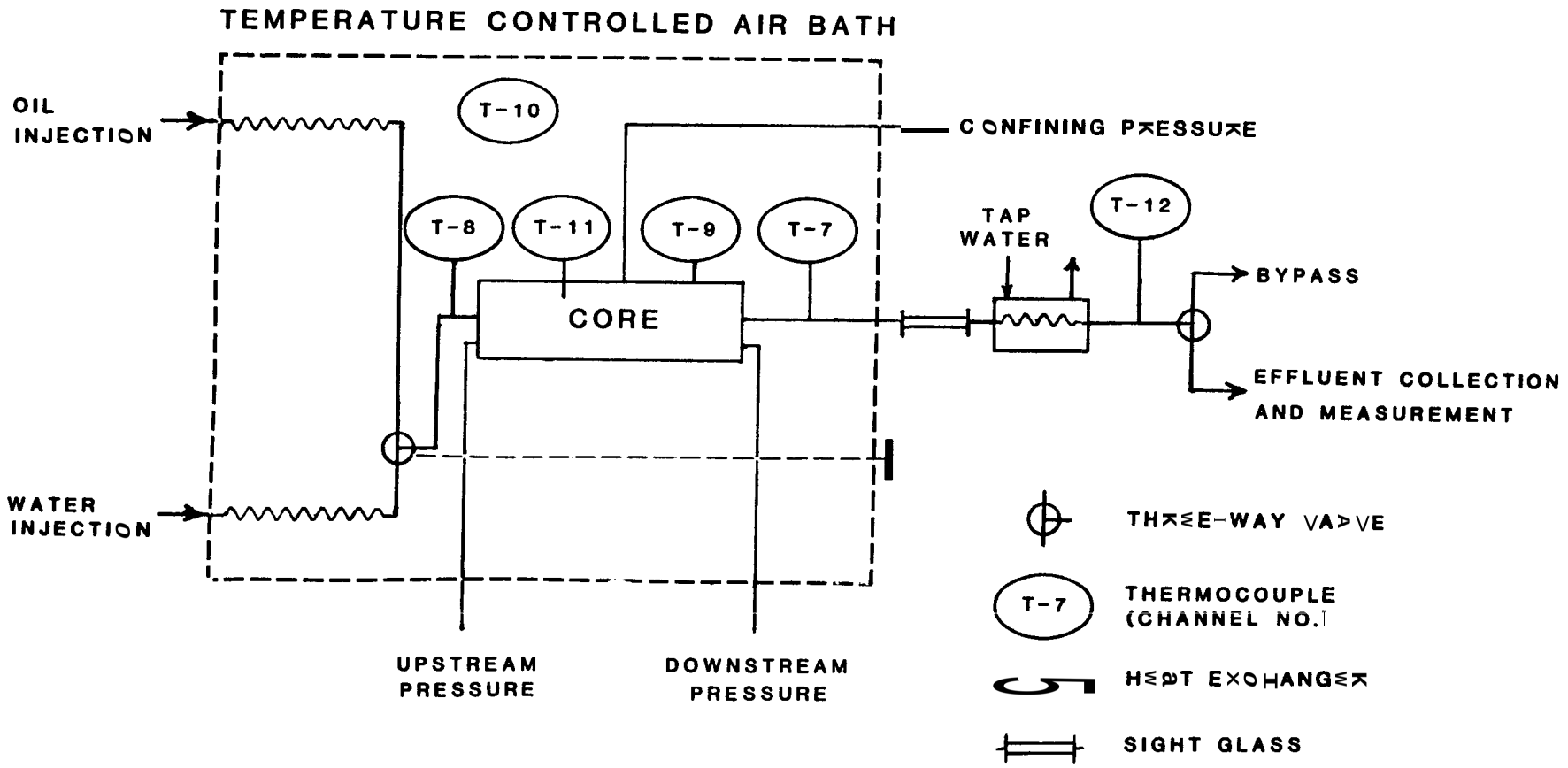

Fig. A.1 Schematic of the Main Flow System of Dynamic Displacement Relative Permeability Apparatus

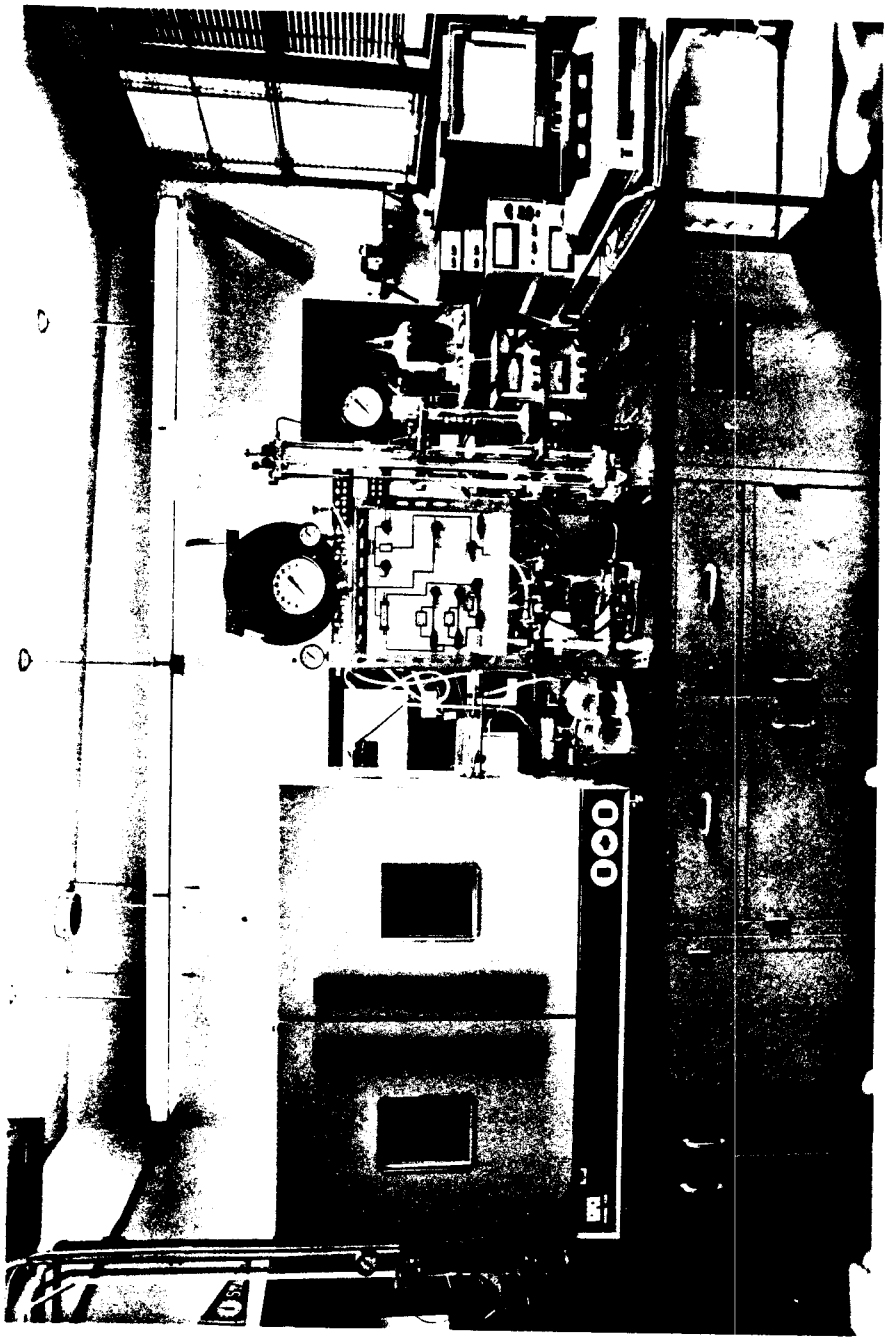

Fig. A.2 Photograph of Dynamic Displacement Relative Permeability Apparatus

Table A.1 - Thermocouple Locations

Location	Channel No.
Downstream flowline	7
Upstream flowline	8
Core holder outer sleeve	9
Air bath	10
Core holder inner sleeve	11
Downstream heat exchanger	12

The temperature recording system was calibrated by placing a thermometer and all thermocouples bundled together inside a hole in a piece of solid brass (to dampen temperature fluctuations from the air bath). Calibration indicated an accuracy of ±1.5°F.

Immediately outside the air bath, a 3-1/2 in. long, 0.10 in. I.D., 0.364 in. O.D. sight glass was used to monitor produced fluids and to visually determine breakthrough. The glass tube was mounted in 3/8 in. Swagelok fittings with Teflon ferrules. The sight glass was tested to 400 psig with nitrogen.

A cooling heat exchanger was placed downstream of the sight glass to cool produced fluids to near room temperature. The heat exchanger was made from 1/8 in. 316-stainless steel tubing inside approximately 1 ft of 1/4 in. 316-stainless steel tubing. Tap water was circulated in the annular space as a cooling medium.

A Whitey three-way switching ball valve was placed downstream of the heat exchanger to direct produced fluids either to the effluent measurement system or to a by-pass line. Placing the three-way valve in a central (shut-off) position also allowed core pressure to be contained.

A.2 Injection System

The injection system used for distilled water runs is shown in Fig. A.3. A single Milton Roy Model R-121A controlled-volume diaphragm pump was used to inject both water and oil. Water was injected directly from the pump, while oil was displaced by water from a 2000 cc pressure vessel in an alternate flow loop. Three-way valve connections were used to fill the vessel with oil by drawing water out on vacuum. Oil and water were both injected through 2 micron Nupro sintered stainless steel filters. For the runs utilizing salt water, the fluid injection arrangement was reversed. Oil was injected directly from the pump, while salt water was displaced by oil from a 1 gal, Teflon-lined, 304-stainless steel pressure vessel. Salt water was de-oxygenated by saturation with nitrogen and addition of sodium sulfite as an oxygen scavenger (see Appendix B.3) prior to being placed in the pressure vessel.

Injection rates were held approximately constant by using an excess flow loop with a 500 psig pressure relief valve. Injection rates were adjusted by a needle valve downstream of the pump. During a run, water flowed continuously through the relief valve. Thus, the needle valve regulated the fraction of water flowing to the core (or pressure vessel). The pump volume could be adjusted to keep excess flow to a minimum.

Since the pressure upstream of the needle valve was regulated at 500 psig, and the pressure drop across the core was always less than around 75 psi (much less at elevated temperature), the majority of the system pressure drop was across the needle valve and the 100 psig pressure regulator in the effluent measurement system. Thus, as the

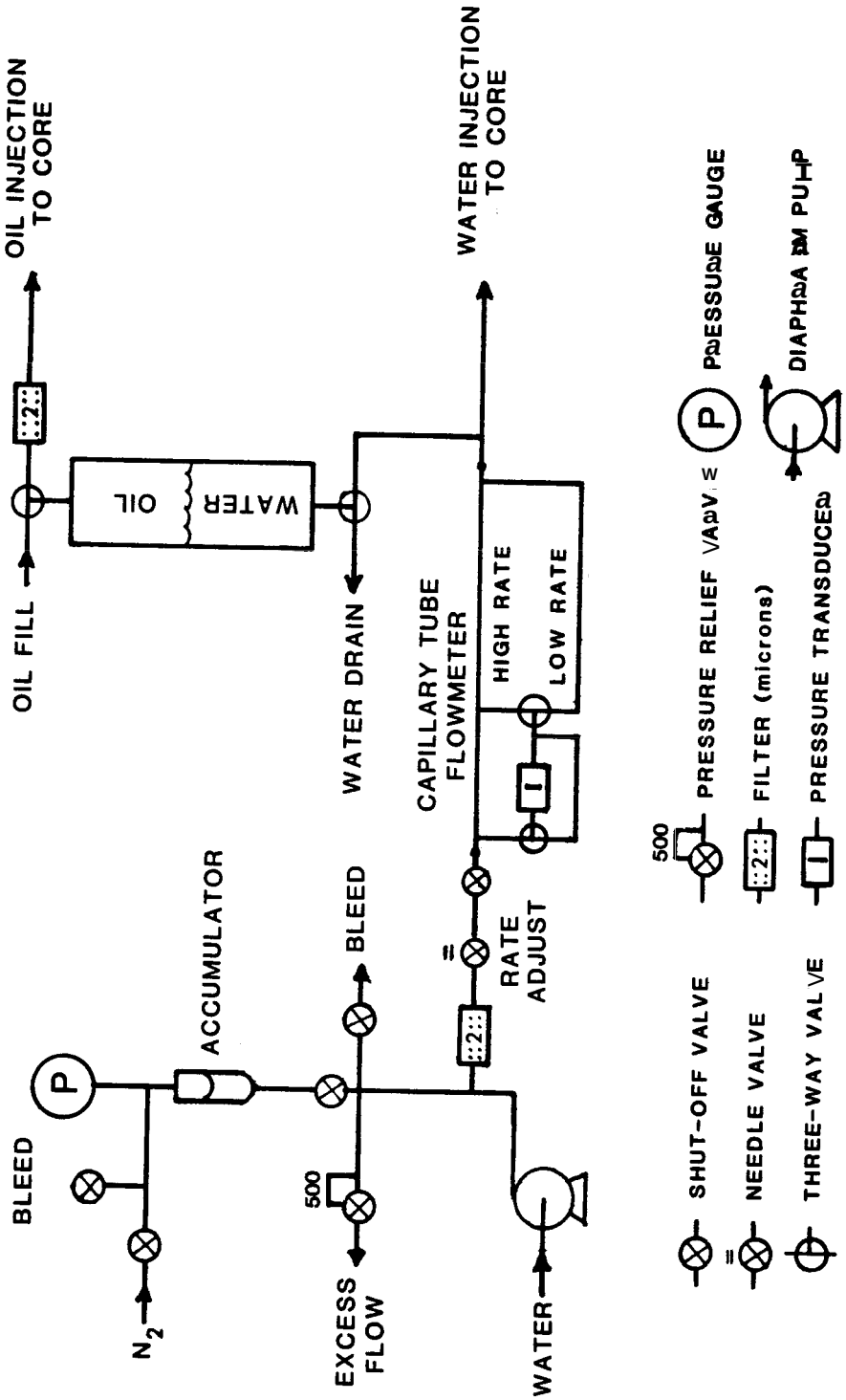

Fig. A.3 Schematic of Injection System for Runs Utilizing Distilled Water and Oil

pressure drop across the core changed during a run, it had only minor effect on the injected fluid flowrate.

A nitrogen-charged Greerolator Model 20-30TMR-S-1/2 WS accumulator was used to dampen pressure pulsations from the pump. The accumulator combined with the large pressure drop across the rate-adjusting needle valve eliminated differential pressure pulsations in the core. The accumulator was charged from a high-pressure nitrogen cylinder to approximately 450 psig with a bleed line open. Once pumping, the bleed line was closed and the accumulator partially filled with water until reaching the 500 psig relief pressure.

A capillary-tube flowmeter was used to determine injection rates. For the distilled water runs, the flowmeter consisted of approximately 4 ft of 1/8 in. O.D., 0.027 in. I.D. 316-stainless steel tubing. Tubing with a 0.085 in. I.D. was used when oil was the pumped fluid (salt water runs). A Celesco KP-15 pressure transducer with a 5 psi plate was connected across the flowmeter to measure the flowing pressure differential. A three-way valve was connected for zeroing the transducer. The pressure transducer was connected to a Celesco Model CD25A transducer indicator and recorded on a Soltec Model 1243 three-pen strip-chart recorder. The flowmeter was "teed" at approximately 10 in. to provide the capability of reading high flowrates,, The 4 ft length of both flowmeters gave full scale readings (5 psi) at a flowrate of approximately 40 cc/min. The shorter length was not: used in any of the runs.

A ball-type shut-off valve just upstream of the! flowmeter was used while heating and cooling the core to keep fluids from expanding back through the pump.

A. 3 Effluent Measurement System

The effluent measurement system (Fig. A.4) was a glass tube separator which allowed visual observation of the oil-water level. The glass tube was 1 in. I.D., 1.25 in. O.D by 32 in. long mounted in machined recesses in two aluminum blocks. Sealing was achieved by compressing O-rings at the tube ends with four threaded steel rods through the aluminum blocks. A graduated scale taped to the glass was used to measure changes in the oil-water interface level.

All produced fluids entered the separator through 1/8 in. 316-stainless steel tubing inserted approximately 2 cm up from the bottom of the glass tube. Connections from the top and bottom of the separator to a three-way switching valve allowed the separator to overflow either water or oil. Thus, the system was capable of measuring either produced oil or produced water volumes. System pressure was regulated by a Grove Mity-Mite Model SD-90-W air dome type pressure regulator. The regulator body was 316-stainless steel, with a Viton diaphragm capable of controlling pressures from 25 to 400 psig. The regulator was charged with nitrogen through a Grove loading tee. Since only single phase fluids passed through the regulator, the usual pressure pulsations from multiphase flow were reduced. The total volume of displacing fluid flowing from the separator was measured in graduated cylinders.

The separator was calibrated at the end of each run to consider fluids sticking to the sides of the glass. Oil and water reservoirs connected to the separator with Tygon tubing were used to displace fluids for calibration (see Appendix B.6 for details).

A.4 Pressure Measurement System

Core differential pressure was measured with a bank of three

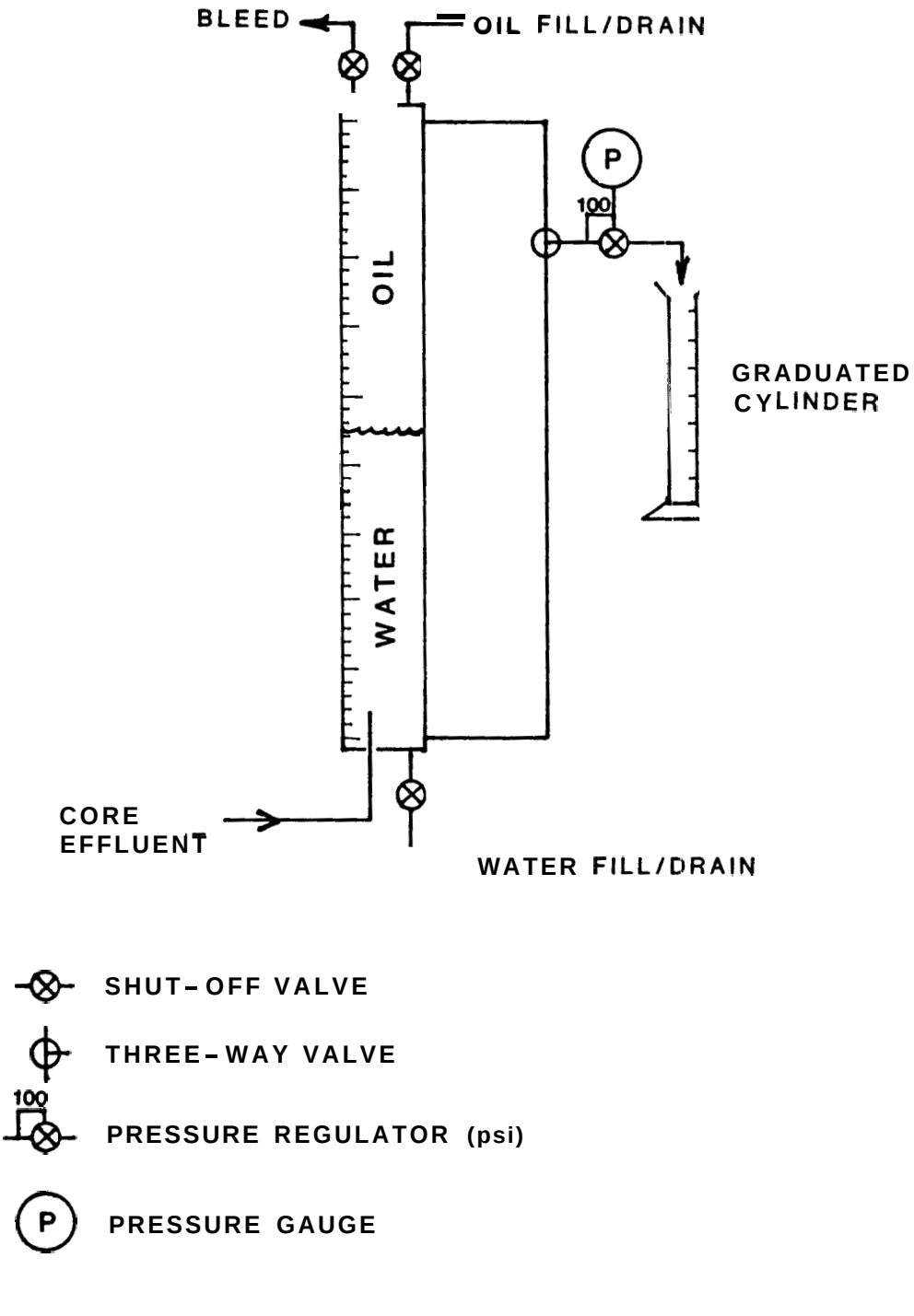

Fig. *A.4* Schematic of Effluent Measurement System

Celesco KP–15 diaphragm–type pressure transducers (see Fig. A.4). For the unconsolidated sand runs, plates were installed for full–scale readings of 5–, 25–, and 100–psi. Plates for 25–, .L00-, and 500–psi were used for the consolidated sand runs. The transducers were connected to Celesco Model CD–25A or CD-10C demodulator/indicators whose output was recorded on a Soltec Model 1243 three-pen strip–chart recorder. Output from any two of the transducers could be recorded simultaneously on the strip–chart (the third trace was used for the flowmeter differential pressure). Three–way switching valves were connected to each transducer for zeroing.

Transducers were disconnected from the system and calibrated using either a dead weight tester (25–, 100–, and 500–psi plates) or a mercury manometer (5 psi plate). Before use during a run, transducer zeroes were adjusted on the strip–chart recorder.

Pressure gauges connected to both the upstream and downstream pressure taps monitored internal core pressure. Valves were also connected to the taps to bleed the lines of air when a fresh core was connected.

A.5 Confining Pressure System

Confining pressure was applied to the core holder using a high–pressure nitrogen cylinder which pressurized the distilled water confining fluid through a 400 cc pressure vessel (see Pig. A.6). This system was used to avoid rapid confining pressure changes during heating and cooling (the nitrogen cushion gave additional system compressibility). After reaching isothermal conditions, a valve was closed to isolate the confining system to water alone. Minor leaks could be detected readily because of the low water compressibility.

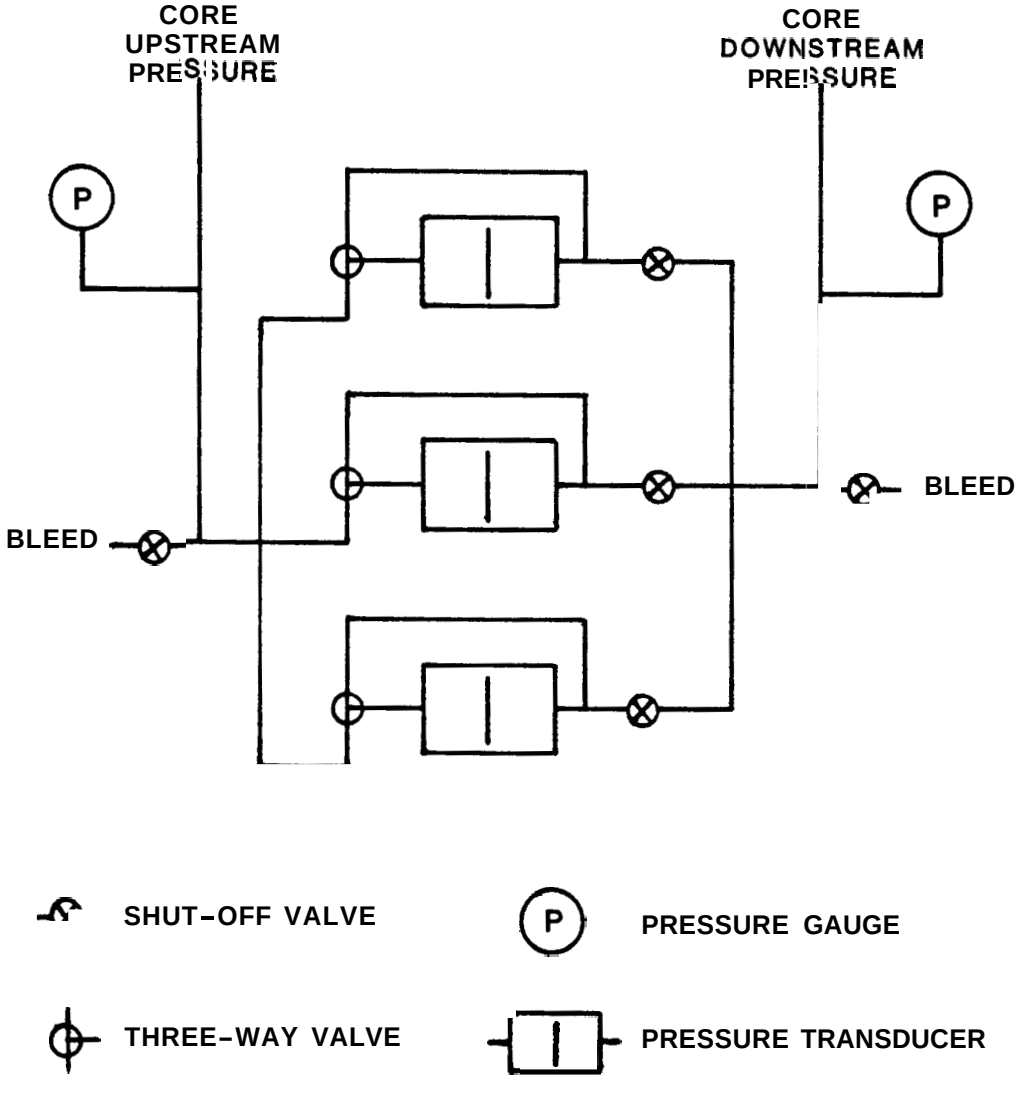

Fig. A.5 Schematic of Pressure Measurement System

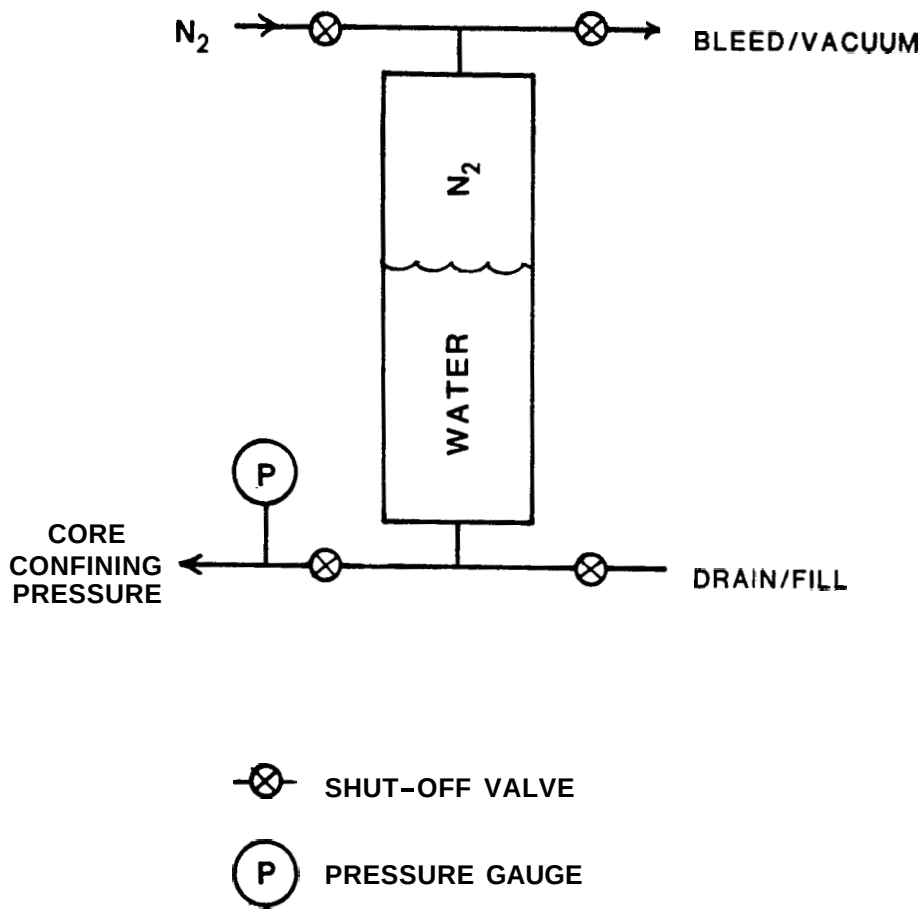

Fig. A.6 Schematic of Confining Pressure System

A.6 Core Holder

The core holder used for unconsolidated sand was originally constructed by Counsil (1979), modified by Jeffers (1981), and further modified for this study. A schematic of the final design is shown in Fig. A.7. Component dimensions are give in Figs. A.8 and A.9. A photograph of the core holder is presented in Fig. A.10.

The outer core holder body is constructed of 304-stainless steel, threaded on both ends for brass retaining caps (brass was used to reduce thread seizure problems). The outer shell is 3.5 in. O.D., 2.62 in. I.D. by 26 in. long. The inside diameter of both ends were machined to 2.65 in. to accept O-ring seals on the end plug assemblies.

To contain the unconsolidated sand, a 316-stainless steel inner sleeve was used. This sleeve was constructed from mechanical grade tubing 2 in. I.D. by 2.25 in. O.D. Both ends were machined to 2.02 in. I.D. to accept end plugs with O-ring seals. The inner sleeve was 23.05 in. long.

The average internal diameter of the inner sleeve was carefully measured by determining the amount of liquid required to fill the empty sleeve from the fixed end plug to a short distance from the opposite end. The average internal diameter was found to be 5.044 cm (1.986 in.).

Confining force for the sand pack was applied uniaxially by a free-traveling end plug. Pressure supplied by the confining pressure system held the end plug tightly against the sand pack. A fixed end plug was used on the opposite end. End plugs were constructed from 316-stainless steel. Both end plugs were drilled with a central hole and six radiating holes to distribute flow across the core face. Concentric

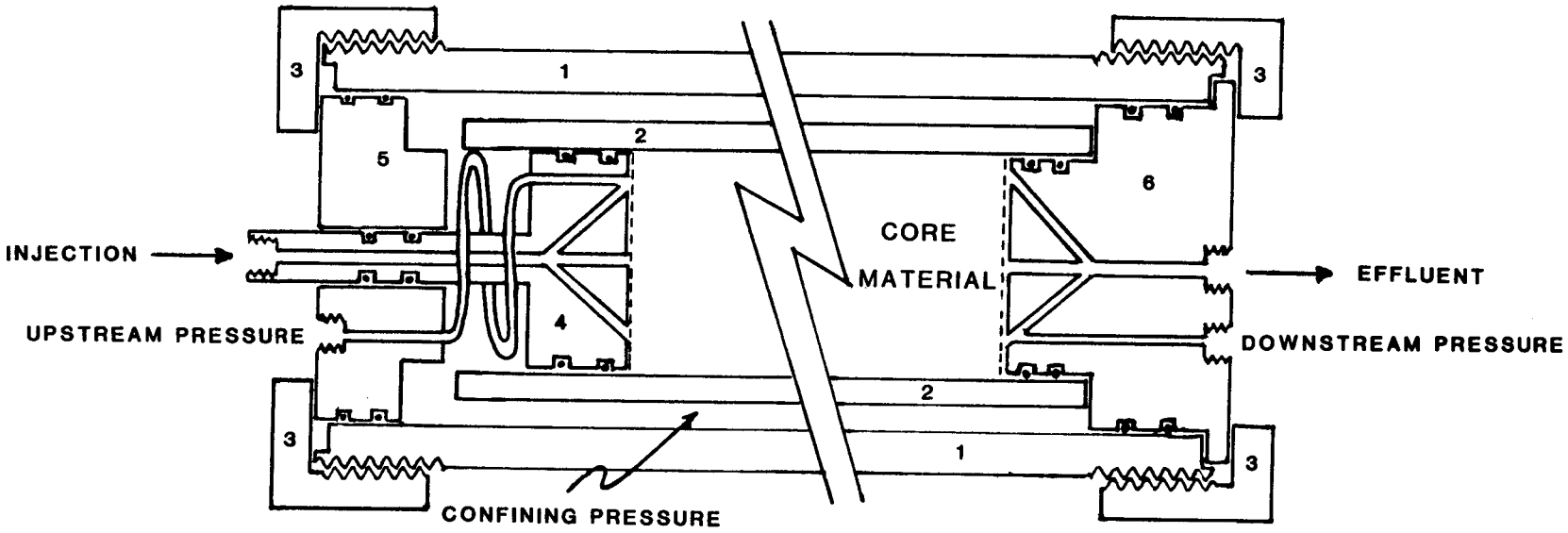

1 - OUTER SLEEVE

2 - INNER SLEEVE

3 - SCREW-ON RETAINER

4 - TRAVELING END PLUG

5 - TRAVELING END PLUG GUIDE

6 - FIXED END PLUG

• O-RING

STAINLESS STEEL SCREEN 270 MESH

Fig. A.7 Schematic of Core Holder Used for Unconsolidated Sands

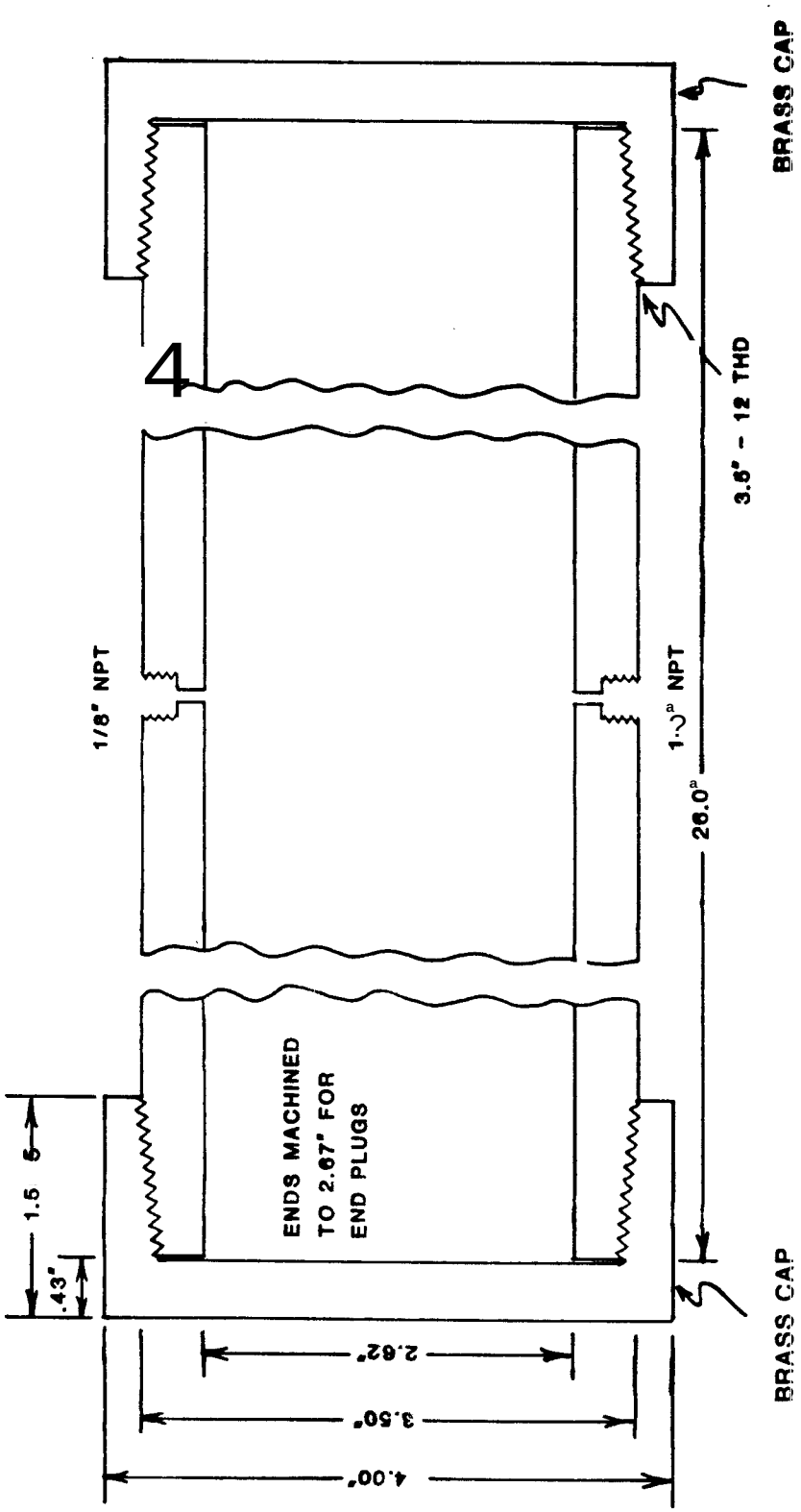

Fig. A.8 Dimensions of Core Holder Outer Shell Components

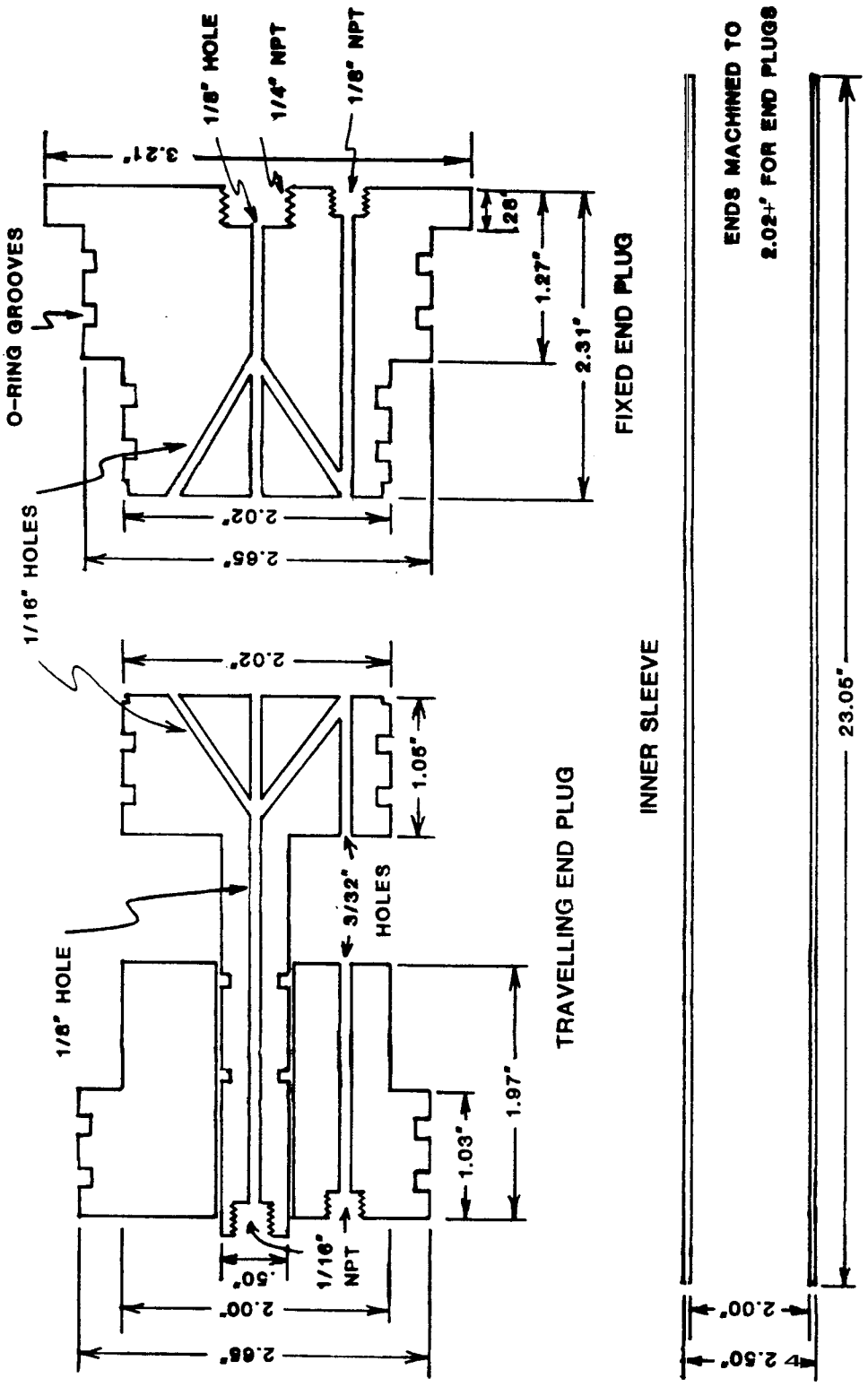

Fig. A.9 Dimensions of Core Holder Inner Sleeve and End Plugs

Fig. A.10 Photograph of Core Holder used for Unconsolidated Sands

circular and linear radiating grooves on the face of the end plugs aided fluid distribution. Both end plugs were covered with 270 mesh stainless steel screens to retain the sand.

A hole was drilled directly through the fixed end plug for the downstream pressure rap. The upstream presure tap consisted of holes drilled through both the traveling end plug and the end plug guide. A 1/16 in. 316-stainless steel tube was silver soldered to both pieces and coiled around the neck of the traveling end plug to allow free movement. The upstream pressure tap arrangement was altered for consolidated sands to facilitate loading of the cores. The coiled tube was removed and a 1/16 in. 316-stainless steel tube was inserted through the main flow channel in the traveling end plug to serve as a pressure tap. This allowed the traveling end plug to be detached from the end plug guide.

The dimensions of the core holder were carefully measured so that an accurate determination of core length could be made. The following was determined from the dimensions shown in Fig. A.7:

$$L = L_m + 19.90 \text{ in. } (50.55 \text{ cm}) \qquad \text{(A.1)}$$

where:

L = length of core

L_m = length of traveling end plug extending from. the end plug guide

The upstream dead volume (between the three-way valve and the core face) was measured by alternately flowing oil and water through the traveling end plug attached to the injection system. Amounts of oil and water displaced from the dead volume were measured several times in a graduated cylinder. The total upstream plus downstream dead volume was

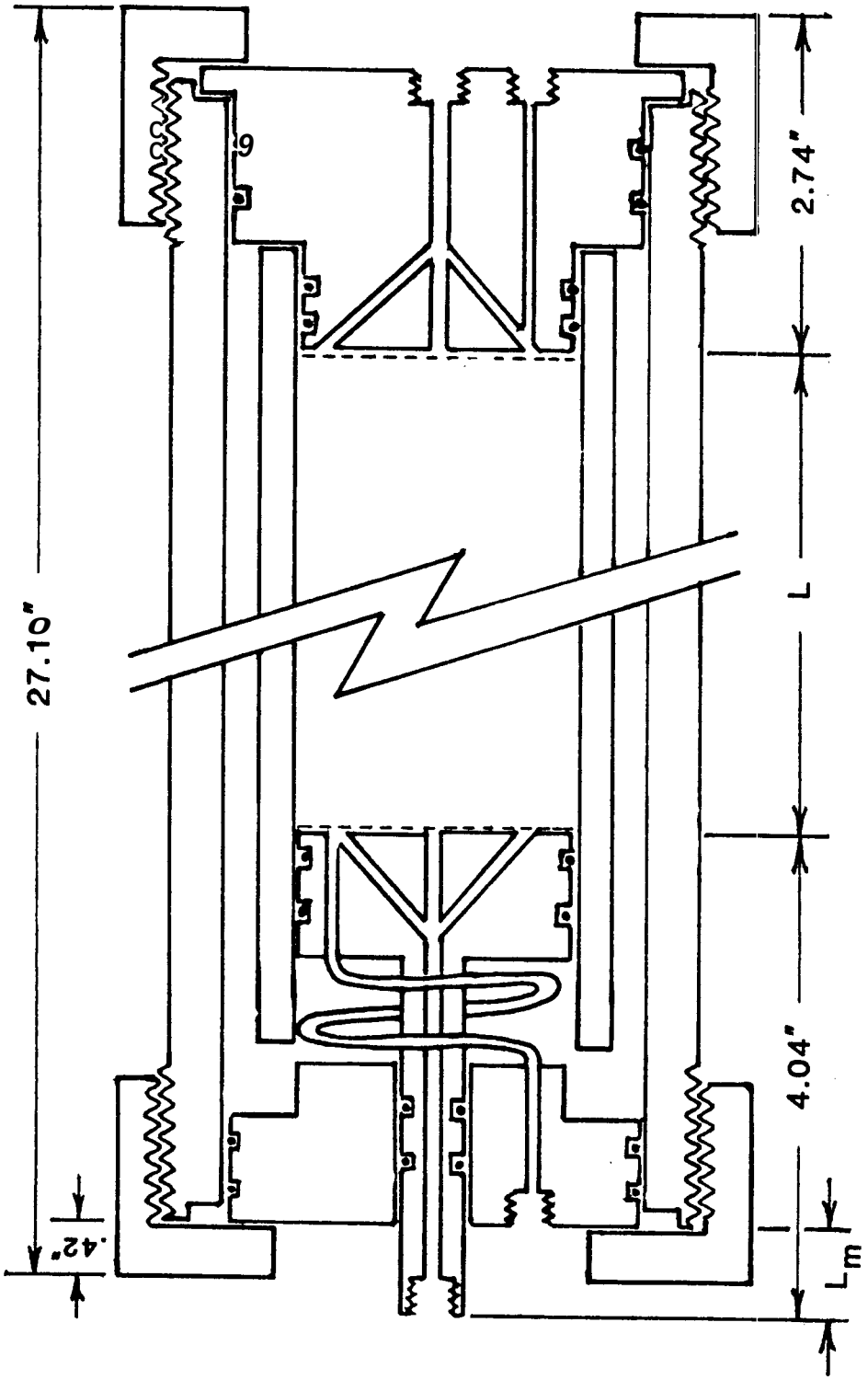

Fig. A.11 Core Holder Dimensions for Determining the Length of Unconsolidated Sand Packs

measured by clamping the end plugs together inside a rubber sleeve and connecting the assembly to both the injection and effluent systems. The combined dead volume was measured by alternately flowing oil and water into the glass tube separator. For the arrangement used for unconsolidated sands, the upstream dead volume was measured to be 2.5 cc. The downstream dead volume was 3.0 cc. For consolidated cores, the 1/16 in. upstream pressure tap reduced the upstream dead volume to 2.2 cc.

A.7 Equipment Suppliers

White Mineral Oil

Van Waters & Rogers
2256 Junction Ave.
San Jose, CA 95131 (408) 263-9900

Ottawa Silica Sand

Barker Industrial and Foundry Supply
1881 Rollins Rd.
Burlingame, CA 94010 (415) 697-8865

Berea Cores

Cleveland Quarries
P.O. Box 261
Amherst, OH 44001 (216) 986-4501

Heat-Shrinking Teflon

Plastic Center
1170 Terra Bella Ave.
Mountain View, CA (415) 969-9280

Stainless Steel Tubing

Tube Service
666 S. Milpitas Blvd.
Milpitas, CA (408) 946-5500

Inner Core Holder Sleeve

Tube Sales
3841 Arden Rd.
Hayward, CA 94545 (415) 887-8900

Stainless Steel Rod

Jorgensen Steel
P.O. Box 4666
Bayshore Annex
Oakland, CA 94623 (415) 835-8222

Stainless Steel Pressure Vessel

Con Val
412 Pendleton Way
Oakland, CA 94621 (415) 568-8922

Valves, Fittings, Filters, Relief Valve, etc.

Sunnyvale Valve
929 Weddell Ct.
Sunnyvale, CA 94086 (408) 734-3145

High-Temperature Three-way Valve

Valco Instruments Co., Inc.
P.O. Box 55603
Houston, TX 77055 (713) 688-9345

High Pressure Glass Tubes

Hickman–Logan
6 Bryant Way
Orinda, CA 94563 (415) 254–6670

Pressure Renulator

Coastal Engineering Corp.
P.O. Box 23526
Harahan, LA 70183 (504) 733–8511

Transducers and Demodulators

Gado Instrument Sales
3997 E. Bayshore Rd., Suite A
Palo Alto, CA 94303 (415) 961–2222

Chart Recorder and Supplies

Electronic Engineering Associates
932 Terminal Way
San Carlos, CA 94070 (415) 593–2189

Much of the equipment used in this study was on hand. See Jeffers (1981) and Counsil (1979) for additional equipment suppliers.

APPENDIX B - PROCEDURE DETAILS

The following sections describe the procedures used for core preparation, salt water treatment, oil and water displacement runs, separator calibration, and heating and cooling the system.

B.1 Unconsolidated Sand Preparation and Core Packing

Sand for the unconsolidated sand packs was prepared from industrial quality F-140 Ottawa silica sand. The sand was sieved using a W. S. Tyler Ro-Tap Testing Sieve Shaker. A double stack of W. S. Tyler U.S.A. Standard Testing Sieves were used in the following sequence (top down): 80-, 100-, 120-, 140-, 170-, and 200-mesh and pan.

Approximately 50 cc (70 g) of sand was placed in each stack and sieved for at least 10 minutes (recommended procedure by W. S. Tyler Co.). Sand on the 80 and 100 mesh screens and the pan was discarded. After enough sand was sieved, approximately 2000 g of total sand were recombined according to the following percentages:

Table B.1 Sieve Analysis of Unconsolidated Sand Packs

U.S.A. Standard Sieve Mesh	Percent
100-120	25
120-140	35
140-170	25
170-200	15
	100

The sand was mixed by shaking in a sealed container and then thoroughly washed with tap water. Washing was done by shaking a sand

and tap water mixture in a sealed jar and then pouring off the dirty water after the sand had settled. This procedure was repeated several times until the water was clear (usually around 10 or more times). The sand was then placed on an aluminum pan and either air dried for a few days or oven dried for a few hours.

Sand was packed in the inner sleeve dry. The fixed end plug was first inserted into the sleeve and the assembly placed upright on a wood block. A pneumatic vibrator was strapped to the sleeve with a strap clamp. A plastic insert containing several wide mesh screens was placed in the top of the sleeve to distribute sand as it was poured. With the vibrator running, sand was poured into the sleeve in batches of approximately 200 cc (usually 6 batches in all). The sand was carefully weighed to determine the porosity (using core dimensions and quartz sand density of 2.65 g/cc). Sand was poured to approximately 4 cm from the top of the sleeve to allow proper end plug travel.

The outer shell was then placed over the inner sleeve and the traveling end plug with guide inserted into the open end of the inner sleeve. The entire assembly was placed in a vise and the retaining caps tightly screwed on with strap wrenches.

The core assembly was placed in the air bath and connected downstream to a shut-off valve and then to a vacuum pump teed to a McLeod vacuum gauge. Upstream, the core was connected to a shut-off valve and then to a water reservoir on top of the air bath. Care was taken to remove all air from the line between the water reservoir and the shut-off valve. Pressure taps were sealed with Swagelok caps.

The confining pressure system was then purged of all water and connected to the core holder. The inner sleeve thermocouple was

connected to the outer shell and 500 psig nitrogen confining pressure applied. The valve between the core and the confining pressure vessel was closed and the vessel bled to atmospheric pressure. The vessel was filled with distilled water using a vacuum and then repressurized with nitrogen. While slowly bleeding nitrogen from the thermocouple connection (to maintain confining pressure), water was displaced from the pressure vessel to fill the core holder.

With the water valve to the core closed and the vacuum valve open, the core was evacuated to less than 50 μTorr. This usually required several hours, or overnight. The vacuum valve was then closed and the water valve opened to saturate the core with water.

After being certain the injection valve was switched to "waterflood" and filled to the end with water, the injection line was connected to the core. The pressure taps and downstream line were then connected and the pump started. While pumping a few pore volumes of water to ensure complete saturation, the pressure tap lines were bled.

After the injection rate and differential pressure stabilized, the absolute permeability of the pack to water was measured several times using a graduated cylinder and a stopwatch to determine flowrates. Measurements were usually repeatable to within ±0.5%.

The core was now ready for oil displacement to establish irreducible water saturation.

B.2 Consolidated Core Preparation and Loading

Two-inch diameter Berea sandstone cores were cut to approximately 20.5 in. long with a core cutter. Each was then furnace-fired at 500°C for five hours to remove organic materials. Both end plugs were clamped against the core inside 24 in. of 2 in. (nominal) diameter heat-

shrinking Teflon tubing. The entire assembly was placed in the air bath at 350°F for approximately 3 hours. Wire was wrapped around the Teflon over the end plugs to provide initial sealing from confining fluid. The core and end plugs were placed in a vertical position and removed from the clamp. The outer shell was then placed over the entire assembly, the traveling end plug guide installed, and the retaining caps were attached.

With the core holder still in a vertical position (to prevent the core from sagging between the end plugs), nitrogen confining pressure was applied. The core was then placed in the air bath horizontally. The core was evacuated and saturated with salt water by the procedure described in Appendix B.l for unconsolidated sand packs. The amount of water required to fill the core was measured using two 250 ml burets. The core pore volume was determined by subtracting the volume of the end plugs and valving (10.9 cc) from the water volume required to fill the system.

After bleeding the pressure taps and determining the absolute permeability to water, the core was ready for oil displacement to establish irreducible water saturation.

B.3 Salt Water Treatment

To prevent clay and fines migration, Berea sandstone runs were conducted using a 2% sodium chloride solution in place of distilled water. To minimize corrosion problems, the salt water was de-oxygenated before being injected into the system.

Sixteen liters of distilled water were placed in a 5 gal Pyrex bottle. Nitrogen was blown into the water through fish tank air stones to reduce the oxygen concentration in the water and to remove oxygen

from the air space in the bottle. In 2 liters of heated distilled water, 367 g of NaCl, 2.5 g of Na_2SO_3, and 0.2 g of $CoCl_2 \cdot 6H_2O$ were added and stirred. Sodium sulfite reacts with dissolved oxygen (with cobalt as a catalyst) to form Na_2SO_4. The amounts of sodium sulfite and cobalt used were recommended by Paulsen (1979), based on at least 50% excess. This solution was poured into the Pyrex bottle. Nitrogen bubbling was continued for a short time to mix the solution thoroughly.

Approximately 1 gal of water at a time was loaded into the salt water pressure vessel. The Pyrex bottle was sealed between loadings to prevent oxygen contamination of the air space above the water.

B.4 Oil Displacement Runs

At the beginning of a set of displacement runs,, the effluent separator was usually dismantled and thoroughly cleaned. The separator was then filled with water from the bottom and oil from the top, being certain to remove air bubbles from the end caps and the lines to the three-way switching valve. Prior to starting an oil- displacement run, the oil/water level was positioned near the bottom of the separator.

For displacing the core to irreducible water saturation, the following procedure is recommended:

1. Be certain the injection system oil vessel is filled with oil (distilled water runs).

2. With both the injection and effluent switching valves set to "waterflood", start the pump briefly to bring the system to 100 psig. This is done by adjusting the nitrogen charge in the pressure regulator (usually to around 125 psig).

3. Measure the separator level.

4. Start the pump, zero the appropriate transducer(s), and begin to record core differential pressure and the flowmeter reading on the strip-chart recorder. A chart speed of 30 cm/hr was used for most runs.

5. Wait for the rate and differential pressure to stabilize.

6. Switch both the injection and effluent switching valves to "oilflood" simultaneously. Immediately begin measuring effluent oil production in a graduated cylinder (usually 100 ml) while simultaneously starting the stopwatch. Record the differential pressure and flowmeter readings just prior to initiation of oil injection (may be done later).

7. When the graduated cylinder is nearly full, do the following simultaneously:

   a) Read separator level.

   b) Change graduated cylinder.

   c) Depress "lap" button on the stopwatch to get an elapsed time reading while letting the internal clock continue to run.

   Immediately depress the "mark" button on the strip-chart recorder to indicate the point at which data was taken.

8. Record:

   a) elapsed time (hr,min,sec) - then restart stopwatch by again pressing "lap" button.

   b) separator level (cm)

   c) volume of oil in graduated cylinder (cc)

d) differential pressure (psi)

e) flowmeter reading at "mark"

f) average flowmeter reading from previous "mark"

Data d), e), and f) may be recorded any time, since they are permanently recorded.

9. Repeat Steps 7 and 8 to the end of the run. Large volume graduated cylinders were generally used after breakthrough, reverting to a 100 ml cylinder at the end to determine an accurate end-point flowrate. Approximately 2 pore volumes of oil were injected to establish irreducible water saturation.

10. Zero transducers, then shut off the pump. Isolate the core with the shut-off valve upstream of the flowmeter and with the switching valve just upstream of the separator (by turning the three-way valve to a neutral shut-off position).

11. Record the final separator level with the pump off. Levels taken with oil flowing are slightly in error, due to the volume of oil in bubbles traveling up the water column.

12. Record the flowmeter reading and differential pressure at oil breakthrough.

13. Bleed the pressure regulator nitrogen charge to bring the separator to atmospheric pressure. Turn the effluent switching valve to neutral. Calibrate the separator (see Appendix B.6).

14. Place the water reservoir on top of the air bath and the oil reservoir on the laboratory bench. Displace oil from the separator

to the oil reservoir, until the oil-water interface is near the top of the separator. Close the valves to the reservoirs.

15. Turn the effluent switching valve to "oilflood". Repressurize the pressure regulator nitrogen charge to the previous level.

16. Slowly turn the switching valve upstream of the separator to "flood". Be careful that boiling does not occur at high temperatures when the core pressure drops slightly (usually there is no difficulty). If necessary, proceed to Step 17 with the switching valve in neutral (shut-off). Turn the valve quickly to "flood" when the core pressure begins to rise.

17. Open the shut-off valve upstream of the flowmeter and start the pump to bring the system to full pressure. The system is now ready for a water displacement run.

B.5 Water Displacement Runs

1. With both the injection and effluent switching valves set to "oilflood", start the pump briefly to bring the system to 100 psig. This is done by adjusting the nitrogen charge in the pressure regulator (usually to around 125 psig).

2. Measure the static separator level.

3. Start the pump, zero the appropriate transducer(s), and record core differential pressure and the flowmeter reading on the strip-chart recorder. A chart speed of 30 cm/hr was used for most runs.

4. Record the dynamic separator level. The difference between this level and the static level is the amount of oil traveling in bubbles up the water column. Corrections for this effect are discussed in Appendix E.2.

5. Wait for the rate and differential pressure to stabilize.

6. Switch both the injection and effluent valves to "waterflood" simultaneously. Immediately begin measuring effluent water production in a graduated cylinder (usually 100 ml) while simultaneously starting the stopwatch. Record the differential pressure and flowmeter readings just prior to initiation of water injection (may be done later).

7. When the graduated cylinder is nearly full, do the following simultaneously:

   a) Read separator level.

   b) Change graduated cylinder.

   c) Depress "lap" button on stopwatch to get an elapsed time reading while letting the internal clock continue to run.

   Immediately depress the "mark" button on the strip-chart recorder to indicate the point data was taken.

8. Record:

   a) elapsed time (hr,min,sec) - then restart stopwatch by again pressing "lap" button.

   b) separator level (cm)

   c) volume of water in graduated cylinder (cc)

   d) differential pressure (psi)

e) flowmeter reading at "mark"

f) average flowmeter reading from previous "mark"

Data d), e), and f) may be recorded at any time, since they are permanently recorded.

9. Repeat Steps 7 and 8 to the end of the run. Watch for water breakthrough in the sight glass to help pick the breakthrough point on the strip-chart recorder. Large volume graduated cylinders were generally used when oil fractional flows became small, reverting to a 100 ml cylinder at the end to determine an accurate end-point flowrate. Up to 10 pore volumes of water were injected for the room temperature runs. The elevated temperature runs were sometimes stopped sooner, usually because of low oil fractional flow.

10. Zero all transducers, then shut off the pump. Isolate the core with the valve upstream of the flowmeter and with the switching valve just upstream of the separator (by turning the three-way valve to a neutral shut-off position).

11. Record the final separator level.

12. Record the flowmeter reading and differential pressure at water breakthrough. Breakthrough is sometimes difficult to establish. Visual observation with the sight glass will give a general idea of breakthrough time.

13. Bleed the pressure regulator nitrogen charge to bring the separator to atmospheric pressure. Turn the effluent switching valve to neutral. Calibrate the separator (see Appendix B.6).

14. Place the oil reservoir on top of the air bath and the water reservoir on the laboratory bench. Displace water from the separator to the water reservoir until the oil-,water interface is near the bottom of the separator. Close the valves to the reservoirs.

15. Turn the effluent switching valve to "waterflood". If the system is at room temperature, bleed the core pressure by turning the valve upstream of the separator to "flood". At elevated temperatures, proceed to Step 16.

16. Repressurize the pressure regulator nitrogen charge to its previous level.

17. Slowly turn the switching valve upstream of the separator to "flood". Be careful that boiling does not occur at high temperatures when the core pressure drops slightly (usually there is no difficulty). If necessary, proceed to Step 18 with the switching valve in neutral (shut-off). Turn the valve quickly to "flood" when the core pressure begins to rise.

18. Open the shut-off valve upstream of the flowmeter and start the pump to bring the system to full pressure. The system is now ready to be cooled to room temperature (see Appendix lB.7).

B.6 Separator Calibration

The separator calibration procedure entails displacing the produced oil or water from the separator into graduated cylinders and measuring the corresponding change in separator level. This was found to give accurate and repeatable measurements of produced volumes for material balance purposes:

1. Place the appropriate reservoir on top of the air bath to displace the desired fluid from the separator. Set the effluent switching valve to the neutral shut-off position, and open the valve to the reservoir.

2. To be sure lines are liquid filled, displace a small amount of produced fluid by turning the effluent switching valve briefly to the appropriate setting ("oilflood" to measure oil, "waterflood" for water). Record the separator level.

3. Place a graduated cylinder (usually 100 ml) under the pressure regulator and turn the effluent switching valve to fill the cylinder with produced fluid.

4. Turn the switching valve to neutral and record the new separator level. Estimate the level if large changes occur in the meniscus shape. A meniscus correction of 0.17 cm was measured as the difference between a perfectly flat meniscus and the bottom of a fully-developed meniscus when the tube is clean. Record the volume of fluid in the graduated cylinder.

5. Repeat Steps 3 and 4 until the separator level is near that at the beginning of the run.

6. Total produced volume is measured as the total measured in the graduated cylinders plus or minus corrections for differences between the beginning and ending calibration levels and the beginning and ending run levels.

B.7 Heating and Cooling

Heating and cooling were both done at the end of water displacement runs. The following procedures were used:

Heating

1. Bring the system to full pressure (100 psig) with the pump. Close the valve upstream of the flowmeter to keep fluid from leaking back through the pump.

2. Record the separator level and place a 50 ml graduated cylinder under the pressure regulator.

3. Open the confining pressure valve to allow fluid to expand back into the pressure vessel.

4. Turn on the air bath (and fan) to the desired setting. Periodically bleed nitrogen from the confining pressure system to keep confining pressure near 500 psig.

5. Wait several hours until all recorded temperatures are identical for at least an hour. The pressure regulator will also cease to drip into the graduated cylinder.

6. Remove the graduated cylinder and record the volume of fluid expanded from the core.

7. Turn on the pump briefly, then record the change in separator level during heating. Use the previous separator calibration to measure oil expansion from the core. The system is now ready for an oil displacement run.

Cooling

1. Bring the system to full pressure (100 psig) with the pump. Close the valve upstream of the flowmeter to keep fluid from leaking back through the pump.

2. Connect a long piece of 1/8 in. tubing to the pressure regulator, so that it will extend to near the bottom of a 50 ml graduated cylinder. Fill a graduated cylinder with water, record the volume, and place it under the pressure regulator.

3. Open the confining pressure valve to the core to allow fluid to expand from the pressure vessel.

4. Turn off the air bath and open the air bath doors. Use either the air bath fan or an external room fan (preferrable) to begin to cool the core holder. Watch the pore pressure and inner sleeve temperature to determine when the system is below atmospheric boiling temperature (inner sleeve temperature must usually be below 150°F and pore pressure on a slight vacuum). Periodically add nitrogen to the confining pressure vessel to keep the confining pressure near 500 psig.

5. Slowly bleed the nitrogen charge from the pressure regulator. If fluid begins flowing into the graduated cylinder (evidence of internal boiling), immediately repressurize the regulator and wait a little longer. If fluid flows from the graduated cylinder, bleed off the pressure regulator and allow the system to cool overnight.

6. Disconnect the long piece of 1/8 in. tubing and record the change in graduated cylinder volume. The system is now ready for an oil displacement run.

APPENDIX C – CORE DATA

Table C.I Core Data

Core Number	Type	Length (cm)	Diameter (cm)	Pore Volume (cc)	'Porosity (%)	Permeability (darcies)
2	Ottawa	51.47	5.044	391.2	38.0	7.16
3	Ottawa	51.69	5.044	395.9	38.3	6.90
4	Ottawa	51.60	5.044	391.4	38.0	6.75
6	Berea	51.85	5.080	200.0	19.0	.220

APPENDIX D - FLUID PROPERTIES

This appendix contains information on the density and viscosity of distilled water, salt water, and the white mineral oil (Blandol) used in these experiments.

D. 1 Distilled Water Density

Distilled water density vs. temperature data was obtained from the ASME Steam Tables (1979), Table 3 - Properties of Superheated Steam and Compressed Water (Temperature and Pressure), p.153. Specific volume data at 115 psia was used, and is given in Table D.1.

The data from 70°F to 300°F was converted to density and curve fit with the following equation:

$$\ln(\rho_w) = a_0 + a_1 T + a_2 T^2 \qquad (D.1)$$

where :

ρ_w = water density, g/cc

T = temperature, °F

$a_0 = 6.52014 \times 10^{-3}$

$a_1 = -4.34333 \times 10^{-5}$

$a_2 = -8.78134 \times 10^{-7}$

Equation D.1 matches the data within a maximum error of ±0.08%. The tabular data and the equation are shown in Fig. D.1.

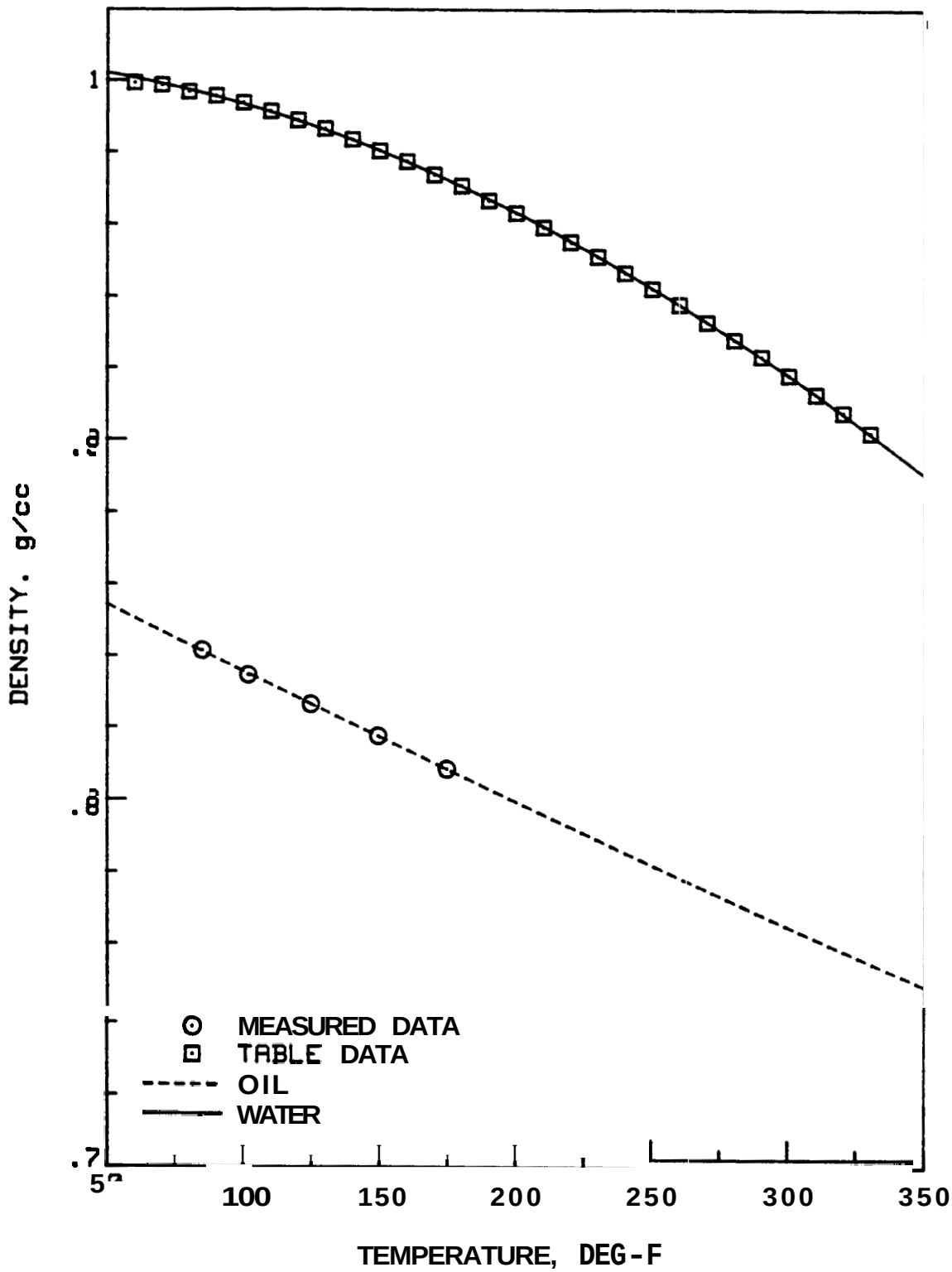

Fig. D.l Density of Distilled Water and Blandol vs. Temperature

Table D.1 Distilled Water Specific Volume and Viscosity vs. Temperature [ASME Steam Tables (1979)]

Temperature (°F)	Specific Volume at 115 psia (ft^3/lbm)	Viscosity at 100 psia (10^{-7} lbf-sec/ft^3)
50		273.0
60	0.01603	
70	0.01604	
80	0.01607	
90	0.01609	
100	0.01612	142.3
110	0.01616	
120	0.01620	
130	0.01624	
140	0.01629	
150	0.01634	89.9
160	0.01639	
170	0.01645	
180	0.01650	
190	0.01657	
200	0.01663	63.4
210	0.01679	
220	0.01677	
230	0.01684	
240	0.01692	
250	0.01700	48.0
260	0.01780	
270	0.01717	
280	0.01726	
290	0.01735	
300	0.01745	38.3
310	0.01755	
320	0.01765	
330	0.01776	

D.2 Distilled Water Viscosity

Distilled water viscosity vs. temperature was also obtained from the ASME Steam Tables (1979), Table 10 - Viscosity of Steam and Compressed Water, p.280. The data for a pressure of 100 psia and temperatures from 50°F to 300°F are shown in Table D.1. The data were converted to centipoise and curve fit with the following equation:

$$\ln \ln(208.9\ \mu_w) = b_0 + b_1[\ln(T)] + b_2[\ln(T)]^2 \qquad (D.2)$$

where:

μ_w = water viscosity, cp

T = temperature, °F

b_0 = 1.3926

b_1 = 3.0841×10^{-1}

b_2 = -5.7139×10^{-2}

This equation represents the data to within a maximum error of ±0.12%. The tabular data and equation are presented in Fig. D.2.

D.3 Salt Water Density

The International Critical Tables (1927), V.3, p.79, lists data for the density of aqueous sodium chloride (NaCl) solutions for temperatures to 100°C (212°F) at atmospheric pressure. The ratio of the density of a 2% NaCl solution to the density of distilled water was calculated to be 1.0137 to 1.0143 over the temperature range of 20°C (68°F) to 100°C (212°F). Since the density ratio is essentially constant, distilled water density data could be used for the salt water runs. This is because only water density ratios between temperatures are required in calculations.

D.4 Salt Water Viscosity

The International Critical Tables, V.5, p.15, also includes data on the viscosity of aqueous NaCl solutions to 100°C (212°F) at atmospheric pressure. This data was in the form of the parameter η vs. temperature and salinity, where η is the ratio of NaCl solution viscosity to distilled water viscosity at the same temperature. Graphing η vs.

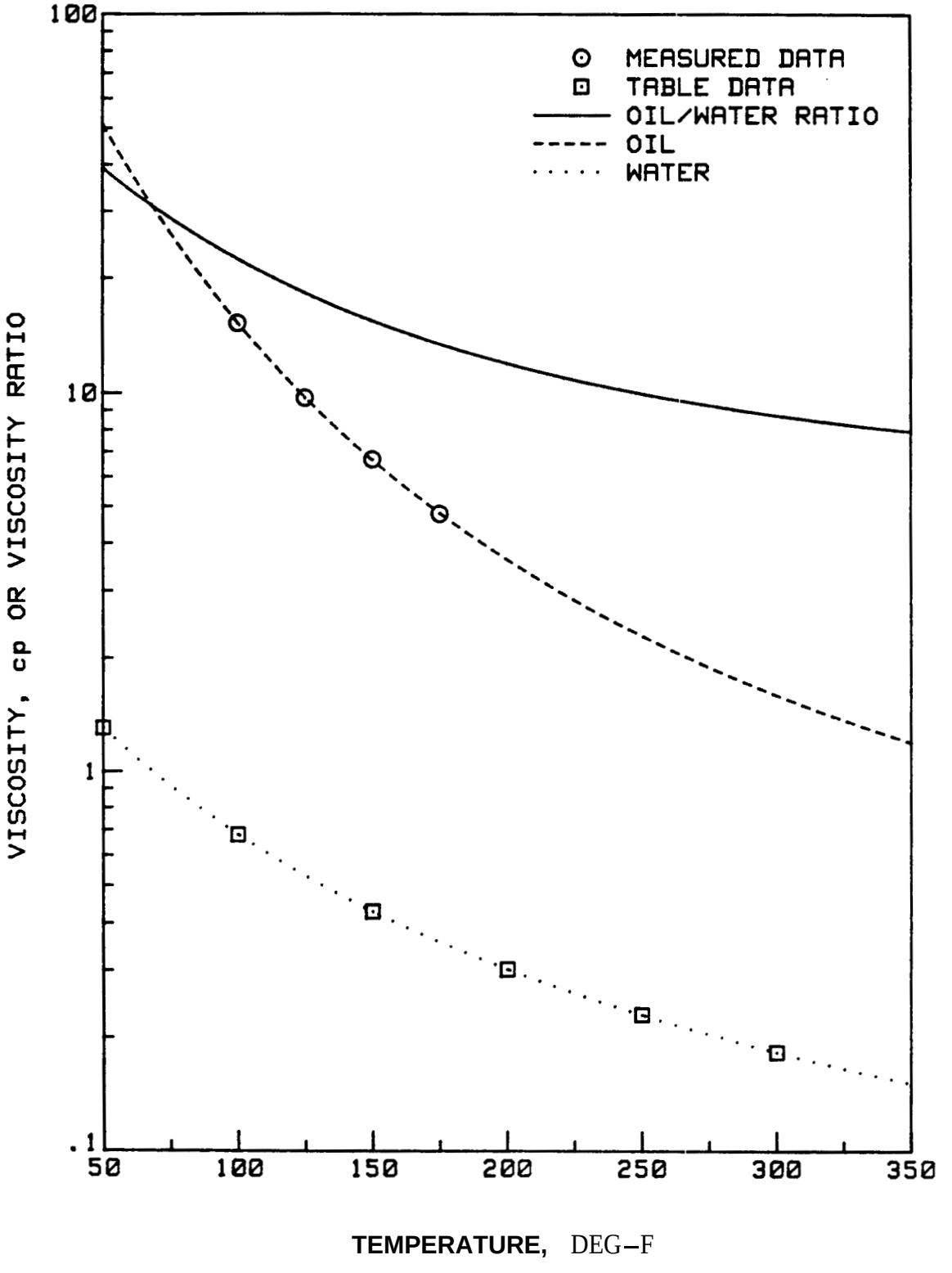

Fig. D.2 Viscosity of Distilled Water and Blandol vs. Temperature

salinity at constant temperature showed a linear relationship over the salinity range of interest. Thus, linear interpolation was used to establish values for 2% NaCl solutions. Also, η became nearly constant with temperature (for a given salinity), approaching 100°C. Table D.2 gives the interpolated values of η vs. temperature for a 2% NaCl solution.

Table D.2 Ratio of 2% NaCl Solution Viscosity to Distilled Water Viscosity vs. Temperature

Temperature (°C)	Ratio of 2% NaCl Solution Viscosity to Distilled Water Viscosity, η
18	1.028
25	1.032
40	1.037
60	1.042
80	1.043
100	1.045

A value for η of 1.030 was selected for use at room temperature (around 20°C). For run temperatures near 200°F (93°C) and 300°F (149°C), a value of 1.045 was used. Since η is nearly constant with temperature above 60°C, and the amount of extrapolation is small, use of this single value was believed to be adequate. The amount of viscosity correction that η represents is small. A slightly inaccurate value will have little effect on the actual viscosity. Even were η as high as 1.05 at 150°C, this would represent only a 0.5% error in the viscosity.

D.5 Oil Density

Blandol density vs. temperature was measured from 85°F to 175°F using a 25 cc pycnometer immersed in a temperature-controlled, circulating water bath. Measurements were made by first weighing the pycnometer dry with a Mettler balance to ±0.0001 g. The pycnometer was filled with oil, capped, and then placed in the water bath for an hour. As the temperature increased, oil expanded through the small hole in the pycnometer cap. The pycnometer was removed from the water bath, the outside dried, and then weighed with a Mettler balance. The water bath was then set to a higher temperature and the procedure repeated. By increasing in temperature, oil continually expanded from the pycnometer. Temporary cooling during weighing did not affect the measurements, since the oil mass remained constant.

This procedure was repeated with distilled water to calibrate the pycnometer, since its volume changed with temperature. The following results were obtained:

Table D.3 Measured Blandol Density vs. Temperature

Temperature (°F)	Blandol Density (g/cc)
84.9	0.8415
101.7	0.8346
124.7	0.8264
149.4	0.8176
174.6	0.8085

Chu and Cameron (1963) analyzed the pressure-volume-temperature behavior of a large number of mineral oils and found that over a

temperature range of 32°F to 400°F, all exhibited a constant thermal expansion coefficient. The American Petroleum Institute (API) recommended procedure for correcting oil gravities for temperature [Frick (1962, p.16-8)] is also based on constant thermal expansion coefficients with temperature. Thus, Eq. D.3 was used to match the oil density data and to extrapolate from 84.9°F to room temperature and from 174.6°F to 300°F.

$$\ln(\rho_o) = c0 + c1T \qquad (D.3)$$

where :

ρ_o = oil density, g/cc

T = Temperature, °F

$c_0 = -1.3539 \times 10^{-1}$

$c_1 = -4.42405 \times 10^{-4}$

This equation matches the data within a maximum error of ±0.05%. The thermal expansion coefficient is approximately 4.4×10^{-4} °F^{-1}. The API recommended procedure for correction of oil gravity for temperature as reported by Frick indicates the following:

Table D.4 API Recommended Thermal Expansion Coefficients for Oils Near 35°API Gravity

Range of API Gravity at 60°F	Thermal Expansion Coefficient, °F^{-1}
15.0-34.9	4.0×10^{-4}
35.0–50.9	5.0×10^{-4}

Blandol has a gravity of 35°API at 60°F. Chu and Cameron correlated thermal expansion coefficients with oil viscosity. For Blandol, this correlation predicts a thermal expansion coefficient of 4.3×10^{-4}. Both sources thus indicate that the measured thermal expansion coefficient is reasonable.

D.6 Oil Viscosity

Blandol viscosity vs. temperature was measured from 100°F to 175°F with a Brookfield Model LTV Synchro-Lectric viscometer. A Brookfield Thermosel system was used to control the oil temperature. This system is controlled by a solid-state proportioning controller capable of stable temperature control from 100°F to 572°F (300°C). However, room temperature data was inaccurate using the Thermosel because of problems in maintaining a uniform and constant temperature at low temperature differentials. In addition, data above 175°F exceeded the lower limit of the recommended reading level for the viscometer (10% of full scale). The following data were measured:

Table D.5 Measured Blandol Viscosity vs. Temperature

Temperature (°F)	Viscosity (cp)
100	15.30
125	9.74
150	6.70
175	4.80

The American Society for Testing and Materials (ASTM) pub ishes Standard Viscosity-Temperature Charts for graphing oil viscosities vs.

temperature. On such paper, kinematic viscosity vs. temperature graphs as a straight line. The correlating equation for this chart is given by [Wright (1969)]:

$$\log \log(cSt + 0.6) = A - B \log(T) \qquad (D.4)$$

where:

cSt = kinematic viscosity, centistokes

T = temperature, °R

A,B = constants

Wright (1969) pre ented n improved correlation which replaced the constant 0.6 with a variable that depends on the range of viscosities being correlated. The increased complexity of this improved correlation, however, was not believed to be justified for this study.

Equation D.4 was used to match measured viscosity data (using the density correlating Eq. D.3 to obtain kinematic viscosity from dynamic viscosity). The following parameters were determined:

$$A = 9.8863$$

$$B = 3.5587$$

The equation matched the data to within ±0.6%. The measured data and the equation are shown in Fig. D.2. Figure D.3 shows the measured data and equation plotted on an ASTM Standard Viscosity-Temperature Chart. The oil-water viscosity ratio vs. temperature is also shown on Fig. D.2.

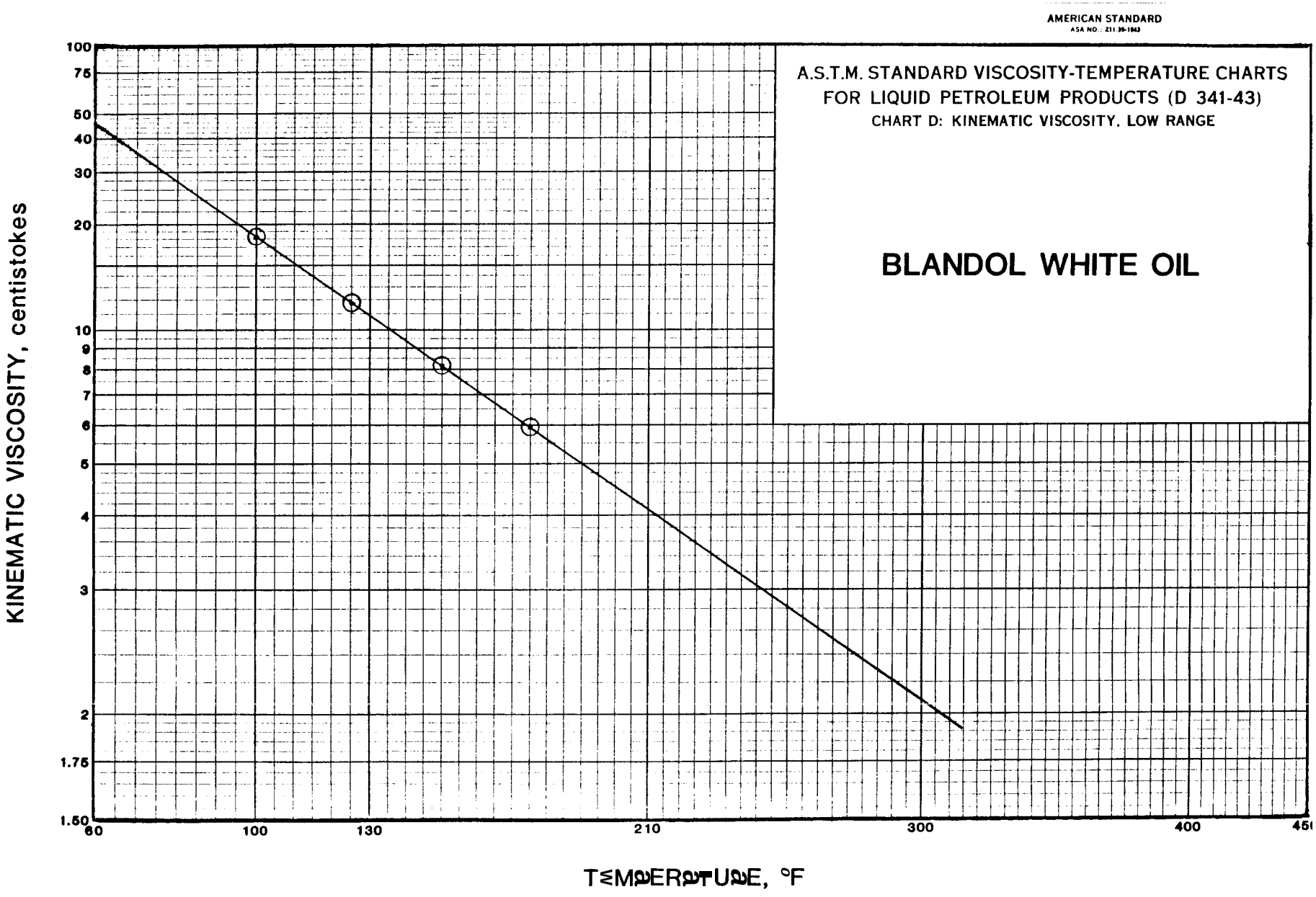

Fig. D.3 Blandol Kinematic Viscosity vs. Temperature on ASTM Standard Viscosity-Temperature Chart

APPENDIX E - DATA ANALYSIS DETAILS

The following raw data were measured from the displacement experiments (symbols in parentheses are used in equations in this section):

a) cumulative separator (produced) volume (Sep), cc

b) cumulative volume of displacing fluid produced from the separator (ΣDv), cc

c) core differential pressure (Ap), psi

d) flowmeter readings - at data point
- average from previous data point

In addition, the following data are also needed to determine recovery and injectivity vs. pore volumes injected:

e) core pore volume (Pv), cc

f) dead volumes, cc - downstream (D)
- upstream (U)

g) core and effluent temperatures, °F

h) oil and water densities vs. temperature

The following sections describe the corrections and calculations used to generate relative permeabilities from the raw data.

E. 1 Dead Volume and Temperature Corrections

Corrections for dead volumes and density changes with temperature were made with the following mass balance calculations. The calculations are for a water displacement run. The same calculations were made for oil displacement, with fluids reversed.

Water:	Initial	$S_{wi}\ Pv\ \rho_{wc}$
	+ In	$+ (W_i Pv + U)\rho_{wc}$
	- out	$- (\Sigma Dv - Sep)\rho_{we}$
	= Final	$(\bar{S}_w Pv + U + D\ f_w)\rho_{wc}$ (E.1)
Oil:	Initial	$[(1-S_{wi})Pv + U + D]\rho_{oc}$
	+ In	0
	- Out	$- Sep\ \rho_{oe}$
	= Final	$[(1-\bar{S}_w)Pv + D(1-f_w)]\rho_{oc}$ (E.2)

where:

S_{wi} = initial core water saturation

$\bar{S}_w$ = average core water saturation

ρ_{wc}, ρ_{oc} = water and oil densities at core temperature

ρ_{we}, ρ_{oe} = water and oil densities at effluent (room) temperature

W_i = pore volumes water injected

f_w = fractional flow of water at outlet

Equations E.1 and E.2 assume that both dead volumes were initially oil-filled and at core temperature (the amount of downstream dead volume at room temperature was small). Also, the relative amounts of oil and water in the downstream dead volume were estimated by the current water fractional flow.

From Eqs. E.1 and E.2, we can derive:

$$\bar{S}_w - S_{wi} = W_i - [(\Sigma Dv - Sep)(\rho_{we}/\rho_{wc}) - D\ f_w]/Pv \qquad (E.3)$$

and,

$$\bar{S}_w - S_{wi} = [Sep(\rho_{oe}/\rho_{oc}) - U - D\ f_w]/Pv \qquad (E.4)$$

Solving for W_i,

$$W_i = \left[Sep\left(\frac{\rho_{oe}}{\rho_{oc}} - \frac{\rho_{we}}{\rho_{wc}}\right) - u + \Sigma Dv \frac{\rho_{we}}{\rho_{wc}}\right]/Pv \qquad (E.5)$$

Since pore volumes of oil recovered, $N_p = \bar{S}_w - S_{wi}$, Eqs. E.4 and E.5 yield the N_p vs. W_i relationship. Total volumetric flowrate and core differential pressure were used directly with Eq. 13.5 to generate the injectivity vs. pore volumes injected data.

E.2 Separator Corrections

Two items were considered to determine accurate data from the separator -- the separator calibration (cc/cm), and a correction for the volume of produced fluid in the bubbles traveling up the water column to the oil-water interface.

The separator calibration section of the computer program used for data analysis (Appendix G) applies calibration information between each data point to compute the incremental produced volume. The method assumes that the average calibration between separator calibration levels (see Appendix B.6) holds for the entire interval. The calculation uses a weighted-average calibration when two measured data levels straddle a calibration level.

Correction for "bubbles" is made by calculating an effective bubble velocity based on the inital static and dynamic separator levels:

$$v_b = \frac{q(h_d - h_o)}{\Delta h(calib)} \qquad (E.6)$$

where:

v_b = average bubble velocity, cm/min

q = total volumetric flowrate, cc/min

h_d = initial dynamic separator level, cm

h_o = level of outlet tube in separator, cm

Δh = difference between initial static and dynamic separator levels, cm

calib = separator calibration, cc/cm

The bubble velocity was assumed to remain constant for any oil-water level in the separator. Thus the following correction was added to the separator volume to consider the amount of oil in the bubbles.

$$\text{Correction} = q\, f_o \frac{(h - h_o)}{v_b} \qquad \text{(E.7)}$$

where:

f_o = fractional flow of oil (in bubbles)

h = separator level, cm

E.3 Flowrate Calculations

The average volumetric flowrate between measurement points was calculated as $\Delta W_i/\Delta t$, where ΔW_i was calculated by the procedure in Appendix E.1. Separator corrections were made using a flowrate calculated from the uncorrected (for bubbles) separator volumes. The fractional flowing volume of displaced phase was also calculated using uncorrected separator data and was estimated by:

$$f_d = 1 - \frac{N_{p_{i+1}} - N_{p_{i-1}}}{W_{i_{i+1}} - W_{i_{i-1}}} \qquad \text{(E.8)}$$

where f_d is the flowing fraction of displaced phase.

Instantaneous flowrates were determined from the capillary tube flowmeter. The average flowrate between measurement points and the average flowmeter reading were used to calculate a flowmeter calibration. This calibration was applied to the flowmeter reading at

the measurement point ("mark" on the strip-chart) to determine the instantaneous flowrate. The flowmeter was thus calibrated continually throughout a run.

E.4 Breakthrough Calculations

Breakthrough times were estimated by visual observation of fluids in the sight glass, combined with the strip-chart records. Differential pressures and flowmeter readings at breakthrough were read from the strip-chart. Pore volumes injected at breakthrough were calculated as that of the measurement before breakthrough, plus the average flowrate multiplied by the elapsed time. Recovery at breakthrough was assumed to be equal to pore volumes injected. Breakthrough flowrate was calculated using the flowmeter calibration between the data points before and after breakthrough.

E.5 Curve Fitting and Relative Permeability Calculations

Recovery and injectivity data were curve fit by least squares methods using the following equations:

$$N_p = a_0 + a_1[\ln(W_i)] + a_2[\ln(W_i)]^2 \qquad \text{(E.9)}$$

$$\ln(W_i I_r) = b_0 + b_1[\ln(W_i)] + b_2[\ln(W_i)]2 \qquad \text{(E.10)}$$

The data point immediately after breakthrough was disregarded in both calculations. This point appeared to have considerable error because of the rapid saturation and flowing volume changes immediately after breakthrough. Differential pressure data sometimes changed unexplainably near the end of certain runs (particularly at elevated temperatures). When this occurred, the questionable injectivity data was ignored. All recovery data was always used.

Relative permeabilities were calculated from the Welge (1952) and Johnson, Bossler, and Naumann (1959) equations:

$$f_o = \frac{d(N_p)}{d(W_i)} = [a_1 + 2a_2 \ln(W_i)]/W_i \qquad \text{(E.11)}$$

$$S_{w2} = S_{wi} + N_p - f_o W_i = S_{wi} + (a_0 - a_1) + (a_1 - 2a_2)\ln(W_i) + a_2[\ln(W_i)]^2 \qquad \text{(E.12)}$$

$$k_{rw}/k_{ro} = (1/f_o - 1)(\mu_w/\mu_o) \qquad \text{(E.13)}$$

$$\frac{f_o}{k_{ro}} = \frac{d\left[\frac{1}{I_r W_i}\right]}{d\left[\frac{1}{W_i}\right]} = \frac{d[\ln(W_i I_r)]}{d[W_i]} \frac{W_i}{I_r} = \frac{[b_1 + 2b_2 \ln(W_i)]W_i}{\exp\{b_0 + b_1 \ln(W_i) + b_2[\ln(W_i)]^2\}} \qquad \text{(E. 14)}$$

Equation E.14 calculates relative permeabilities relative to oil permeability at irreducible water saturation (the relative injectivity base is the injectivity just prior to initiation of water injection). Relative permeabilities were normalized to absolute permeability using the calculated effective oil permeability at irreducible water saturation.

E. 6 End-Point Saturation Calculations

End-point saturations were calculated considering fluid expansion with temperature, but assuming the core pore volume remained constant. The amount of liquid that expanded from the core during heating was also considered. Equations E.15 and E.16 were used to adjust the saturations for temperature changes (core near residual saturation):

$$\bar{S}_{o2} = \bar{S}_{o1} \frac{\rho_{oc1}}{\rho_{oc2}} - \frac{V_e}{Pv} \frac{\rho_{oe}}{\rho_{oc2}} \qquad \text{(E.15)}$$

$$\bar{S}_{w2} = 1 - \bar{S}_{o2} \qquad \text{(E.16)}$$

where :

$\bar{S}_{o1}$ = average oil saturation before temperature change

$\bar{S}_{o2}$ = average oil saturation after temperatuare change

$\bar{S}_{w2}$ = average water saturation after temperature change

ρ_{oc1} = oil density before temperature change, g/cc

ρ_{oc2} = oil density after temperature change, g/cc

ρ_{oe} = oil density at effluent temperature , g/cc

V_e = volume of oil expanded out of the core with heating (zero, if core was cooled), cc

Similar equations were used if heating or cooling was done after an oil displacement run (core at irreducible water saturation).

The end-point saturation following an oil displacement run was calculated by:

$$\bar{S}_{wf} = \bar{S}_{W} - \left[V_p \frac{\rho_{we}}{\rho_{wc2}} - (U+D) \right]/Pv \qquad \text{(E. 17)}$$

where :

$\bar{S}_{wf}$ = final average water saturation

$\bar{S}_{W}$ = initial average water saturation

V_p = water production measured at effluent temperature, cc

ρ_{we} = water density at effluent temperature, g/cc

ρ_{wc2} = water density at core temperature, g/cc

End-point saturations were calculated similarly following a water displacement run.

APPENDIX F - COMPUTER PROGRAM FOR END-POINT SATURATION CALCULATIONS (ENDSAT)

Program ENDSAT calculates end-point saturation changes from displacement runs and from heating and cooling of the core. The equations used are described in Appendix E.6. Fluid property equations are given in Appendix D. ENDSAT was written in BASIC for a Hewlett-Packard 9845B desk-top minicomputer. User instructions, example output, and a program listing are presented in this Appendix.

F.1 Operating Instructions and Flow Chart

The program was written to be self-prompting. The following chart presents the program flow and required input data.

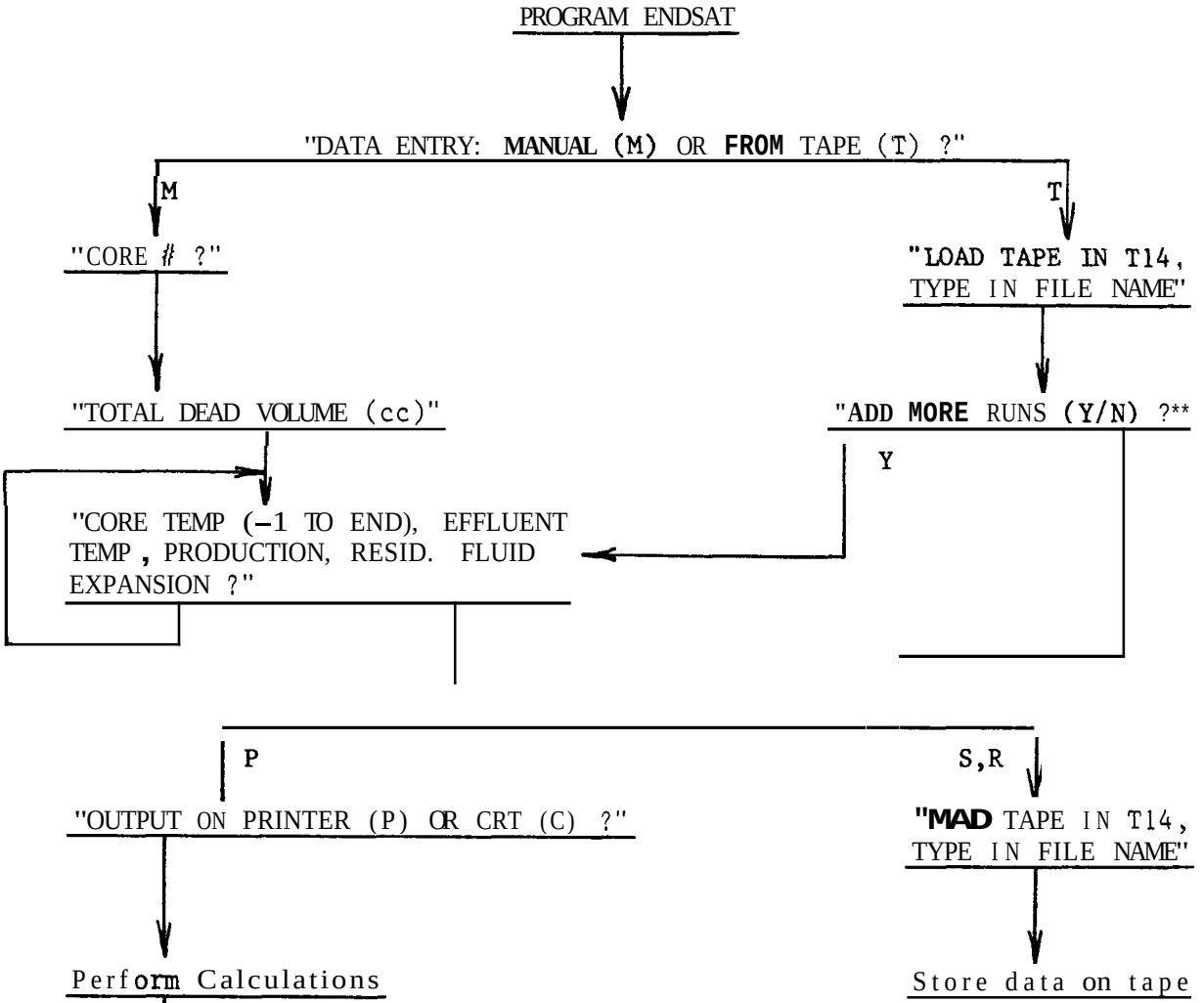
PROGRAM ENDSAT
"DATA ENTRY: MANUAL (M) OR FROM TAPE (T) ?"
M
T
"CORE # ?"
"LOAD TAPE IN T14, TYPE IN FILE NAME"
"TOTAL DEAD VOLUME (cc)"
"ADD MORE RUNS (Y/N) ?**
Y
"CORE TEMP (-1 TO END), EFFLUENT TEMP, PRODUCTION, RESID. FLUID EXPANSION ?"
P
S,R
"OUTPUT ON PRINTER (P) OR CRT (C) ?"
"MAD TAPE IN T14, TYPE IN FILE NAME"
Perform Calculations
Store data on tape
Print Output

F.2 Example Output

CORE # 2
PORE VOLUME 391.2 cc
DEAD VOLUME 5.5 cc

RUN	DISPL FLUID	TEMP (F) CORE	TEMP (F) EFFLU	EXPAN COEFF WHTER	EXPAN COEFF OIL	PROD/EXP(cc) ACTUAL	PROD/EXP(cc) CORE	WATER SAT cc	WATER SAT %	OIL SAT cc	OIL SAT %
				1.0000	1.0000	0.0	0.0	391.2		0.0	0.0
1	OIL	71.0	71.0	1.0000	1.0000	368.3	362.8	28.4	7.3	362.8	
				1.0002	1.0004	0.0	0.0	28.4	7.3	362.8	
	WHTER	72.0	72.0	1.0000	1.0000	295.5	290.0	318.4		72.8	18.6
				.9994	.9985	0.0	0.0	318.5		72.7	18.6
2	OIL	68.5	68.5	1.0000	1.0000	291.9	286.4	32.1	8.2	359.1	
				1.0002	1.0007	0.0	0.0	32.1	8.2	359.1	
	WHTER	70.0	70.0	1.0000	1.0000	286.3	280.8	312.9		78.3	20.8
				1.0359	1.0578	4.5	4.8	313.2		78.0	20.0
3	OIL	197.0	74.0	1.8352	1.0559	272.8	276.9	36.2	9.3	355.0	
				1.0000	1.0000	0.0	0.0	36.2	9.3	355.0	
	WATER	197.0	74.0	1.0352	1.0559	277.9	287.9	324.2		67.0	17.1
				.9653	.9454	0.0	0.8	327.8		63.4	16.2
4	OIL	*70.0*	*70.0*	1.0000	1.0080	298.8	288.3	39.5	10.1	351.7	
				1.0807	1.8018	0.0	0.0	39.6	10.1	351.6	
	WHTEF	74.0	**74.0**	1.0000	1.0000	284.8	279.3	318.9		72.3	18.5
				.9988	.9969	0.0	0.0	319.1		72.1	18.4
5	OIL	67.0	67.0	1.0000	1.0008	291.6	296.1	33.8	8.4	358.2	
				1.0005	1.0813	0.0	0.0	33.0	8.4	358.2	
	WHTEP	70.0	70.0	1.0000	1.0000	283.7	278.2	311.2		80.0	20.4
				1.0872	1.1061	14.3	15.8	3185		72.7	18.6
6	OIL	298.8	**74.0**	1.0864	1.1042	261.1	278.2	48.3	10.3	350.9	
				.9994	.9996	0.0	0.0	40.3	10.3	350.9	
	WATER	*297.0*	74.0	1.0858	1.1037	266.7	288.9	320.2		62.0	15.9

Displacement Run

Temperature Change

F.3 Program Listing

```
10   ! PROGRAM ENDSAT
20    DIM Tc(20),Te(20),Prod(20),Expan(20),Fluid$[5],Ic$[1]
30    INTEGER Core,N
40    N1=0
50    INPUT "DATA ENTRY: MANUAL (M) OR FROM TAPE(T) ?",Ic$
60    IF Ic$="M" THEN GOSUB Man
70    IF Ic$="T" THEN GOSUB Tape
80    INPUT "PRINT (P), STORE (S), OR RE-STORE (R) ?",Ic$
98    IF Ic$="P" THEN GOSUB Calc
100   IF Ic$="S" THEN GOSUB Str
110   IF Ic$="R" THEN GOSUB Rstr
120   GOTO 80
130   ! ************************ MANUAL ENTRY **********************************
140 Man:  INPUT "CORE # ?",Core
150   INPUT "PORE VOLUME (cc) ?",Pv
160   INPUT "TOTAL DEAD VOLUME (cc) ?",Dv
170   FOR I=1 TO 20
180   INPUT "CORE TEMP (-1 TO END), EFFLUENT TEMP, PRODUCTION, RESID. FLUID EXPA
NSION ?",Tc(I),Te(I),Prod(I),Expan(I)
190   IF Tc(I)<0 THEN 220
200   NEXT I
210   PRINT "MORE THAN 20 RUNS"
220   N=I-1
230   RETURN
240   ! ***************************** CALCULATIONS *******************************
250 Calc:   PRINTER IS 16
260   INPUT "OUTPUT ON PRINTER (P) OR CRT (C) ?",Ic$
270   IF Ic$="P" THEN PRINTER IS 0
280   Run=0
290   So=0
300   Sw=Pv
310   Tc(0)=Tc(1)
320   PRINT USING 330;Core,Pv,Dv
330   IMAGE 56X,"CORE #",6X,5D/56X,"POPE VOLUME ",3 .D," cc"/56X,"DEAD VOLUME  "
,2D.D," cc"//
340   PRINT USING 350
350   IMAGE 4X,"DISPL  TEMP (F)  | EXPAN COEFF | PROD/EXP(cc)   WATER
 SRT  |  OIL SAT  "
360   PRINT USING 370
370   IMAGE "HUN FLUID  CORE EFFLU | WATER  OIL   ACTUAL  CORE
  |   cc     %  |  cc     %"/22X,"|",15X,"|",14X," ",13X,"|
380   FOR I=1 TO N STEP 2
390   Run=Run+1
400   Fluid$="OIL"
410   T1=Tc(I)                          ! CURRENT CORE TEMPERATURE
420   T2=Tc(I-1)                        ! PREVIOUS CORE TEMPERRTURE
430   T3=Te(I)                          ! EFFLUENT TEMPERATURE
440   Cto=FNRhoo(T2)/FNRhoo(T1)         ! THERMAL EXPANSION - OIL, RUN TO RUN
450   Ctw=FNRhow(T2)/FNRhow(T1)         ! THERMAL EXPANSION - WATER, RUN TO RUN
460   Ctp=FNRhow(T3)/FNRhow(T1)         ! THERMAL EXPANSION - PRODUCED FLUID
470   Cte=FNRhoo(T3)/FNRhoo(T1)         ! THERMAL EXPANSION - RESIDUAL FLUID
480   Procor=Prod(I)*Ctp-Dv
490   Expcor=Expan(I)*Cte
500   Sol=So*Cto-Expcor
510   Swl=Pv-Sol
520   Sw=Swl-Procor
530   So=Pv-Sw
540   PRINT USING 550; Ctw, Cto, Expan(I),Expcor, Sw1, So1,So1*100/Pv
550   IMAGE 22X,"|",X,D.4D, X, D.4D, X, "|",X,3D.D,2X,3D.D,X,"|",X,3D.D,7X,"|",X,3D.
D,X,3D.D
560   PRINT USING 570;Run,Fluidf,Tc(I),Te(I),Ctp, Cte, Prod(I),Procor,Sw,Sw*100/Pv
,So
570   IMAGE 2D,2X,5A,X,3D.D,X,3D.D, X, "|",X,D.4D,X,D.4D,X,"|",X, 3D.D, 2X, 3D.D, X, "|
",X,3D.D,X,3D.D,X,"|",X,3D.D/22X,"|",15X,"|",14X,"|",13X,"|"
580   J=I+1                             ! T1=PREVIOUS CORE TEMPERATURE
590   IF J>N THEN RETURN
600   Fluid$="WATER"
610   T2=Tc(J)                          ! CURRENT CORE TEMPERATURE
620   T3=Te(J)                          ! EFFLUENT TEMPERATURE
630   Ctw=FNRhow(T1)/FNRhow(T2)         ! THERMAL EXPANSION - WATER, RUN TO RUN
640   Cto=FNRhoo(T1)/FNRhoo(T2)         ! THERMAL EXPANSION - OIL, RUN TO RUN
```

```
658   Ctp=FNRhoo(T3)/FNRhoo(T2)       ! THERMAL EXPANSION - IPRODUCED FLUID
668   Cte=FNRhow(T3)/FNRhow(T2)       ! THERMAL EXPANSION - RESIDUAL FLUID
670   Procor=Prod(J)*Ctp-Dv
680   Expcor=Expan(J)*Cte
690   Swl=Sw*Ctw-Expcor
700   so1=Pv-Swl
710   So=Sol-Procor
720   Sw=Pv-So
730   PRINT USING 740;Ctw,Cto,Expan(J),Expcor,Swl,Swl*100/Pv,Sol
740   IMAGE 22X,"|",X,D.4D,X,D.4D,X,"|",X,3D.D,2X,3D.D,X,"|",X,3D.D,X,3D.D,X,"|"
,X,3D.D
750   PRINT USING 760;Fluid$,Tc(J),Te(J),Cte,Ctp,Prod(J),Procor,Sw,So,So*100/Pv
760   IMACE 4X,5A,X,3D.D,X,3D.D,X,"|",X,D.4D,X,D.4D,X,"|",X,3D.D,2X,3D.D,X,"|",X
,3D.D,7X,"|",X,3D.D,X,3D.D/22X,"|",15X,"|",14X,"|",13X,"|"
770   NEXT I
780   RETURN
790   ! ***************************** READ DATA FROM TAPE **********************
880 Tape:  INPUT "LOAD TAPE IN T14, TYPE IN FILE NAME",If1$
818   RSSIGN #1 TO If1$&":T14"
828   REHD #1;Core,Pv,Dv,N
830   FOR I=1 TO N
848   READ #1;Tc(I),Te(I),Prod(I),Expan(I)
858   NEXT I
860   N1=N
E78   INPUT "HDD MORE RUNS (Y/N) ?",Ic$
888   IF Ic$="N" THEN RETURN
890   FOR I=N+1 TO 28
988   INPUT "CORE TEMP (-1 TO END), EFFLUENT TEMP, PRODUCTION, RESID. FLUID EXPA
NSION ?",Tc(I),Te(I),Prod(I),Expan(I)
918   IF Tc(I)<0 THEN 940
928   NEXT I
938   PRINT "NO MORE THRN 20 RUNS"
948   N=I-1
950   N1=0
968   RETURN
978   ! ************************** STORE DHTA ON TAPE ***************************
980 Str:  INPUT "LOAD TAPE IN T14, TYPE IN FILE NAME",If1$
998   CRERTE If1$&":T14",N+1,32
1088  GOSUB Rstrl
1010  RETURN
1020 Rstr:  IF N1=N THEN Rstrl
1030  PURGE If1$&":T14"
1840  CREATE If1$,":T14",N+1,32
1050 Rstrl:  ASSIGN #1 TO If1$&":T14"
1060  N1=N
1070  PRINT #1;Core,Pv,Dv,N
1088  FOR 1=1 TO N
1090  PRINT #1;Tc(I),Te(I),Prod(I),Expan(I)
1100  NEXT I
1110  PRINT #1;END
1120  ASSIGN #1 TO *
1130  RETURN
1140  END
1158  ! ************************** DENSITY FUNCTIONS ***************************
1160  DEF FNRhow(T)
1170  Rhow=EXP(6.52014E-3-4.34333E-5*T-8.78134E-7*T*T)
1180  RETURN Rhow
1190  FNEND
1200  DEF FNRhoo(T)
1210  Rhoo=EXP(-.13539-4.42405E-4*T)
1220  RETURN Rhoo
1230  FNEND
```

APPENDIX G - COMPUTER PROGRAM FOR ANALYZING DISPLACEMENT DATA AND CALCULATING RELATIVE PERMEABILITY CURVES (DSPCLC)

Program DSPCLC calculates recovery and relative injectivity vs. pore volumes injected from the raw data collected from a displacement run. The equations used are outlined in Appendixes E.1 through E.4. Fluid property equations are described in Appendix D. DSPCLC curve matches the recovery and injectivity data and calculates relative permeability relationships using equations outlined in Appendix E.5.

DSPCLC was written in BASIC for a Hewlett-Packard 9845B desk-top minicomputer. The program utilizes the plotting capabilities of the computer to generate hard-copy graphs of recovery and injectivity times pore volumes injected vs. pore volumes injected and vs. the reciprocal of pore volumes injected, the logarithm of relative permeability ratio vs. water saturation, and relative permeabilities vs. water saturation.

User instruction, example output, and a program listing are presented in this Appendix.

G.1 Operating Instructions and Flow Chart

The program was written to be self-prompting. The following chart presents the program flow and required input data.

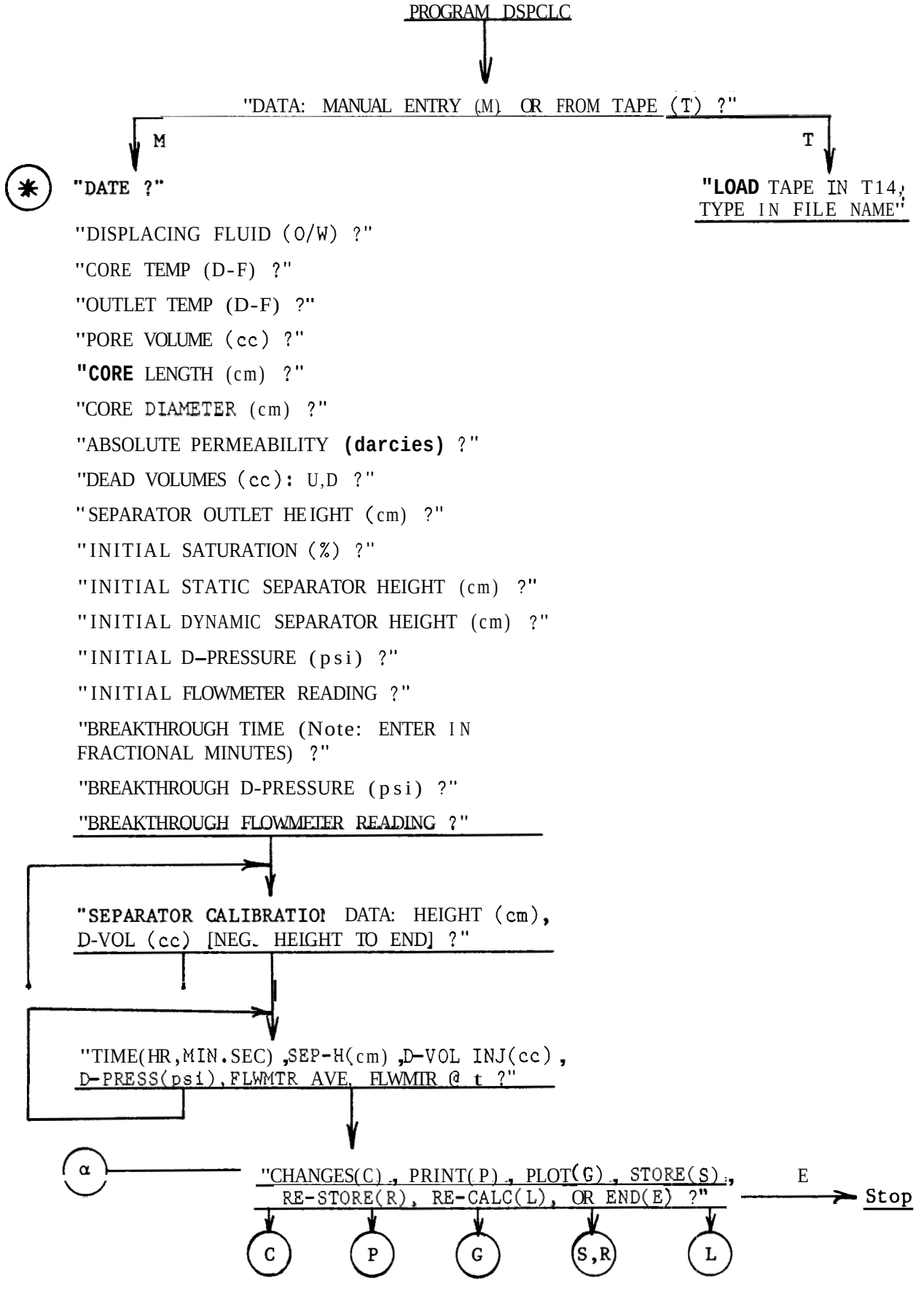
PROGRAM DSPCLC
"DATA: MANUAL ENTRY (M) OR FROM TAPE (T) ?"
M
T
"DATE ?"
"LOAD TAPE IN T14; TYPE IN FILE NAME"
"DISPLACING FLUID (O/W) ?"
"CORE TEMP (D-F) ?"
"OUTLET TEMP (D-F) ?"
"PORE VOLUME (cc) ?"
"CORE LENGTH (cm) ?"
"CORE DIAMETER (cm) ?"
"ABSOLUTE PERMEABILITY (darcies) ?"
"DEAD VOLUMES (cc): U,D ?"
"SEPARATOR OUTLET HEIGHT (cm) ?"
"INITIAL SATURATION (%) ?"
"INITIAL STATIC SEPARATOR HEIGHT (cm) ?"
"INITIAL DYNAMIC SEPARATOR HEIGHT (cm) ?"
"INITIAL D-PRESSURE (psi) ?"
"INITIAL FLOWMETER READING ?"
"BREAKTHROUGH TIME (Note: ENTER IN FRACTIONAL MINUTES) ?"
"BREAKTHROUGH D-PRESSURE (psi) ?"
"BREAKTHROUGH FLOWMETER READING ?"
"SEPARATOR CALIBRATION DATA: HEIGHT (cm), D-VOL (cc) [NEG. HEIGHT TO END] ?"
"TIME(HR,MIN.SEC),SEP-H(cm),D-VOL INJ(cc), D-PRESS(psi),FLWMTR AVE, FLWMTR @ t ?"
α
"CHANGES(C), PRINT(P), PLOT(G), STORE(S), RE-STORE(R), RE-CALC(L), OR END(E) ?"
E
Stop
C
P
G
S,R
L

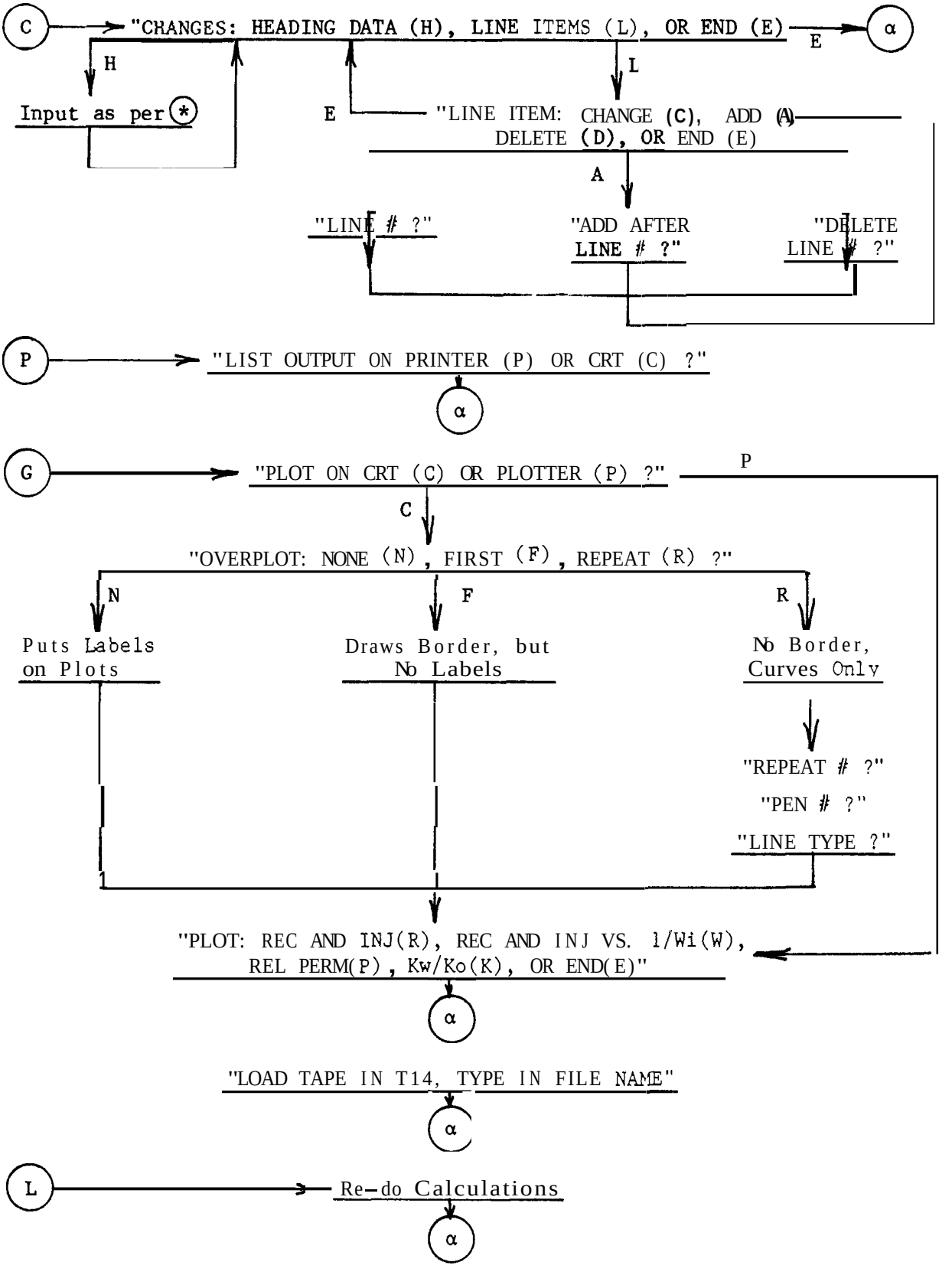
C
"CHANGES: HEADING DATA (H), LINE ITEMS (L), OR END (E)
E
α
H
L
Input as per (*)
E
"LINE ITEM: CHANGE (C), ADD (A)
DELETE (D), OR END (E)
A
"LINE # ?"
"ADD AFTER
LINE # ?"
"DELETE
LINE # ?"
P
"LIST OUTPUT ON PRINTER (P) OR CRT (C) ?"
α
G
"PLOT ON CRT (C) OR PLOTTER (P) ?"
P
C
"OVERPLOT: NONE (N), FIRST (F), REPEAT (R) ?"
N
F
R
Puts Labels
on Plots
Draws Border, but
No Labels
No Border,
Curves Only
"REPEAT # ?"
"PEN # ?"
"LINE TYPE ?"
"PLOT: REC AND INJ(R), REC AND INJ VS. 1/Wi(W),
REL PERM(P), Kw/Ko(K), OR END(E)"
α
"LOAD TAPE IN T14, TYPE IN FILE NAME"
α
L
Re-do Calculations
α

G.2 Example Output

OIL DISPLACEMENT RUN

DISPLACEMENT EXPERIMENT CALCULATIONS

FORE VOLUME	391.2	cc	DATE	10/12/82	
CORE LENGTH	51.47	cm	CORE/RUN	2/1	
CORE DIAMETER	5.844	cm	DISPLACEMENT	OIL-Dist W	
DEAD VOL'S: U	2.5	cc	CORE TEMPERATURE	71.0	F
D	3.0	cc	OUTLET TEMPERATURE	71.8	F
SEPARATOR OUTLET	82.72	cm	WATER VISCOSITY	.966	cp
BUBBLE VELOCITY	0.00	cm/sec	OIL VISCOSITY	29.08	cp
ABSOLUTE PERM	7.060	darcies	VISCOSITY RATIO	38.11	
INIT SAT - OIL	0.0	%	WATER DENSITY PATIO	1.0000	
FINHL SAT - WATER	7.3	%	OIL DENSITY RATIO	1.0880	

	TIME	SEFAPATOR HEIGHT	CALIB	D-VOL INJ	D-F	FLOWRATE CHART			cc	PVi	Rec	1/Inj
	(min)	(cm)	(cc/cm)	(cc)	(psi)	AVG	Et.	CHL	min			
ST		81.80										
0	0.00	81.86	4.99	0.0	1.95	.607	.607	37.2	22.6	0.000	.000	1.00
1	4.97	62.50	4.99	96.0	28.40	.559	.510	37.2	19.0	.239	.240	12.45
2	10.62	41.58	4.99	104.8	43.28	.499	.488	37.2	18.1	.507	.508	27.56
3	17.25	18.88	4.99	117.3	65.88	.475	.462	37.2	17.2	.807	.802	44.27
BT	19.15				72.68		.458	37.2	17.8	.888	.888	49.31
4	45.30	8.00	4.99	470.6	65.40	.451	.450	37.2	16.7	2.010	.927	45.21

Krw - INITIAL = .999
Kro - FINAL = .665

WATER DISPLACEMENT RUN

DISPLACEMENT EXPERIMENT CALCULATIONS

PORE VOLUME	391.2 cc	DATE	18/12/82
CORE LENGTH	51.47 cm	CORE/RUN	2/1
CORE DIAMETER	5.044 cm	DISPLACEMENT	Dist W-OIL
DEAD VOL'S: U	2.5 cc	CORE TEMPERATURE	72.0 F
D	3.0 cc	OUTLET TEMPERATURE	72.0 F
SEPARATOR OUTLET	82.72 cm	WATER VISCOSITY	.953 cp
BUBBLE VELOCITY	7.58 cm/sec	OIL VISCOSITY	28.37 cp
ABSOLUTE PERM	7.060 darcies	VISCOSITY RATIO	29.77
INIT SAT - WHTER	7.3 %	WATER DENSITY RATIO	1.0000
FINAL SAT - OIL	18.6 %	OIL DENSITY RATIO	1.0000

	TIME	SEPHRHTOR HEIGHT	SEPHRHTOR CALIB	D-VOL INJ	D-P	FLOWRATE CHART AVG	CHART @t	CHART CAL	cc/min	PVi	Rec	Inj
	(min)	(cm)	(cc/cm)	(cc)	(psi)							
ST		8.00										
0	0.80	7.40	4.96	0.0	66.10	.440	.440	40.3	17.7	8.008	.000	1.08
1	4.55	26.80	4.96	95.9	49.96	.516	.531	40.3	21.4	.239	.238	1.60
ET	8.61				22.50		.554	40.3	22.3	.466	.466	3.70
2	9.02	46.80	4.89	97.6	20.70	.542	.554	40.3	22.3	.488	.472	4.02
3	13.18	50.95	4.88	93.0	13.40	.566	.570	40.2	22.9	.726	.528	6.38
4	17.22	53.00	4.88	94.4	11.30	.570	.571	40.2	23.0	.967	.553	7.58
5	21.25	54.60	4.88	93.0	9.93	.571	.571	40.4	23.1	1.205	.572	8.65
6	25.08	55.80	4.88	88.2	*9.08*	.571	.571	40.3	23.0	1.430	.587	9.44
7	29.50	57.00	4.88	101.0	8.33	.571	.572	40.0	22.9	1.689	.602	10.25
8	33.45	56.00	4.88	92.1	7.80	.572	.571	40.8	23.3	1.924	.614	11.12
9	37.30	58.75	4.88	89.2	7.33	.571	.571	40.6	23.2	2.152	.624	11.78
10	41.27	59.35	4.88	92.0	6.88	.570	.570	40.7	23.2	2.387	.631	12.56
11	45.12	60.00	4.88	90.0	6.55	.570	.570	41.0	23.4	2.617	.639	13.38
12	49.02	60.67	4.88	91.2	6.28	.570	.570	41.0	23.4	2.850	.648	13.88
13	53.09	61.18	4.88	92.4	6.85	.570	.570	40.7	23.2	3.087	.654	14.29
14	**56.93**	61.72	4.88	91.3	5.88	.570	.569	40.7	23.2	3.320	.661	14.68
15	68.97	62.20	4.88	93.1	5.78	.569	.568	40.6	23.0	3.558	.667	15.06
16	64.93	62.60	4.88	92.2	5.58	.567	.567	41.0	23.2	3.794	.672	15.75
17	85.58	64.35	4.88	478.0	4.83	.565	.563	41.0	23.1	5.016	.693	17.80
18	185.92	65.70	4.88	471.0	4.38	.562	.561	41.2	23.1	6.220	.710	19.67
19	126.85	66.82	4.88	483.0	-.00	.560	.560	41.2	23.1	7.454	.724	-.00
20	147.38	67.50	4.88	475.0	-.00	.558	.556	41.5	23.1	8.668	.733	-.08
21	166.27	68.21	4.68	482.0	-.00	.554	.552	41.7	23.0	9.901	.741	*-.00*

CURVE FITS	C0	C1	c2	%E-MAX	%E-AVG
Recovery	5.5606E-01	9.1831E-02	-4.4486E-03	.3	.1
Inj. X Pore Vol. Inj.	2.0443E+00	1.5914E+00	-4.3987E-02	1.5	.6

	PVi	R-ACT	R-CALC	R-%E	I*P-ACT	I*P-CALC	I*P-%E	Sw	Krw	Kro	Kw/Ko
								.073	0.000	.680	0.006
BT		.466	.488		1.72	2.41					
3	.726	.528	.526	.3	4.63	4.62	.3	.505	.078	.349	.224
4	.967	.553	.553	.1	7.33	7.32	.0	.534	.098	.308	.319
5	1.205	.572	.573	.1	10.43	10.38	.5	.556	.116	.278	.415
6	1.430	.587	.588	.2	13.51	13.58	.5	.573	.130	.257	.508
7	1.689	.602	.603	.1	17.30	17.57	1.5	.589	.146	.236	.617
8	1.924	.614	.614	.0	21.40	21.48	.4	.601	.159	.221	.718
9	2.152	.624	.624	.0	25.35	25.49	.5	.612	.171	.209	.817
10	2.387	.631	.633	.2	29.99	29.84	.5	.622	.182	.198	.920
11	2.617	.639	.640	.2	34.81	34.29	1.5	.630	.192	.188	1.022
12	2.850	.648	.647	.0	39.55	38.98	1.4	.638	.202	.180	1.127
13	3.087	.654	.654	.0	44.10	43.91	.4	.645	.212	.172	1.234
14	3.320	.661	.660	.1	48.75	48.94	.4	.652	.221	.165	1.341
15	3.558	.667	.665	.2	53.68	54.23	1.2	.658	.230	.159	1.450
16	3.794	.672	.671	.1	59.74	59.62	.2	.664	.238	.153	1.560
17	5.016	.693	.693	.1	89.25	89.67	.5	.688	.278	.130	2.141
18	6.220	.710	.709	.2	122.35	122.24	.1	.706	.310	.114	2.731
19	7.454	.724	.723	.2	-.00	-.00	-.0	.722	-.000	-.000	3.352
20	8.668	.733	.734	.1	-.00	-.00	-.0	.734	-.000	-.000	3.976
21	9.901	.741	.743	.2	-.00	-.00	-.0	.745	-.000	-.000	4.622

G.3 Program Listing

```
10    ! PROGRAM DSPCLC
20    DIM Date$[10],Fluid$[10],Fld$[5],Fldd$[5],Core$[10],Ic$[1],Id$[1],Ifl$[6],
If$[1],Ia$[1],Ii$[1],Iwtyp$[1],Wat$[6]
30    DIM Time(100),Tim(100),Seph(100),Tbcal(100),Op(100),Cop(100),Delv(100),Fma
vg(100),Fmt(100),Fmc(100),Dp(100),Q(100),Wi(100),Rec(100),Inj(100)
40    DIM Hs(7),Dvs(7),Hsc(7),Dvsc(7),Tbsc(7),Pctr(100),Pctp(100)
50    DIM S(100),Krw(100),Kro(100),Kwko(100) Drr(2),Drp(2),Ar(2,2),Ap(2,2),Ai(2,
2),Br(2),Bp(2)
60    COM Cr(2),Cp(2)
70    INTEGER N,Nsc
80    !          PAPER TYPE (1 = 8.5x11, 2 = 11x12.5)
90    Paper=1
100   !          FEN FOR BORDER
110   Pb=1
120   !          BASE RELATIVE PERMEABILITY  0=Absolute, 1=Ko@Swi>
130   Ibs=0
140   !          PLOTTING SPEED
150   Spd=36
160   Ltype=1
170   DEG
180   Del=2
190   Nv=2
200   Flag=0
210   PRINTER IS 16
220   PRINT PAGE
230   INFUT "DATA:  MANUAL ENTRY (M) OR FROM TAPE (T) ?",Id$
240   IF Id$="T" THEN GOSUB Tape
250   IF Id$="M" THEN GOSUB Man
260   INPUT "CHANGES(C), PRINT(P), PLOT(G), STORE(S), RE-STORE(R), RE-CALC(L), O
R END(E) ?",Id$
270   IF Id$="E" THEN STOP
280   IF Id$="C" THEN GOSUB Chg
290   IF Id$="P" THEN GOSUB Prnt
300   IF Id$="G" THEN GOSUB Plot
310   IF Id$="S" THEN GOSUB Str
320   IF Id$="R" THEN GOSUB Rstr
330   IF Id$="L" THEN GOSUB Calc
340   GOTO 260
350   ! ******************************** INPUT NEW DATA ************************
360 Man:   GOSUB 380
370   GOTO 710
380   INPUT "DATE ?",Date
390   INPUT "CORE/RUN ?",Core$
400   INPUT "DISPLACING FLUID (O/W) ?",If$
410   INPUT "WATER TYPE (D=DISTILLED, S=SALT) ?",Iwtyp$
420   INPUT "CORE TEMP (D-F) ?",Tc
430   INPUT "OUTLET TEMP (D-F) ?",Te
440   INPUT "PORE VOLUME (cc) ?",Pv
450   INPUT "CORE LENGTH (cm) ?",Lc
460   INFUT "CORE DIAMETER (cm) ?",Dc
470   INPUT "ABSOLUTE PERMEABILITY (darcies) ?",Kabs
480   INPUT "DEAD VOLUMES (cc): U,D  ?",U,D
490   INPUT "SEPARATOR OUTLET HEIGHT (cm) ?",Ho
500   INPUT "INITIAL SATURATION (%) ?",Sati
510   INPUT "INITIRL STATIC SEPARATOR HEIGHT (cm) ?",Seps
520   INPUT "INITIRL DYNAMIC SEPARATOR HEIGHT (cm) ?",Seph(0)
530   INPUT "INITIAL D-PRESSURE (psi) ?",Dp(0)
540   INPUT "INITIAL FLOWMETER READING ?",Fmt(0)
550   INPUT "BREAKTHROUGH TIME (Note:  ENTER IN FRACTIONAL MINUTES) ?",Tbt
560   INPUT "BRERKTHROUGH D-PRESSURE (psi) ?",Dpbt
570   INPUT "BREAKTHROUGH FLOWMETER READING ?",Fmbt
580   PRINTER IS 16
590   PRINT USING 600
600   IMAGE 6X,"Hs",5X,"Dvs"/
610   FOR I=0 TO 6
620   INPUT "SEPARATOR CALIBRATION DATA:  HEIGHT (cm), D-VOL (cc) [NEG. HEIGHT T
O END] ?",Hs(I),Dvs(I)
630   IF Hs(I)<0 THEN 690
640   PRINT USING "D,2X,3D.2D,2X,3D.D";I,Hs(I),Dvs(I)
650   NEXT I
660   PRINT "MAX NUMBER (6) OF CALIBRATION DATA REACHED"
```

```
670   BEEP
680   I=6
690   Nsc=I-1
700   RETURN
710   PRINT "       Time   Seph   Delv     Dp   Fmavg    Fmt"
720   PRINT USING "4X,4D.2D,2X,2D.2D,8X,3D.3D,9X,D.3D";Time(0),Seph(0),Dp(0),Fmt
(0)
730   N=0
740   FOR 1=1 TO  00
750   INPUT "TIME(HR,MIN.SEC),SEP-H(cm),D-VOL INJ(cc),D-PRESS(psi),FLWMTR AVC, FL
WMTR @ t,?",Time(I),Seph(I),Delv(I),Dp(I),Fmavg(I),Fmt(I)
760   IF Time(I)<0 THEN 840
770   N=N+1
780   PRINT USING 790;I,Time(I),Seph(I),Delv(I),Dp(I),Fmavg(I),Fmt(I)
796   IMAGE 2D,2X,4D.2D,2X,2D.2D,2X,3D.D,X,3D.3D,2X,D.3D,2X,I. 3D
800   BEEP
810   NEXT I
820   PRINT "MORE THAN 10U DATA POINTS"
830   BEEP
840   RETURN
850   ! ********************** CHANGES ************************************
866 Chg:  INPUT "CHHNGES: HEADING DATA (H), LINE ITEMS (L), OR END (E) ?",Id$
870   IF Id$="E" THEN 1250
880   IF Id$="L" THEN 910
890   GOSUB 380
900   GOTO 860
910   INPUT "LINE ITEM: CHANGE (C), ADD (A), DELETE ID),  OR END (E) ?",Id$
920   IF Id$="E" THEN 860
938   IF Id$="C" THEN 960
940   IF Id$="A" THEN 1000
950   IF Id$="D" THEN 1140
960   INPUT "LINE # ?",I
970   INPUT "TIME,SEP-H,D-VOL,D-PRESS,FLOWMTR-AVG,FLOWMTR@t",Time(I),Seph(I),Del
v(I),Dp(I),Fmavg(I),Fmt(I)
980   PRINT USING 790;I,Time(I),Seph(I),Delv(I),Dp(I),Fmavg(I),Fmt(I)
990   GOTO 910
1000  INPUT "ADD AFTER LINE # ?",Iadd
1010  N=N+1
1020  FOR I=N TO Iadd+2 STEP -1
1030  Time(I)=Time(I-1)
1840  Seph(I)=Seph(I-1)
1050  Delv(I)=Delv(I-1)
1060  Dp(I)=Dp(I-1)
1070  Fmavg(I)=Fmavg(I-1)
1080  Fmt(I)=Fmt(I-1)
1090  NEXT I
1100  I=Iadd+1
1110  INPUT "TIME,SEP-H,D-VOL D-PRESS FLOWMTR-AVG,FLOWMTR@t",Time(I), Seph(I),Del
v(I),Dp(I),Fmavg(I),Fmt(I)
1120  PRINT USING 790;I,Time( ),Seph( ),Delv(I), Dp(I), Fmavg(I),Fmt(I)
1130  GOTO 910
1140  INPUT "DELETE LINE # ?" Idel
1150  FOR I=Idel TO N-1
1160  Time(I)=Time(I+1)
1170  Seph(I)=Seph(I+1)
1180  Delv(I)=Delv(I+1)
1190  Dp(I)=Dp(I+1)
1200  Fmavg(I)=Fmavg(I+1)
1210  Fmt(I)=Fmt(I+1)
1220  NEXT I
1230  N=N-1
1240  GOTO 910
1250  F1ag=0
1260  RETURN
1270  ! ********************** STORE DHTA ON TAPE ****************************
1280 Str:  ON ERROR GOTO El
1290  INPUT "LOAD TAPE IN T14, TYPE IN FILE NAME",If1$
1300  CREATE If1$&":T14",6+N,56
1310  GOSUB Rstr
1320  OFF ERROR
1330  RETURN
```

```
1340 El: BEEF
1350  DISP "NAME UNACCEPTABLE ----- ";
1360  GOTO 1290
1370 Rrtr: ASSIGN #1 TO If1$&":T14"
1380  PRINT #1;Date$,Core$,If$,N,Nsc,Dpbt
139b  PRINT #1;Tc,Te,Pv,Lc,Dc,Tbt,Fmbt
1400  PRINT #1;Ho,Kabs,U,D,Seps,Sat1,Iwtyp$
1410  PRINT #1;Hs(*)
1420  PRINT #1;Dvs(*)
1430  FOR 1=0 TO N
1440  PRINT #1;Time(I),Seph(I),Delv(I),Dp(I),Fmavg(I),Fmt(I)
1450  NEXT I
1460  PRINT #1;END
1470  ASSIGN #1 TO •
1480  RETURN
1490  ! ****************** READ DATH FROM TAPE **********************
1500 Tape: INPUT "LOAD TAPE IN T14, TYPE IN FILE NAME",If1$
1510  ASSIGN #1 TO If1$&":T14"
1520  REHD #1;Date$,Core$,If$,N,Nsc,Dpbt
1530  REHD #1;Tc,Te,Pv,Lc,Dc,Tbt,Fmbt
1548  READ #1;Ho,Kabs,U,D,Seps,Sati,Iwtyp$
1550  READ #1;Hs(*)
1560  READ #1;Dvs(*)
1570  FOR 1=0 TO N
1580  READ #1;Time<I),Seph(I),Delv(I),Dp(I),Fmavg(I),Fmt(I)
1590  NEXT I
1600  RETURN
1610  ! ************************** CALCULHTIONE ****************************
1620 Calc: Ck=4*Lc/(PI*Dc*Dc*4.0827)
1630  Iwt=1
1640  Wat$="Dist W"
1650  IF Iwtyp$="D" THEN 1688
1660  Iwt=2
1670  Wat$="Salt W"
1680  CALL Watp(Tc,Rhow,Muw,Iwt)
1690  CALL Oilp(Tc,Rhoo,Muo)
1700  CALL Watp(Te,Rhowe,M,Iwt)
1710  CALL Oilp(Te,Rhooe,M)
1720  Drw=Rhowe/Rhow
1730  Dro=Rhooe/Rhoo
1740  Mur=Muo/Muw
1750  IF If$="O" THEN 1810
1760  Fld$="WATER"
1770  Fluid$=Wat$&"-0IL"
1780  Drd=Drw
1790  Dre=Dro
1800  GOTO 1850
1810  Fluid$="0IL-"&Wat$
1820  Fld$="OIL"
1830  Drd=Dro
1840  Dre=Drw
1850  Time(0)=0
1860  Fmavg(0)=Fmt(0)
1870  Delv(0)=0
1880  Tim(0)=0
1890  Cop(0)=0
1900  Wi(0)=0
1910  Rec(0)=0
1920  Inj(0)=1
1930  !                          SEPARATOR CALIBPHTION
1940  Op(0)=0
1950  FOR I=1 TO N
1960  Op(I)=ABS(Seph(I)-Seps)
1970  NEXT I
1980  IF Hs(Nsc)-Seps>20 THEN 2100
1990  Sign=1
2000  IF Seps>Hs(1) THEN Sign=-1
2010  FOR I=0 TO Nsc-1
2020  Hsc(Nsc-I)=Sign*(Hs(I)-Seps)
2036  Tbsc(Nsc-I)=Dvs(I+1)/ABS(Hs(I)-Hs(I+1))
2040  NEXT I
```

```
2050  IF Nscil THEN 2080
2060  Hsc(1)=Sign*(Hs(0)-Seps)
2070  Tbsc(1)=Dvs(1)/ABS(Hs(0)-Hs(1))
2080  Hsc(0)=Sign*(Hs(Nsc)-Seps)
2090  GOTO 2150
2100  FOR I=1 TO Nsc
2110  Hsc(I)=Hs(I)-Seps
2120  Tbsc(I)=Dvs(I)/ABS(Hs(I)-Hs(I-1))
2130  NEXT I
2140  Hsc(0)=Hs(0)-Seps
2150  Tbsc(0)=Tbsc(1)
2160  FOR I=1 TO Nsc
2170  IF Hsc(I)>0 THEN 2190
2180  NEXT I
2190  Is=I-1
2200  IF Nsc=1 THEN Is-0
2210  Hsc(Is)=0
2220  FOR I=Nsc-1 TO 0 STEP -1
2230  IF Hsc(I)<Op(N) THEN 2250
2240  NEXT I
2250  If=I+1
2260  Hsc(If)=Op(N)
2270  J=1
2280  FOR I=Is+1 TO If
2290  IF Op(J)>Hsc(I) THEN 2340
2300  Tbcal(J)=Tbsc(I)
2310  J=J+1
2320  IF J<=N THEN 2290
2330  J=N
2340  Dop=(Hsc(I)-Op(J-1))*Tbsc(I)
2350  FOR K=I+1 TO If
2360  IF Hsc(K)>Op(J) THEN 2400
2370  Dop=Dop+(Hsc(K)-Hsc(K-1))*Tbsc(K)
2380  NEXT K
2390  GOTO 2410
2400  Dop=Dop+(Op(J)-Hsc(K-1))*Tbsc(K)
2410  IF Op(J)=Op(J-1) THEN Op(J-1)=Op(J)-.000131
2420  Tbcal(J)=Dop/(Op(J)-Op(J-1))
2430  I=K-1
2440  J=J+1
2450  NEXT I
2460  Tbcal(0)=Tbcal(1)
2470  !                                   BUBBLE CORRECTION
2480  Qo=Fmt(0)*Delv(1)/FNTcon(Time(1))/Fmavg(1)
2490  Vbi=1/(Qo*ABS(Seph(0)-Ho))*ABS(Seph(0)-Seps)*Tbcal(0)
2500  !
2510  Sdv=0
2520  Ni=N
2530  FOR I=1 TO N
2540  Tim(I)=FNTcon(Time(I))
2550  Dt=Tim(I)-Tim(I-1)
2560  Sdv=Sdv+Delv(I)
2570  Cop(I)=Cop(I-1)+(Op(I)-Op(I-1))*Tbcal(I)
2580  Wi(I)=(Cop(I)*(Dre-Drd)-U+Sdv*Drd)/Pv
2590  Qavg=(Wi(I)-Wi(I-1))*Pv/Dt
2600  Fmc(I)=Qavg/Fmavg(I)
2610  Q(I)=Fmt(I)*Fmc(I)
2620  NEXT I
2630  Fmc(1)=Fmc(2)
2640  Q(1)=Fmc(1)*Fmt(1)
2650  Fmc(0)=Fmc(1)
2660  Q(0)=Fmc(0)*Fmt(0)
2670  Inji=Q(0)/Dp(0)
2680  FOR I=1 TO N
2690  IF Dp(I)>0 THEN 2730
2700  Dp(I)=-.0001
2710  Inj(I)=-.0001
2720  GOTO 2740
2730  Inj(I)=Q(I)/Dp(I)/Inji
2740  Qdqt=1
2750  IF I<N THEN Qdqt=1-(Cop(I+1)-Cop(I-1))*Dre/(Wi(I+1)-Wi(I-1))/Pv
```

```
2760  Cop(I)=Cop(I)+(1-Qdqt)*Q(I)*ABS(Seph(I)-Ho)*Vbi
2770  Rec(I)=(Cop(I)*Dre-U-D*Qdqt)/Pv
2780  NEXT I
2790  FOR I=1 TO N
2800  IF Tim(I)>Tbt THEN 2820
2810  NEXT I
2820  Isabt=I
2830  Isc=Isabt+1
2840  Fmcbt=Fmc(I)
2850  Qbt=Fmbt*Fmcbt
2860  Wibt=Wi(I-1)+(Wi(I)-Wi(I-1))*(Tbt-Tim(I-1))/(Tim(I)-Tim(I-1))
2870  Recbt=Wibt
2880  Injbt=Qbt/Dpbt/Inji
2890  Satf=(1-Rec(N))*100-Sati
2900  IF If$="0" THEN 3490
2910  !                                   CURVE FIT CALCULATIONS
2920  MAT Cr=ZER
2930  MAT Cp=ZER
2940  MAT Br=ZER
2950  MAT Bp=ZER
2960  MAT Ar=ZER
2970  MRT Ap=ZER
2980  FOR I=Isc TO N
2990  FOR K=O TO Nu
3000  Drr(K)=LOG(Wi(I))^K
3010  Drp(K)=LOG(Wi(I))^K
3020  Br(K)=Br(K)+Rec(1)*Drr(K)
3030  IF Inj(I)>0 THEN Bp(K)=Bp(K)+LOG(Wi(I)*Inj(I))*Drp(K)
3040  NEXT K
3050  FOR K=0 TO Nu
3060  FOR L=K TO Nu
3070  Ar(K,L)=Ar(K,L)+Drr(K)*Drr(L)
3080  IF Inj(I)>0 THEN Ap(K,L)=Ap(K,L)+Drp(K)*Drp(L)
3090  NEXT L
3100  NEXT K
3110  NEXT I
3120  FOR K=O TO Nu
3130  FOR L=K+1 TO Nu
3140  Ar(L,K)=Ar(K,L)
3158  Ap(L,K)=Ap(K,L)
3160  NEXT L
3170  NEXT K
3180  MAT Ai=INV(Ar)
3190  MAT Cr=Ai*Br
3200  MAT Ai=INV(Ap)
3210  MAT Cp=Ai*Bp
3220  Pctmr=0
3230  Pctmp=0
3240  Spctr=0
3250  spctp=0
3260  FOR I=Isc TO N
3270  Rc=FNFr(Wi(I),1)
3280  Pctr(I)=ABS(Rc-Rec(I))*100/Rec(I)
3290  Spctr=Spctr+Pctr(I)
3300  IF Pctr(I)<Pctmr THEN 3340
3310  Pctmr=Pctr(I)
3320  Imr=I
3330  Rm=Rc
3340  IF Inj(I)<0 THEN 3450
3350  Ni=I
3360  Injc=Wi(I)*FNFi(Wi(I),1)
3370  Winjc=Wi(I)*Inj(I)
3380  Pctp(I)=ABS(Injc-Winjc)*100/Winjc
3390  spctp=Spctp+Pctp(I)
3400  IF Pctp(I)<Pctmp THEN 3460
3410  Pctmp=Pctp(I)
3420  Imp=I
3430  Injm=Injc
3440  GOTO 3460
3450  Pctp(I)=-.001
3460  NEXT I
```

```
3470  Pctar=Spctr/(N-Isabt+1)
3480  Pctap=Spctp/(Ni-Isabt+1)
3490  IF If$="0" THEN 3530    .
3500  Ko=Ck*Q(0)*Muo/Dp(0)
3510  Kw=Ck*Q(Ni)*Muw/Dp(Ni)
3520  GOTO 3550
3530  Kw=Ck*Q(0)*Muw/Dp(0)
3540  Ko=Ck*Q(Ni)*Muo/Dp(Ni)
3558  Kroswi=1
3560  IF Ibs=0 THEN Kroswi=Ko/Kabs
3570  IF If$="0" THEN 3800
3580  FOR I=Isc TO N                        ! REL PERM CALCS
3590  W=Wi(I)
3600  R=FNFr(W,1)
3610  Fo=FNFr(W,2)
3620  IF Fo>0 THEN 3680
3630  Kwko(I)=9999.999
3640  S(I)=-.999
3650  Kro(I)=0
3660  Krw(I)=1
3670  GOTO 3790
3680  Kwko(I)=(1/Fo-1)/Mur
3690  S(I)=Sati/100+R-Fo*W
3768  IF Inj(I)>0 THEN 3746
3710  Kro(I)=-.0001
3728  Krw(I)=-.0001
3730  GOTO 3780
3740  Ir=FNFi(W,1)
3750  Dirdw=FNFi(W,2)
3760  Kro(I)=Fo/Dirdw*Kroswi
3770  KrW(I)=Kwko(I)*Kro(I)
3786  IF Kwko(I)>=10000 THEN Kwko(I)=9999.999
3796  NEXT I
3860  Wbt=Wibt
3810  IF If$="0" THEN 3900
3820  Wbt1=.5
3830  FOR I=1 TO 20
3840  Wbt=FNFr(Wbt1,1)
3850  IF ABS(Wbt-Wbt1)<.0001 THEN 3880
3860  Wbt 1=Wbt
3870  NEXT I
3888  Inbt=FNFi(Wbt,1)
3898  GOTO 4020
3960  Sx=0
3910  Sx2=0
3920  Sxy=0
3930  IF Isabt>1 THEN 3960
3940  Inbt=Wbt
3950  GOTO 4020
3960  FOR I=1 TO Isabt-1
3970  Sx=Sx+Wi(I
3980  Sx2=Sx2+Wi I)^2
3990  Sxy=Sxy+Wi I)/Inj(I)
4000  NEXT I
4010  Inbt=(Sxy-Sx)/Sx2*Wbt+1
4020  Flag=1
4030  RETURN
4040  ! ************************ PRINT OUTPUT *********************************
4050 Prnt:  INPUT "LIST OUTPUT ON PRINTER (P) OR CPT (C) ?",Ic$
4060  PRINTER IS 16
4070  IF Ic$="P" THEN PRINTER IS 0
4080  IF Flag=0 THEN GOSUB Calc
4090  PRINT USING 4100
4100  IMAGE 23X,"DISPLACEMENT EXPERIMENT CALCULATIONS"/
4110  PRINT USING 4120;Pv,Date$
4120  IMAGE "PORE VOLUME",7X,3D.D," cc",23X,"DATE",17X,10A
4130  PRINT USING 4140;Lc,Core$
4140  IMAGE "CORE LENGTH",7X,2D.2D," cm",23X,"CORE/RUN",13X,10A
4150  PRINT USING 4160;Dc,Fluid$
4160  IMAGE "CORE DIAMETER",5X,D.3D," cm",23X,"DISPLACEMENT    ",5X,10A
4170  PRINT USING 4180;U,Tc
```

```
4180  IMAGE "DEAD VOL/S: U",6X,2D.D," cc",23X,"CORE TEMPERATURE",5X,3D.D," F"
4190  PRINT USING 4200;D,Te
42061 IMAGE 12X,"D",6X,2D.D," cc",23X,"OUTLET TEMPERATURE",3X,3D.D," F"
4210  PRINT USING 4220;Ho,Muw
4220  IMAGE "SEPARATOR OUTLET  ",2D.2D," cm",23X,"WATER VISCOSITY",6X,D.3D," cp"
4230  Vb=0
4240  IF Vbi<>0 THEN Vb=1/Vbi
4250  PRINT USING 4260;Vb/60,Muo
4260  IMAGE "BUBBLE VELOCITY",3X,2D.2D," cm/sec",19X,"OIL VISCOSITY",8X,2D.2D,"
cp"
4270  PRINT USING 4280;Kabs,Mur
4280  IMACE "RESOLUTE PERM",5X,D.3D," darcies",18X,"VISCOSITY RATIO",6X,2D.2D
4290  PRINT USING 4300;Fld$,Sati,Drw
4300  IMAGE "INIT SAT  - ",5A,  2X,2D.D," %",24X,"WATER DENSITY RATIO ",D.4D
4310  Fldd$="OIL"
4320  IF If$="O" THEN Fldd$="WATER"
4330  PRINT USING 4340;Fldd$,Satf,Dro
4340  IMAGE "FINAL SAT - ",5A,  2X,2D.D," %",24X,"OIL DENSITY RATIO",3X,D.4D/
4350  '
4360  PRINT USING 4370
4370  IMAGE 10X,"  SEPARATOR  "," D-VOL",8X,"      FLOWRATE      ",X
4380  PRINT USING 4390
4390  IMAGE 5X,"TIME HEIGHT  CALIB   INJ    D-P  ","     CHART     ",3X,"  cc"
4400  IF If$="O" THEN PRINT USING 4410
4410  IMAGE 3X,"  (min)  (cm)  (cc/cm)  (cc)  (psi)  AVG   Ct  CAL
  min |  PVi   Rec 1/Inj",X,"|"
4420  IF If$="W" THEN PRINT USING 4430
4430  IMAGE 3X,"  (min)  (cm)  (cc/cm)  (cc)  (psi)  AVG   @t  CAL
  min |  PVi   Rec  Inj ",X,"|"
4440  PRINT USING 4450;Seps
4450  IMAGE "ST",9X,2D.2D,43X,"|",19X,"|"
4460  FOR I=0 TO Isabt-1
4470  In=Inj(I)
4480  IF If$="O" THEN In=1/In
4490  PRINT USING 4500;I,Tim(I),Seph(I),Tbcal(I),Delv(I),Dp(I),Fmavg(I),Fmt(I),F
mc(I),Q(I),Wi(I),Rec(I), In
4580  IMAGE 2D,X,3D.2D,2X,2D.2D,3X,D.2D,2X,3D.D,X,3D.2D,X,.3D,X,. 3D,X,2D.D,2X,2D
.D,X,"|",X,2D.3D,X,.3D,X, 2D.2D,X,"|"
4510  NEXT I
4520  In=Injbt
4530  IF If$="O" THEN In=1/In
4540  PRINT USING 4550;Tbt,Dpbt,Fmbt,Fmcbt,Qbt,Wibt,Recbt,In
45561 IMAGE "BT",X,3D.2D,22X,3D.2D,6X,.3D,X,2D.D,2X,2D.D,X,"|",X,2D.3D,X,.3D,X, 2
D.2D,X,"|"
4560  FOR J=Isabt TO N
4570  In=Inj(J)
4580  IF If$="O" THEN In=1/In
4590  PRINT USING 4500;J,Tim(J),Seph(J),Tbcal(J),Delv(J),Dp(J),Fmavg(J),Fmt(J),F
mc(J),Q(J),Wi(J),Rec(J),In
4600  NEXT J
4610  IF If$="O" THEN 4830
4620  PRINT USING 4630
4630  IMAGE /"     CURVE FITS     ",4X,"   C0   ",2X,"   C1   ",2X,"
  C2   ",3X,"%E-MAX",X,"%E-AVG"
4640  PRINT USING 4650:"Recovery",Cr(*),Pctmr,Pctar
4650  IMAGE 21A,2X,3(MD.4DE,X),3X,2D.D,2X,2D.D
4660  PRINT USING 4650;"Inj. X Pore Vol. Inj.",Cp(*),Pctmp,Pctap
4670  PRINT USING 4680
4680  IMAGE /3X,"  PVi  R-ACT R-CALC R-%E I*P-ACT I*P-CALC I*P-%E"
, 4X," Sw ",2X," Krw",2X," Kro",4X,"Kw/Ko"
4690  PRINT USING 4700;Sati/100,0,Kroswi,0
4700  IMAGE 55X, .3D,1X,D.3D,X,D.3D,4X,D.3D
4710  PRINT USING 4720;Wibt,Wbt,Wibt*Injbt,Wbt*Inbt
4720  IMAGE "BT",7X,D.3D,2X,D.3D,7X,3D.2D,2X,3D.2D
4730  FOR I-Isc TO N
4740  Rc=FNFr(Wi(I),1)
4750  Injc=Wi(I)*FNFi(Wi(I),1)
4760  IF Inj(I)<0 THEN Injc=-.0001
4770  In=Wi(I)*Inj(I)
4780  IF In<0 THEN In=-.0001
4790  PRINT USING 4800;I,Wi(I),Rec(I),Rc,Pctr(I),In,Injc,Pctp(I),ABS(S(I)),Krw(I
```

```
),Kro(I),Kwko(I)
4800  IMAGE 2D, X, 2D. 3D,X,.3D,3X,.3D,X,2D. D, 2X, 3D. 2D, 2X,3D. 2D,4X,2D.D, 5X,.3D,X, D
.3D,X,D.3D,X,4D.3D
4810  NEXT I
4820  RETURN
4830  PRINT USING 4840;Kw/Kabs,Ko/Kabs
4840  IMAGE /"Krw - INITIAL =",D.3D/"Kro - FINAL   =",D.3D
4850  RETURN
4860  ! ********************** PLOTS ****************************************
4870 Plot:  IF Flag=0 THEN GOSUB Calc
4880  INPUT "PLOT-ON CRT (C) OR PLOTTER (P) ?",Ic$
4890  Ia$="N"
4900  Pen=1
4910  IF Ic$="P" THEN 4970
4920  PLOTTER IS 13,"GRAPHICS"
4930  LIMIT 0,184.47,0,149.8
4940  Loct=97
4950  LOCATE 11,RATIO*100-3,11,97
4960  GOTO 5170
4970  PLOTTER IS "9872A"
4980  IF If$="W" THEN 5020
4990  Ia$="N"
5000  Id$="R"
5010  GOTO 5140
5020  INPUT "OVERPLOT:  NONE (N), FIRST (F), REPEAT (R) ?",Ia$
5030  Pen=1
5040  Ltype=1
5050  Szl=1
5060  Rep=1
5070  IF Ia$<>"R" THEN 5140
5080  INPUT "REPEAT # ?",Rep
5090  INPUT "PEN # ?",Pen
5100  INPUT "LINE TYPE ?",Ltype
5110  IF Ltype=6 THEN Szl=4
5120  IF Ltype=3 THEN Szl=.5
5130  IF Ltype=5 THEN Szl=2
5140  PRINTER IS 7,5
5150  PRINT "VS "&VAL$(Spd)
5160  PRINTER IS 16
5170  Wf=INT(Wi(N))+1
5180  Wfi=INT(Wi(Ni))+1
5190  IF If$="O" THEN Wf=INT(Wi(N)*2+1)/2
5200  Rf=INT(Rec(N)*5+1)/5
5210  Injm=MAX(INT(LGT(Inj(Ni)*Wi(Ni))+1),2)
5220  IF If$="O" THEN Injm=INT(1/Injbt/10+1)*10
5230  IF If$="O" THEN GOSUB Rec
5240  INPUT "PLOT:  REC AND INJ(R), REC AND INJ VS. 1/Wi(W), REL PERM(P), Kw/Ko(K
), OR END(E)",Id$
5250  IF Id$="E" THEN 5320
5260  IF Id$="R" THEN GOSUB Rec
5270  IF If$="O" THEN 5240
5280  IF Id$="W" THEN GOSUB Recwi
5290  IF Id$="P" THEN GOSUB Rel
5300  IF Id$="K" THEN GOSUB Kwku
5310  GOTO 5240
5320  GCLEAR
5330  EXIT GRAPHICS
5340  RETURN
5350  ! ********************** SET PLOT LIMITS ****************************
5366 V:  IF Ic$="C" THEN 5540
5370  Hp=8.5
5380  Vp=11
5390  Lm=1.5
5400  Rm=1
5410  Tm=1
5420  Bm=2
5430  IF Paper=1 THEN 5500
5440  Hp=11
5450  Vp=12.5
5460  Lm=2.3
5470  Rm=1.2
```

```
5480  Tm=1.2
5490  Bm=1.05
5500  GOSUB Lim
5518  Loct=100/RATIO-3
5520  LOCATE 11,97,11,Loct
5530  RETURN
5540  GRAPHICS
5550  Loct=97
5560  LOCATE 11,97,11,97
5570  RETURN
5580 Lim:  Add=MIN((Hp-Lm-Rm)*25.4,(Vp-Tm-Bm)*25.4)/100
5590  LIMIT Lm*25.4-12-Add,(Hp-Rm)*25.4-12+3*Add,Bm*25.4-6-Add,(Vp-Tm)*25.4-6+3*
Add
5608  RETURN
5610  ! ************************** LOG SCALE ************************************
5620 Logscl:   LDIR 0
5630  LORC 8
5640  CSIZE 3
5650  FOR Yex=Ks TO Kf-1
5660  MOVE Xs,Yex
5670  LABEL 10^Yex
5680  FOR Inc=2 TO 9
5690  MOVE Xs,LGT(Inc*10^Yex)
5700  SETGU
5710  RPLOT .5,0,-1
5720  SETUU
5730  NEXT Inc
5740  NEXT Yrx
5750  RETURN
5760  ! ************************** RUN LABELS ***************************
5770 Lblrt:   LORG 9
5780  SETGU
5790  RPLOT -5,-5,-2
5880  SETUU
5810  CSIZE 3
5820  LABEL "RUN "&Core$&"("&VAL$(Tc)&" DEG-F)"
5830  RETURN
5840 Lbllt:   LORG 3
5850  SETGU
5860  RPLOT 5,-5,-2
5870  SETUU
5880  CSIZE 3
5890  LABEL "HUN "&Core$&" ("&VAL$(Tc)&" DEG-F)"
5900  RETURN
5910 Lblrb:   LOHG 3
5920  SETGU
5930  CSIZE 3
5940  LABEL "RUN "&Core$&" ("&VAL$(Tc)&" DEG-F)"
5950  IF If$="W" THEN 5980
5960  IPLOT 0,-2,-2
5970  LABEL "OIL DISPLACEMENT"
5980  IPLOT Del/2,-3,-2
5996  CALL Plsym(Del,2)
6000  SETGU
6010  RPLOT 3,0,-2
6020  LORG 2
6030  CSIZE 2.5
6040  Bthru$="TRUE BREAKTHROUGH"
6858  IF If$="O" THEN Bthru$="BREAKTHROUGH"
6060  LABEL Bthru$
6070  IF If$="O" THEN 6130
6080  IPLOT -3,-2,-2
6090  CALL Plsym(Del,3)
6100  SETGU
6110  RPLOT 3,0,-2
6120  LABEL "INFERRED BREAKTHROUGH"
6130  SETUU
6140  RETURN
6150  ! ********************** RECOVERY AND INJECTIVITY PLOTS ****************
6160 Rec: GOSUB V
6170  PEN 1
```

```
6180  PEN Pb
6190  FRAME
6200  PEN 1
6210  LOCATE 11,97,(Loct+11)/2,Loct
6220  SCALE 0,Wf,0,Rf
6230  IF If$="W" THEN 6260
6240  AXES .5,.1,0,0,2,2,3
6250  GOTO 6270
6260  AXES 1,.1,0,0,2,2,3
6270  CALL Lobe1(0,Wf,-1,0,Rf,.2,"","RECOVERY")
6280  MOVE 0,0
6290  IF If$="W" THEN 6320
6300  DRAW Wibt,Recbt
6310  GOTO 6410
6320  DRAW Wbt,Wbt
6330  CALL Plsym(Del,3)
6340  IF If$="O" THEN 6400
6350  FOR W=Wbt TO Wf STEP .1
6360  R=FNFr(W,1)
6370  DRAW W,R
6380  NEXT W
6390  DRAW Wf,FNFr(Wf,1)
6400  MOVE Wibt,Recbt
6410  CALL Plsym(Del,2)
6420  FOR I=1 TO N
6430  MOVE Wi(I),Rec(I)
6440  CALL Plsym(Del,1)
6450  NEXT I
6460  MOVE Wf/2,Rf/3
6470  GOSUB Lblrb
6480  LOCATE 11,97,11,(Loct+11)/2          ! INJECTIVITY PLOT
6490  IF If$="W" THEN 6680
6500  SCALE 0,Wf,0,Injm                    ! OILFLOOD
6510  IF Injm<=10 THEN 6550
6520  AXES .5,5,0,0,2,2,3
6530  CALL Label(0,Wf,1,0,Injm,-10,"PORE VOLUMES INJECTED","1/INJECTIVITY")
6540  GOTO 6570
6550  AXES .5,1,0,0,2,2,3
6560  CALL Label(0,Wf,1,0,Injm,-2,"PORE VOLUMES INJECTED","1/INJECTIVITY")
6570  MOVE 0,1
6580  DRAW Wbt,Inbt
6590  MOVE Wibt,1/Injbt
6600  CALL Plsym(Del,2)
6610  FOR I=1 TO Ni
6620  MOVE Wi(I),1/Inj(I)
6630  CALL Plsym(Del,1)
6640  NEXT I
6650  MOVE Wf/2,Injm/3
6660  GOTO 6950
6670  GOTO 6890
6680  SCALE 0,Wf,-1,Injm                   ! WATERFLOOD
6690  AXES 1,1,0,-1,1,1,3
6700  Ks=-1
6710  Kf=Injm
6720  Xs=0
6730  GOSUB Logscl
6740  CALL Label(0,Wf,1,-1,Injm,-99,"PORE VOLUMES INJECTED","INJECTIVITY X PORE
VOL. INJ.")
6750  FOR W=.02 TO Wbt STEP .1
6760  Injp=1/(1+W*(1/Inbt-1)/Wbt)
6770  IF W=.02 THEN MOVE W,LGT(Injp*W)
6780  DRAW W,LGT(Injp*W)
6790  NEXT W
6800  DRAW Wbt,LGT(Inbt*Wbt)
6810  CALL Plsym(Del,3)
6820  FOR W=Wbt TO Wfi STEP .1
6830  Ir=FNFi(W,1)*W
6840  DRAW W,LGT(Ir)
6850  NEXT W
6860  DRAW Wfi,LGT(FNFi(Wfi,1)*Wfi)
6870  MOVE Wibt,LGT(Injbt*Wibt)
```

```
6880  CALL Plsym(Del,2)
6890  FOR I=1 TO Ni
6900  Ir=Inj(I)*Wi(I)
6910  MOVE Wi(I),LGT(Ir)
6920  CALL Plsym(Del,1)
6930  NEXT I
6940  MOVE Wf/2,(Injm+1)/3-1
6950  GOSUB Lblrb
6960  PEN 0
6970  PAUSE
6980  CCLEAR
6990  RETURN
7000  ! ******************** RECOVERY AND INJECTIVITY VS. 1/Wi ****************
7010 Recwi: GOSUB V
7020  PEN Pb
7030  Rsp=INT(FNFr(1,1)*10)/10
7040  FRAME
7050  PEN 1
7060  LOCATE 11,97,(Loct+11)/2,Loct
7070  SCALE 0,1,Rsp,Rf
7080  AXES .1,.05,0,Rsp,2,2,3
7090  CALL Label(0,1,-999,Rsp,Rf,.1,"","RECOVERY")
7100  MOVE 1/Wf,FNFr(Wf,1)
7110  FOR Winv=1/Wf TO 1 STEP .02
7120  DRAW Winu,FNFr(1/Winu,1)
7130  NEXT Winv
7140  DRAW 1,FNFr(1,1)
7150  FOR I=1 TO N
7160  IF Wi(I)<1 THEN 7190
7170  MOVE 1/Wi(I),Rec(I)
7180  CALL Plsym(Del,1)
7190  NEXT I
7200  MOVE 1,Rf
7210  GOSUB Lblrt
7220                                ! INJECTIVITY
7230  LOCATE 11,97,11,(Loct+11)/2
7240  SCALE 0,1,0,Injm
7250  AXES .1,1,0,0,2,1,3
7260  Ks=0
7270  Kf=Injm
7280  Xs=0
7290  GOSUB Logscl
7300  CALL Label(0,1,.2,0,Injm,-999,"1/PORE VOLUMES INJECTED","INJECTIVITY X POR
E VOL. INJ.")
7310  MOVE 1/Wfi,LGT(FNFi(Wfi,1)*Wfi)
7320  FOR Winv=1/Wfi TO 1 STEP .02
7330  Ir=LGT(FNFi(1/Winv,1)/Winv)
7340  DRAW Winv,Ir
7350  NEXT Winv
7360  DRAW 1,LGT(FNFi(1,1))
7370  FOR I=1 TO Ni
7380  IF Wi(I)<1 THEN 7410
7398  MOVE 1/Wi(I),LGT(Inj(I)*Wi(I))
7400  CALL Plsym(Del,1)
7410  NEXT I
7420  MOVE 1,Injm
7430  GOSUB Lblrt
7440  PEN 0
7450  PAUSE
7460  GCLEAR
7470  RETURN
7480  ! ************************** REL PERMS *************************
7490 Rel: IF Ic$="C" THEN 7650
7500  Hp=8.5
7510  Vp=11
7520  Lm=1.5
7530  Rm=1
7540  Tm=2
7550  Bm=3
7560  IF Paper=1 THEN 7630
7570  Hp=11
```

```
7580  Vp=12.5
7590  Lm=2.3
7600  Rm=1.2
7610  Tm=1.95
7620  Bm=3.05
7630  GOSUB Lim
7640  GOTO 7660
7650  GRAPHICS
7660  Loct=97
7670  LOCATE 11,97,11,Loct
7680  SCRLE 0,1,0,1
7690  IF Ia$="R" THEN 7790
7700  PEN Pb
7710  FRRME
7720  PEN 1
7730  AXES .1,.1,0,0,2,2,3
7740  CALL Label(0,1,.2,0,1,.2,"WATER SATURATION","RELATIVE PERMEABILITY")
7750  IF Ia$="F" THEN 7790
7760  MOVE 1,1
7770  COSUB Lblrt
7780  GOTO 7910
7790  LORG 2
7880  PEN Pen
7810  MOVE .4,1
7820  SETGU
7830  IPLOT 0,-5*Rep,-2
7840  LINE TYPE Ltype,Sz1
7850  IPLOT 8,0,-1
7860  IPLOT 2,0,-2
7878  CSIZE 3
7880  LINE TYPE 1
7890  LABEL "RUN "&Core$&" ("&VAL$(Tc)&" DEG-F)"
7900  SETUU
7510  MOVE Sati/100,MIN(1,Kroswi)
7920  CALL Plsym(Del,2)
7930  LINE TYPE Ltype,Sz1
7940  Iss=Isc
7950  HOVE S(Iss),Kro(Iss)
7960  IF Ia$<>"N" THEN 8058
7970  CSIZE 3
7980  LORG 7
7990  RPLOT -.02,0,-2
8880  LABEL "Oil"
8010  MOVE Sati/100,0
8028  CALL Plsym(Del,2)
8036  LINE TYPE Ltype,Sz1
8040  MOVE S(Iss),Kro(Iss)
8050  FOR I=Iss+1 TO Ni
8060  IF S(I)<0 THEN 8080
8070  DRAW S(I),Kro(I)
8080  NEXT I
8050  MOVE S(Iss),Krw(Iss)
8100  FOR I=Iss+1 TO Ni
8110  IF S(I)<0 THEN 8130
8128  DRAW S(I),Krw(I)
8130  NEXT I
8140  LINE TYPE 1
8150  IF Ia$<>"N" THEN 8200
8160  LORC 1
8170  RPLOT .02,0,-2
8180  LABEL "Water"
8190  GOTO 8240
8200  IF Ibs=1 THEN 8240
8210  MOVE Sati/100+.02,MIN(Kroswi,1)
8220  LORC 2
8230  LABEL Cores
8240  PEN 0
8250  PAUSE
8260  GCLEAR
8270  RETURN
8288  ! ***************************** Kw/Ko PLOT ****************************
```

```
8290 Kwko:   GOSUB V
8300  Ks=-1
8310  Kf=2
8320  Xs=0
8330  FEN Fen
8340  SCALE Xs,1,Ks,Kf
8350  IF Ia$="R" THEN 8480
8360  PEN Pb
8370  FRAME
8380  FEN 1
8390  AXES .1,1,Xs,Ks,2,1,3
8400  GOSUB Logscl
8410  MOVE Xs,Kf
8420  LRBEL 10^Kf
8430  CALL Label(Xs,1,.2,Ks,Kf,-999,"WATER SATURATION","WATER/OIL PERMEABILITY R
ATIO")
8440  IF Ia$="F" THEN 8480
8450  MOVE 0,Kf
8460  GOSUB Lblit
8470  GOTO 8600
8480  LORG 2
8490  MOVE 0,Kf
8500  SETGU
8510  IPLOT 5,-5*Rep,-2
8520  FEN Pen
8530  LINE TYPE Ltype,Sz1
8540  IPLOT 8,0,-1
8550  IPLOT 2,0,-2
8560  CSIZE 3
8570  LINE TYPE 1
8580  LRBEL "RUN "&Core$&" ("&VAL$(Tc)&" DEG-F)"
8590  SETUU
8600  LINE TYPE Ltype,Sz1
8610  MOVE S(Isc),LGT(Kwko(Isc))
8620  FOR I=Isc TO N
8630  IF S(I)<0 THEN 8650
8640  DRAW S(I),LGT(Kwko(I))
8650  NEXT I
8660  LINE TYPE 1
8670  FEN 0
8680  PAUSE
8690  GCLEAR
8700  RETURN
8710  ! ************************** SUBROUTINES ******************************
8720  !
8730  ! ********************** WATER PROPERTIES ****************************
8740  SUB Watp(T,Rhow,Muw,I)
8750  Rhow=EXP(6.52014E-3-4.34333E-5*T-8.78134E-7*T*T)
8760  Muw=EXP(EXP(1.3926+3.0841E-1*LOG(T)-5.7139E-2*LOG(T)*LOG(T)))/208.9
8770  IF I=1 THEN 8820
8780  Rhow=Rhow*1.0137
8790  M=1.03
8800  IF T>150 THEN M=1.045
8810  Muw=Muw*M
8820  SUBEND
8830  ! ************************* OIL PROPERTIES ************************
8840  SUB Oilp(T,Rhoo,Muo)
8850  Rhoo=EXP(-.13539-4.42405E-4*T)
8860  Tr=T+460
8870  Nu=10^(10^(9.8863-3.5587*LGT(Tr)))-.6
8880  Muo=Nu*Rhoo
8890  SUBEND
8900  ! ********************** TIME CONVERSION ************************
8910  DEF FNTcon(Time)
8920  Ti=Time/100
8930  Hr=INT(Ti)
8940  Min=INT(FRACT(Ti)*100)
8950  Sec=FRACT(Time)
8960  RETURN Hr*60+Min+Sec/.6
8970  FNEND
8980  END
```

```
8990  ! **********************PLOT SYMBOLS ********************************
9000  SUB Plsym(Del,Sym)
9010  DEG
9020  SETGU
9030  D=De1/2
9040  RPLOT 0,0,-1
9050  ON Sym GOTO 9090,9060,9170
9060  Nsds=20
9070  D=D/1.2
9080  GOTO 9180
9090  Nsds=4
9100  PDIR -135
9110  RPLOT D,0,-2
9120  FOR Dir=-135 TO 225 STEP 360/Nsds
9130  PDIR Dir
9140  RPLOT D,0,-1
9150  NEXT Dir
9160  GOTO 9230
9170  PDIR -30
9180  RPLOT D,0,-2
9190  FOR Dir=-30 TO 330 STEP 120
9200  PDIR Dir
9210  RPLOT D,0,-1
9220  NEXT Dir
9230  RPLOT 0,0,-2
9240  PDIR 0
9250  SETUU
9260  SUBEND
9270  ! ****************************** RECOVERY FUNCTION ***********************
9280  DEF FNFr(X,I)
9290  COM Cr(2),Cp(2)
9300  X1=LOG(X)
9310  ON I GOTO 9328,9340
9320  F=Cr(0)+Cr(1)*X1+Cr(2)*X1^2    ! FUNCTION
9330  RETURN F
9340  Fp=(Cr(1)+2*Cr(2)*X1)/X        ! DERIVITIVE
9358  RETURN Fp
9360  FNEND
9370  ! ************************** INJECTIVITY FUNCTION ***********************
9380  DEF FNFi(X,I)
9390  COM Cr(2),Cp(2)
9400  X1=LOG(X)
9410  Ex=EXP(Cp(0)+Cp(1)*X1+Cp(2)*X1^2)
9428  ON I GOTO 9438,9450
9430  F=Ex/X                                          ! FUNCTION
9440  RETURN F
9450  Fp=X*(Cp(1)+2*Cp(2)*X1)/Ex       ! DERIVITIVE
9460  RETURN Fp
9470  FNEND
9480  ! ************************** LAEELLING SUBROUTINE ************************
9490  SUB Label(Xs,Xf,Xstep,Ys,Yf,Ystep,Xlbl$,Ylbl$)
9500  DEG
9510  STANDARD
9520  LDIR 0
9530  CSIZE 3
9540  IF Xstep<0 THEN 9640
9550  LORG 6
9560  FOR X=Xs TO Xf STEP Xstep
9570  MOVE X,Ys
9580  SETGU
9590  RPLOT 0,-1,-2
9600  SETUU
9610  LABEL X
9620  NEXT X
9630  Dy=0
9640  Dy=0
9650  IF Ystep<=-99 THEN 9740
9660  IF Ystep>=0 THEN 9690
9670  Dy=Ystep
9680  Ystep=-Ystep
9690  LORG 8
```

```
9700  FOR Y=Ys TO Yf+Dy STEP Ystep
9710  MOVE Xs,Y
9720  LRBEL Y
9730  NEXT Y
9740  CSIZE 3                          ! LABELS
9750  IF Xlbl$="" THEN 9820
9760  LORC 4
9770  MOVE (Xs+Xf)/2,Ys
9780  SETGU
9790  RPLOT 0,-10,-2
9800  SETUU
9810  LABEL Xlbl$
9820  LDIR 90
9830  LORC 6
9640  MOVE Xs,(Ys+Yf)/2
9850  SETCU
9860  RPLOT -10,0,-2
9870  SETUU
9880  LABEL Ylblt
9890  LDIR 0
9900  SUBEND
```

APPENDIX H - RELATIVE PERMEABILITY AND PERMEABILITY RATIO CURVES

Figures H.1 through H.24 present the logarithm of relative permeability ratio vs. saturation and relative permeability vs. saturation curves for the unconsolidated sand runs.

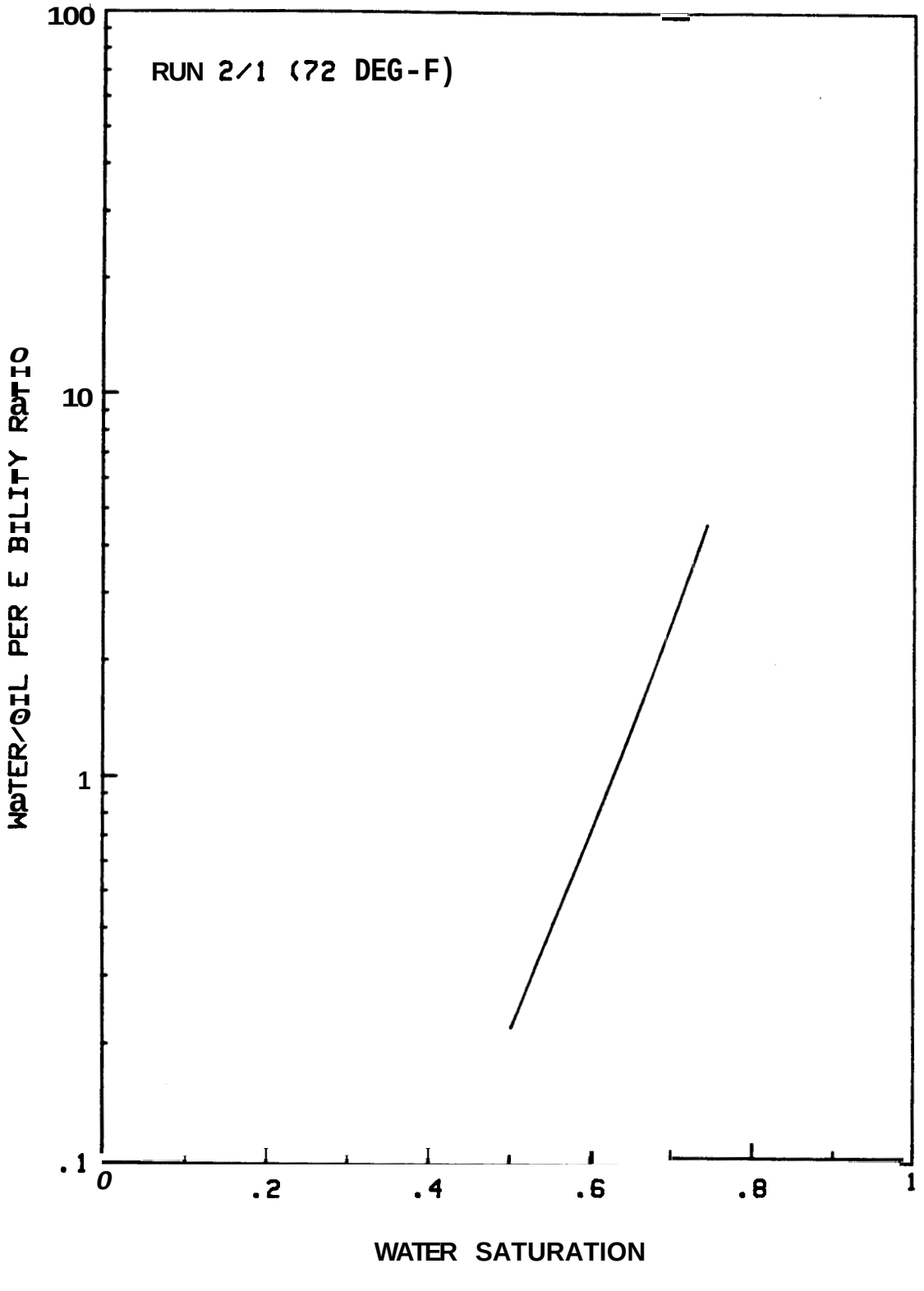

Fig. H.l Relative Permeability Ratio vs. Water Saturation -- Run 2/1

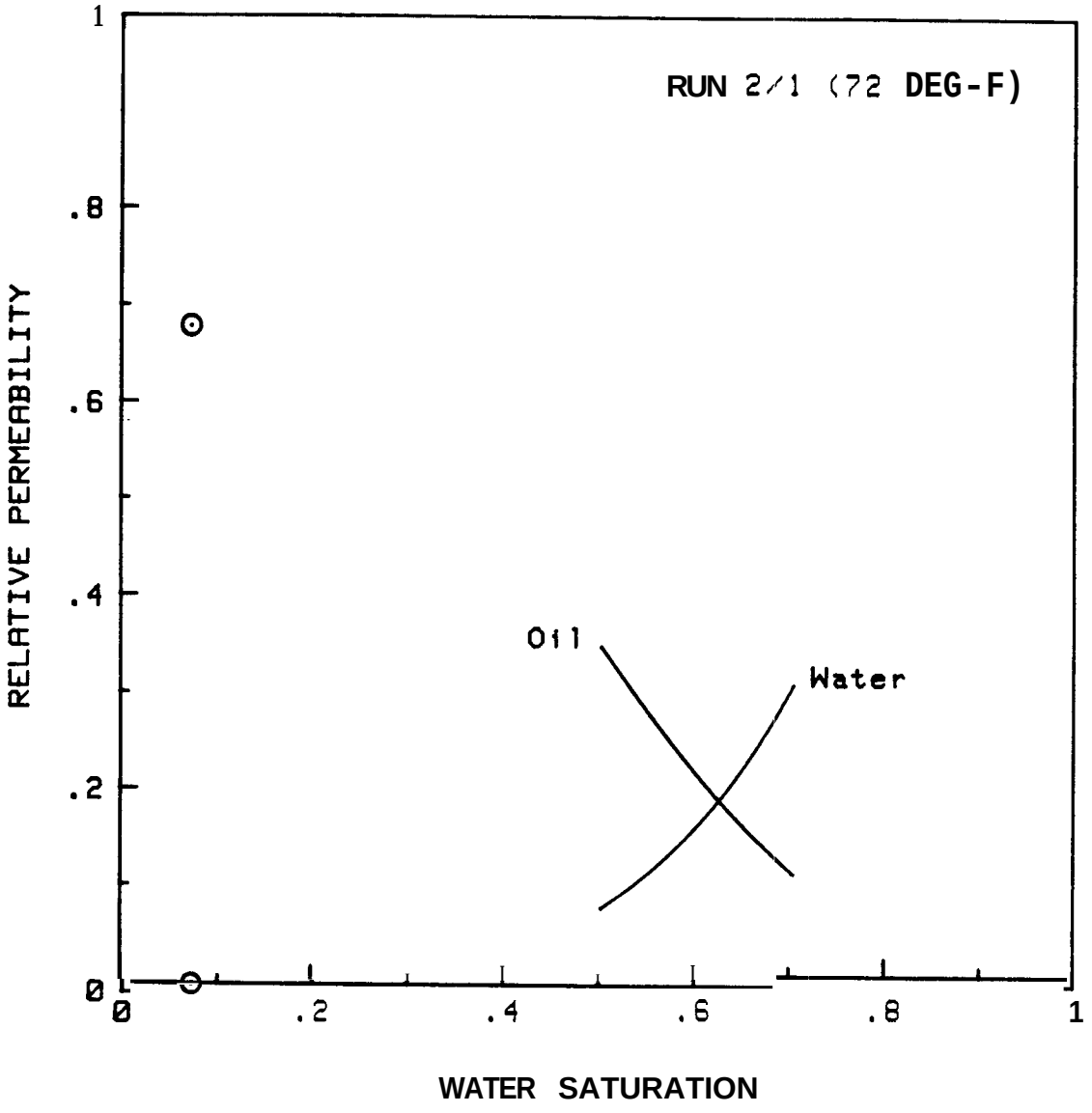

Fig. H.2 Relative Permeabilities vs. Water Saturation -- Run 2/1

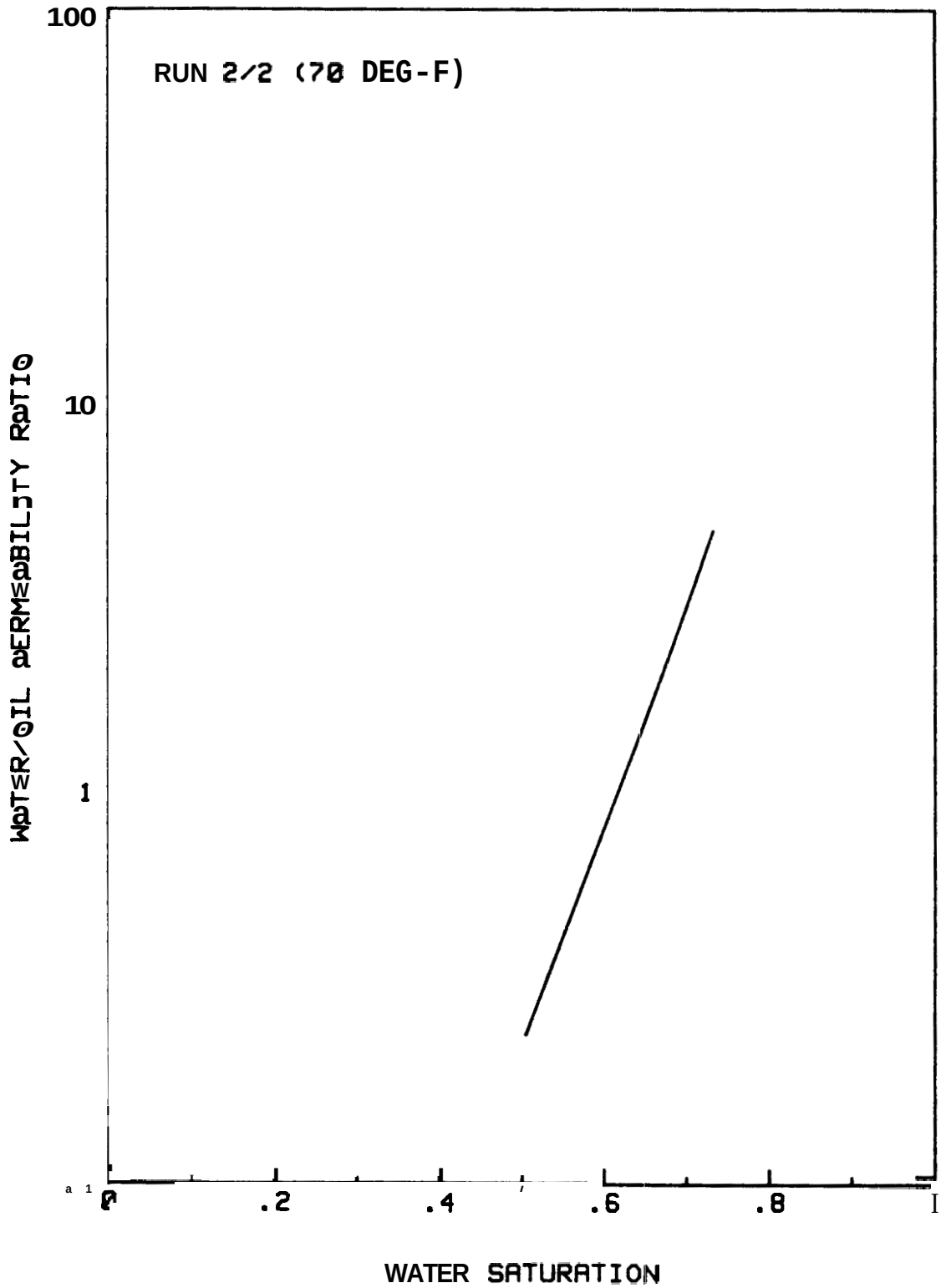

Fig. H.3 Relative Permeability Ratio **vs. Water Saturation -- Run 2/2**

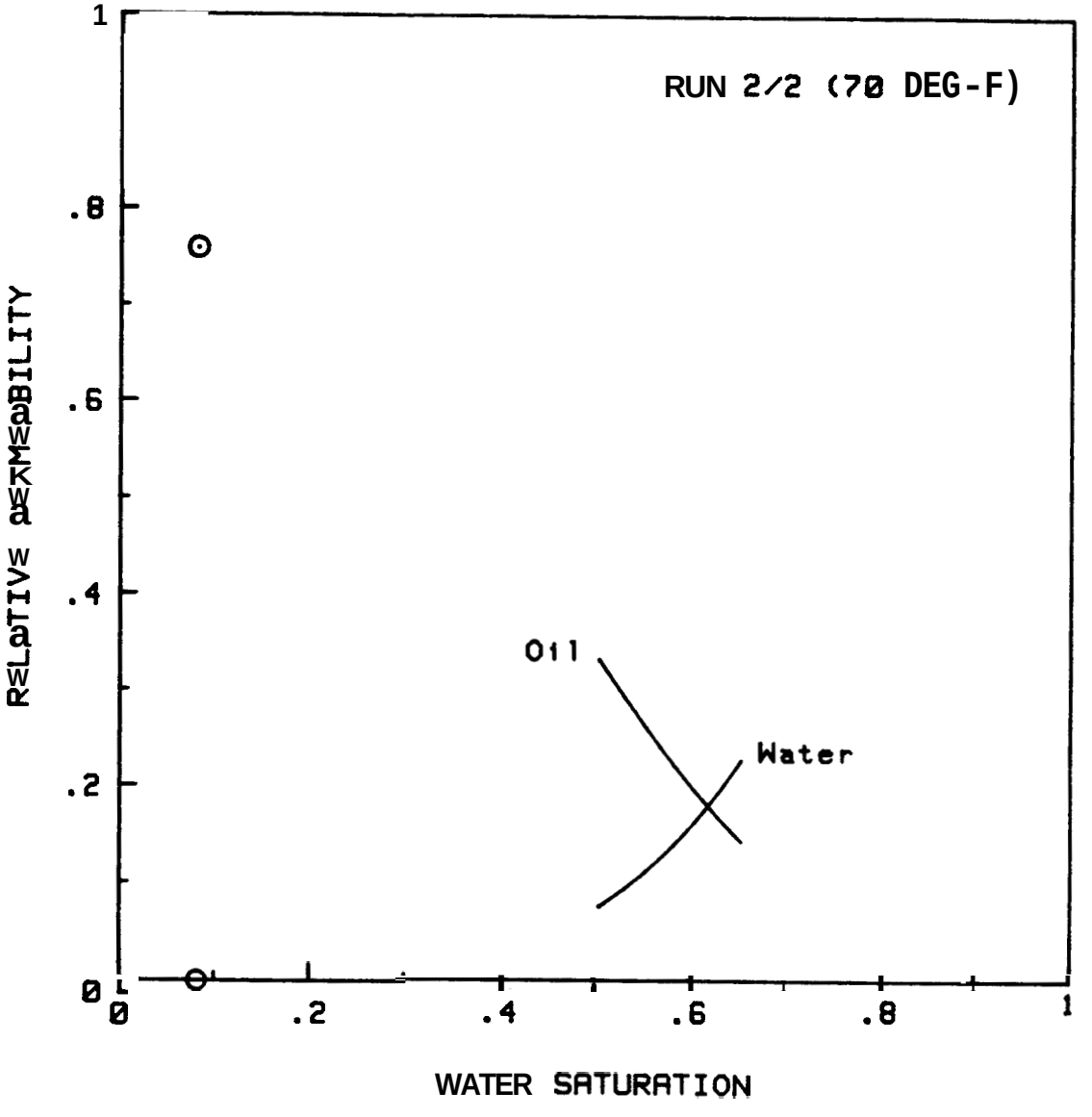

Fig. *H.4* Relative Permeabilities vs. Water Saturation -- Run 2/2

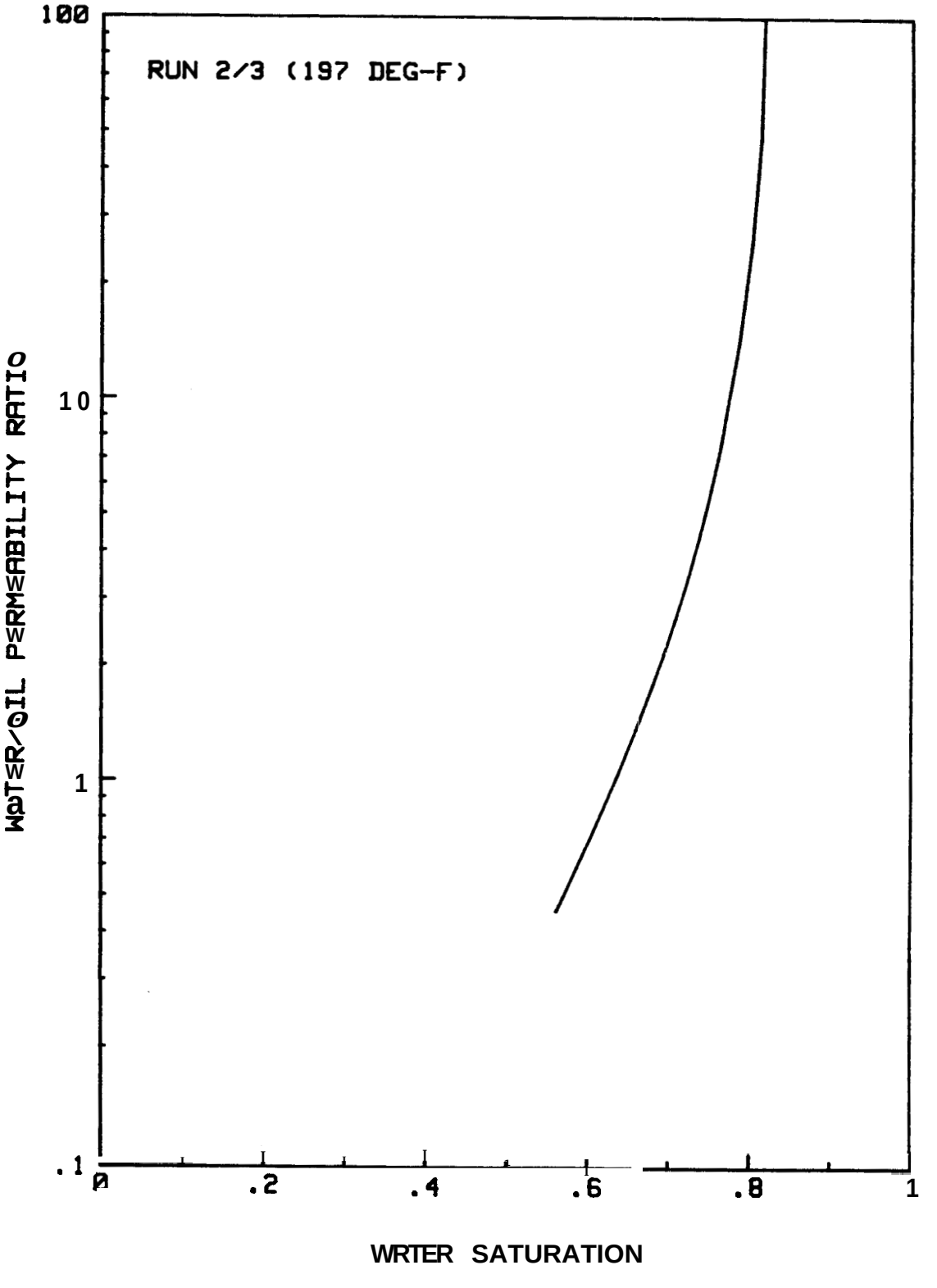

Fig. H.5 Relative Permeability Ratio vs. Water Saturation -- Run 2/3

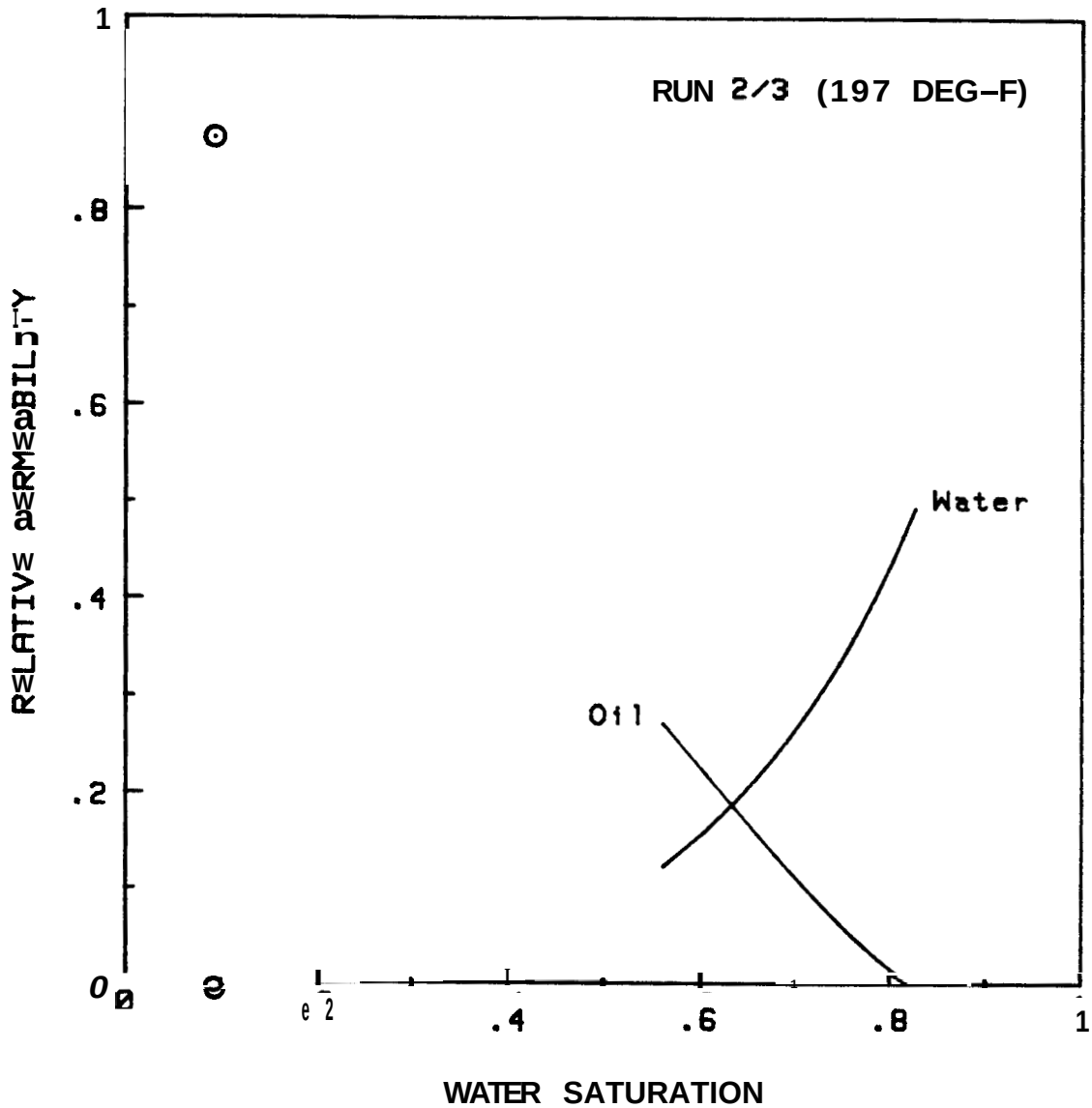

Fig. H.6 Relative Permeabilities vs. Water Saturation -- Run 2/3

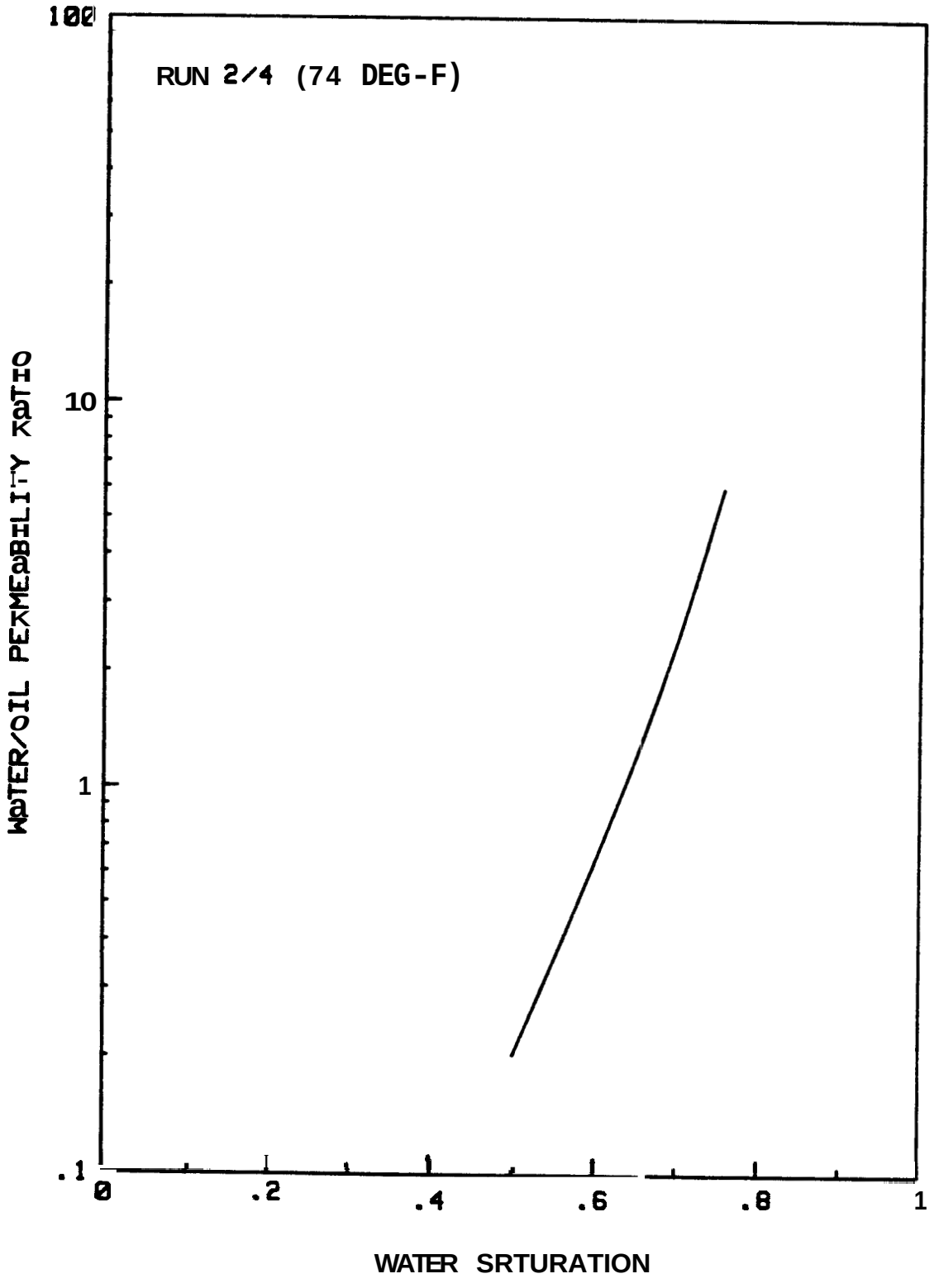

Fig. H.7 Relative Permeability Ratio vs. Water Saturation -- Run 2/4

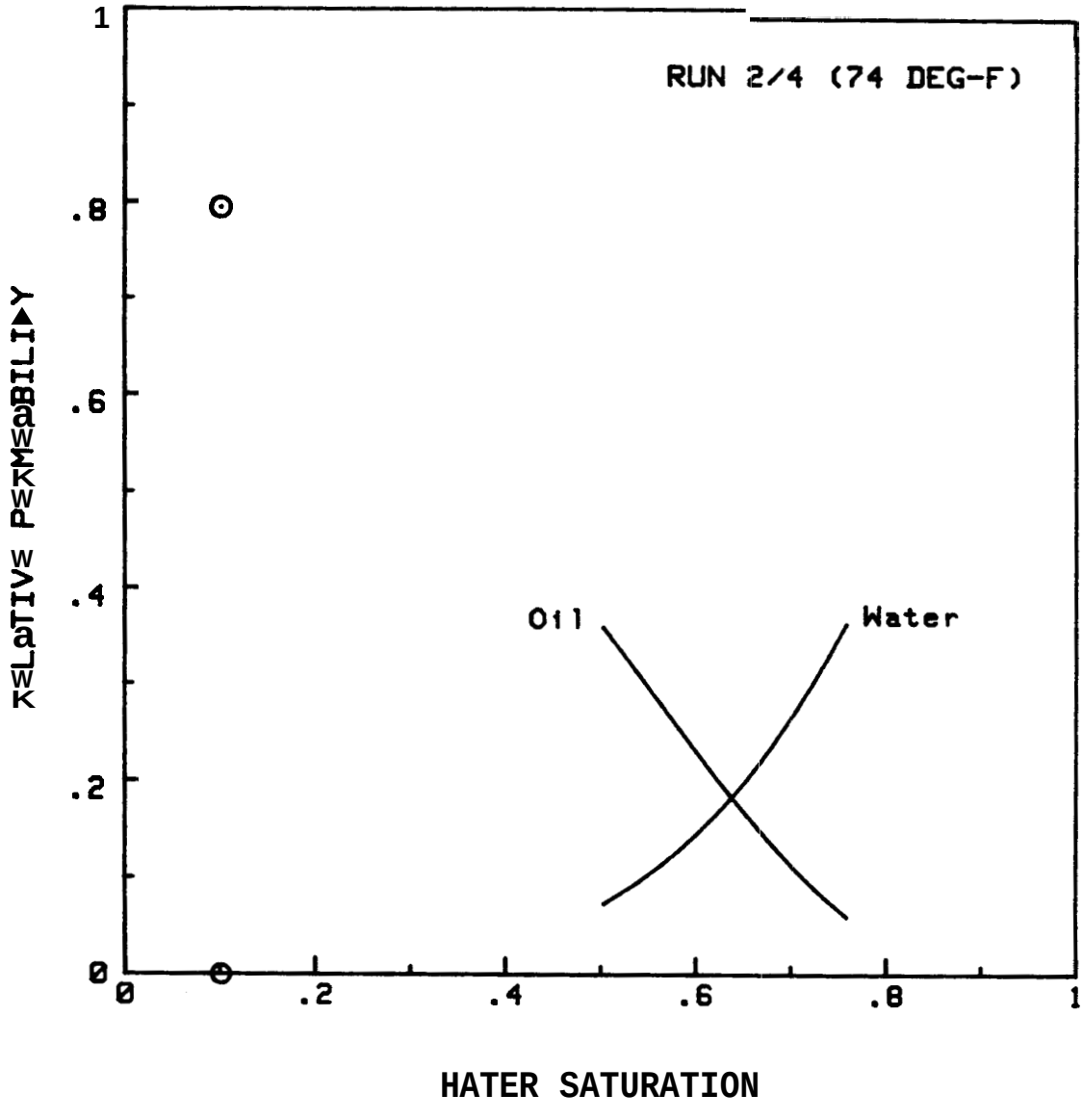

Fig. H.8 Relative Permeabilities vs. Water Saturation -- Run *2/4*

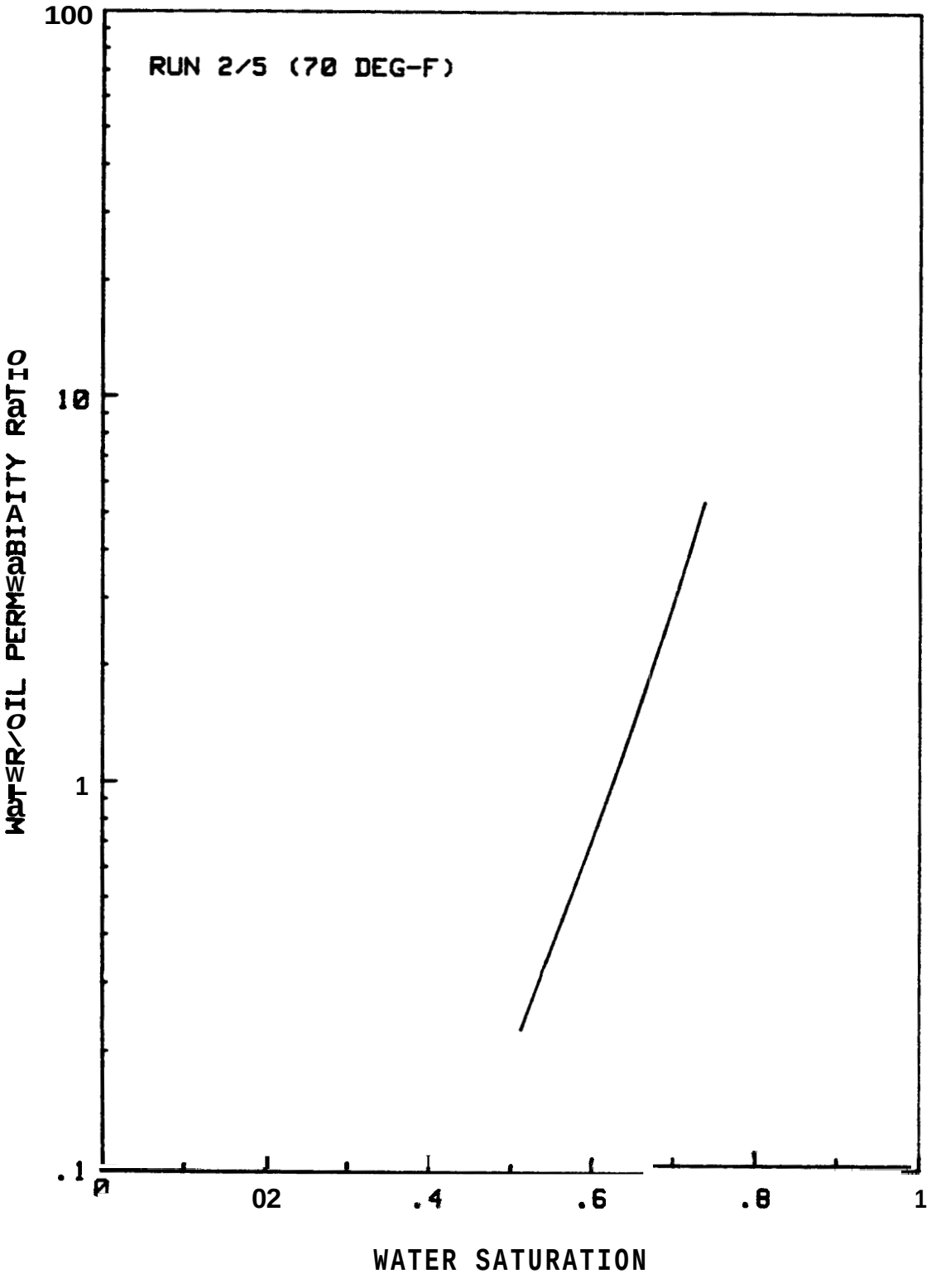

Fig. H.9 Relative Permeability Ratio vs. Water Saturation — Run 2/5

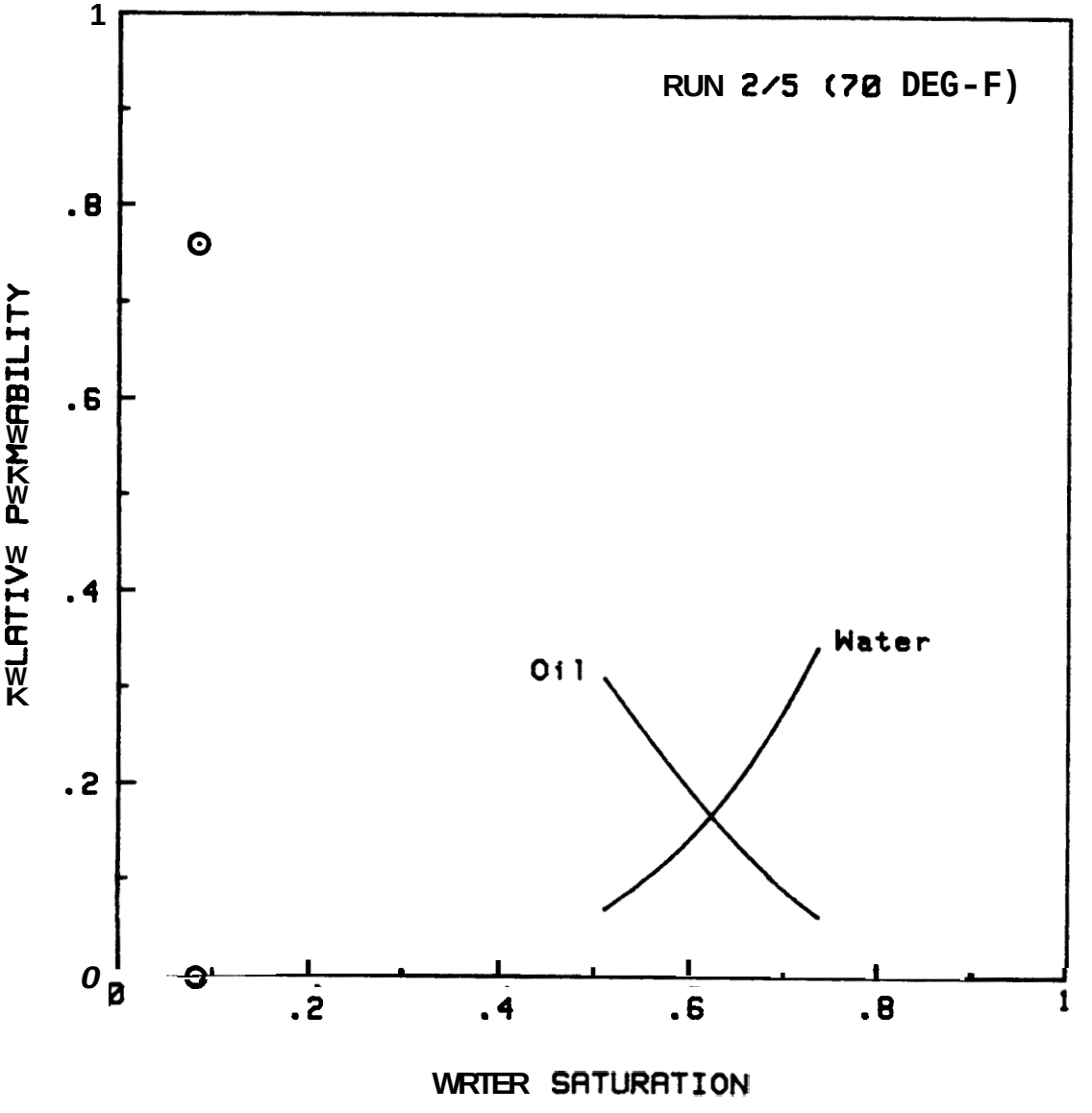

Fig. H.10 Relative Permeabilities vs. Water Saturation -- Run 2/5

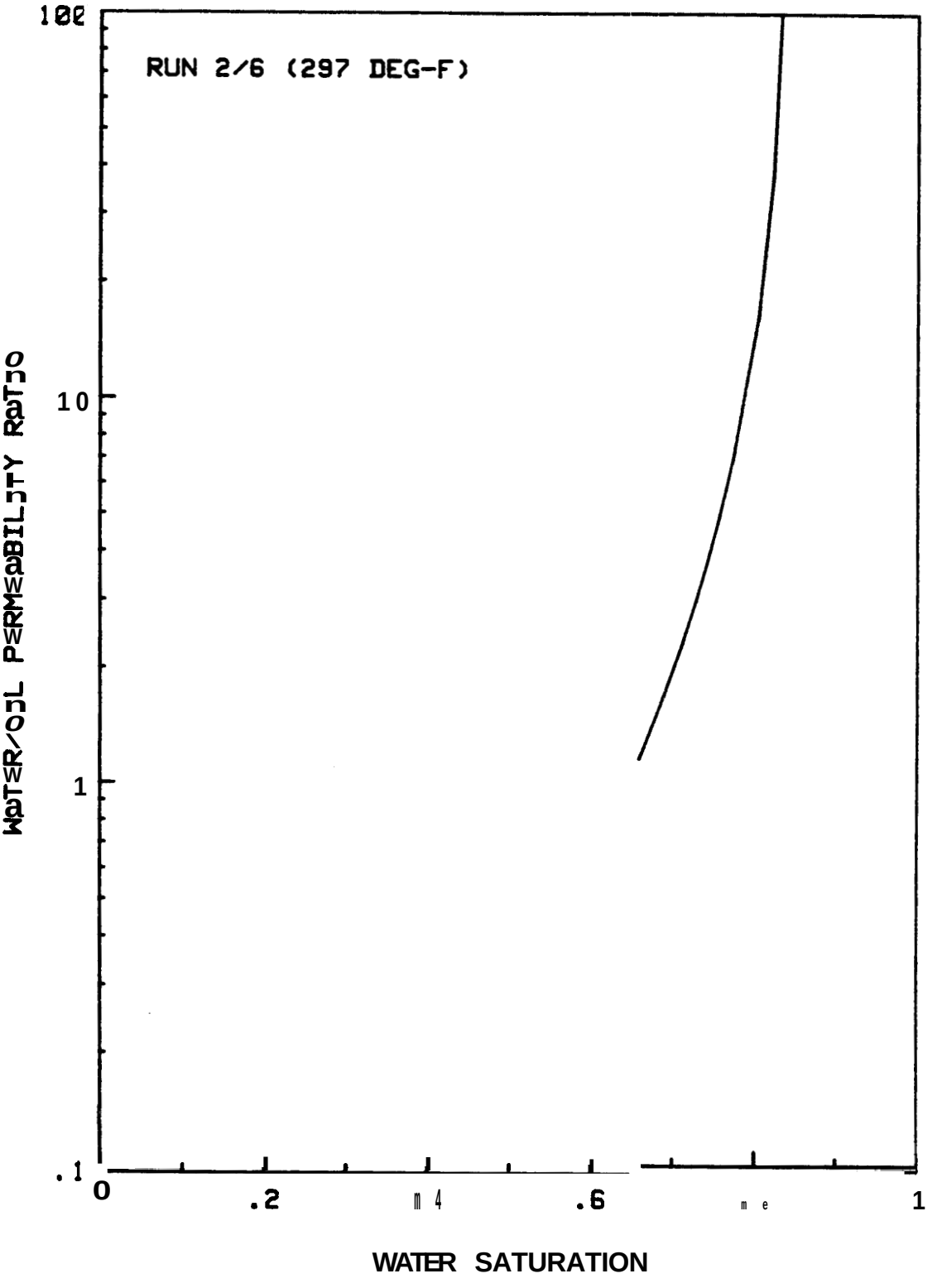

Fig. H.11 Relative Permeability Ratio vs. Water Saturation -- Run 2/6

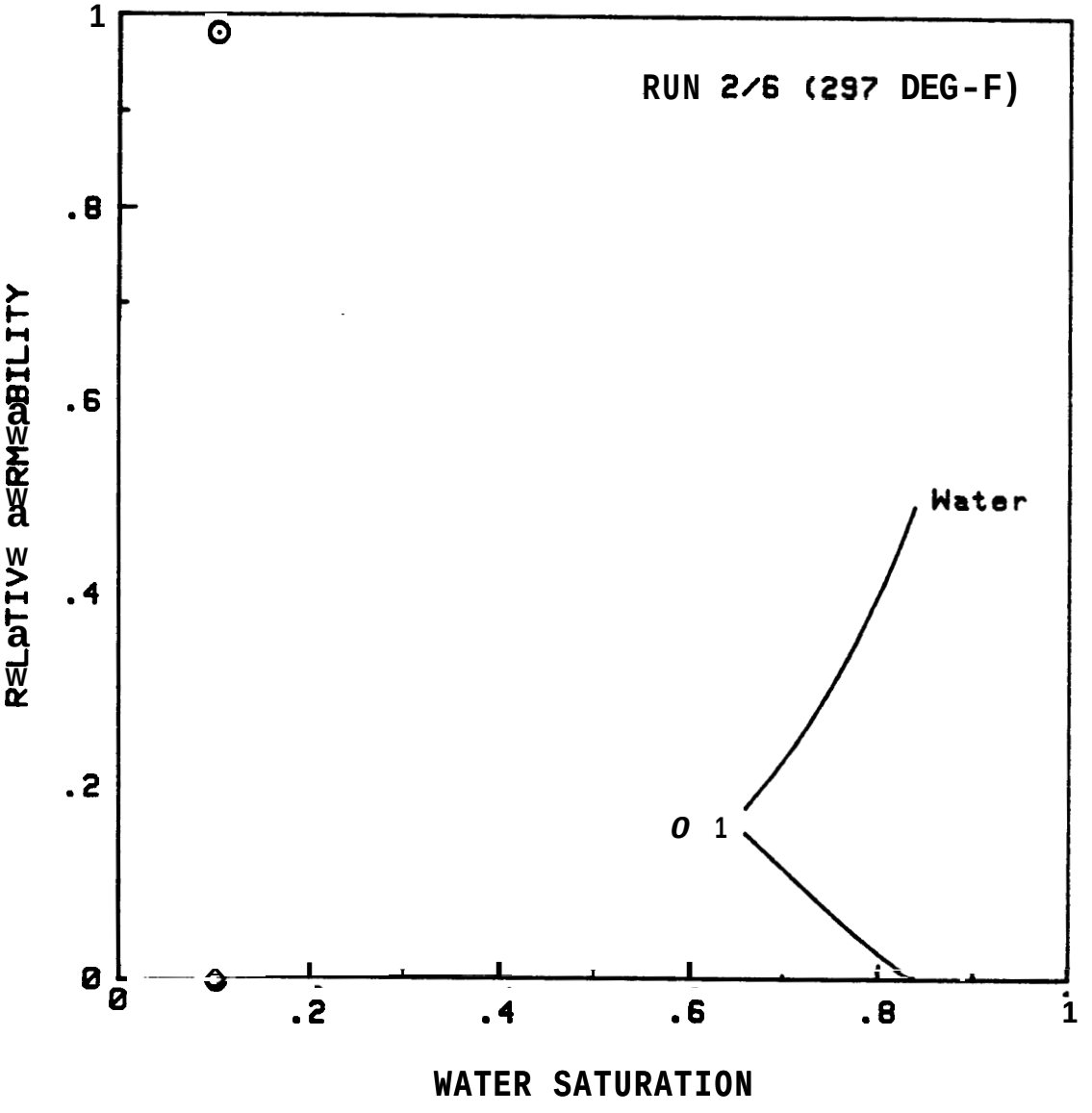

Fig. H.12 Relative Permeabilities vs. Water Saturation — Run 2/6

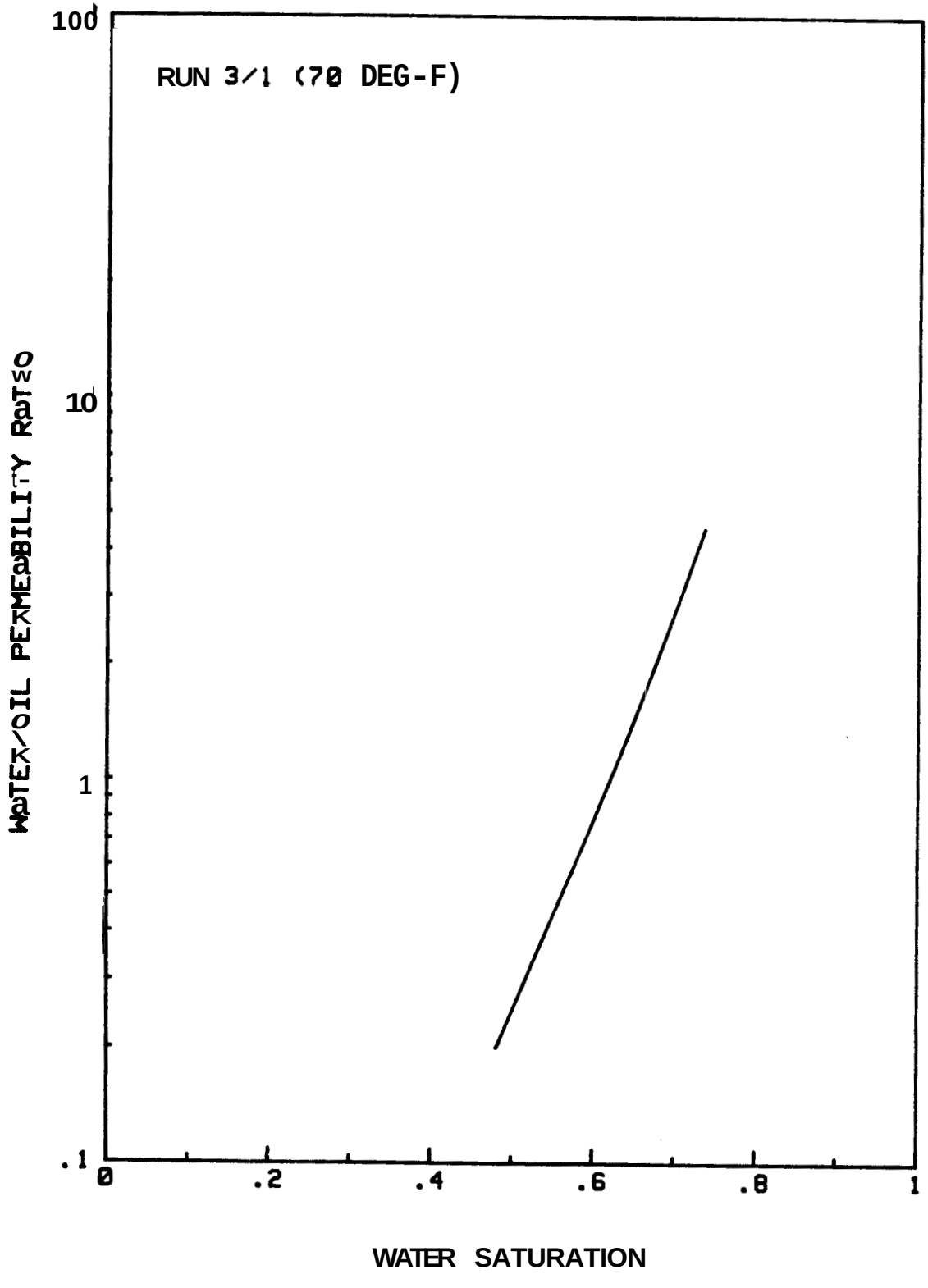

Fig. H.13 Relative Permeability Ratio vs. Water Saturation -- Run 3/1

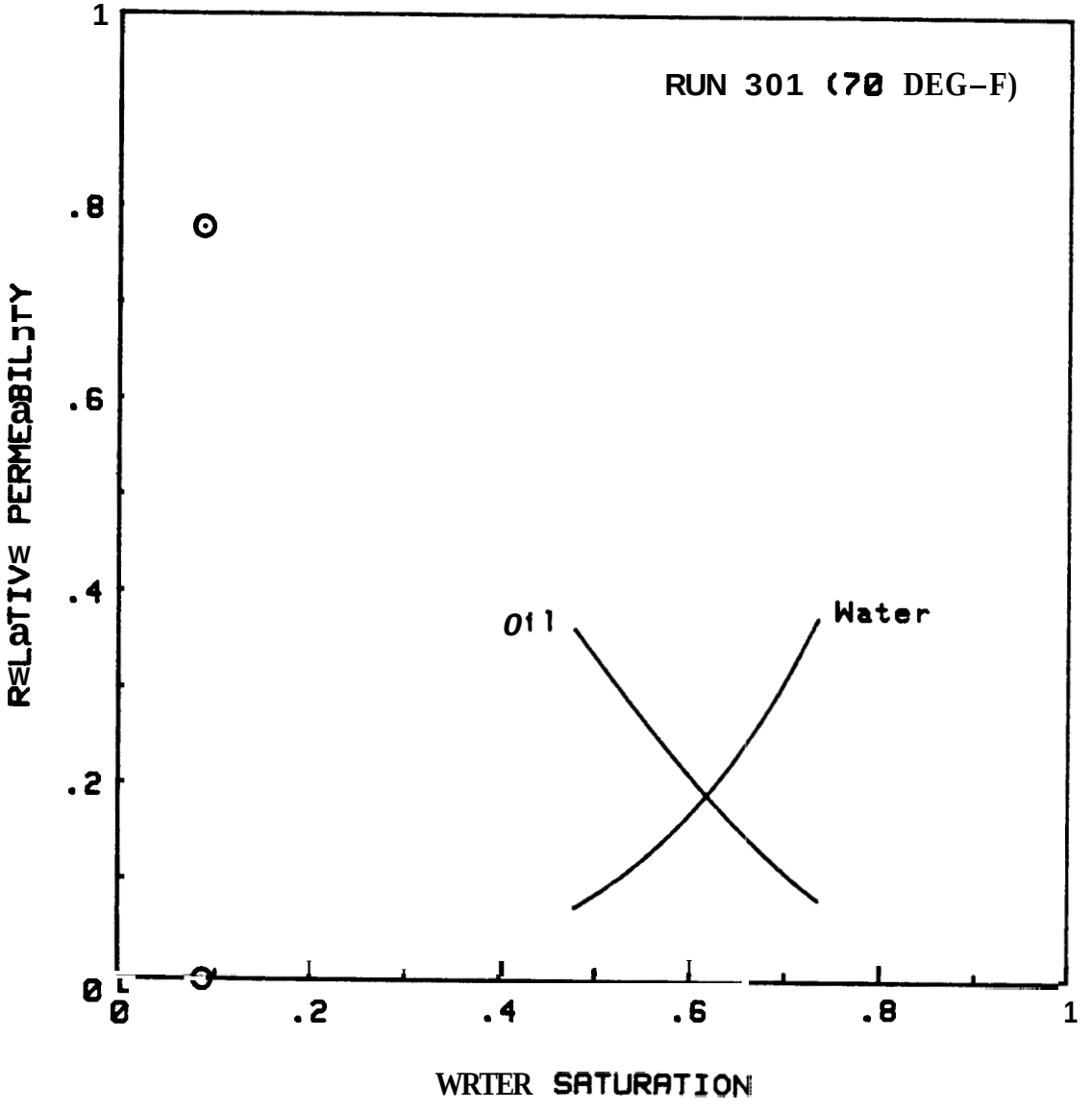

Fig. H. 14 Relative Permeabilities vs. Water Saturation -- Run 3/1

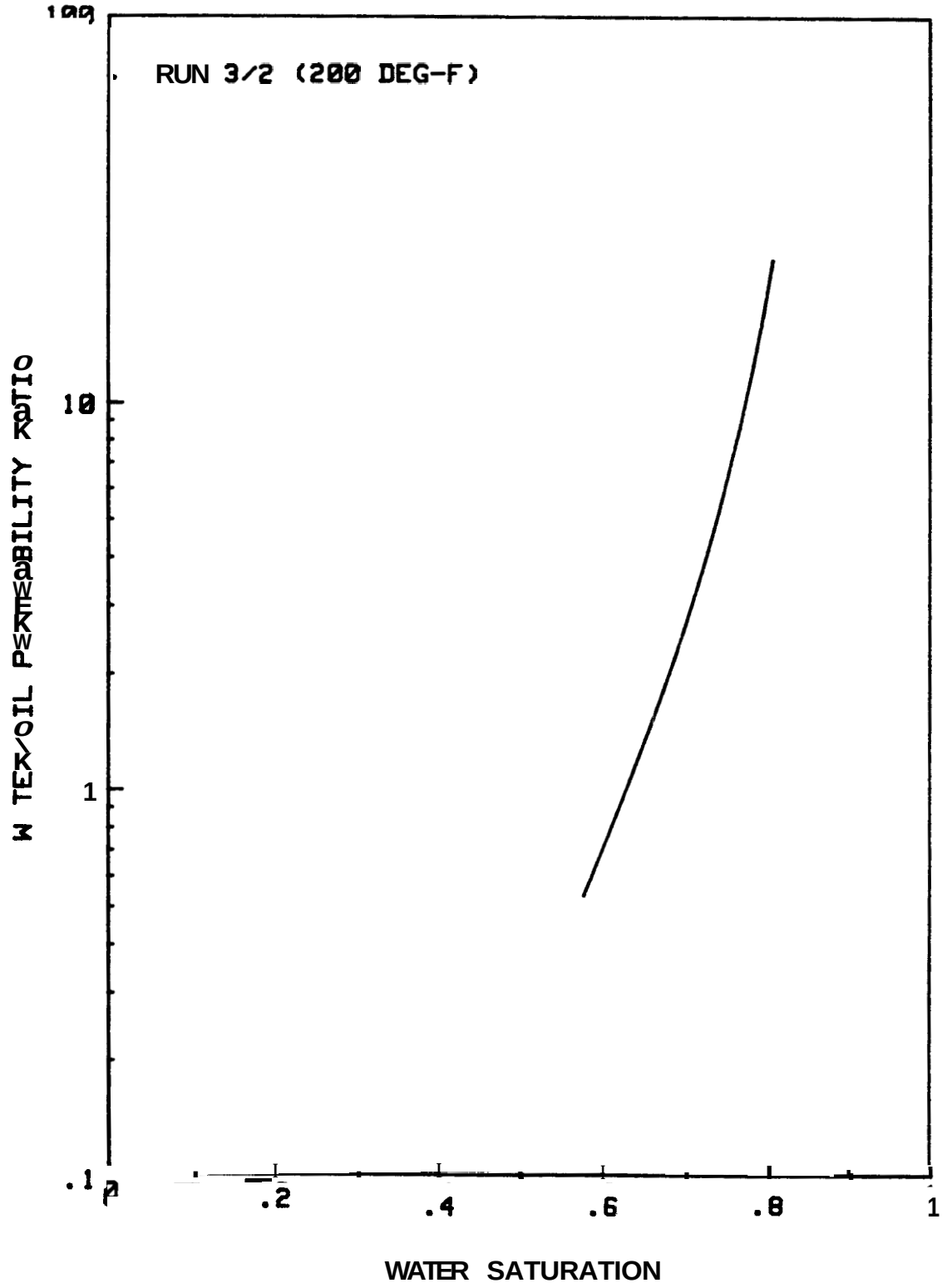

Fig. H.15 Relative Permeability Ratio vs. Water Saturation -- Run 3/2

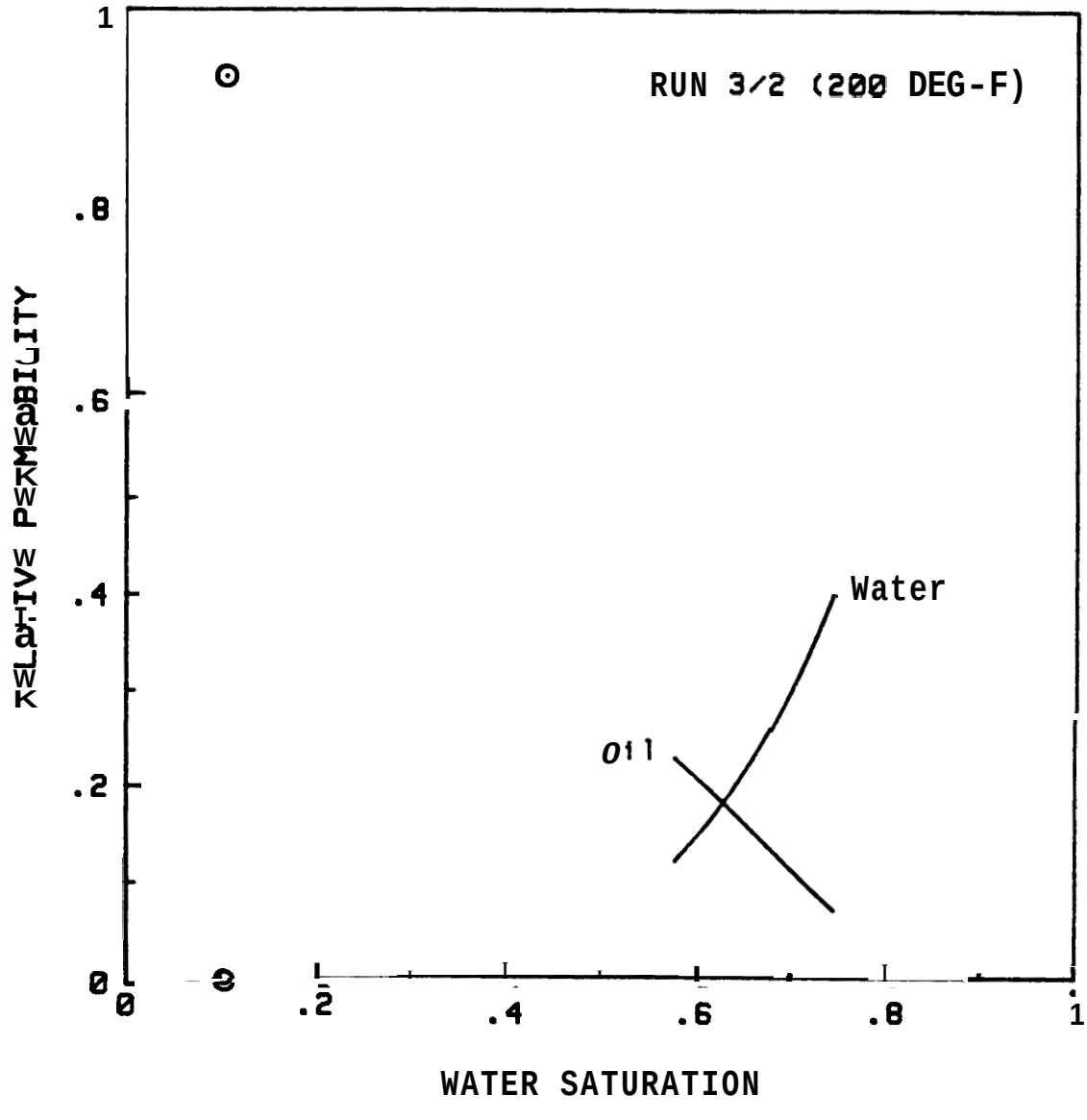

Fig. H.16 Relative Permeabilities vs. Water Saturation — Run 3/2

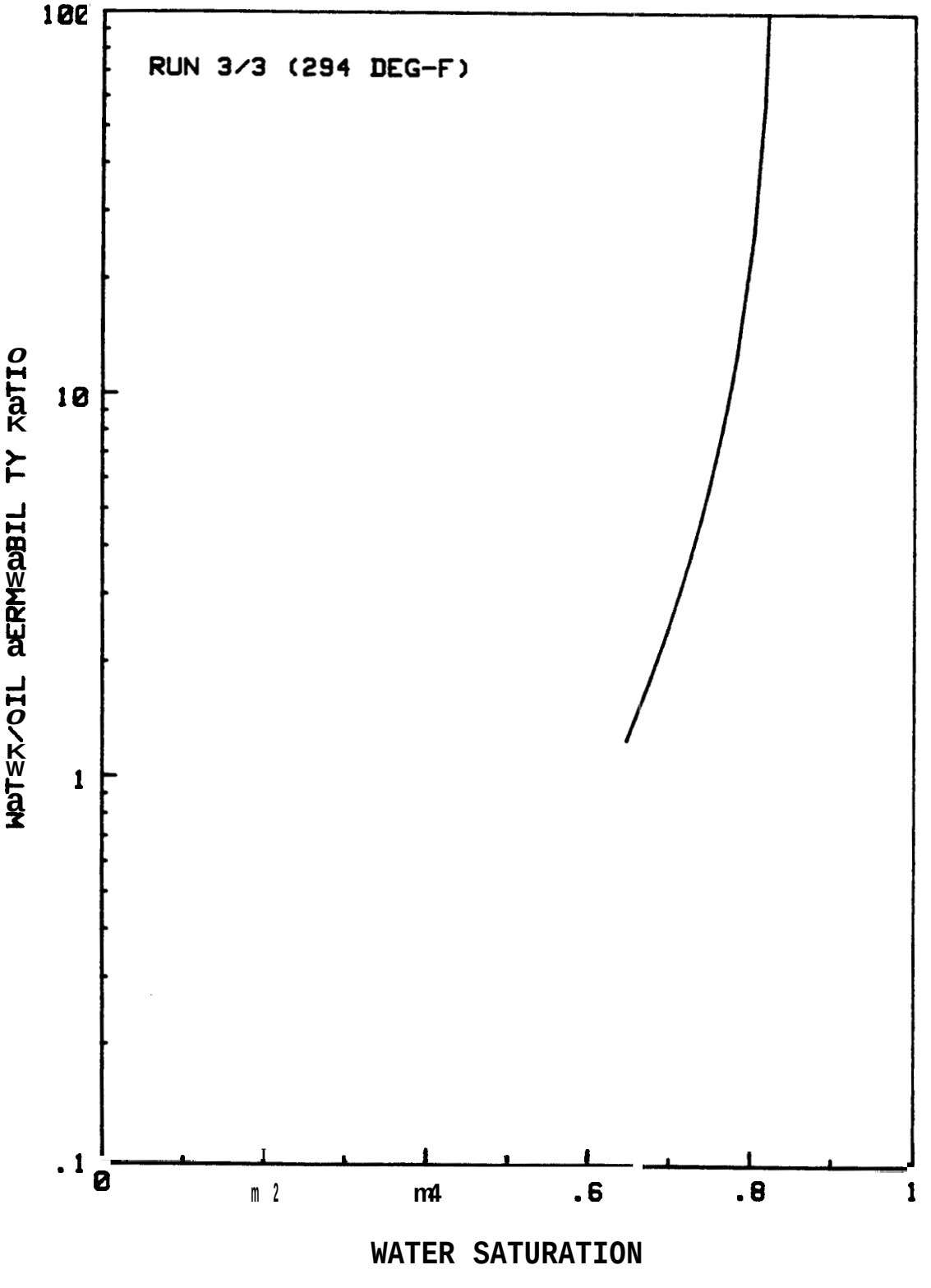

Fig. H.17 Relative Permeability Ratio vs. Water Saturation -- Run 3/3

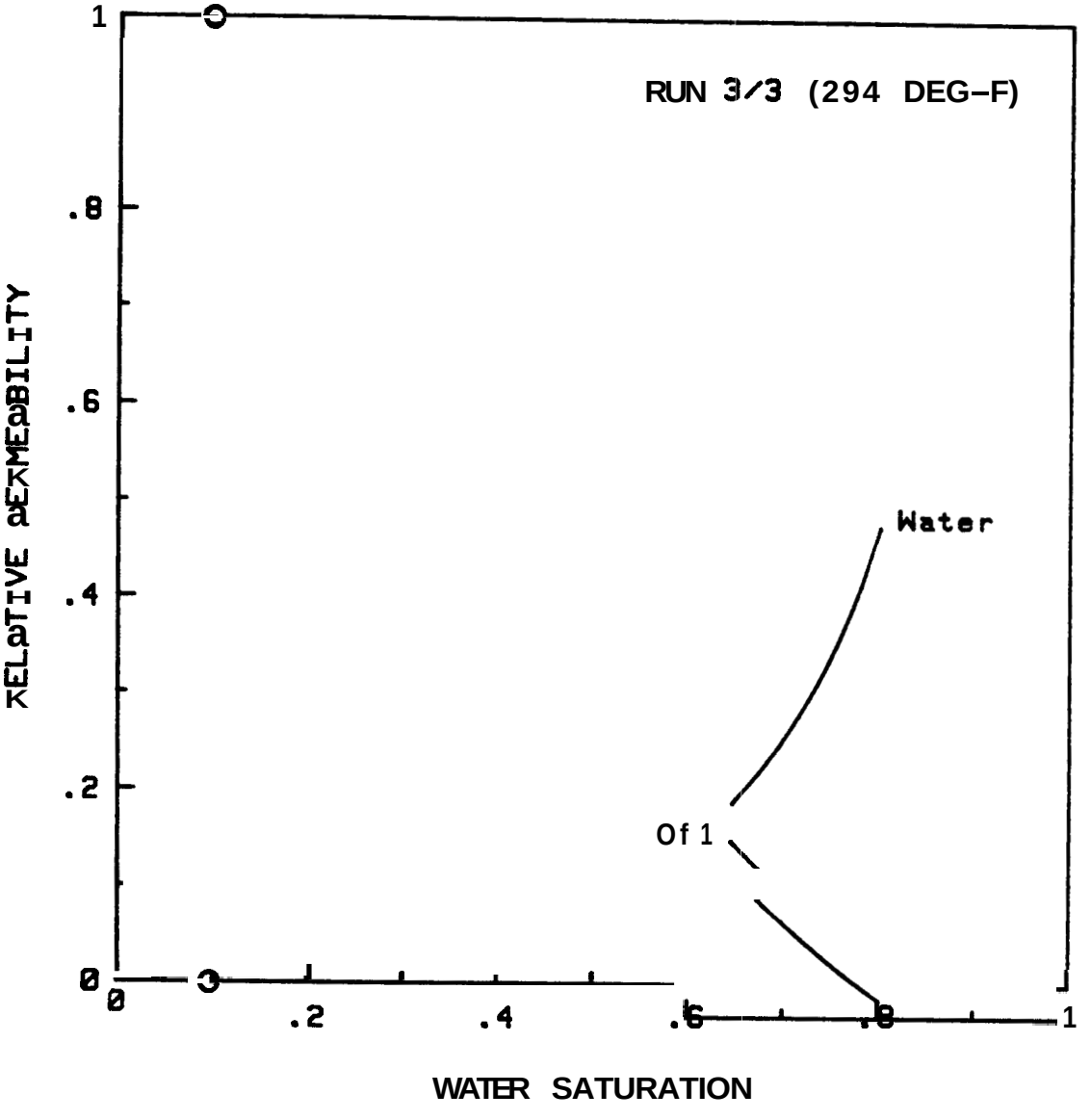

Fig. H. 18 Relative Permeabilities vs. Water Saturation -- Run 3/3

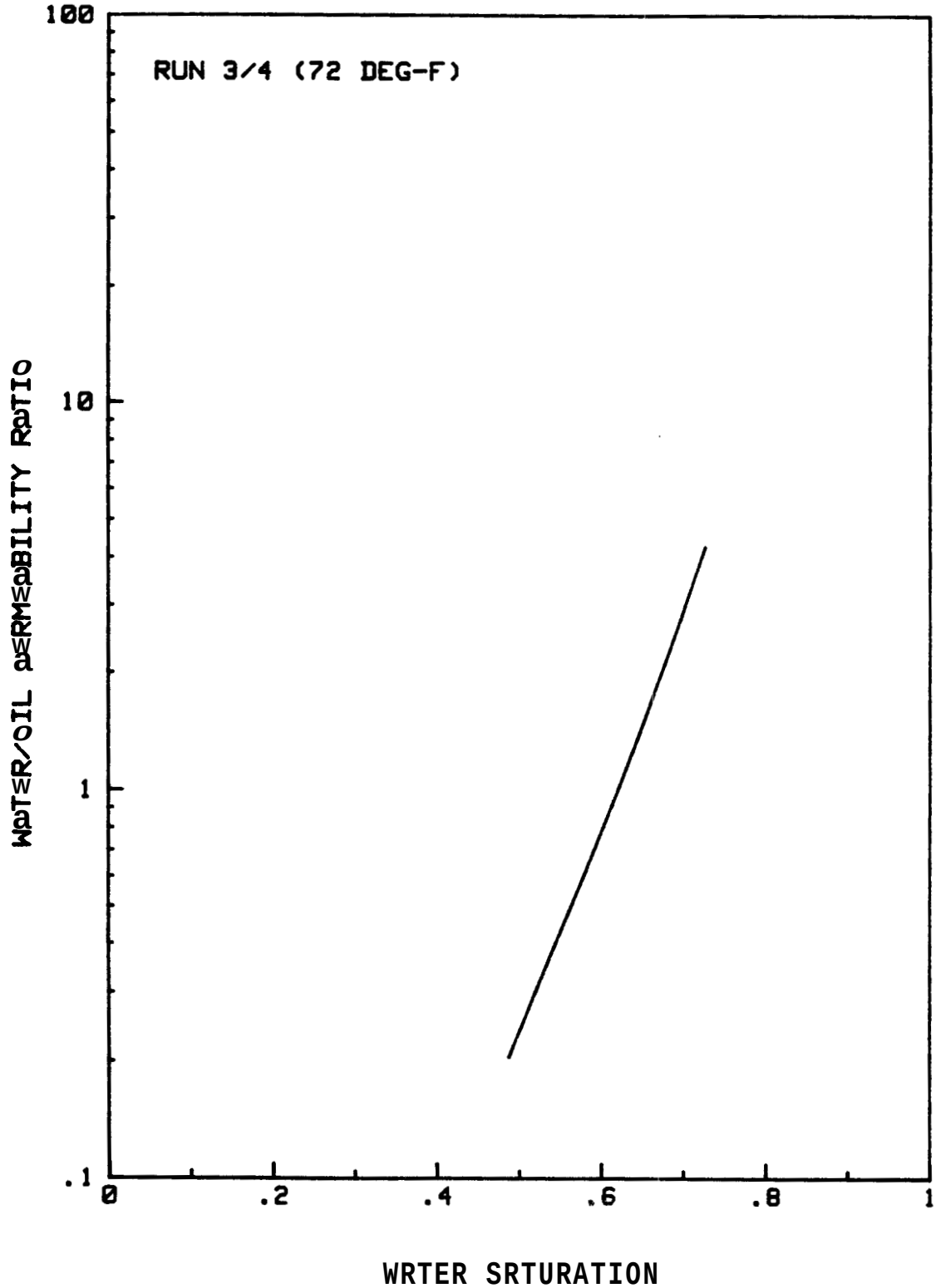

Fig. H.19 Relative Permeability Ratio vs. Water Saturation -- Run 3/4

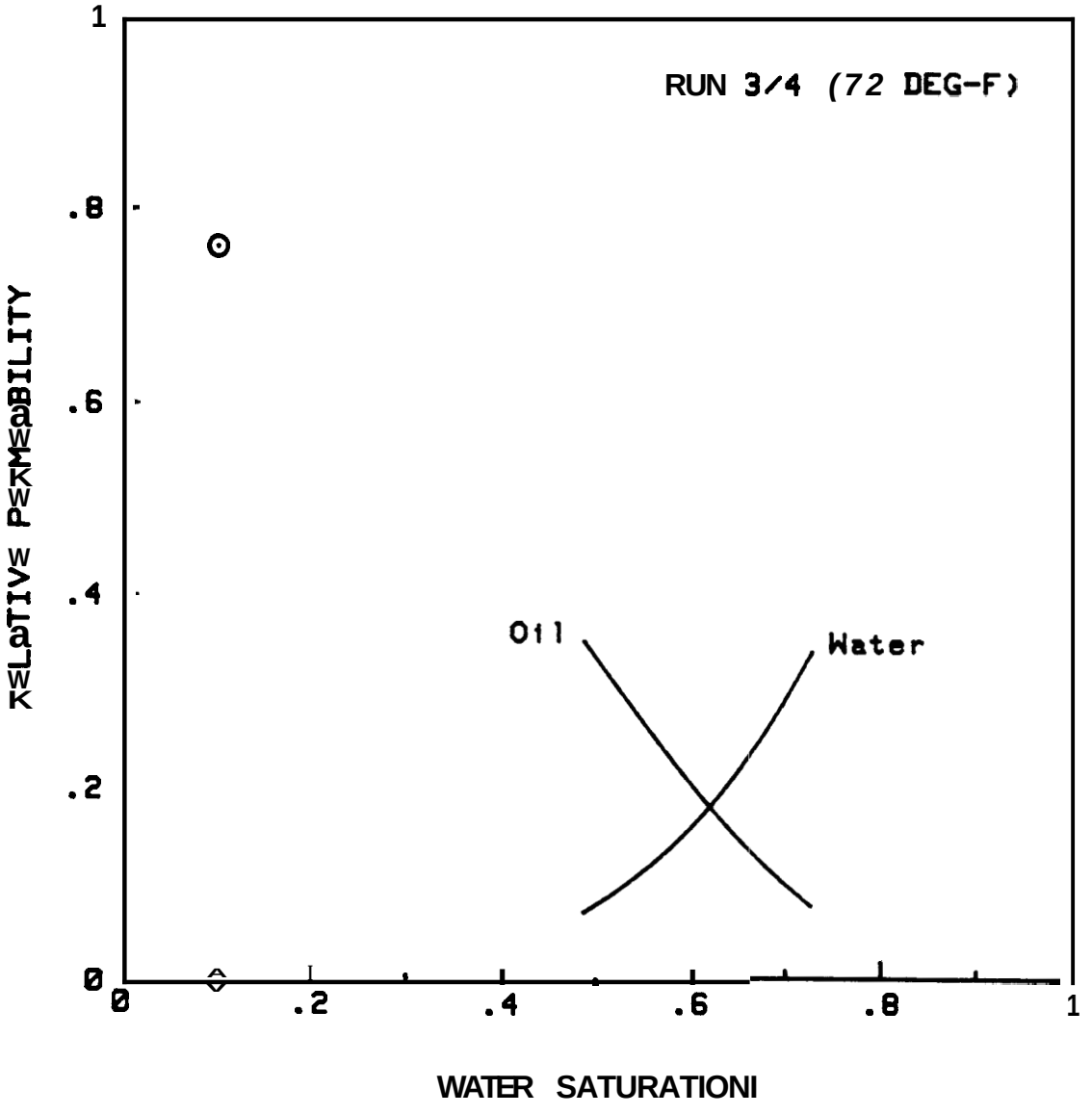

Fig. H.20 Relative Permeabilities vs. Water Saturation -- Run 3/4

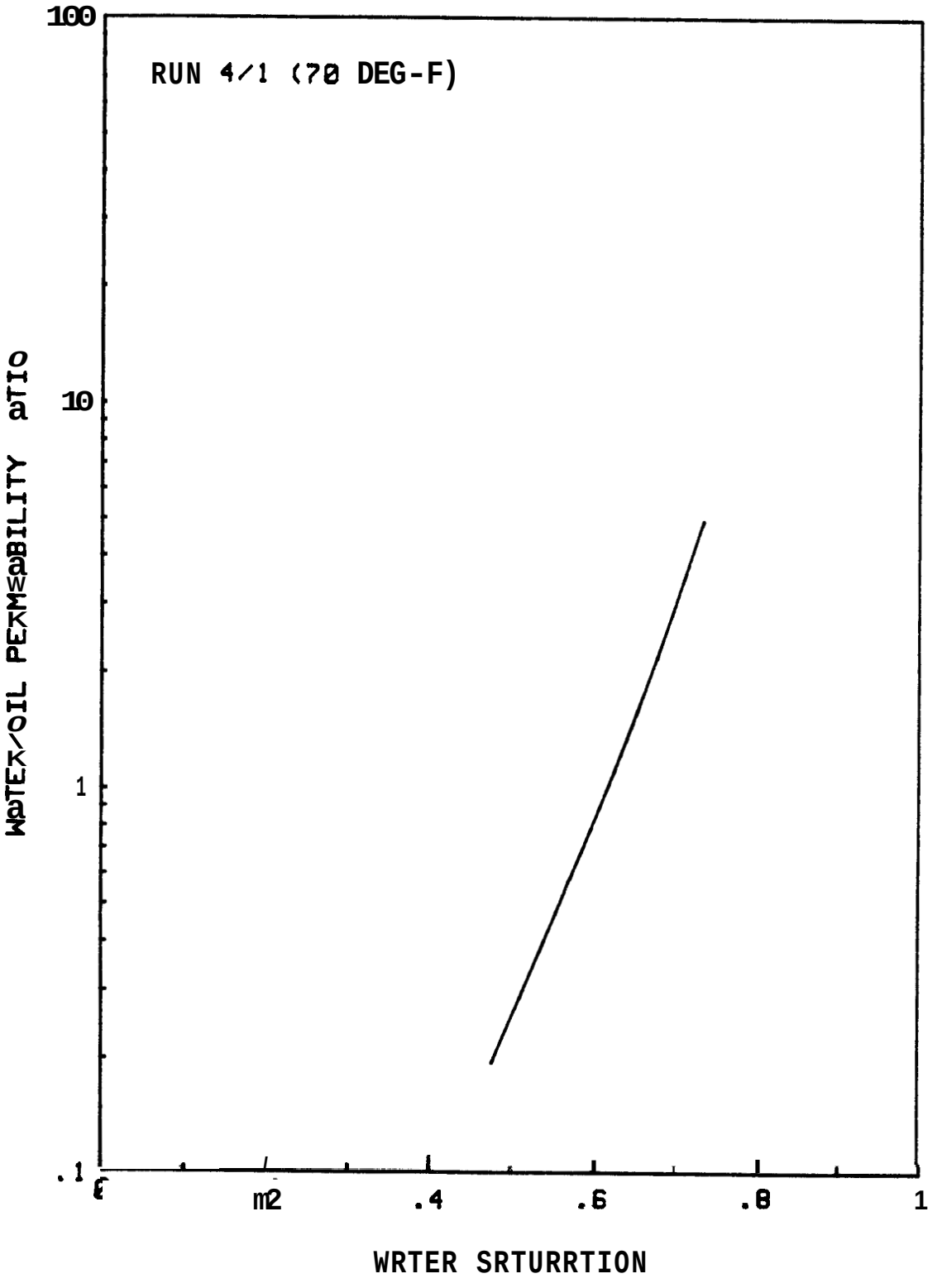

Fig. H.21 Relative Permeability Ratio vs. Water Saturation -- Run 4/1

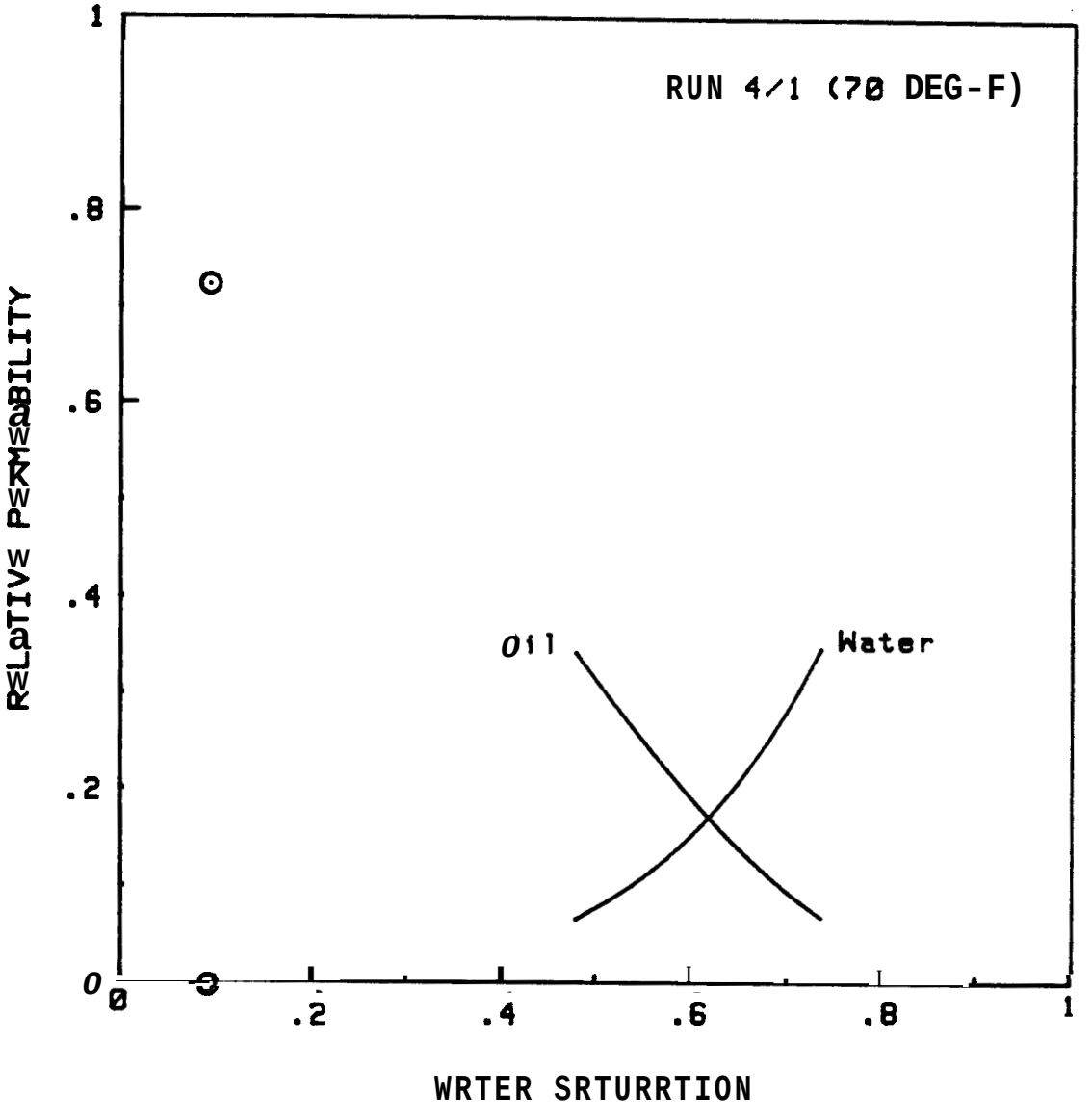

Fig. H.22 Relative Permeabilities vs. Water Saturation -- Run 4/1

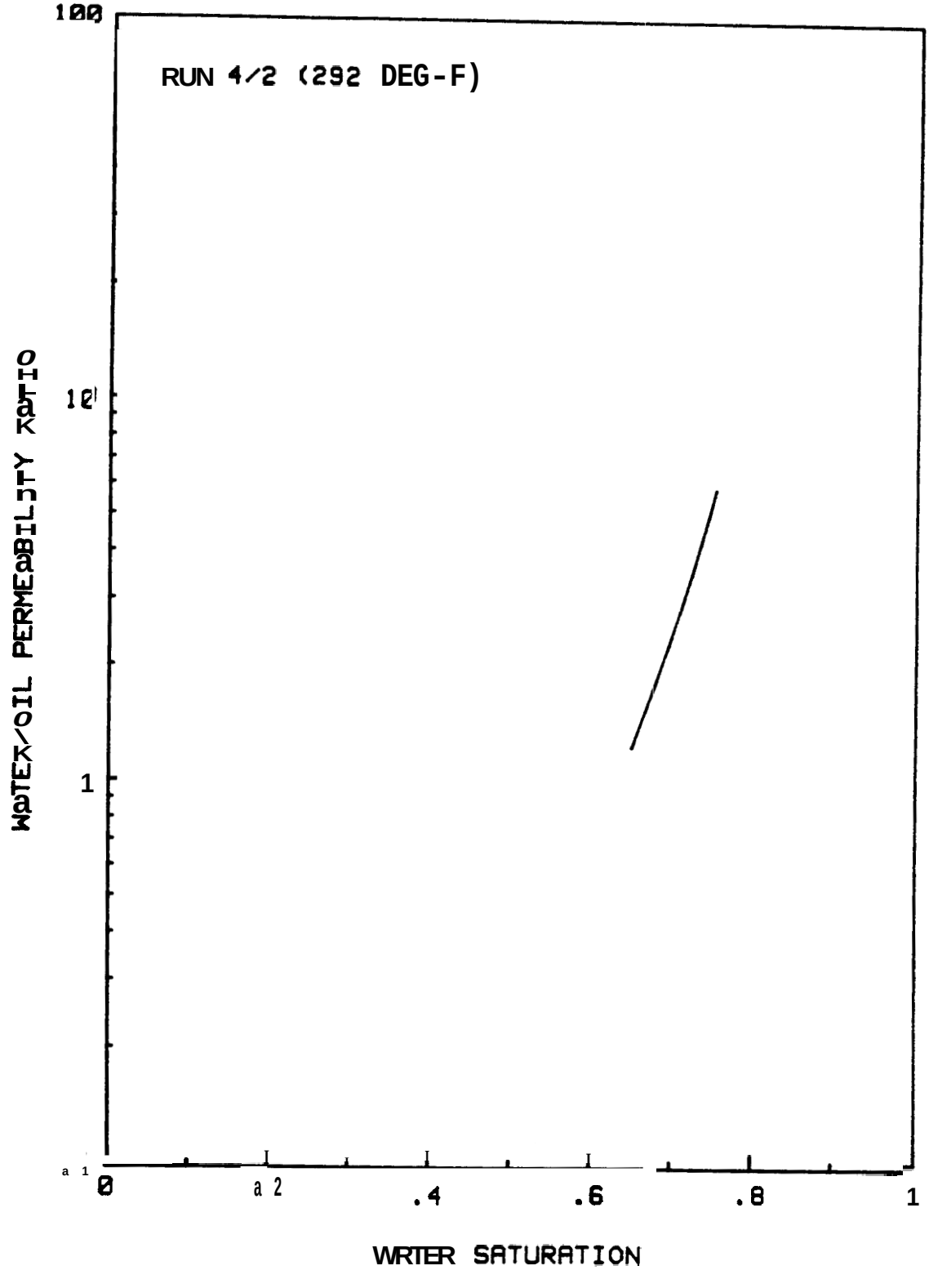

Fig. H.23 Relative Permeability Ratio vs. Water Saturation -- Run *4/2*

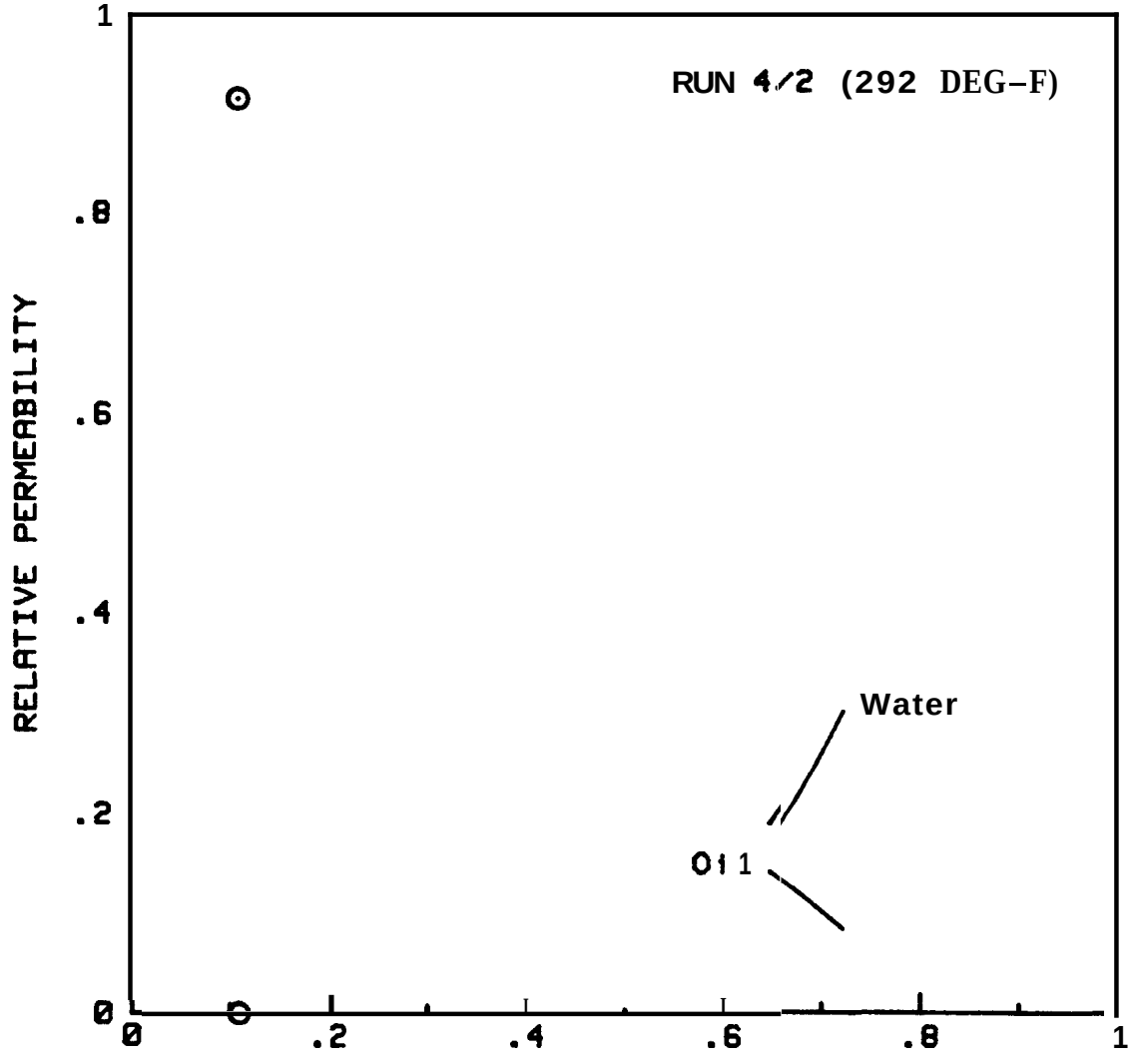

Fig. H.24 Relative Permeabilities vs. Water Saturation — Run 4/2

APPENDIX I - END-POINT SATURATION CALCULATIONS

Tables 1.1 through 1.3 present the end-point saturation calculations from computer program ENDSAT (see Appendix F) for the three unconsolidated sand cores run in this study.

Table I.1 End-Point Saturation Calculations; -- Core 2

CORE # 2
PORE VOLUME 391.2 cc
DEAD VOLUME 5.5 cc

RUN	DISPL FLUID	TEMP (F) CORE	TEMP (F) EFFLU	EXPAN COEFF WATER	EXPAN COEFF OIL	PROD/EXP(cc) ACTUAL	PROD/EXP(cc) CORE	WATER SAT cc	WATER SAT %	OIL SAT cc	OIL SAT %
				1.0000	1.0000	0.0	0.0	391.2		0.0	0.0
1	OIL	71.0	71.0	1.0000	1.0000	366.3	362.8	28.4	7.3	362.8	
				1.0002	1.0804	0.0	0.0	28.4	7.3	362.8	
	WATER	72.0	72.0	1.0000	1.0000	295.5	290.0	318.4		72.8	18.6
				.9994	.9985	0.0	0.0	318.5		72.7	18.6
2	OIL	68.5	68.5	1.0000	1.0000	291.9	286.4	32.1	8.2	359.1	
				1.0802	1.0007	0.0	0.0	32.1	8.2	359.1	
	WHTEF	78.8	70.0	1.0000	1.0000	286.3	280.8	312.9		78.3	20.9
				1.0359	1.0578	4.5	4.8	313.2		78.0	20.8
3	OIL	197.8	74.0	1.0352	1.0559	272.8	276.9	36.2	9.3	355.0	
				1.0008	1.0000	0.0	0.0	36.2	9.3	355.0	
	WATER	197.0	74.0	1.0352	1.0559	277.9	287.8	324.2		67.0	17.1
				.9653	.9454	0.0	0.0	327.8		63.4	16.2
4	OIL	70.0	70.0	1.8080	1.0080	293.8	288.3	39.5	10.1	351.7	
				1.0807	1,001 8	0.13	0.8	39.6	10.1	351.6	
	WHTER	74.0	74.0	1.0000	1.0000	284.8	279.3	318.9		72.3	18.5
				.9988	.9969	0.8	0.0	319.1		72.1	18.4
5	OIL	67.0	67.0	1.0080	1.00013	291.6	296.1	33.0	8.4	358.2	
				1.0005	1.0013	8.9	0.8	33.0	8.4	358.2	
	WATER	70.0	70.0	1.0088	1.0806	283.7	278.2	311.2		80.0	20.4
				1.0872	1.1061	14.3	15.8	316.9		72.7	18.6
6	OIL	298.0	74.0	1.0864	1.1042	261.1	278.2	40.3	10.3	358.9	
				.9994	.9996	0.0	0.0	40.3	10.3	350.9	
	WATER	297.8	74.0	1.0858	1.1037	266.7	288.9	329.2		62.0	15.9

Table 1.2 End-Point Saturation Calculations -- Core 3

CORE # 3
PORE VOLUME 395.9 cc
DEAD VOLUME 5.5 cc

RUN	DISPL FLUID	TEMP (F) CORE	TEMP (F) EFFLU	EXPAN COEFF MATER	EXPAN COEFF OIL	PROD/EXP(cc) ACTUAL	PROD/EXP(cc) CORE	WATER SAT cc	WATER SAT %	OIL SAT cc	OIL SAT %
				1.0000	1.0000	0.0	0.0	395.9		0.0	0.0
1	OIL	70.0	70.0	1.0000	1.0000	366.8	361.3	34.16	8.7	361.3	
				1.0000	1.0000	9.0	0.0	34.6	8.7	361.3	
	MATER	70.0	74.0	.9993	.9982	290.7	284.1	319.3		76.6	19.4
				1.0371	1.0592	3.0	3.2	317.9		78.0	19.7
2	OIL	208.0	76.0	1.0361	1.0564	272.6	276.9	41.0	10.4	354.9	
				1.0000	1.0000	0.0	0.0	41.0	10.4	354.9	
	WATER	200.0	76.0	1.0361	1.0564	280.9	291.2	332.2		63.7	16.1
				1.0465	1.0429	.0	.0	329.5		66.4	16.8
3	OIL	295.0	74.0	1.0846	1.1027	273.4	291.0	38.15	9.7	357.4	
				.9994	.9996	0.0	0.0	38.4	9.7	357.5	
	WRTER	294.8	75.0	1.0838	1.1017	268.4	290.2	328.6		67.3	17.0
				.9569	.9601	1.0	1.1	332.4		63.5	16.0
4	OIL	202.0	72.0	1.0376	1.0592	294.7	300.3	32.1	8.1	363.8	
				.9637	.9441	-9.5	-9.5	40.4	10.2	355.5	
	WRTER	72.0	72.0	1.0000	1.0000	279.4	273.9	314.3		81.6	20.6

Table 1.3 End-Point Saturation Calculations -- Core *4*

CORE # 4
PORE VOLUME 391.4 cc
DEAD VOLUME *5.5* cc

RUN	DISPL FLUID	TEMP (F) CORE	TEMP (F) EFFLU	EXPAN COEFF WATER	EXPAN COEFF OIL	PROD/EXP(cc) ACTUAL	PROD/EXP(cc) CORE	WATER SAT cc	WATER SAT %	OIL SAT cc	OIL SAT %
				1.0000	1.0000	0.0	0.0	391.4		0.0	0.0
1	OIL	67.0	67.0	1.0000	1.0000	360.2	354.7	36.7	9.4	354.7	
				1.0085	1.0013	0.0	0.0	36.7	9.4	354.7	
	WATER	70.0	69.0	1.0002	1.0004	281.8	276.4	313.1		78.3	20.0
				1.0853	1.1047	4.0	4.4	309.4		82.0	21.0
2	OIL	295.0	70.0	1.0853	1.1047	250.7	266.6	42.8	10.9	348.6	
				.9983	.9987	0.8	0.0	42.7	10.9	348.7	
	WATEF	292.0	78.8	1.0835	1.1032	251.8	272.3	315.0		76.4	19.5
				.9225	.9053	0.8	0.0	322.2		69.2	17.7
3	OIL	67.0	66.0	1.0082	1.0084	296.4	290.9	31.3	8.0	360.1	

APPENDIX J - DISPLACEMENT CALCULATIONS AND PLOTS OF RECOVERY AND INJECTIVITY DATA

This Appendix contains the displacement calculations from computer program DSPCLC (see Appendix G) and graphs of the recovery and injectivity data for the runs made in this study.

J.1 Oil Displacement Data

Tables J.1 through J.12 present the computer calculations for all oil displacement runs.

Table J.1 Oil Displacement Calculations -- Run 2/1

DISPLACEMENT EXPERIMENT CALCULATIONS

PORE VOLUME	391.2	cc	DATE	10/12/82
CORE LENGTH	51.47	cm	CORE/RUN	2/1
CORE DIAMETER	5.044	cm	DISPLACEMENT	OIL – Dist W
DEAD VOL'S: U	2.5	cc	CORE TEMPERATURE	71.0 F
D	3.0	cc	OUTLET TEMPERATURE	71.0 F
SEPARATOR OUTLET	82.72	cm	WATER VISCOSITY	.966 cp
BUBBLE VELOCITY	0.00	cm/sec	OIL VISCOSITY	29.08 cp
ABSOLUTE PERM	7.060	darcies	VISCOSITY RATIO	30.11
INIT SAT - OIL	0.0	%	WATER DENSITY RATIO	1.0000
FINAL SAT - WATER	7.3	%	OIL DENSITY RATIO	1.0000

	TIME	SEPARATOR HEIGHT	CALIB	D-VOL INJ	D-P	FLOWRRTE CHART AVG	@t	CAL	cc min	PVi	Rec	1/Inj
	(min)	(cm)	(cc/cm)	(cc)	(psi)							
ST		81.80										
0	0.00	81.86	4.99	9.8	1.95	.607	.607	37.2	22.6	0.008	.000	1.00
1	4.97	62.50	4.99	96.0	20.46	.559	.510	37.2	19.0	.239	.240	12.45
2	10.62	41.58	4.99	104.8	43.20	.499	.488	37.2	18.1	.507	.508	27.56
3	17.25	18.06	4.99	117.3	65.80	.475	.462	37.2	17.2	.807	.802	44.27
BT	19.15				72.66		.458	37.2	17.0	.888	.888	49.31
4	45.38	8.66	4.99	470.6	65.46	.451	.450	37.2	16.7	2.010	.927	45.21

Krw - INITIAL = .999
Kro - FINAL = .665

Table 5.2 Oil Displacement Calculations — Run 2/2

DISPLRCEMENT EXPERIWENT CALCULATIONS

PORE VOLUME	391.2	cc	DATE	10/18/82	
CORE LENGTH	51.47	cm	CORE/RUN	2/2	
CORE DIAMETER	5.044	cm	DISPLACEMENT	OIL – Dist W	
DEAD VOL'S: U	2.5	cc	CORE TEMPERATURE	68.5	F
D	3.0	cc	OUTLET TEMPERATURE	68.5	F
SEPARATOR OUTLET	82.72	cm	URTER VISCOSITY	.999	cp
BUBBLE VELOCITY	0.00	cm/sec	OIL VISCOSITY	30.95	cp
RESOLUTE PERM	7.060	darcies	VISCOSITY RATIO	30.98	
INIT SAT - OIL	18.6	%	UATER DENSITY RATIO	1.0000	
FINAL SAT - UATER	8.2	%	OIL DENSITY RATIO	1.0088	

	TIME	SEPARATOR HEIGHT	SEPARATOR CHLIB	D–VOL INJ	D–P	FLOWRATE CHART AVG	FLOWRATE CHART @t	FLOWRATE CHART CAL	cc min	PVi	Rec	1/Inj
	(min)	(cm)	(cc/cm)	(cc)	(psi)							
ST		81.53										
8	0.00	R1.53	4.96	*0.0*	4.15	.592	.592	35.1	20.8	0.008	.000	1.00
1	5.32	62.50	4.96	93.9	24.40	.506	.492	35.1	17.3	.234	,235	7.07
2	10.97	43.28	4.93	95.4	44.98	.481	.470	35.1	16.5	.478	.478	13.63
3	16.56	25.68	4.92	91.1	63.20	.460	.450	35.3	15.9	.710	,704	19.95
BT	16.74				63.58		.450	35.3	15.9	.717	.717	20.81
4	22.45	23.45	4.93	92.0	60.80	,444	.442	35.3	15.6	.946	.720	19.50
5	49.60	22.46	4.93	426.6	58.16	.438	.433	35.3	15.3	2.019	.732	19.02

Krw - INITIAL = .447
Kro - FINAL = .728

Table 5.3 Oil Displacement Calculations -- Run 2/3

DISPLACEMENT EXPERIMENT CALCULATIONS

PORE VOLUME	391.2 cc	DATE	10/19/82
CORE LENGTH	51.47 cm	CORE/RUN	2/3
COPE DIAMETEP:	5.044 cm	DISPLACEMENT	OIL-Dist W
DEAD VOL'S: U	2.5 cc	CORE TEMPERATURE	197.0 F
D	3.0 cc	OUTLET TEMPERATURE	74.0 F
SEPARATOR OUTLET	82.72 cm	UATER VISCOSITY	.309 cp
BUBBLE VELOCITY	0.00 cm/sec	OIL VISCOSITY	3.75 cp
ABSOLUTE PERM	7.060 darcies	VISCOSITY RATIO	12.16
INIT SAT - OIL	20.8 %	WATER DENSITY RATIO	1.0352
FINAL SAT - WATER	9.2 %	OIL DENSITY RATIO	1.0559

	TIME	SEPARATOR HEIGHT	CALIE	D-VOL INJ	D-P	FLOWRATE CHAPT AVG	@t	CAL	cc min	PVi	Rec	1/Inj
	(min)	(cm)	(cc/cm)	(cc)	<psi:@							
ST		81.70										
0	0.00	81.70	4.96	0.0	1.50	,548	.548	39.0	21.3	0.000	.000	1.00
1	4.88	62.58	4.96	95.2	5.18	.507	.504	39.0	19.6	.246	.246	3.70
2	9.82	43.58	4.91	93.0	8.58	.501	.498	39.0	19.4	.492	.492	6.24
BT	12.86				11.25		.492	39.2	19.3	.642	.642	8.31
3	14.78	27.50	4.88	92.5	10.85	.494	.490	39.2	19.2	.737	.695	8.05
4	19.93	26.90	4.88	95.0	9.45	.490	.490	39.7	19.5	.993	.699	6.91
5	24.97	26.68	4.88	93.5	8.75	.490	.488	48.0	19.5	1.246	.703	6.38
6	30.03	26.45	4.88	94.0	8.33	.487	.486	40.2	19.5	1.499	.705	6.06
7	35.13	26.27	4.88	94.8	8.05	.485	.484	40.1	19.4	1.753	.707	5.98
8	48.12	26.26	4.88	93.8	7.93	.483	.483	48.8	19.7	2.084	.708	5.73
9	44.00	26.25	4.88	72.5	7.83	.483	.482	40.8	19.7	2.208	.708	5.66

Erw - INITIAL = .393
Kro - FINAL = .843

Table J.4 Oil Displacement Calculations -- Run 2/4

DISPLACEMENT EXPERIMENT CALCULATIONS

PORE VOLUME	391.2 cc		DATE	10/20/82
CORE LENGTH	51.47 cm		CORE/RUN	2/4
CORE DIAMETER	5.044 cm		DISPLACEMENT	OIL - Dist W
DEAD VOL'S: U	2.5 cc		CORE TEMPERATURE	70.0 F
D	3.8 cc		OUTLET TEMPERATURE	70.0 F
SEPRRRTOR OUTLET	82.72 cm		URTER VISCOSITY	.979 cp
BUBBLE VELOCITY	8.00 cm/sec		OIL VISCOSITY	29.81 cp
RESOLUTE PERM	7.860 darcies		VISCOSITY RRTIO	30.45
INIT SAT - OIL	16.2 %		WATER DENSITY RRTIO	1.0000
FINAL SRT - WATER	10.1 %		OIL DENSITY RATIO	1.0000

	TIME	SEPARATOR HEIGHT	SEPARATOR CALIB	D-VOL INJ	D-P	FLOWRATE CHART AVG	CHART @t	CHART CAL	cc min	PVi	Rec	1/Inj
	(min)	(cm)	(cc/cm)	(cc)	(psi)							
ST		78.70										
0	0.66	78.70	4.84	0.0	3.56	.520	.520	35.2	18.3	0.000	.000	1.00
1	5.82	59.50	4.14	93.5	20.08	.460	.449	35.2	15.8	.233	.231	6.62
2	11.92	40.50	5.04	94.5	35.80	.440	.430	35.2	15.1	.474	.476	12.37
BT	18.26				51.20		.418	35.0	14.6	.715	.715	18.31
3	18.27	21.56	4.85	94.2	51.20	.424	.418	35.0	14.6	.715	.708	18.31
4	24.65	19.36	4.84	93.0	49.20	.412	.410	35.4	14.5	.953	.731	17.75
E	54.67	18.86	4.84	437.0	48.00	.406	.402	35.9	14.4	2.670	.737	17.42

Krw - INITIAL = .458
Kro - FINAL = .800

Table J.5 Oil Displacement Calculations — Run 2/5

DISPLACEMENT EXPERIMENT CALCULATIONS

PORE VOLUME	391.2 cc		DATE	11/29/82	
CORE LENGTH	51.47 cm		CORE/RUN	2/5	
COKE DIAMETER	5.044 cm		DISPLACEMENT	OIL - Dist W	
DEAD VOL'S: U	2.5 cc		CORE TEMPERHTURE	67.0 F	
D	3.0 cc		OUTLET TEMPERATURE	67.0 F	
SEPARATOR OUTLET	82.72 cm		UATER VISCOSITY	1.820 cp	
BUBBLE VELOCITY	0.00 cm/sec		OIL VISCOSITY	32.14 cp	
ABSOLUTE PERM	7.060 darcies		VISCOSITY RATIO	31.53	
INIT SAT - OIL	18.4 %		UATER DENSITY RATIO	1.0000	
FINAL SAT - WATER	8.5 %		OIL DENSITY RATIO	1.0000	

	TIME	SEPARATOR HEIGHT	SEPARATOR CALIB	D-VOL INJ	D-P	FLOWRATE CHART AVG	CHART @t	CHART CAL	cc min	PVi	Rec	1/Inj
	(min)	(cm)	(cc/cm)	(cc)	(psi)							
ST		79.12										
0	0.80	79.12	4.97	0.0	5.15	.812	.812	33.8	26.8	0.000	.000	1.08
1	4.27	68.50	4.97	91.0	29.90	.654	.632	33.0	20.9	.226	.230	7.46
2	8.92	41.50	4.95	94. 0	53.28	.612	.591	33.0	19.5	.467	.470	14.1%
3	13.90	22.50	4.69	94.2	74.48	.574	.557	32.9	18.3	.707	.704	21.12
BT	14.88				74.50		.557	33.5	18.6	.712	.712	28.62
4	19.12	20.30	4.88	95.6	71.06	.546	.543	33.5	18.2	.952	.728	26.35
5	24.25	20.20	4.88	93.0	70.08	.542	.540	33.5	18.1	1.189	.729	20.13
6	29.63	20.20	4.88	97.9	69.20	.539	.539	33.7	18.2	1.440	.729	19.82
7	35.02	20.20	4.88	98. 0	68.38	.536	.533	34.0	18.1	1.690	.729	19.65
8	40.32	20.10	4.88	96.0	67.88	.531	.530	34.1	18.1	1.936	.730	19.53
9	42.52	20.08	4.88	39.9	67.30	.530	.530	34.2	18.1	2.038	.731	19.33

Krw - INITIAL = .474
Kro - FINAL = ,774

Table 5.6 Oil Displacement Calculations -- Run 2/6

DISPLACEMENT EXPERIMENT CALCULATIONS

PORE VOLUME	391.2 cc	DATE	11/30 82
CORE LENGTH	51.47 cm	CORE/RUN	2/6
CORE DIAMETEP	5.044 cm	DISPLACEMENT	OIL-D st W
DEAD VOL S: U	2.5 cc	CORE TEMPERATURE	298.0 F
D	3.0 cc	OUTLET TEMPERATURE	74.0 F
SEPARATOR OUTLET	82.72 cm	CIATER VISCOS ITY	.184 cp
BUBBLE VELOCITY	0.08 cm/sec	OIL VISCOSITY	1.62 cp
ABSOLUTE PEPM	7.068 darcies	VISCOSITY RATIO	8.81
INIT SAT - OIL	18.6 %	WATEF DENSITY RATIO	1.0864
FINHL SAT - YATEP	16.3 %	OIL DENSITY RATIO	1.1042

	TIME	SEPHPHTOP HEIGHT	CHLIE	D-VOL INJ	D-P	FLOWRATE CHART		CAL	cc min	PVi	Rec 1/	nj
	(min)	(cm)	(cc/cm)	(cc)	(psi)	AVG	@t					
ST		81.82										
8	0.00	81.82	4.92	0.0	.eS	.568	.568	41.1	23.3	0.000	.000	1.08
1	4.65	62.58	4.92	94.8	2.84	.531	.527	41.1	21.7	.257	.258	3.46
2	9.45	43.08	4.93	95.0	4.58	.523	.520	41.1	21.4	.521	.523	5.65
BT	12.53				5.45		.511	41.5	21.2	.689	.689	6.78
3	14.23	30.50	4.86	93.5	5.83	.515	.510	41.5	21.2	.782	.688	6.27
4	19.05	29.65	4.86	94.0	4.64	.509	.508	42.3	21.5	1.047	.697	5.78
5	23.90	29.20	4.86	94.8	4.43	.506	.503	42.3	21.3	1.312	.703	5.58
6	28.68	28.95	4.86	92.5	4.28	.502	.500	42.5	21.3	1.573	.706	5.31
7	33.52	28.75	4.86	93.8	4.89	.500	.499	42.9	21.4	1.838	.709	5.85
8	38.32	28.61	4.86	93.8	3.95	.499	.498	42.9	21.3	2.188	.711	4.88
9	42.32	28.60	4.86	77.0	3.82	.496	.493	42.9	21.1	2.318	.711	4.77

Krw - INITIHL = .435
Kro - FINAL = .803

Table 5.7 Oil Displacement Calculations -- Run 3/1

DISPLACEMENT EXPERIMENT CALCULATIONS

PORE VOLUME	395.9 cc	DATE	12/8/82
CORE LENGTH	51.69 cm	CORE/RUN	3/1
CORE DIAMETER	5.044 cm	DISPLACEMENT	OIL-Dist W
DEAD VOL'S: U	2.5 cc	CORE TEMPERATURE	70.0 F
D	3.0 cc	OUTLET TEMPERATURE	70.0 F
SEPARATOR OUTLET	81.41 cm	WATER VISCOSITY	.979 cp
BUBBLE VELOCITY	0.00 cm/sec	OIL VISCOSITY	29.81 cp
ABSOLUTE PEPM	6.900 darcies	VISCOSITY RATIO	30.45
INIT SAT - OIL	0.0 %	WATER DENSITY RATIO	1.0000
FINHL SAT - UATER	8.7 %	OIL DENSITY RATIO	1.0000

		SEPARATOR		D-VOL		FLOWRATE						
	TIME	HEIGHT	CALIB	INJ	D-P	CHART			cc			
	(min)	(cm)	(cc/cm)	(cc)	(psi)	AVG	@t	CHL	min	PVi	Rec 1/	nj
ST		79.15										
0	0.88	79.15	4.99	0.0	1.95	.601	.601	35.8	21.5	0.000	.000	1.00
1	5.40	68.00	4.99	95.6	17.70	.497	.482	35.8	17.3	.235	.235	11.32
2	11.00	41.68	5.08	94.5	31.98	.471	.460	35.8	16.5	.474	.475	21.37
3	16.92	22.66	5.01	95.0	46.28	.449	.437	35.8	15.6	.714	.715	32.65
BT	20.86				56.70		.423	35.6	15.2	.867	.867	41.33
4	22.98	7.36	4.95	93.0	55.30	.428	.418	35.8	15.0	.949	.894	48.79
5	29.32	6.70	4.95	94.7	54.90	.415	.413	36.0	14.9	1.188	.899	40.74
6	35.58	6.48	4.95	93.2	54.20	.411	.410	36.2	14.8	1.423	.903	46.34
7	41.82	6.15	4.95	93.8	53.96	.409	.408	36.5	14.9	1.658	.906	39.99
8	46.06	5.58	4.95	93.8	53.38	.407	.406	36.8	14.9	1.895	.909	39.42
5	54.28	5.68	4.95	91.4	53.00	.405	.404	36.9	14.9	2.126	.913	39.26

Krw - INITIHL = .992
Kro - FINAL = .770

Table J.8 Oil Displacement Calculations -- Run 3/2

DISPLACEMENT EXPERIMENT CALCULATIONS

PORE VOLUME	395.9 cc		DATE	12/9/82
CORE LENGTH	51.69 cm		COREf RUN	3f2
COKE DIAMETER	5.044 cm		DISPLACEMENT	OIL- Dist W
DEAD VOL'S: U	2.5 cc		CORE TEMPERATURE	200.0 F
D	3.0 cc		OUTLET TEMPERATURE	76.0 F
SEPARATOR OUTLET	81.41 cm		URTER VISCOSITY	.303 cp
BUBBLE VELOCITY	0.00 cm/sec		OIL VISCOSITY	3.64 cp
ABSOLUTE PERM	6.900 drrcies		VISCOSITY RATIO	12.00
INIT SAT - OIL	19.7 %		WATER DENSITY RATIO	1.0361
FINAL SAT - MATER	10.3 %		OIL DENSITY RATIO	1.0564

	TIME	SEPARATOR HEIGHT	CALIE	D-VOL INJ	D-P	FLOWRATE CHART AVG	@t	CAL	cc min	PVi	Rec	1/Inj
	(min)	(cm)	(cc/cm)	(cc)	(psi)							
ST		77.70										
0	0.00	77.78	5.00	0.0	1.33	.574	.574	40.3	23.1	0.008	.000	1.00
1	4.75	58.08	5.00	97.0	5.53	.524	.516	46.3	20.8	.247	.251	4.63
a	9.5;	39.00	4.99	95.0	8.23	.513	.510	48.3	20.5	.496	.498	6.96
BT	12.62				10.10		.505	40.6	20.5	.658	.658	8.55
3	14.22	24.76	4.97	93.0	9.50	.507	.500	48.6	20.3	.741	.678	8.13
4	38.33	23.88	4.9;	465.0	7.98	.494	.490	41.2	28.2	1.981	.700	6.86
5	42.96	23.08	0.08	91.1	7.96	.490	.489	42.2	20.7	2.224	.700	6.64

Krw - INITIAL = .483
Kro - FINAL = .873

Table J.9 Oil Displacement Calculations — Run 3/3

DISPLACEMENT EXPERIMENT CALCULATIONS

PORE VOLUME	395.9 cc	DATE	12/18/82
CORE LENGTH	51.69 cm	CORE/RUN	3/3
CORE DIAMETER	5.044 cm	DISPLACEMENT	OIL – Dist W
DEAD VOL'S: U	2.5 cc	CORE TEMPERATURE	295.0 F
D	3.0 cc	OUTLET TEMPERATURE	74.0 F
SEPARATOR OUTLET	81.41 cm	WATER VISCOSITY	.187 cp
BUBBLE VELOCITY	0.00 cm/sec	OIL VISCOSITY	1.66 cp
ABSOLUTE PERM	6.900 darcies	VISCOSITY RATIO	8.87
INIT SAT - OIL	16.8 %	WATER DENSITY RATIO	1.0846
FINAL SAT - UATER	9.7 %	OIL DENSITY RATIO	1.1027

	TIME	SEPARATOR HEIGHT	SEPARATOR CRLIB	D–VOL INJ	D–P	FLOWRATE CHART AVG	FLOWRATE CHART @t	FLOWRATE CHART CAL	FLOWRATE cc/min	PVi	Rec	1/Inj
	(min)	(cm)	(cc/cm)	(cc)	(psi)							
ST		77.83										
0	0.00	77.83	4.56	0.0	.77	.575	.575	42.0	24.1	8.086	.000	1.08
1	4.52	59.00	4.96	93.5	3.58	,534	.528	42.0	22.2	.250	.250	4.95
2	9.25	39.50	4.98	96.0	4.53	.524	.520	42.0	21.8	.513	.515	6.94
BT	12.84				5.78		.515	41.9	21.6	.709	.709	8.46
3	14.12	24.16	5.08	96.6	5.28	.516	.511	41.9	21.4	.778	.720	7.74
4	38.77	22.90	5.00	480.0	3.84	.507	.499	42.3	21.1	2.115	.735	5.76
5	43.33	22.90	0.00	9'5.2	3.74	.498	.497	43.3	21.5	2.375	.735	5.45

Krw - INITIAL = .538
Kro - FINAL = .875

Table J.10 Oil Displacement Calculations -- Run 3/4

DISPLACEMENT EXPERIMENT CALCULATIONS

PONE VOLUME	395.9 cc	DATE	12/11/82
CORE LENGTH	51.69 cm	CORE/RUN	3/4
CORE DIAMETEP	5.044 cm	DISPLACEMENT	OIL-Dist W
DEAD VOL'S: U	2.5 cc	CORE TEMPERATURE	202.0 F
D	3.8 cc	OUTLET TEMPERATURE	72.0 F
SEPARATOR OUTLET	81.41 cm	MATER VISCOSITY	.299 cp
BUBBLE VELOCITY	0.80 cm/sec	OIL VISCOSITY	3.56 cp
ABSOLUTE PERM	6.900 darcies	VISCOSITY RATIO	11.90
INIT SAT - OIL	16.0 %	WATER DENSITY RATIO	1.0376
FINAL SAT - UATER	8.1 %	OIL DENSITY RATIO	1.0592

	TIME	SEPARATOR HEIGHT	SEPARATOR CALIE	D-VOL INJ	D-P	FLOWPHTE CHART AVG	FLOWPHTE CHART @t	FLOWPHTE CHART CAL	cc mrn	PVi	Rec	1/Inj
	(min)	(cm)	(cc/cm)	(cc)	(psi)							
ST		*77.88*										
0	0.08	77.80	4.96	0.0	1.31	.598	.598	39.1	23.4	0.088	.000	1.08
1	4.47	59.00	4.96	92.1	5.43	.553	.544	39.1	21.3	.235	.238	4.56
2	9.11	48.08	4.91	94.0	10.95	.537	.530	39.1	28.7	.481	.483	9.43
ET	14.80				16.78		,516	39.1	28.2	.733	.733	14.76
3	14.82	28.58	4.92	96.2	16.60	.521	.512	39.1	28.0	.734	.730	14.79
4	18.97	19.80	4.92	93.2	15.00	.508	.504	39.2	19.8	.983	.746	13.54
5	41.86	18.00	4.92	425.8	12.78	.495	.486	39.7	19.3	2.119	.759	11.75
&	46.65	18.88	0.00	8S.R	12.48	.485	.484	48.7	19.7	2.357	.759	11.23

Krw - INITIAL = .490
Kro - FINRL = .520

Table J.11 Oil Displacement Calculations -- Run 4/1

DISPLACEMENT EXPERIMENT CALCULATIONS

PORE VOLUME	391.4	cc	DATE	12/28/82	
CORE LENGTH	51.60	cm	CORE/RUN	4/1	
CORE DIAMETER	5.044	cm	DISPLACEMENT	OIL - Dist W	
DEAD VOL'S: U	2.5	cc	CORE TERPERATUKE	67.0	F
D	3.0	cc	OUTLET TEMPERATURE	67.0	F
SEPARATOF OUTLET	61.40	cm	UATER VISCOSITY	1.020	cp
BUBBLE VELOCITV	0.00	cm/sec	OIL VISCOSITY	32.14	cp
ABSOLUTE PERM	6.750	darcies	VISCOSITY RATIO	31.53	
INIT SAT - OIL	0.0	%	WATER DENSITY RATIO	1.0800	
FINAL SAT - MATEP	9.4	%	OIL DENSITY RRTIO	1.0000	

	TIME	SEPARATOR HEIGHT	D-VOL CHLIB	INJ	D-P	FLOWRATE CHAFT			cc			
	(min)	(cm)	(cc/cm)	(cc)	(psi)	AVG	@t	CAL	mim	PVi	Rec	1/Inj
ST		77.18										
0	0.08	77.18	4.98	0.0	2.28	.676	.676	34.1	23.6	0.008	.000	1.08
1	4.95	57.50	4.98	95.1	28.18	.566	.552	34.1	18.8	.237	.238	11.19
2	10.07	38.90	4.59	94.1	39.20	.540	.527	34.1	17.9	.477	.480	22.86
3	15.48	20.00	5.04	94.9	59.00	.513	.499	34.2	17.0	.719	.722	36.23
BT	18.96				70.10		,483	34.4	16.6	.869	.869	44.28
4	21.10	6.30	5.00	94.0	68.50	.487	.476	34.4	16.4	.960	.892	43.82
5	43.83	5.10	5.80	375.8	65.50	.469	.462	35.2	16.2	1.918	.906	42.18
6	49.42	5.10	0.80	91.3	64.70	.461	.460	35.5	16.3	2.151	.906	41.58

C'rw - INITIAL =1.000
Kro - FINHL = .760

Table 5.12 Oil Displacement Calculations -- Run 4/2

DISPLACEMENT EXPERIMENT CALCULATIONS

PORE VOLUME	391.4 cc	DATE	12/21/82
CORE LENGTH	51.60 cm	CORE/RUN	4/2
CORE DIAMETER	5.044 cm	DISPLACEMENT	OIL-Dist W
DEHD VOL'S: U	2.5 cc	CORE TEMPERATURE	295.6 F
D	3.0 cc	OUTLET TEMPERATURE	70.0 F
SEFRPATOR OUTLET	81.40 cm	WATER VISCOSITY	.187 cp
BUBBLE VELOCITY	0.00 cm/sec	OIL VISCOSITY	1.66 cp
ABSOLUTE PERM	6.750 darcies	VISCOSITY RATIO	8.87
INIT SAT - OIL	21.0 %	WATER DENSITY RATIO	1.0853
FINHL SAT - WATER	10.9 %	OIL DENSITY RATIO	1.1047

	TIME	SEPARATOR HEIGHT	CALIB	D-VOL INJ	D-P	FLOWRHTE CHAFT AVG	@t	CAL	cc min	PVi	Rec	1/Inj
	(min)	(cm)	(cc/cm)	(cc)	(psi)							
ST		76.40										
0	0.00	76.46	4.97	8.0	1.27	.648	.648	39.6	25.6	0.000	.000	1.00
1	4.15	50.00	4.97	92.0	3.66	.601	.599	39.6	23.7	.249	.248	3.08
2	8.48	25.061	5.00	94.5	4.83	.598	.598	39.6	23.7	.511	.510	4.14
ET	10.92				5.55		.594	39.7	23.6	.658	.658	4.77
3	12.78	27.10	5.01	92.8	5.00	.594	.591	39.7	23.5	.770	.670	4.32
4	29.88	26.20	5.01	362.8	4.37	.586	.580	39.9	23.1	1.791	.681	3.83
5	34.45	2E.28	6.60	97.5	4.33	.580	.580	461.7	23.6	2.066	.681	3.72

Krw - INITIAL = .355
Kro - FINAL = .846

5.2 Water Displacement Data and Recovery and Injectivity Plots

Tables J.13 through 5.24 present the computer output for all water displacement runs. Figures J. 1 through J.24 present graphs of recovery and injectivity times pore volumes injected vs. pore volumes injected and vs. the reciprocal of pore volumes injected.

Table J.13 Water Displacement Calculations -- Run 2/1

DISPLACEMENT EXPERIMENT CALCULATIONS

PORE VOLUME	391.2 cc	DATE	18/12/82
CORE LENGTH	51.47 cm	CORE/RUN	2/1
CORE DIAMETER	5.044 cm	DISPLACEMENT	Dist W-OIL
DEAD VOL'S: U	2.5 cc	CORE TEMPERATURE	72.8 F
D	3.8 cc	OUTLET TEMPERATURE	72.8 F
SEPARATOR OUTLET	82.72 cm	UATER VISCOSITY	.953 cp
BUBBLE VELOCITY	7.58 cm/sec	OIL VISCOSITY	28.37 cp
ABSOLUTE PERM	7.060 darcies	VISCOSITY RATIO	29.77
INIT SAT - WATER	7.3 %	WATER DENSITY RATIO	1.8000
FINAL SAT - OIL	18.6 %	OIL DENSITY RATIO	1.8000

	TIME	SEPARATOR HEIGHT	SEPARATOR CALIB	D-VOL INJ	D-P	FLOWRATE CHART AVG	CHART @t	CHART CAL	cc/min	PVi	Rec	Inj
	(min)	(cm)	(cc/cm)	(cc)	(psi)							
ST		8.80										
0	0.08	7.40	4.96	0.0	66.10	.440	.440	40.3	17.7	0.800	.000	1.00
1	4.55	26.80	4.96	95.9	49.90	.516	.531	40.3	21.4	.239	.238	1.60
BT	8.61				22.50		.554	40.3	22.3	.466	.466	3.70
2	9.02	46.00	4.89	97.6	20.70	.542	.554	40.3	22.3	.488	.472	4.02
3	13.10	50.95	4.88	93.0	13.40	.566	.570	461.2	22.9	.726	.528	6.38
4	17.22	53.06	4.88	94.4	11.30	.570	.571	48.2	23.8	.967	.553	7.58
5	21.25	54.68	4.88	93.0	9.93	.571	.571	40.4	23.1	1.205	.572	8.65
6	25.08	55.80	4.88	89.2	9.08	.571	.571	40.3	23.0	1.430	.587	9.44
7	29.50	57.00	4.88	101.0	8.33	.571	.572	40.0	22.9	1.689	.602	10.25
8	33.45	58.00	4.88	92.1	7.80	.572	.571	40.8	23.3	1.924	.614	11.12
9	37.30	58.75	4.88	89.2	7.33	.571	.571	40.6	23.2	2.152	.624	11.78
10	41.27	59.35	4.88	92.0	6.88	.570	.570	40.7	23.2	2.387	.631	12.56
11	45.12	60.00	4.88	90.0	6.55	.570	.570	41.0	23.4	2.617	.639	13.30
12	49.02	60.67	4.88	91.2	6.28	.570	.570	41.0	23.4	2.850	.648	13.88
13	53.00	61.18	4.88	92.4	6.05	.570	.570	40.7	23.2	3.087	.654	14.29
14	56.93	61.72	4.88	91.3	5.88	.570	.569	40.7	23.2	3.320	.661	14.68
15	60.97	62.20	4.88	93.1	5.70	.569	.568	48.6	23.0	3.558	.667	15.06
16	64.93	62.60	4.88	92.2	5.56	.567	.567	41.0	23.2	3.794	.672	15.75
17	85.58	64.35	4.88	478.0	4.83	.565	.563	41.0	23.1	5.016	.693	17.80
18	105.92	65.70	4.88	471.0	4.38	.562	.561	41.2	23.1	6.220	.710	19.67
19	126.85	66.82	4.88	483.0	-.00	.560	.560	41.2	23.1	7.454	.724	-.00
20	147.38	67.50	4.88	475.0	-.00	.558	.556	41.5	23.1	8.668	.733	-.00
21	168.27	68.21	4.88	482.0	-.00	.554	.552	41.7	23.0	9.901	.741	-.00

CURVE FITS	C0	C1	c2	%E-MAX	%E-AVG
Recovery	5.5606E-01	9.1831E-02	-4.4486E-03	.3	.1
Inj. X Pore Vol. Inj.	2.0443E+00	1.5914E+00	-4.3987E-02	1.5	.6

	PVi	R-ACT	R-CALC	R-%E	I*P-ACT	I*P-CALC	I*P-%E	Sw	Krw	Kro	Kw/Ko
								.073	0.000	.680	0.000
BT		.466	.488		1.72	2.41					
3	.726	.528	.526	.3	4.63	4.C2	.3	.505	.078	.349	.224
4	.967	.553	.553	.1	7.33	7.32	.0	.534	.098	.308	.319
5	1.205	.572	.573	.1	10.43	10.38	.5	.556	.116	.278	.415
6	1.430	.587	.588	.2	13.51	13.58	.5	.573	.130	.257	.508
7	1.689	.602	.603	.1	17.30	17.57	1.5	.589	.146	.236	.617
8	1.924	.614	.614	.0	21.40	21.48	.4	.601	.159	.221	.718
9	2.152	.624	.624	.0	25.35	25.49	.5	.612	.171	.209	.817
10	2.387	.631	.633	.2	29.99	29.84	.5	.622	.182	.198	.920
11	2.617	.639	.640	.2	34.81	34.25	1.5	.630	.192	.188	1.022
12	2.850	.648	.647	.0	39.55	58.98	1.4	.638	.202	.180	1.127
13	3.087	.654	.654	.0	44.10	43.91	.4	.645	.212	.172	1.234
14	3.320	.661	.660	.1	48.75	48.94	.4	.652	.221	.165	1.341
15	3.558	.667	.665	.2	53.60	54.23	1.2	.658	.230	.159	1.450
16	3.794	.672	.671	.1	59.74	59.62	.2	.664	.238	.153	1.560
17	5.016	.693	.693	.1	89.25	89.67	.5	.688	.278	.130	2.141
18	6.220	.710	.709	.2	122.35	122.24	.1	.706	.310	.114	2.731
19	7.454	.724	.723	.2	-.00	-.00	-.0	.722	-.800	-.800	3.352
20	8.668	.733	.734	.1	-.00	-.80	-.0	.734	-.000	-.800	3.976
21	9.901	.741	.743	.2	-.00	-.80	-.0	.745	-.800	-.800	4.622

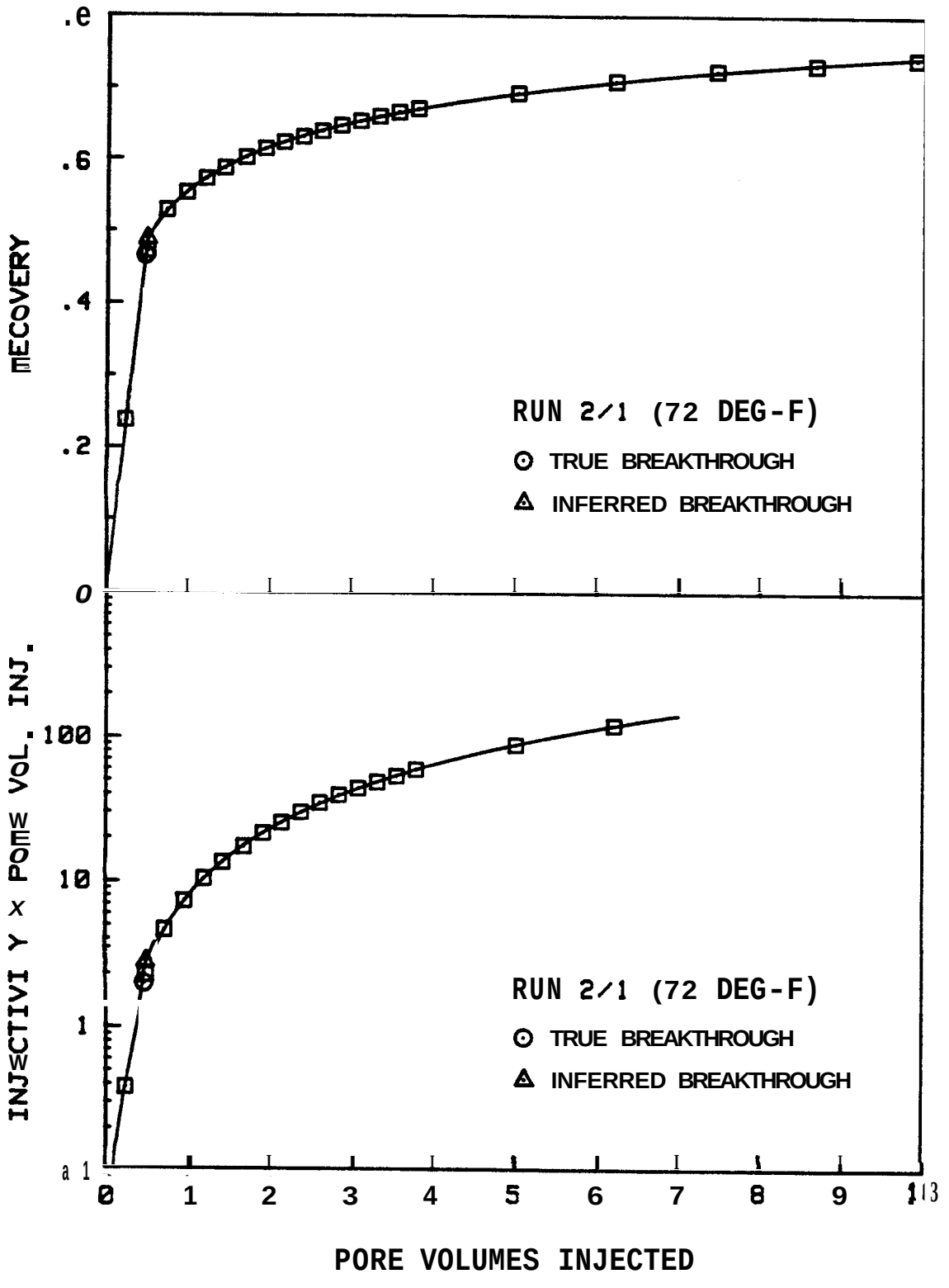

Figure J.1 Recovery and Injectivity x Pore Volumes Injected vs. Pore Volumes Injected -- Run 2/1

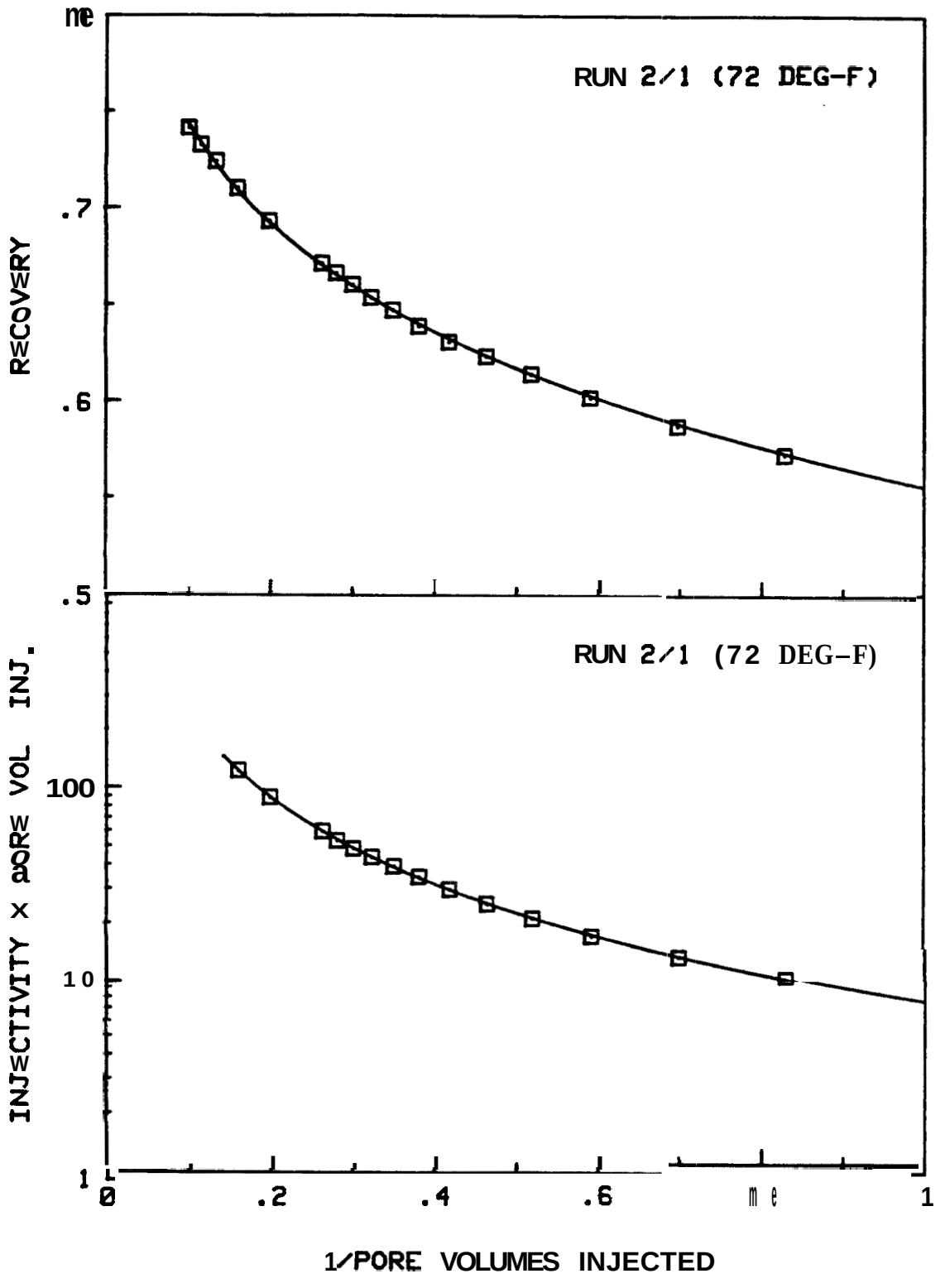

Fig. 5.2 Recovery and Injectivity x Pore Volumes Injected vs. 1/Pore Volumes Injected — Run 2/1

Table 5.14 Water Displacement Calculations -- Run 2/2

DISPLACEMENT EXPERIMENT CALCULATION$[

PORE VOLUME	391.2	cc	
CORE LENGTH	51.47	cm	
CORE DIAMETER	5.044	cm	
DEAD VOL'S: U	2.5	cc	
D	3.0	cc	
SEPARATOR OUTLET	82.72	cm	
BUBBLE VELOCITY	6.29	cm/sec	
ABSOLUTE PERM	7.060	darcies	
INIT SAT - UATER	8.2	%	
FINAL SAT - OIL	20.0	%	

DATE	18/18/82
CORE/RUN	2/2
DISPLACEMENT	Dist W-OIL
CORE TEMPERATURE	70.0 F
OUTLET TEMPERATURE	70.0 F
UATER VISCOSITY	.979 cp
OIL VISCOSITY	29.81 cp
VISCOSITY RATIO	30.45
WATER DENSITY RATIO	1.0000
OIL DENSITY RATIO	1.0000

	TIME	SEPARATOR HEIGHT	SEPARATOR CALIB	D-VOL INJ	D-P	FLOWRATE CHART AVG	CHART @t	CHART CAL	cc min	PVi	Rec	Inj
	(min)	(cm)	(cc/cm)	(cc)	(psi)							
ST		9.69										
0	0.00	9.00	4.96	0.0	58.60	.442	.442	37.9	16.7	0.000	.000	1.00
1	4.62	27.60	4.96	93.9	43.90	.513	.526	37.9	19.9	.234	.228	1.5%
BT	8.58				21.80		.546	37.9	20.7	.440	.440	3.32
2	9.22	46.80	4.88	93.9	18.78	.539	.551	37.9	20.9	.474	.451	3.91
3	13.67	51.80	4.78	93.8	13.10	.559	.559	37.7	21.1	.713	.516	5.63
4	18.03	53.20	4.80	92.5	11.10	.559	.559	37.9	21.2	.950	.532	6.68
5	22.30	54.90	4.80	90.6	9.78	.559	.558	38.0	21.2	1.181	.552	7.59
6	26.72	56.30	4.80	94.0	8.83	.558	.556	38.1	21.2	1.422	.569	8.41
7	31.13	57.30	4.80	93.5	8.23	.556	.555	38.1	21.1	1.661	.582	8.99
8	35.55	58.38	4.81	94.2	7.70	.555	.556	38.4	21.4	1.902	.594	9.71
9	39.85	59.00	4.90	92.0	7.25	.557	.555	38.4	21.3	2.137	.602	10.29
10	44.18	59.75	4.90	93.0	6.85	.555	.555	38.7	21.5	2.374	.612	10.97
11	48.42	66.40	4.90	90.9	6.55	.555	.553	38.7	21.4	2.607	.620	11.43
12	52.75	60.95	4.90	93.0	6.28	.553	.552	38.8	21.4	2.845	.627	11.94
13	57.17	61.46	4.90	94.7	6.03	.551	.550	38.9	21.4	3.087	.632	12.43
14	61.48	62.00	4.90	93.0	5.83	.550	.550	39.2	21.5	3.324	.640	12.94
15	65.85	62.40	4.90	94.5	5.70	.550	.550	39.3	21.6	3.566	.645	13.29
16	70.27	62.85	4.90	95.0	5.50	.550	.550	39.1	21.5	3.809	.650	13.69
17	83.93	63.95	4.90	288.0	-.00	.540	.549	39.0	21.4	4.545	.664	-.00
18	88.42	64.25	4.90	96.0	-.00	.549	.549	39.0	21.4	4.790	.668	-.00
19	91.47	64.50	4.90	65.0	-.00	.550	.550	38.7	21.3	4.957	.671	-.00
20	114.52	65.90	4.90	491.0	-.00	.546	.545	39.0	21.3	6.212	.688	-.00
21	137.72	66.92	4.90	495.0	-.00	.543	.541	39.3	21.3	7.477	.701	-.00
22	183.48	68.25	4.90	985.0	-.00	.540	.540	39.9	21.5	9.995	.718	-.00

CURVE FITS	c0	c1	c2	%E-MAX	%E-AVG
Recovery	5.3996E-01	8.6123E-02	-3.1677E-03	1.0	.2
Inj. X Pore Vol. Inj.	1.9273E+00	1.5679E+00	-3.7855E-02	1.0	.3

	PVi	R-ACT	R-CALC	R-%E	I*P-ACT	I*P-CALC	I*P-%E	Sw	Krw	Kro	Kw/Ko
								.082	0.000	.761	0.000
BT		.440	.474		1.46	2.09					
3	.713	.516	.511	1.0	4.02	4.03	.3	.504	.078	.334	.233
4	.950	.532	.536	.7	6.35	6.34	.1	.531	.096	.294	.328
5	1.181	.552	.554	.3	8.96	8.92	.5	.551	.112	.266	.423
6	1.422	.569	.570	.1	11.95	11.87	.7	.568	.127	.243	.524
7	1.661	.582	.583	.2	14.93	15.07	1.0	.582	.141	.225	.625
8	1.902	.594	.594	.1	18.47	18.53	.3	.594	.153	,211	.728
9	2.137	.602	.604	.2	22.00	22.11	.5	.604	.165	.198	.830
10	2.374	.612	.612	.0	26.04	25.92	.5	.613	.175	.188	.934
11	2.607	.620	,620	.0	29.81	29.81	.0	.622	.185	.179	1.036
12	2.845	.627	.627	.0	33.97	33.96	.0	.629	.195	.171	1.142
13	3.087	.632	,633	.1	38.35	38.34	.0	.636	.204	.163	1.250
14	3.324	.640	.639	.2	43.01	42.78	.5	.642	.213	.157	1.358
15	3.566	.645	.644	.1	47.40	47.45	.1	.648	.221	.151	1.467
16	3.809	.650	.649	.1	52.14	52.27	.2	.654	.229	.145	1.578
17	4.545	.664	.663	.2	-.00	-.00	-.0	.669	-.000	-.000	1.917
18	4.790	.668	.667	.1	-.00	-.00	-.0	.673	-.000	-.000	2.032
19	4.957	.671	.670	.2	-.00	-.00	-.0	.676	-.000	-.000	2.109
20	6.212	.688	.687	.3	-.00	-.00	-.0	.694	-.000	-.000	2.703
21	7.477	.701	,700	.1	-.00	-.00	-.0	.709	-.000	-.000	3.313
22	9.995	.718	.721	.5	-.00	-.00	-.0	.732	-.000	-.000	4.555

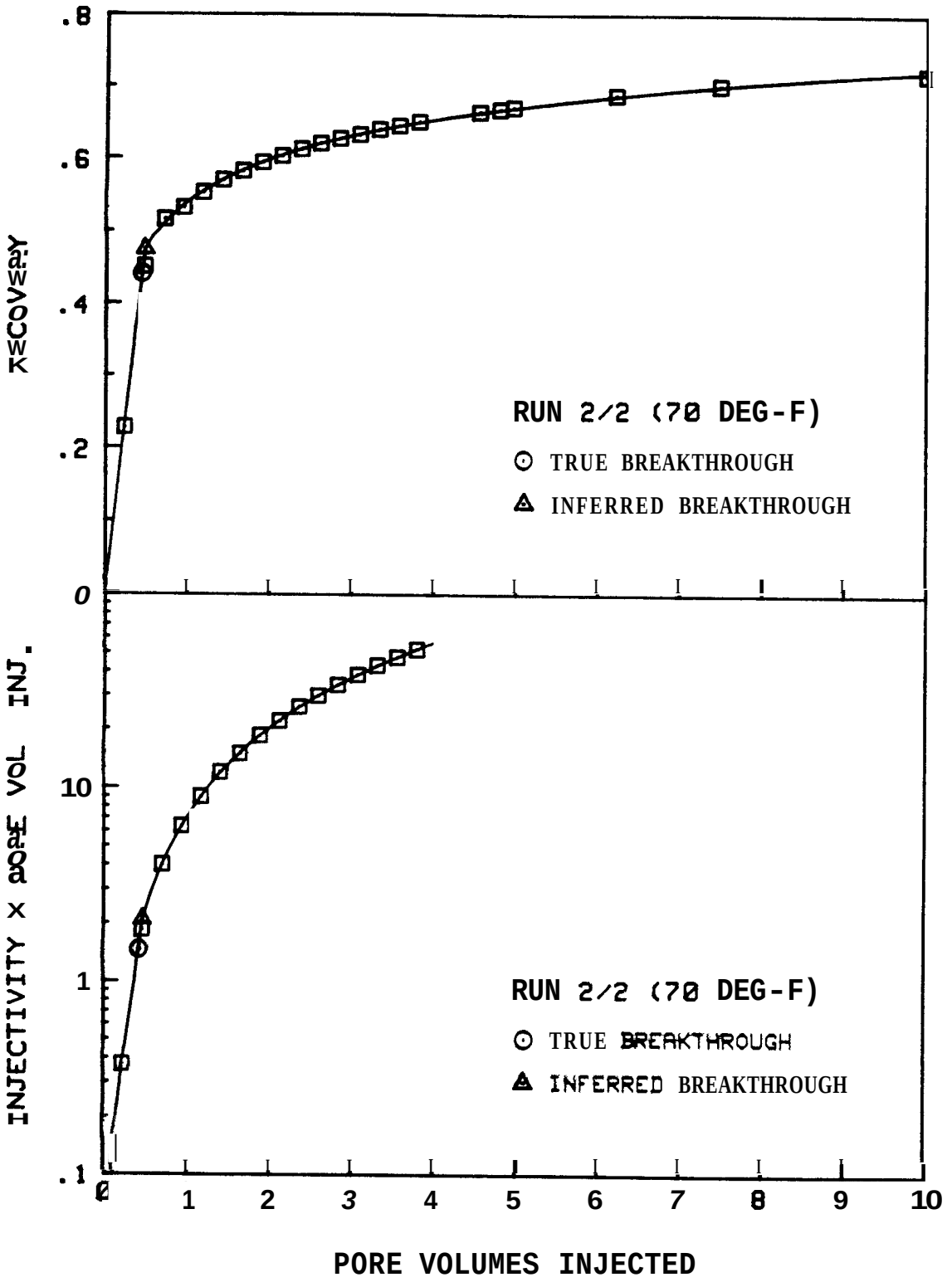

Figure 5.3 Recovery and Injectivity x Pore Volumes Injected vs. Pore Volumes Injected — Run 2/2

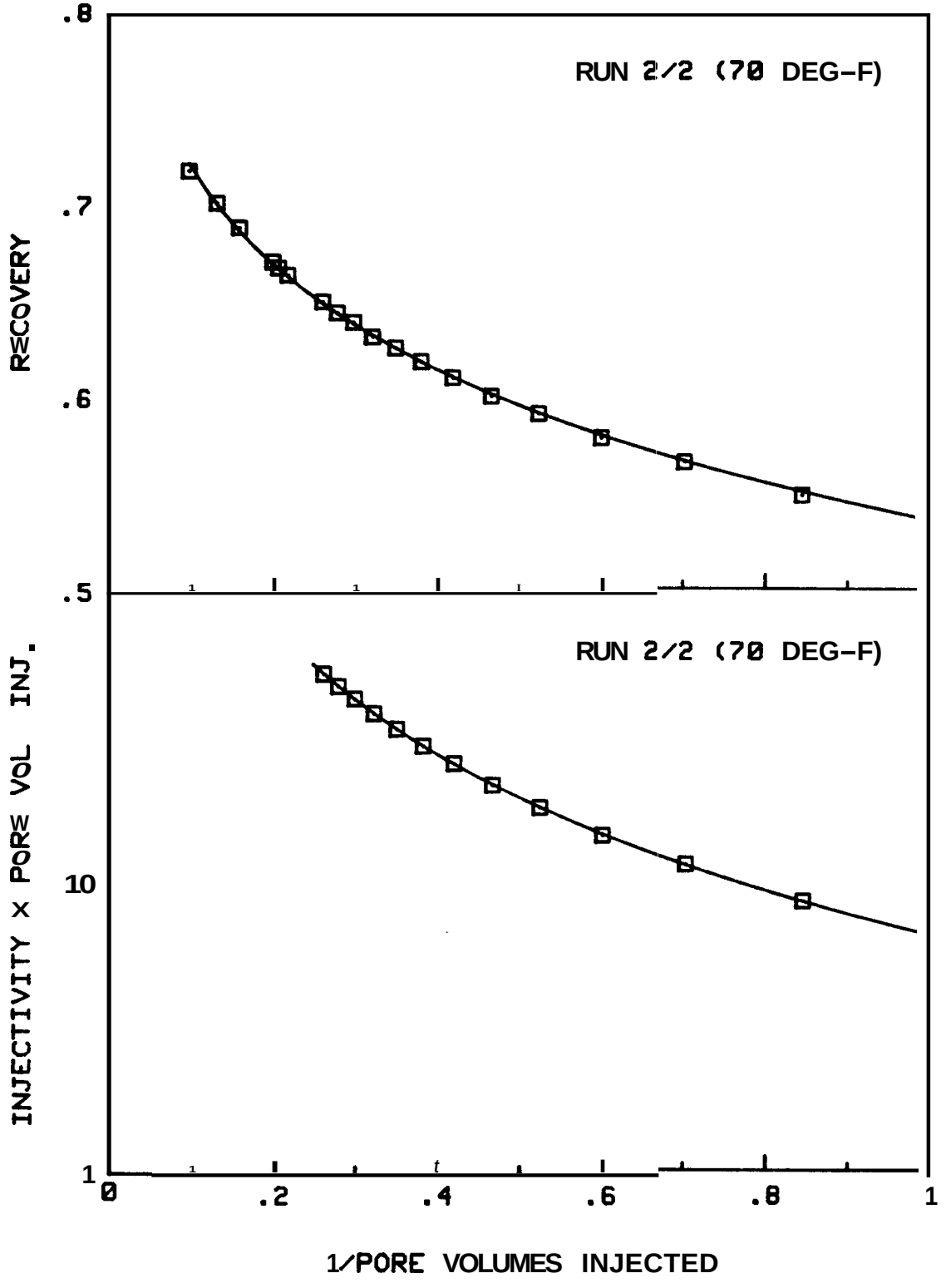

Fig. 5.4 Recovery and Injectivity x Pore Volumes Injected vs. 1/Pore Volumes Injected -- Run 2/2

Table J.15 Water Displacement Calculations — Run 2/3

DISPLACEMENT EXPERIMENT CALCULATIONS

PORE VOLUME	391.2 cc	DATE	10/19/92
CORE LENGTH	51.47 cm	COREfRUN	2f3
CORE DIAMETER	5.044 cm	DISPLACEMENT	Dist U-OIL
DEAD VOL'S: U	2.5 cc	CORE TEMPERATURE	197.0 F
D	3.0 cc	OUTLET TEHPERATURE	74.0 F
SEPARATOR OUTLET	82.72 cm	UATER VISCOSITY	.309 cp
BUBBLE VELOCITY	8.56 cm/sec	OIL VISCOSITY	3.75 cp
ABSOLUTE PERM	7.060 darcies	VISCOSITY RATIO	12.16
INIT SAT - UATER	9.3 %	UATER DENSITY RATIO	1.0352
FINAL SAT - OIL	17.1 %	OIL DENSITY RATIO	1.0559

	TIME	SEPARATOR HEIGHT	SEPARATOR CALIB	D-VOL INJ	D-P	FLOWRATE CHART AVG	CHART @t	CHART CAL	cc min	PVi	Rec	Inj
	(min)	(cm)	(cc/cm)	(cc)	(psi)							
ST		21.00										
0	0.80	20.50	4.97	0.0	7.96	.509	.509	40.9	20.8	0.000	.000	1.00
1	4.48	40.40	4.97	97.0	5.94	.537	.536	40.9	21.9	.255	.259	1.41
BT	7.42				4.09		.536	40.9	21.9	.420	.420	2.05
2	8.82	59.06	4.92	89.9	3.54	.536	.535	40.9	21.9	.498	.500	2.37
3	13.32	65.88	4.91	93.2	2.69	.536	.535	40.3	21.6	.747	.586	3.07
4	17.77	68.00	4.94	92.1	2.14	.534	.532	40.2	21.4	.991	.614	3.83
5	22.27	69.50	4.97	93.1	1.92	.531	.530	40.4	21.4	1.238	.633	4.27
6	26.77	70.75	4.97	92.5	1.79	.530	.530	40.2	21.3	1.483	.650	4.56
7	31.27	71.60	4.97	93.0	1.68	.530	.530	40.4	21.4	1.729	.661	4.8%
8	35.82	72.40	4.97	94.0	1.62	.530	.530	40.4	21.4	1.978	.672	5.07
9	40.33	73.10	4.97	93.6	1.54	.530	.529	40.5	21.4	2.226	.681	5.34
10	44.87	73.65	4.97	93.7	1.49	.529	.529	40.5	21.4	2.474	.689	5.51
11	49.40	74.15	4.97	93.2	1.45	.528	.529	40.3	21.3	2.721	.695	5.64
12	53.95	74.50	4.97	93.5	1.41	.528	.527	40.3	21.2	2.968	.700	5.78
13	58.50	74.90	4.97	94.0	1.39	.526	.525	40.7	21.4	3.217	.705	5.89
14	63.15	75.20	4.97	96.0	1.38	.524	.523	48.8	21.3	3.471	.709	5.93
15	67.72	75.50	4.97	94.5	1.36	.526	.528	40.7	21.5	3.721	.713	6.07
16	72.35	75.75	4.97	96.9	1.34	.528	.527	41.0	21.6	3.978	.717	6.19
17	96.28	76.35	4.97	495.0	1.27	.523	.520	40.9	21.3	5.288	.725	6.43
18	120.45	76.65	4.97	498.0	1.23	.519	.519	41.1	21.3	6.606	.729	6.66
19	144.15	76.80	4.97	485.0	1.19	.517	.515	41.0	21.1	7.889	.731	6.81
20	188.27	77.20	4.97	898.0	1.13	.511	.509	41.2	21.0	10.266	.736	7.13

CURVE FITS	c0	C1	C2	%E-MAX	%E-AVG
Recovery	6.1453E-01	1.0144E-01	-2.1285E-02	.4	.2
Inj. X Pore Vol. Inj.	1.3237E+00	1.5145E+00	-1.0837E-01	4.4	1.2

	PVi	R-ACT	R-CALC	R-%E	I*P-ACT	I*P-CALC	I*P-%E	Sw	Krw	Kro	Kw/Ko
								.093	0.000	.878	0.000
BT		.420	,545		.86	1.44					
3	.747	.586	.583	.4	2.29	2.39	4.4	.562	.124	.272	,457
4	.991	.614	.614	.0	3.80	3.71	2.4	.605	.160	.222	.718
5	1.238	.633	,635	.3	5.29	5.16	2.4	.636	.190	.186	1.020
6	1.483	.650	.651	.2	6.77	6.71	.8	.660	.215	.159	1.358
7	1.729	.661	.664	.4	8.45	8.34	1.4	.679	.238	.137	1.738
8	1.978	.672	.674	.3	10.02	10.04	.2	.694	.258	.119	2.164
9	2.226	.681	.682	.1	11.88	11.78	.9	.708	.276	.105	2.634
10	2.474	.689	.689	.0	13.63	13.55	.6	.719	.292	.093	3.153
11	2.721	.695	.695	.1	15.36	15.35	.0	.729	.307	.083	3.721
12	2.968	.?00	.700	.0	17.15	17.17	.1	.738	.320	.074	4.346
13	3.217	.705	.704	.2	18.96	19.02	.3	.745	.333	.066	5.035
14	3.471	.709	.708	.2	20.59	20.92	1.6	.752	.345	.059	5.808
15	3.721	.713	.711	.3	22.58	22.80	1.0	.759	.355	.053	6.643
16	3.978	.717	.714	.4	24.62	24.73	.5	.764	.365	.048	7.585
17	5.288	,725	.724	.0	34.02	34.65	1.9	.787	.408	.029	14.153
18	6.606	.729	.730	.2	43.98	44.55	1.3	.802	.439	.017	25.695
19	7.889	.731	.733	.4	53.71	54.03	.6	.813	.463	.010	47.919
20	10.266	.736	.735	.1	73.22	71.02	3.0	.826	.494	.001	365.823

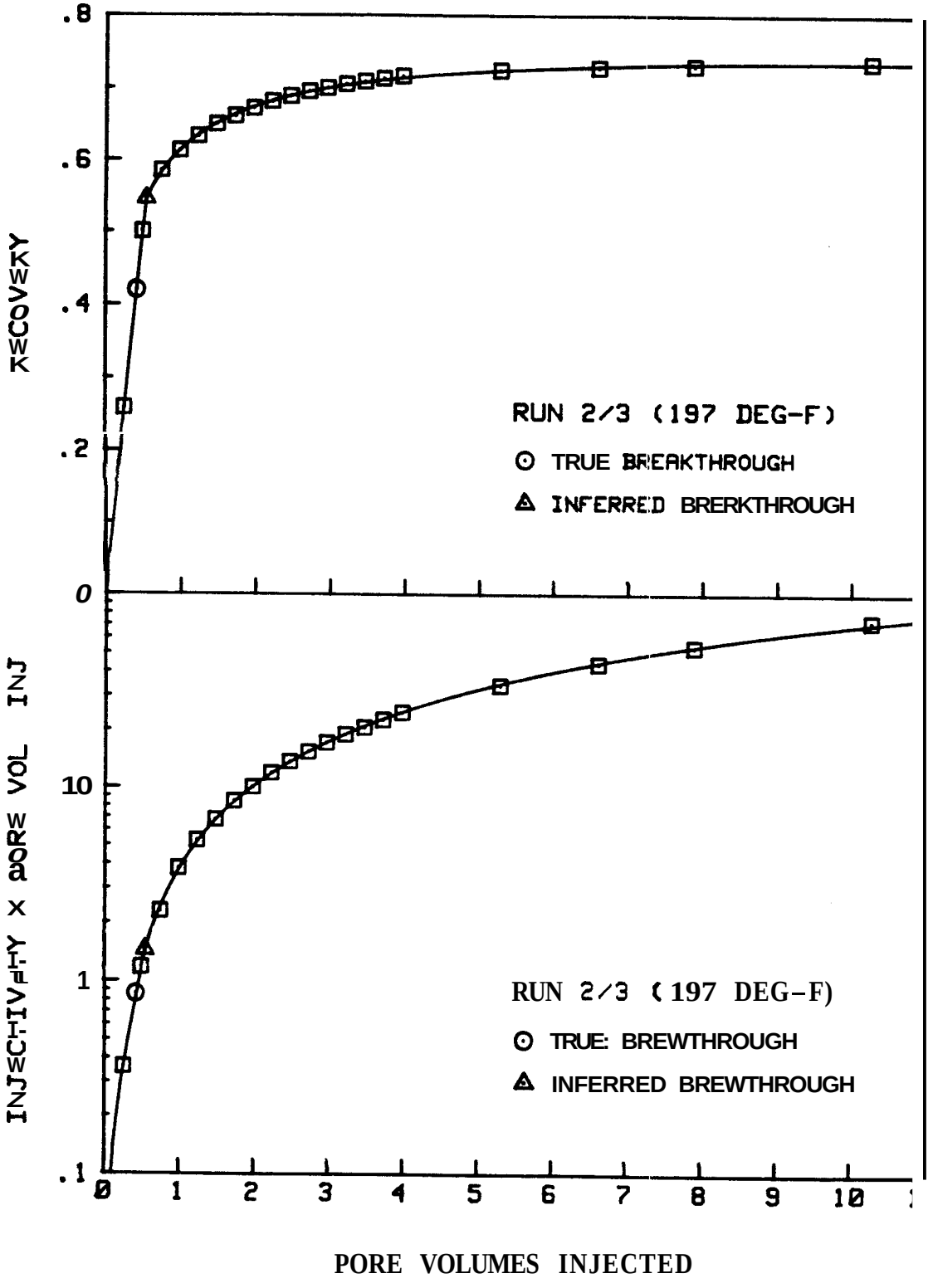

Figure 5.5 Recovery and Injectivity x Pore Volumes Injected vs. Pore Volumes Injected — Run 2/3

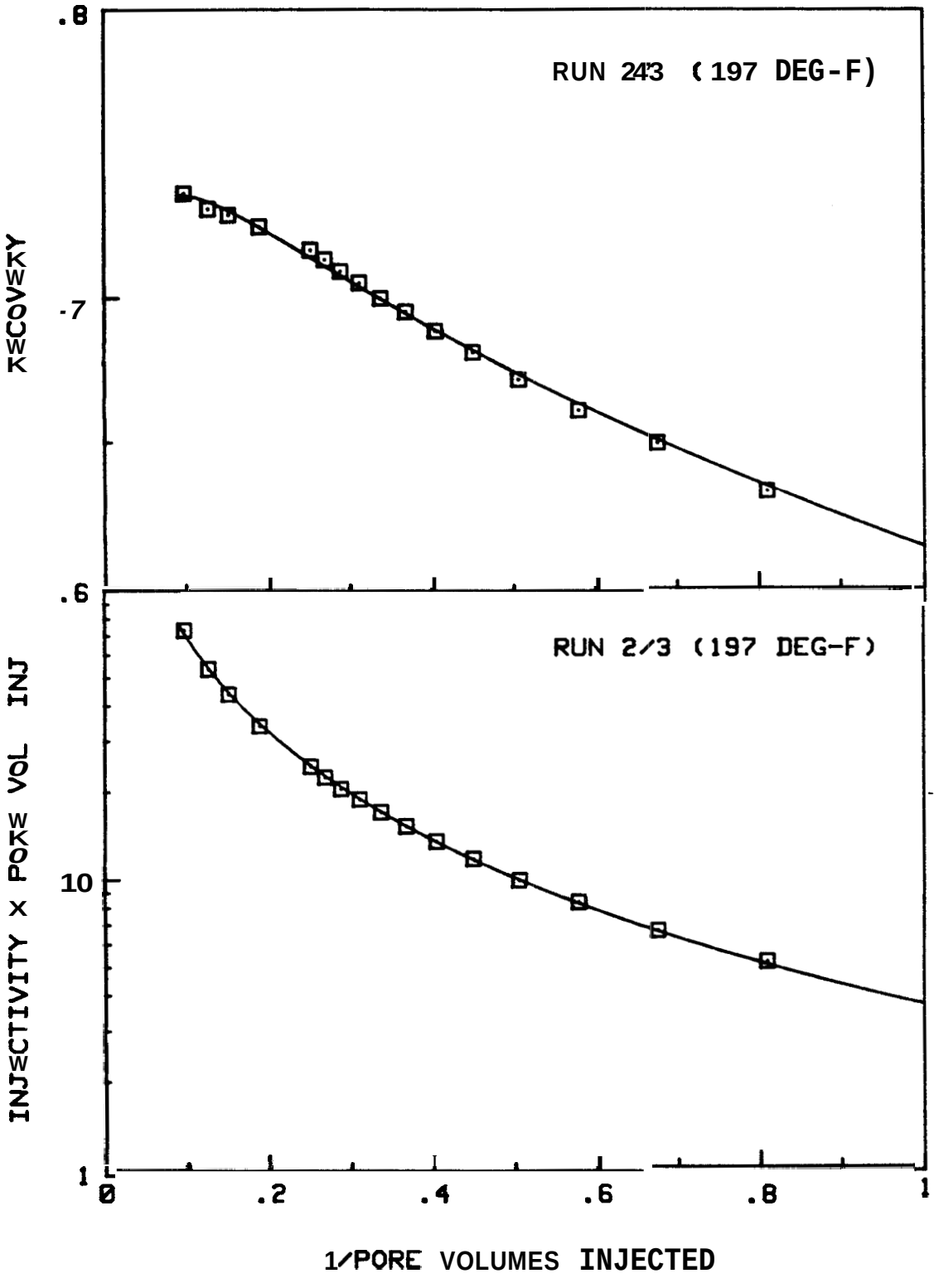

Fig. 5.6 Recovery and Injectivity x Pore Volumes Injected vs. 1/Pore Volumes Injected — Run 2/3

Table 5.16 Water Displacement Calculations -- Run 2/4

DISPLACEMENT EXPERIMENT CALCULATIONS

PORE VOLUME	391.2 cc	DATE	18/28/82
CORE LENGTH	51.47 cm	CORE/RUN	2/4
CORE DIAMETER	5.044 cm	DISPLACEMENT	Dirt U-OIL
DEAD VOL'S: U	2.5 cc	CORE TEMPERATURE	74.0 F
D	3.0 cc	OUTLET TEMPERATURE	74.0 F
SEPARATOR OUTLET	82.72 cm	UATER VISCOSITY	.928 cp
BUBBLE VELOCITY	10.12 cm/sec	OIL VISCOSITY	27.83 cp
ABSOLUTE PERM	7.060 drrcies	VISCOSITY RATIO	29.12
INIT SAT - WATER	10.1 %	YATER DENSITY RATIO	1.8800
FINAL SAT - OIL	18.5 %	OIL DENSITY RATIO	1.0000

	TIME (min)	SEPARATOR HEIGHT (cm)	SEPARATOR CRLIB (cc/cm)	D-VOL XNJ (cc)	D-P (psi)	FLOWRATE CHART AVG	FLOWRATE CHART @t	FLOWRATE CHART CAL	cc min	PVi	Rec	Inj
ST		16.08										
6	0.00	9.60	5.06	0.0	50.60	.431	.431	39.0	16.8	0.000	.000	1.00
1	4.80	28.50	5.06	93.4	36.30	.499	.470	39.0	18.3	.232	.237	1.52
BT	7.51				25.50		.485	39.0	18.9	.363	.363	2.23
2	9.63	46.20	4.79	94.7	17.35	.482	.493	39.0	19.2	.474	.448	3.34
3	14.68	51.26	4.81	93.0	11.25	.501	.500	38.3	19.1	.712	.505	5.12
4	19.58	53.46	4.81	94.0	9.40	.501	.501	38.3	19.2	.952	.532	6.14
5	24.43	55.40	4.81	93.7	8.35	.501	.502	38.6	19.4	1.192	.556	6.97
6	29.27	56.50	4.81	93.5	7.55	.502	.502	38.5	19.3	1.431	.569	7.71
7	34.10	57.86	4.81	94.0	7.00	.501	.500	38.8	19.4	1.671	.585	8.34
8	38.86	59.60	4.61	91.1	6.55	.500	.500	38.8	19.4	1.904	.600	8.90
9	43.68	59.70	4.81	93.2	6.23	.500	.498	38.8	19.3	2.142	.609	9.34
10	48.33	60.48	4.81	92.1	5.86	.499	.499	39.0	19.5	2.378	.617	9.95
11	53.17	60.90	4.81	93.7	5.60	.498	.497	38.9	19.3	2.617	.623	0.39
12	57.98	61.50	4.81	94.0	5.38	.497	.495	39.3	19.4	2.858	.631	0.87
13	62.80	62.00	4.81	94.2	5.20	.498	.498	39.3	19.6	3.098	.637	1.31
14	67.55	62.48	4.81	93.0	5.05	.497	.496	39.4	19.5	3.336	.642	1.64
15	72.36	62.80	4.81	92.2	4.90	.495	.494	39.2	19.4	3.572	.646	11.89
16	77.23	63.10	4.81	96.0	4.78	.494	.493	39.4	19.4	3.817	.650	12.22
17	102.82	64.81	4.81	496.8	4.25	.491	,489	39.5	19.3	5.085	.671	13.66
18	127.85	66.16	4.81	485.0	4.00	.486	.482	39.9	19.2	6.325	.687	14.45
19	153.22	67.65	4.81	490.0	3.75	.481	.479	40.2	19.2	7.577	.699	15.43
20	200.43	66.30	4.81	908.0	3.45	.477	.472	40.3	19.0	9.899	.714	16.57

CURVE FITS	c0	c1	c2	LE-MAX	LE-AVG
Recovery	5.3845E-01	9.6709E-02	-8.8560E-03	.5	.2
Inj. X Pore Vol. Inj.	1.8401E+00	1.5934E+00	-7.4563E-02	1.5	.4

	PVi	R-ACT	R-CALC	R-LE	I*P-ACT	I*P-CALC	I*P-%E	Sw	Krw	Kro	Kw/Ko
								.101	0.000	.803	0.006
BT		.363	.457		.81	1.73					
3	.712	.505	.505	.2	3.64	3.64	.2	.503	.073	.360	.204
4	.952	.532	.534	.4	5.85	5.83	.4	.537	.095	.314	.301
5	1 192	.556	.555	.2	8.31	8.31	.0	.563	.113	.281	.403
6	1 431	.569	.572	.5	11.03	11.04	.1	.583	.129	,254	.510
7	1 671	.585	.586	.1	13.94	14.00	.4	.599	,144	.232	.621
8	1 904	.600	,597	.5	16.95	17.04	.5	.613	.157	.215	.732
9	2 142	.609	.607	.2	20.00	20.30	1.5	.625	.170	.200	.850
10	2 376	.617	.616	.2	23.67	23.67	.0	.635	.181	.187	.969
11	2 617	.623	.623	.0	27.28	27.23	.1	.645	.192	.175	1.094
12	2 858	.631	.630	.1	31.05	30.91	.5	.653	.202	.165	1.222
13	3.098	.637	.636	.0	35.05	34.78	1.0	.661	.211	.156	1.353
14	3.336	.642	.642	.1	38.82	38.54	.7	.668	.220	.148	1.486
15	3.572	.646	.647	.1	42.47	42.43	.1	.674	.229	.141	1.628
16	3.817	.650	.652	.3	46.64	46.56	.2	.680	.237	.134	1.762
17	5.085	.671	.672	.2	69.48	69.01	.7	.705	.273	.108	2.538
18	6.325	.687	.687	.0	91.38	92.33	1.0	.724	.302	.090	3.358
19	7.577	.699	.698	.1	116.91	116.88	.0	.738	.327	.077	4.243
26	9.899	.714	.714	.0	164.03	164.17	.1	.758	.363	.060	6.025

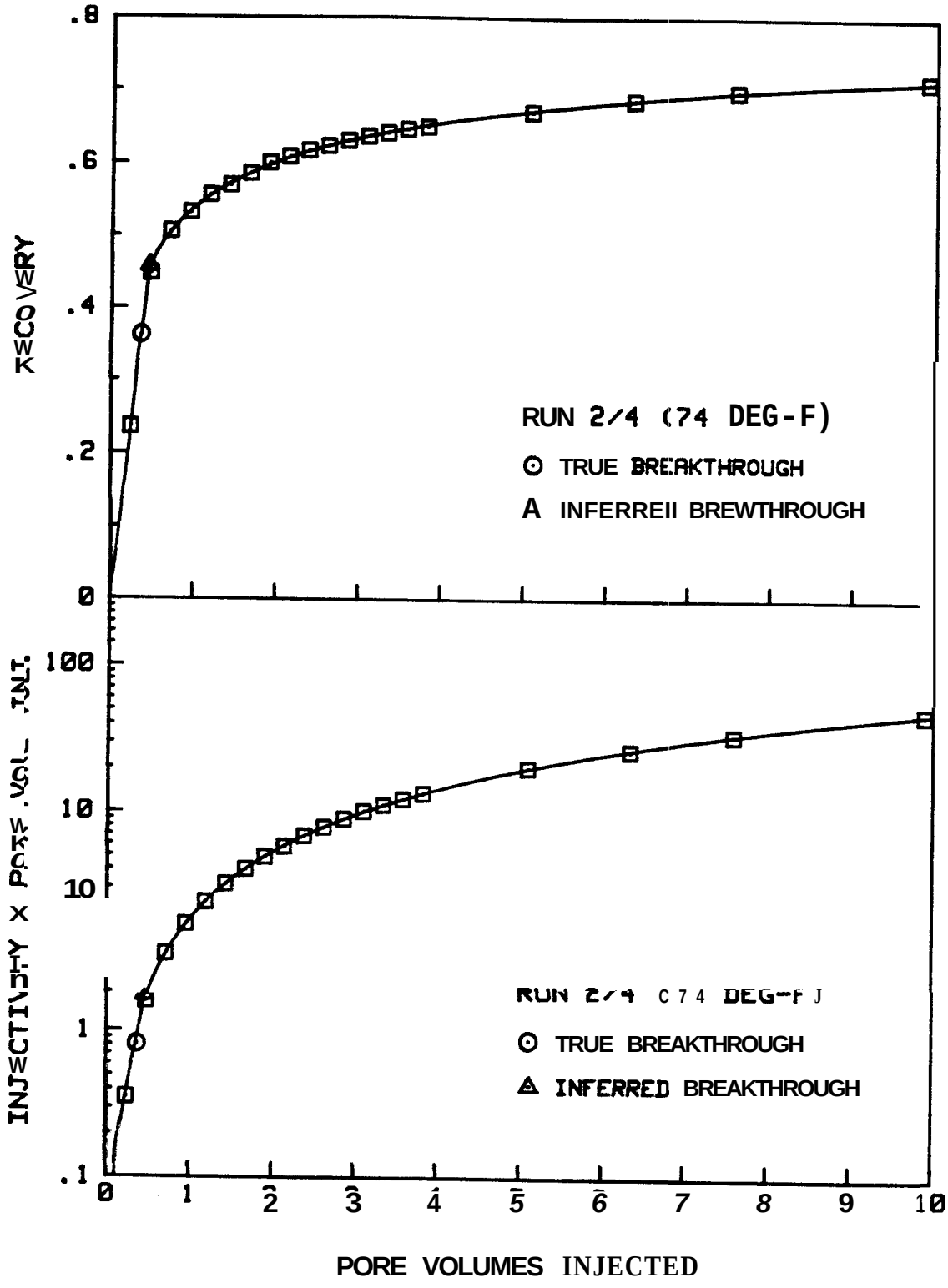

Figure 5.7 Recovery and Injectivity x Pore Volumes Injected vs. Pore Volumes Injected — Run *2/4*

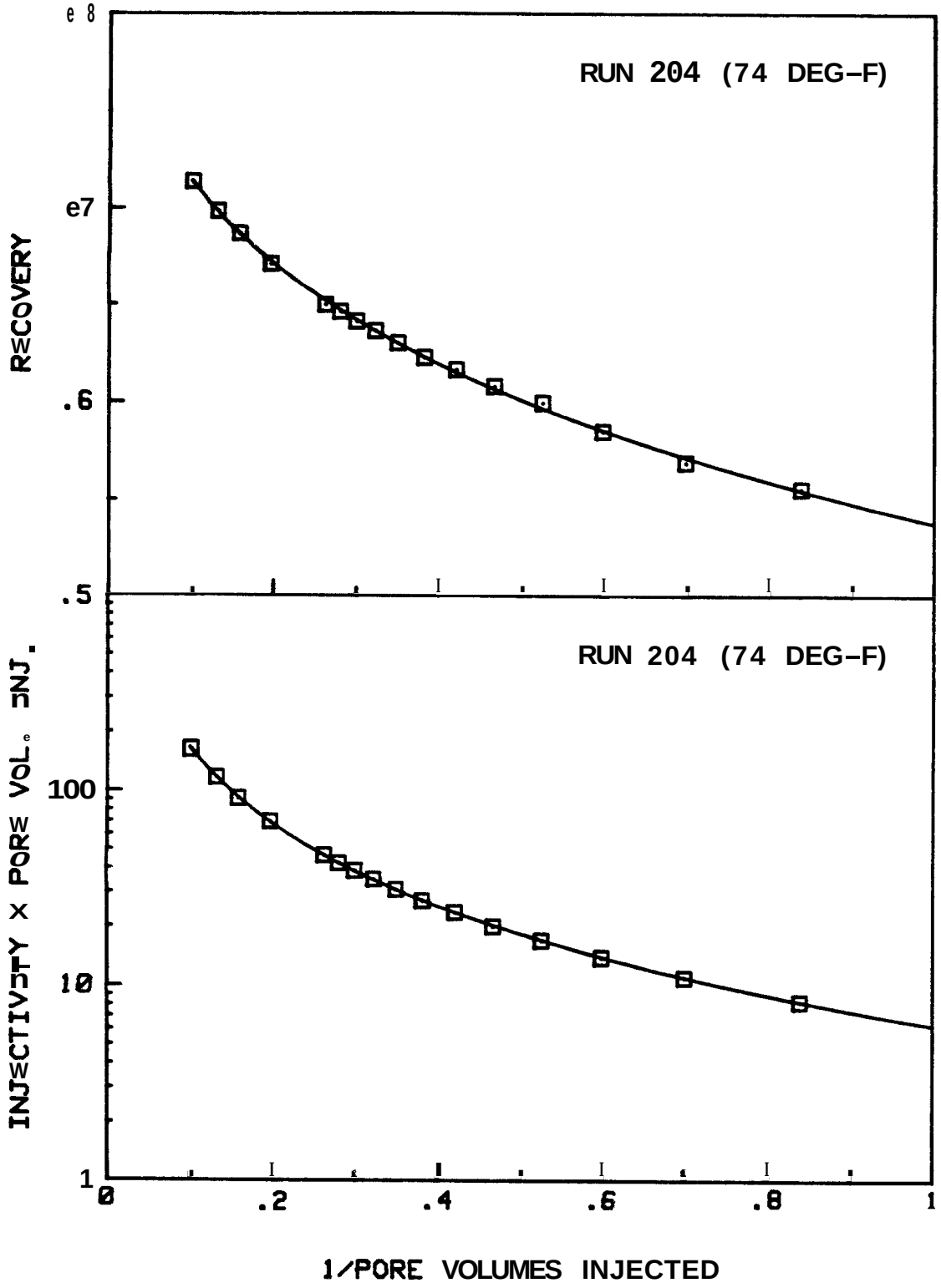

Fig. 5.8 Recovery and Injectivity x Pore Volumes Injected vs. 1/Pore Volumes Injected -- Run *2/4*

Table J.17 Water Displacement Calculations -- Run 2/5

DISPLACEMENT EXPERIHENT CALCULATIONS;

PORE VOLUME	391.2 cc	DATE	11/29/82
CORE LENGTH	51.47 cm	COREfRUN	2/5
CORE DIAMETER	5.044 cm	DISPLACEMENT	Dirt U-OIL
DERD VOL'S: U	2.5 cc	CORE TEMPERATURE	70.0 F
D	3.0 cc	OUTLET TEMPERATURE	70.0 F
SEPARATOR OUTLET	82.72 cm	YATER VISCOSITY	.979 cp
BUBBLE VELOCITY	7.27 cm/sec	OIL VISCOSITY	29.81 cp
ABSOLUTE PERM	7.060 darcies	VISCOSITY RATIO	30.45
INIT SAT - UATER	8.4 %	UATER DENSITY RATIO	1.0000
FINAL SAT - OIL	20.5 %	OIL DENSITY RATIO	1.0000

	TIME	SEPARATOR HEIGHT	SEPARATOR CALIB	D-VOL INJ	D-P	FLOWRATE CHART AVG	CHART @t	CHART CAL	cc min	PVi	Rec	Inj
	(min)	(cm)	(cc/cm)	(cc)	(psi)							
ST		19.70										
0	0.00	19.00	5.00	0.0	76.00	.605	.605	35.9	21.7	0.000	.000	1.00
1	3.07	37.00	5.00	93.0	59.70	.766	.792	35.9	28.4	.231	.222	1.67
BT	4.60				45.00		.816	35.9	29.3	.346	.346	2.28
2	6.20	55.50	4.80	92.0	32.50	.818	.844	35.9	30.3	.467	.442	3.26
3	9.25	62.50	4.81	93.1	20.50	.858	.869	35.6	30.9	.704	.523	5.28
4	12.35	63.80	4.82	95.0	16.90	.870	.871	35.2	30.7	.947	.537	6.35
5	15.40	65.40	4.82	94.6	15.00	.870	.869	35.7	31.0	1.189	.557	7.23
6	18.47	66.70	4.82	94.8	13.50	.868	.868	35.6	30.9	1.431	.573	8.01
7	21.47	68.00	4.82	93.0	12.58	.866	.863	35.8	30.9	1.669	.589	8.65
8	24.48	68.90	4.82	93.8	11.65	.862	.861	36.1	31.1	1.909	.600	9.33
9	27.63	69.90	4.82	96.5	10.98	.859	.857	35.7	30.6	2.156	.612	9.74
10	30.68	78.40	4.e2	94.2	10.45	.855	.852	36.1	30.8	2.396	.618	10.31
11	33.72	71.00	4.82	94.0	9.93	.852	.851	36.4	31.0	2.637	.625	10.91
12	36.78	71.50	4.82	94.8	9.50	.850	.848	36.1	30.6	2.877	.631	11.27
13	39.82	72.00	4.82	93.3	9.18	.845	.842	36.4	30.6	3.116	.638	11.68
14	42.93	72.20	4.82	95.5	8.80	.840	.840	36.5	30.6	3.360	.640	12.19
15	46.05	72.60	4.82	95.5	8.58	.838	.837	36.6	30.6	3.604	.645	12.48
16	49.15	73.00	4.82	95.5	8.38	.835	.833	36.9	30.7	3.848	.650	12.83
17	65.25	74.70	4.82	486.0	7.35	.826	.819	36.5	29.9	5.090	.671	14.25
18	81.38	75.88	4.82	488.0	6.70	.812	.804	37.3	29.9	6.338	.685	15.64
19	97.77	76.82	4.82	492.0	6.23	.797	.790	37.7	29.8	7.595	.697	16.72
20	125.45	77.99	4.82	819.0	5.70	.780	.769	37.9	29.2	9.689	.711	17.91
21	128.78	77.99	0.00	95.0	5.65	.766	.764	38.2	29.2	9.932	.711	18.06

CURVE FITS	C0	C1	c2	%E-MRX	LE-AVG
Recovery	5.4666E-01	8.4555E-02	-5.3021E-03	1.2	.3
Inj. X Pore Vol. Inj.	1.8772E+00	1.5807E+00	-5.9644E-02	1.2	.4

	PVi	R-RCT	R-CRLC	R-LE	I*P-ACT	I*P-CALC	I*P-%E	Sw	Krw	Kro	Kw/Ko
								.084	0.000	.761	0.000
BT		.346	.482		.79	2.00					
3	.704	.523	.516	1.2	3.72	3.73	.3	.512	.071	,311	.229
4	.947	.537	.542	.9	6.02	6.00	.3	.541	.091	.273	.333
5	1.189	.557	.561	.8	8.60	8.58	.2	,562	.108	.245	.439
6	1.431	.573	.576	.6	11.47	11.43	.3	.580	.122	.223	.549
7	1.669	.589	.589	.0	14.44	14.46	.2	.593	.136	.206	.660
8	1.909	.600	.599	.1	17.81	17.71	.5	,605	.148	.191	.774
9	2.156	.612	.608	.6	21.00	21.25	1.2	.616	.160	.179	.894
10	2.396	.618	.617	.2	24.70	24.86	.6	,625	.170	.168	1.012
11	2.637	.625	.624	.3	28.76	28.61	.5	.633	.180	.159	1.133
12	2.877	.631	.630	.2	32.41	32.49	.3	.641	.189	.151	1.255
13	3.116	.638	.636	.3	36.40	36.47	.2	,647	.198	.143	1.378
14	3.360	.640	.641	.2	40.94	40.66	.7	.654	.206	.137	1.506
15	3.604	.645	.646	.2	44.99	44.95	.1	.659	.214	.131	1.635
16	3.848	.650	.651	.2	49.39	49.35	.1	,665	.222	.126	1.765
17	5.090	.671	.670	.1	72.54	73.08	.7	.687	.255	.104	2.451
18	6.338	.685	.685	.1	99.15	98.75	.4	.704	,283	.089	3.170
19	7.595	.697	.696	.1	127.01	126.08	.7	.717	.307	.078	3.922
20	9.689	.711	.711	.0	173.51	174.04	.3	.735	.341	.065	5.228
21	9.932	.711	.713	.2	179.35	179.77	.2	.737	.344	.064	5.383

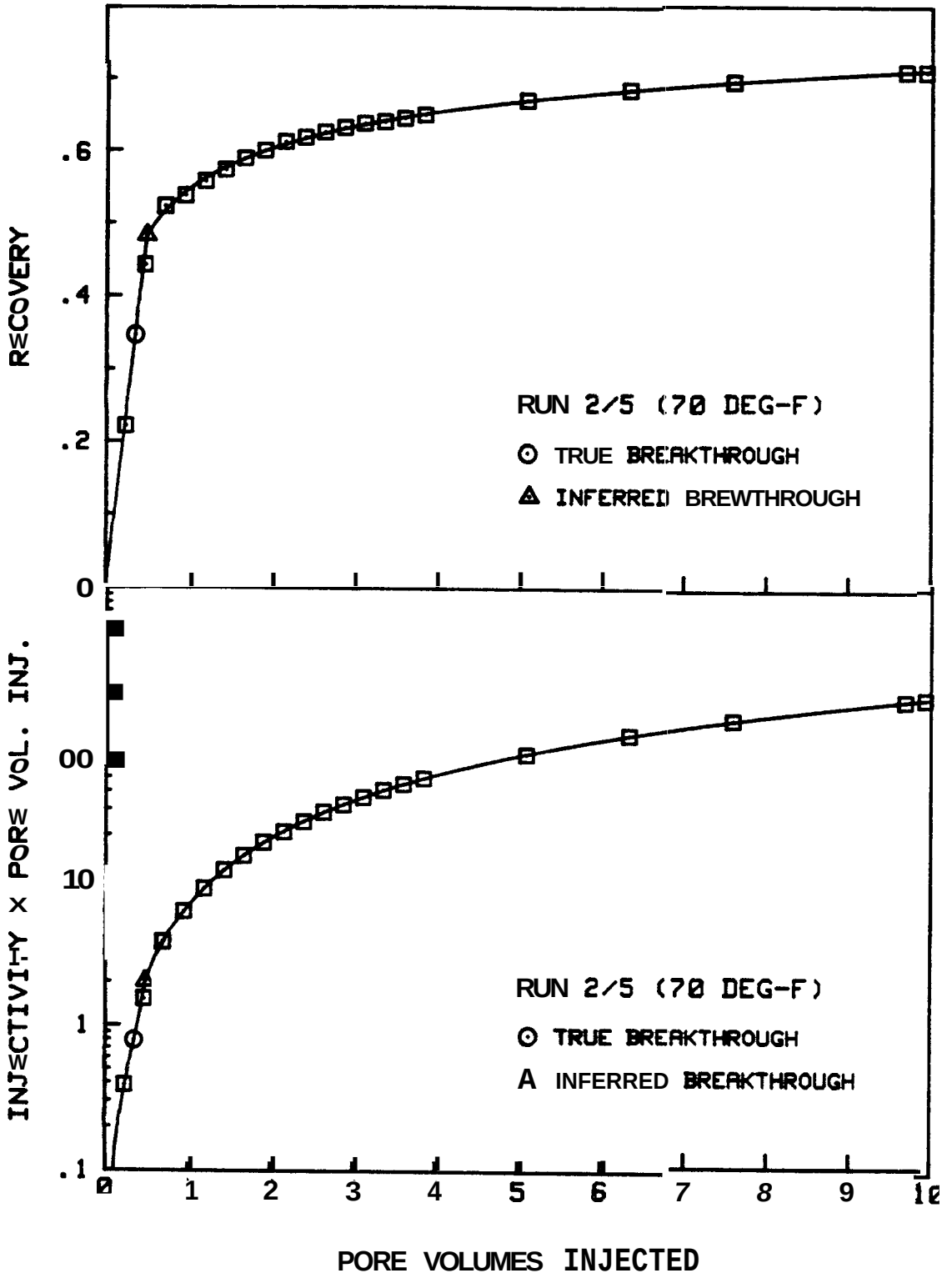

Figure J.9 Recovery and Injectivity x Pore Volumes Injected vs. Pore Volumes Injected — Run 2/5

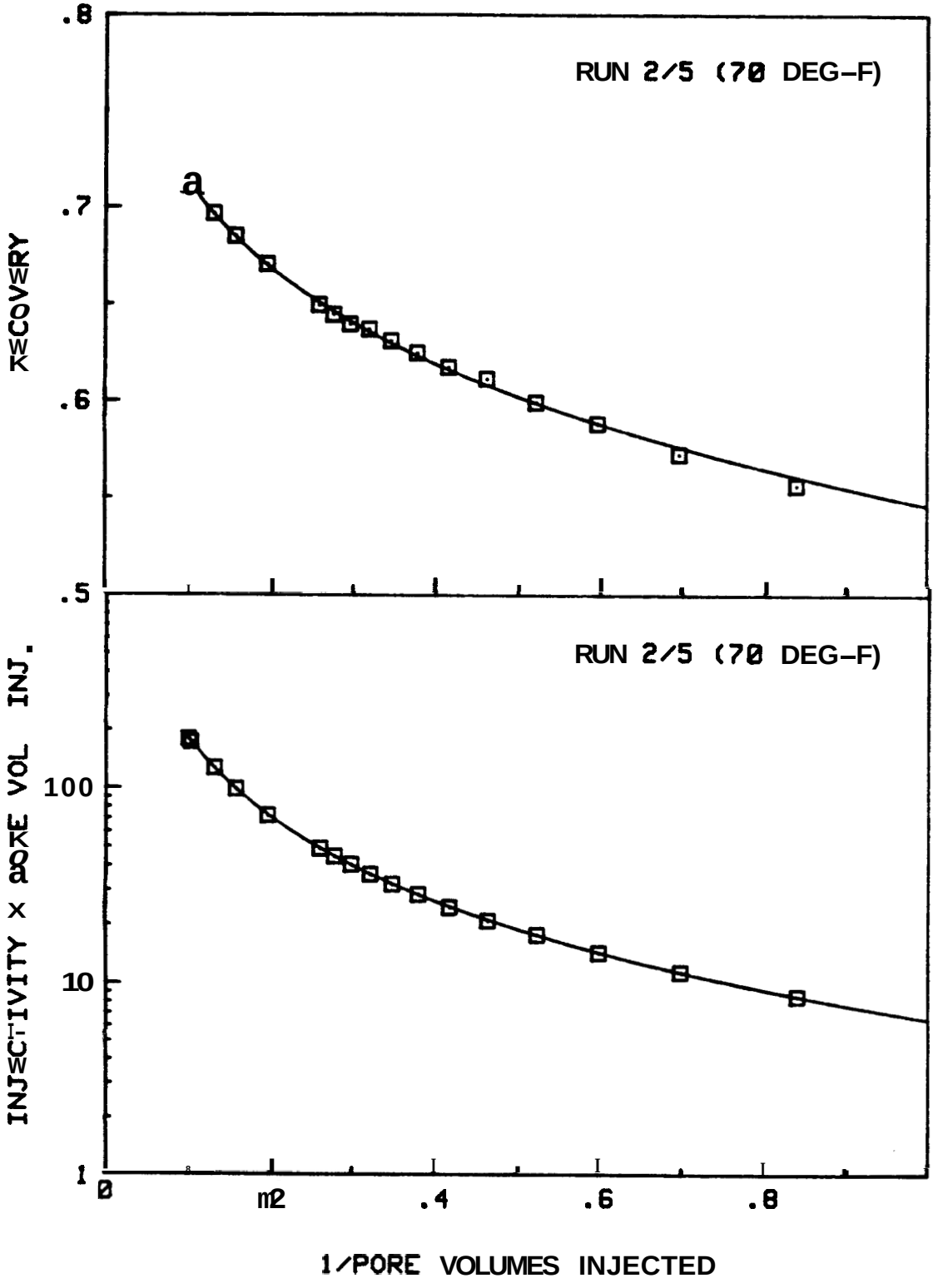

Fig. J.10 Recovery and Injectivity x Pore Volumes Injected vs. 1/Pore Volumes Injected -- Run 2/5

Table J.18 Water Displacement Calculations — Run 2/6

DISPLACEMENT EXPERIMENT CALCULATIONS

PORE VOLUNE	391.2 cc	DATE	11/38/82
CORE LENGTH	51.47 cm	CORE/RUN	2/6
CORE DIAMETER	5.044 cm	DISPLACEMENT	Dirt U-OIL
DEAD VOL'S: U	2.5 cc	CORE TEMPERATURE	297.0 F
D	3.0 cc	OUTLET TEMPERATURE	74.0 F
SEPARATOR OUTLET	82.72 cm	YATER VISCOSITY	.185 cp
BUBBLE VELOCITY	19.17 cm/sec	OIL VISCOSITY	1.64 cp
ABSOLUTE PERM	7.060 darcies	VISCOSITY RATIO	8.83
INIT SAT - YATER	10.3 %	YATER DENSITY RATIO	1.0858
FINAL SAT - OIL	15.9 %	OIL DENSITY RATIO	1.1037

	TINE	SEPARATOR HEIGHT	SEPARATOR CALIB	D-VOL INJ	D-P	FLOWRATE CHART AVG	CHART @t	CHART CAL	cc min	PVi	Rec	Inj
	(min)	(cm)	(cc/cm)	(cc)	(psi)							
ST		27.00										
0	0.00	26.80	4.97	0.0	3.26	.515	.515	42.6	21.9	0.000	.000	1.00
1	4.37	46.00	4.97	93.8	2.48	.541	.540	42.6	23.0	.258	.262	1.38
2	8.80	65.00	4.93	92.0	1.62	.538	.534	42.6	22.7	.518	.522	2.09
BT	9.32				1.53		.534	42.3	22.6	.548	.548	2.19
3	13.32	72.50	4.89	92.9	1.35	.532	.530	42.3	22.4	.777	.622	2.47
4	17.82	74.50	4.89	92.5	1.21	.529	.528	42.3	22.3	1.035	.648	2.74
5	22.37	75.90	4.89	93.0	1.10	.526	.524	42.2	22.1	1.293	.667	2.99
6	26.93	76.85	4.89	93.0	1.01	.523	,522	42.3	22.1	1.551	.680	3.25
7	31.50	77.70	4.89	93.0	.97	.521	.520	42.5	22.1	1.810	.692	3.40
8	36.07	78.30	4.89	92.9	.91	.519	.518	42.6	22.1	2.068	.700	3.60
9	40.73	78.80	4.89	94.1	.86	.516	.514	42.4	21.8	2.329	.707	3.77
10	45.35	79.10	4.89	92.5	.84	.513	.511	42.4	21.7	2.586	.711	3.86
11	49.97	79.55	4.89	92.6	.80	.510	.510	42.7	21.8	2.643	.717	4.05
12	72.90	80.60	4.89	456.0	.73	.505	.500	42.8	21.4	4.109	.731	4.35
13	95.97	80.90	4.89	452.0	.71	.495	.489	43.0	21.0	5.364	.736	4.43
14	120.68	81.10	4.89	478.0	.70	.484	.480	43.4	20.8	6.690	.738	4.42
15	125.55	81.10	0.00	92.9	.70	.480	.480	43.2	20.7	6.948	.738	4.43

CURVE FITS	C0	C1	C2	%E-MAX	%E-AVG
Recovery	6.4460E-01	9.2773E-02	-2.2846E-02	.2	.1
Inj. X Pore Vol. Inj.	9.7534E-01	1.5299E+00	-1.3510E-01	1.8	.8

	PVi	R-ACT	R-CALC	R-%E	I*P-ACT	I*P-CALC	I*P-%E	Sw	Krw	Kro	Kw/Ko
								.103	0.000	.983	0.000
BT		.548	.589		1.20	1.14					
4	1.035	.648	.648	.1	2.84	2.79	1.5	.660	.180	.154	1.171
5	1.293	.667	.667	.0	3.87	3.89	.7	.689	.215	.127	1.694
6	1.551	.680	.681	.1	5.04	5.06	.3	.711	.245	.106	2.303
7	1.810	.692	.692	.0	6.16	6.27	1.8	.729	.271	.090	3.008
8	2.068	.700	.700	.0	7.45	7.50	.7	.743	.294	.077	3.817
9	2.329	.707	.707	.0	8.78	8.78	.1	.756	.315	.066	4.759
10	2.586	.711	.712	.2	9.98	10.04	.6	.766	.333	.057	5.820
11	2.843	.717	.717	.1	11.51	11.32	1.7	.775	.350	.050	7.037
12	4.109	.731	.730	.2	17.89	17.59	1.7	.805	.412	.025	16.387
13	5.364	.736	.736	.1	23.77	23.66	.5	.823	.455	.012	37.788
14	6.690	.738	.738	.0	29.59	29.82	.8	.835	.488	.004	127.712
15	6.948	.738	.739	.El	30.80	30.98	.6	.837	.493	.003	187.256

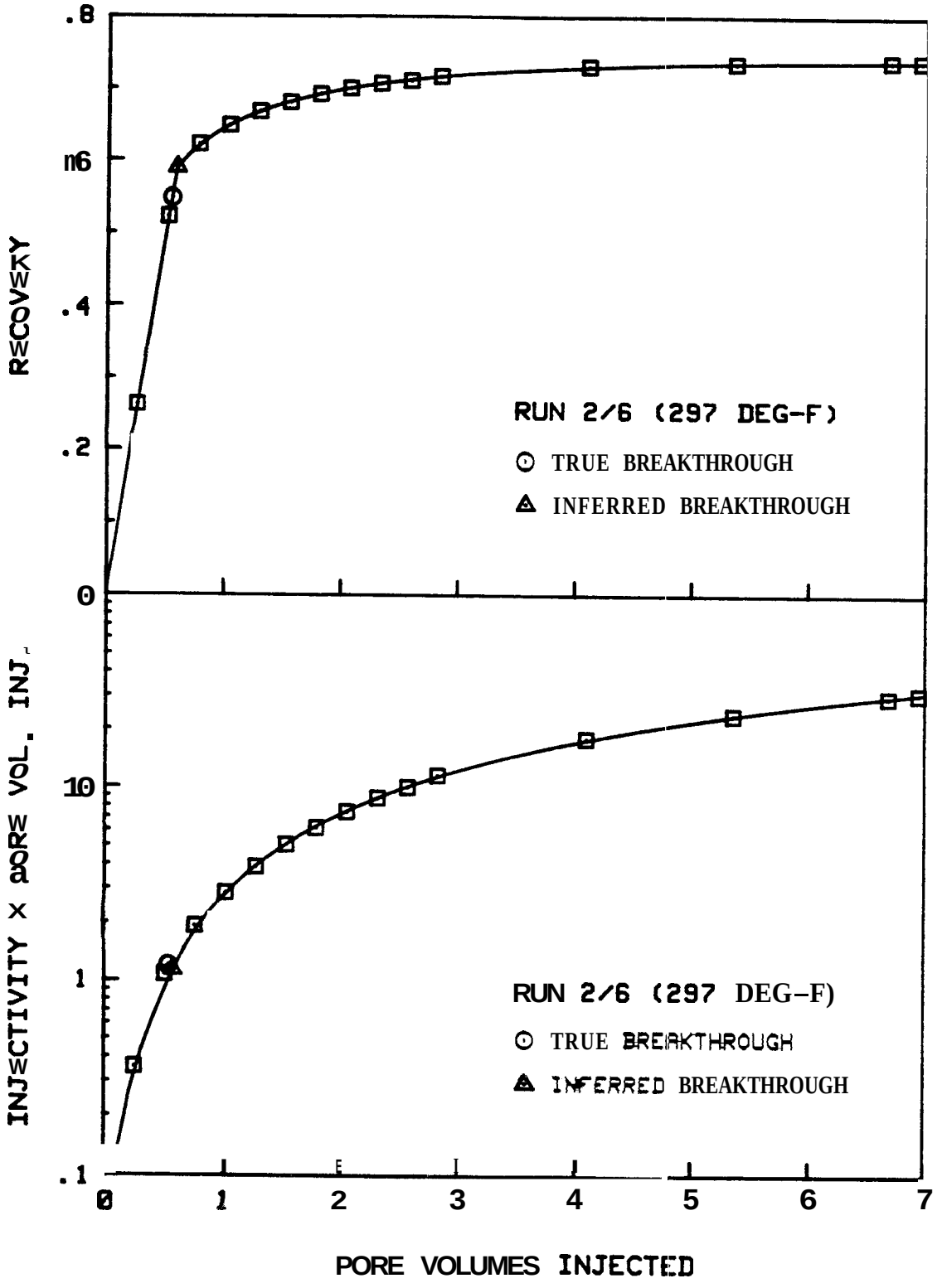

Figure J.11 Recovery and Injectivity x Pore Volumes Injected vs. Pore Volumes Injected -- Run 2/6

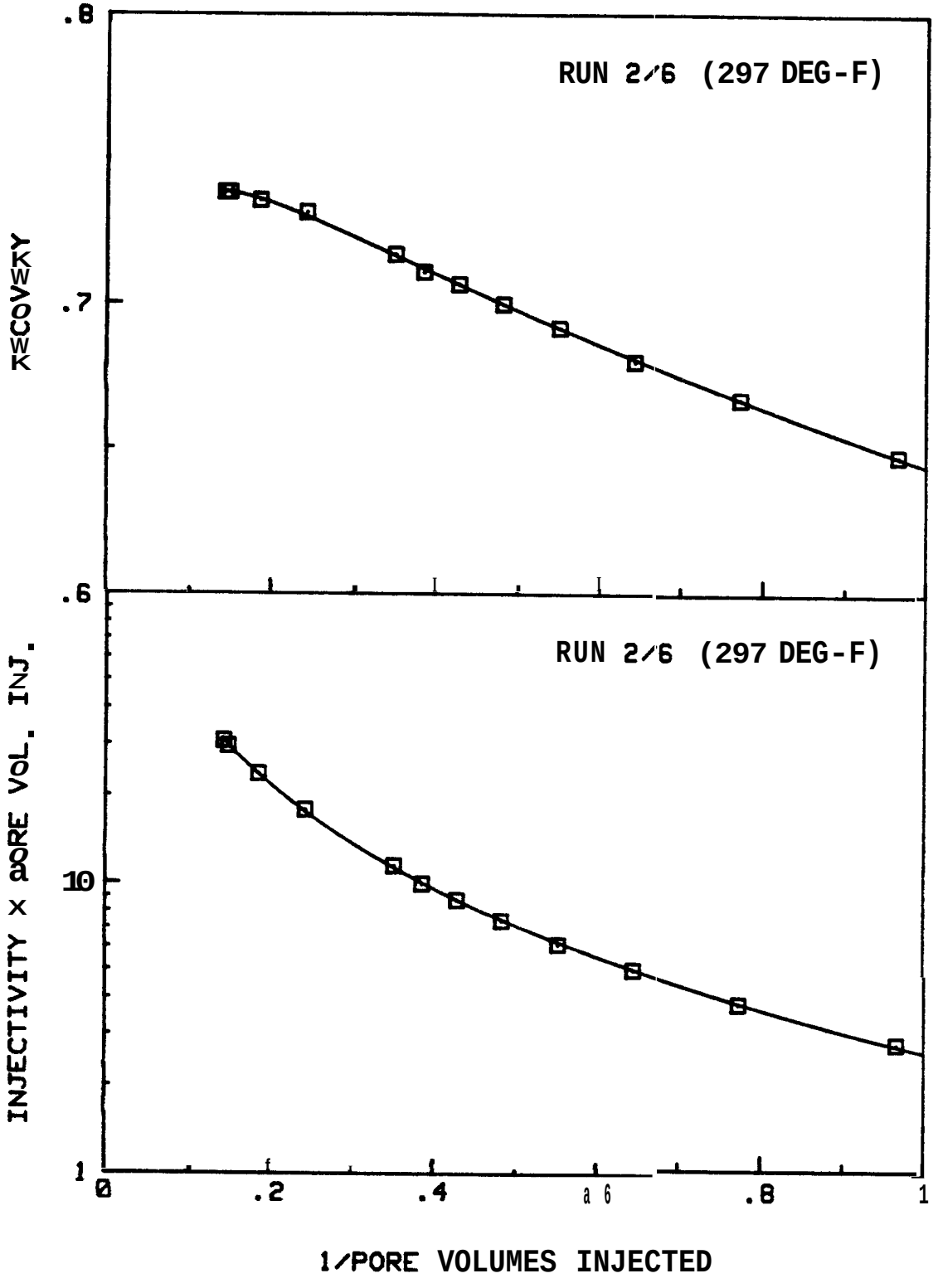

Fig. 5.12 Recovery and Injectivity x Pore Volumes Injected vs. 1/Pore Volumes Injected — Run 2/6

Table J.19 Water Displacement Calculations -- Run 3/1

DISPLACEMENT EXPERIMENT CALCULATIONS

PORE VOLUME	395.9 cc	DATE	12/8/82
CORE LENGTH	51.69 cm	CORE/RUN	3/1
CORE DIAMETER	5.044 cm	DISPLACEMENT	Dist U-OIL
DEAD VOL'S: U	2.5 cc	CORE TENPERATURE	78.0 F
D	3.8 cc	OUTLET TEMPERATURE	74.8 F
SEPARATOR OUTLET	81.41 cm	UATER VISCOSITY	.979 cp
BUBBLE VELOCITY	9.31 cm/sec	OIL VISCOSITY	29.81 cp
ABSOLUTE PERM	6.900 drrcies	VISCOSITY RATIO	30.45
INIT SAT - UATER	8.7 %	URTER DENSITY RATIO	.9993
FINAL SAT - DIL	19.4 %	OIL DENSITY RATIO	.9982

		SEPARRTOR		D-VDL		FLOWRRTE						
	TIME	HEIGHT	CALIB	INJ	D-P	CHRRT			cc	PVi	Rec	Inj
	(min)	(cm)	(cc/cm)	(cc)	(psi)	AVG	@t	CAL	min			
ST		9.82										
0	0.00	9.40	4.97	0.0	56.20	.426	.426	37.6	16.0	0.000	.000	1.00
1	4.87	29.00	4.97	96.2	40.30	.520	.538	37.6	20.2	.236	.237	1.76
BT	5.27				38.50		.542	37.6	20.4	.257	.257	1.86
2	9.45	44.00	4.89	95.7	22.90	.554	.569	37.6	21.4	.478	.417	3.28
3	13.85	50.50	4.88	95.0	14.55	.575	.581	37.5	21.8	.717	.494	5.25
4	18.17	53.10	4.86	94.9	11.75	.584	.584	37.6	22.0	.957	.524	6.55
5	22.45	54.86	4.86	94.9	10.28	.583	.582	38.0	22.1	1.196	.545	7.54
6	26.77	56.30	4.86	95.0	9.28	.582	.581	37.8	22.0	1.436	.563	8.29
7	31.05	57.35	4.86	94.8	8.63	.582	.582	38.0	22.1	1.675	.576	8.98
8	35.33	58.40	4.86	94.6	8.03	.581	.580	38.0	22.0	1.914	.589	9.62
9	39.58	59.20	4.86	93.9	7.55	.578	.577	38.2	22.0	2.151	.598	10.23
10	43.85	60.00	4.86	94.0	7.20	.577	.576	38.2	22.0	2.388	.608	10.70
11	48.23	60.70	4.86	97.0	6.88	.575	.573	38.5	22.0	2.633	.617	11.23
12	52.60	61.25	4.86	96.2	6.58	.573	.572	38.4	22.0	2.876	.623	11.71
13	56.87	61.80	4.86	95.0	6.30	.571	.570	39.0	22.2	3.116	.630	12.36
14	61.07	62.30	4.86	93.5	6.08	.570	.570	39.8	22.2	3.352	.636	12.83
15	65.38	62.80	4.86	96.0	5.90	.568	.565	39.1	22.1	3.594	.642	13.13
16	87.72	64.80	4.86	492.0	5.20	.562	.560	39.2	21.9	4.836	.667	14.79
17	109.10	66.10	4.86	470.0	4.70	.557	.553	39.4	21.8	6.022	.682	16.27
18	131.07	67.28	4.86	483.0	4.33	.551	.549	39.9	21.9	7.242	.697	17.72
19	375.23	69.10	4.86	966.0	3.80	.542	.536	40.3	21.6	9.680	.719	19.92
20	179.55	69.10	0.00	93.1	3.78	.537	.537	40.6	21.8	9.915	.719	20.22

CURVE FITS	C0	C1	c2	XE-MAX	%E-AVC
Recovery	5.2759E-01	9.7049E-02	-5.7978E-03	.2	.1
Inj. X Pore Vol. Inj.	1.8930E+00	1.6030E+00	-5.3617E-02	2.9	.9

	PVi	R-ACT	R-CALC	R-%E	I*P-ACT	I*P-CALC	I*P-%E	Sw	Krw	Kro	Kw/Ko
								.087	0.000	.781	0.000
BT		.257	.445		.48	1.75					
3	.717	.494	.495	.2	3.77	3.87	2.9	.481	.073	.362	.201
4	.957	.524	.523	.2	6.27	6.18	1.4	.513	.093	.320	.289
5	1.196	.545	.545	.0	9.02	8.83	2.0	.537	.110	.289	.381
6	1.436	.563	.562	.2	11.91	11.78	1.1	.556	.126	.265	.475
7	1.675	.576	.576	.1	15.05	14.97	.6	.572	.140	.245	.571
8	1.914	.589	.588	.1	18.41	18.38	.2	.586	.153	.229	.669
9	2.151	.598	.599	.0	22.01	21.96	.2	.597	.165	.215	.768
10	2.388	.608	.608	.1	25.56	25.74	.7	.608	.176	.203	.869
11	2.633	.617	.616	.1	29.57	29.81	.8	.617	.187	.192	.975
12	2.876	.623	.624	.1	33.67	34.01	1.0	.626	.197	.183	1.081
13	3.116	.630	.630	.1	38.51	38.36	.5	.634	.207	.174	1.187
14	3.352	.636	.636	.1	42.99	42.67	.8	.640	.216	.167	1.293
15	3.594	.642	.642	.0	47.21	47.28	.1	.647	.225	.160	1.403
16	4.836	.667	.666	.1	71.52	72.70	1.6	.674	.264	.133	1.983
17	6.022	.682	.683	.1	97.96	99.32	1.4	.694	.296	.116	2.561
18	7.242	.697	.697	.0	128.35	28.58	.2	.710	.324	.102	3.177
19	9.680	.719	.718	.2	192.80	91.64	.6	.734	.371	.083	4.461
20	9.915	.719	.720	.1	208.51	97.99	1.3	.736	.375	.082	4.589

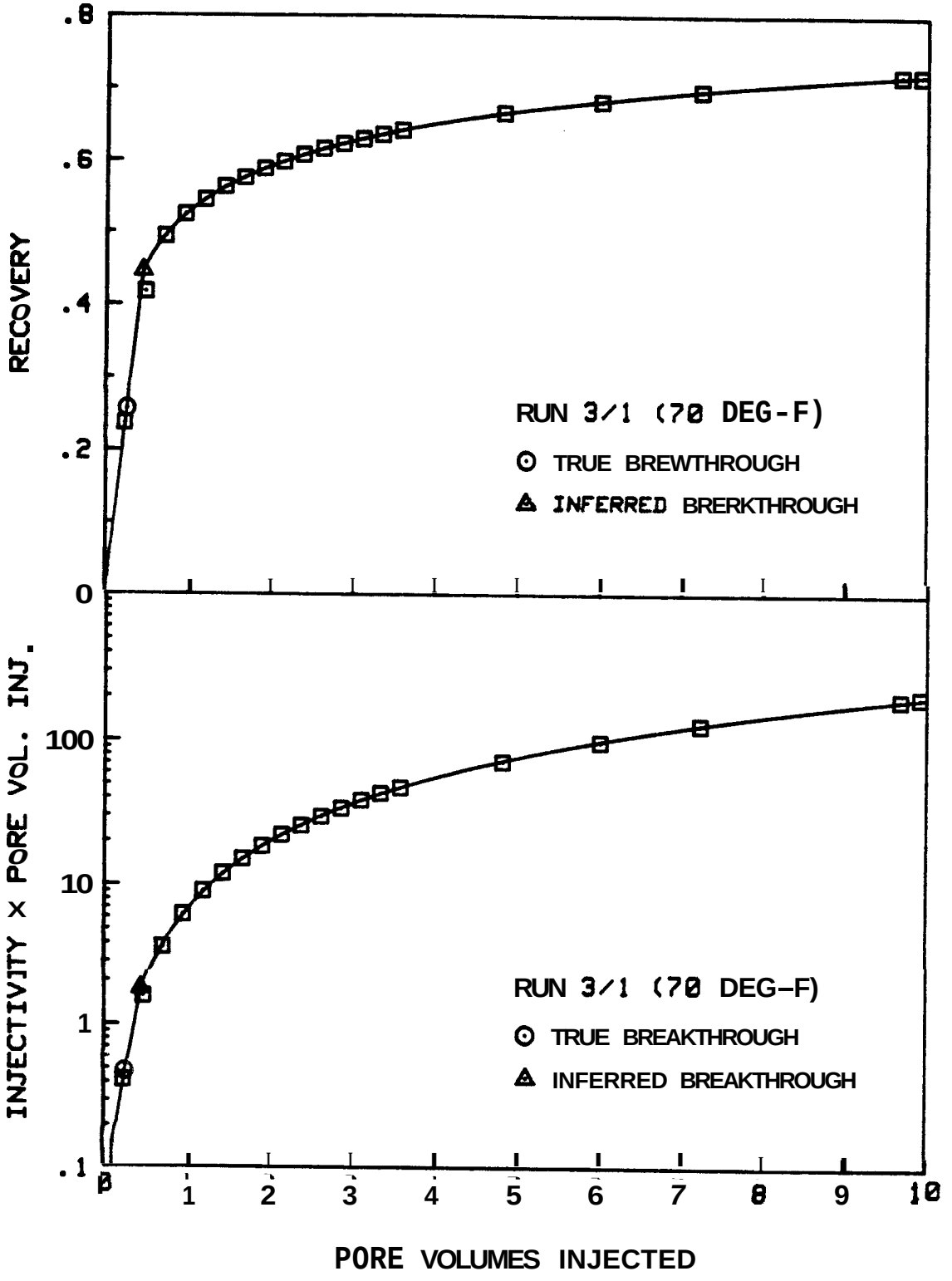

Figure 5.13 Recovery and Injectivity x Pore Volumes Injected vs. Pore Volumes Injected — Run 3/1

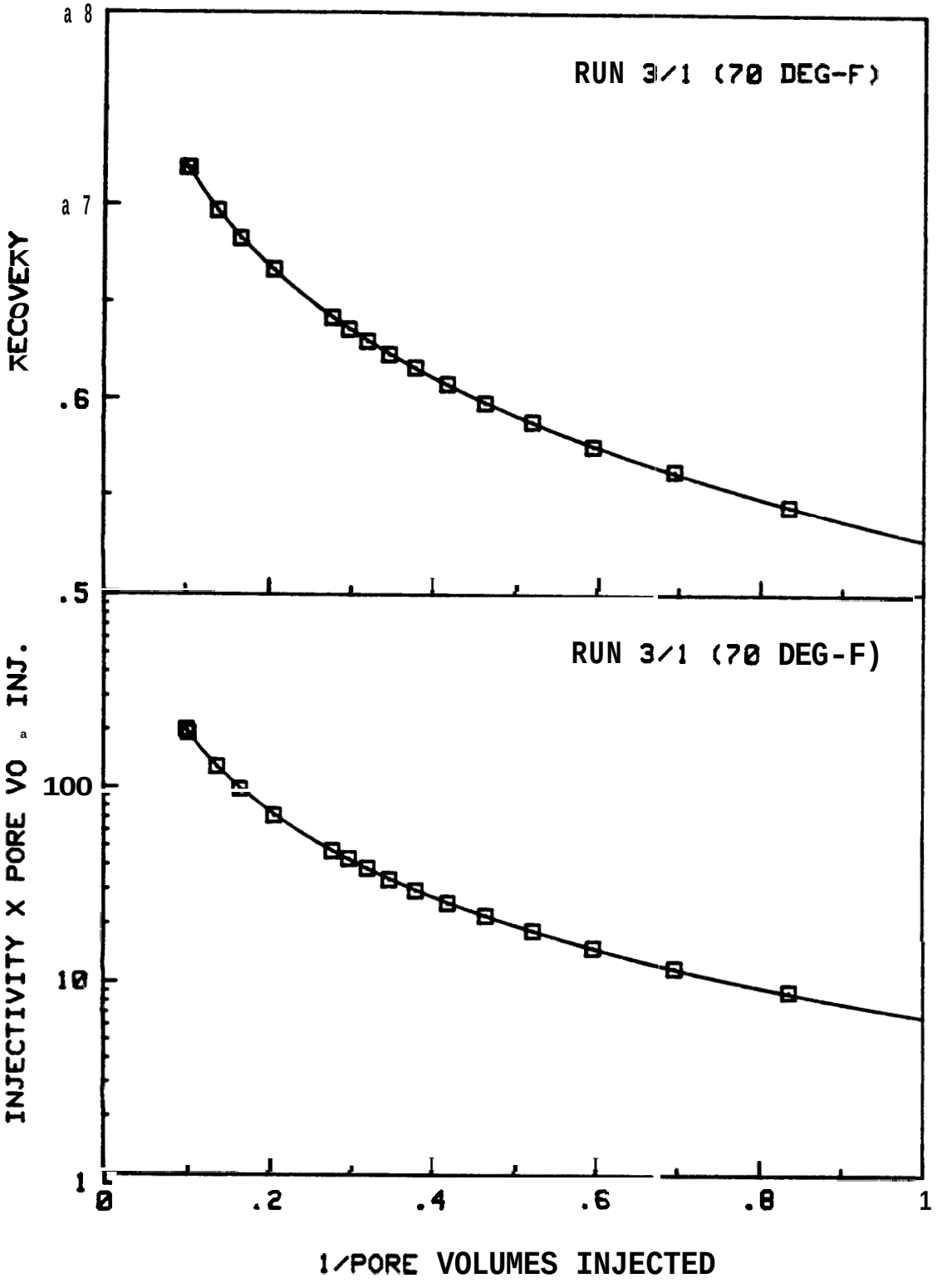

Fig. 5.14 Recovery and Injectivity x Pore Volumes Injected vs. 1/Pore Volumes Injected -- Run 3/1

Table 5.20 Water Displacement Calculations -- Run 3/2

DISPLACEMENT EXPERIMENT CALCULATION?

FORE VOLUME	395.9 cc	DATE	12/9/82
CORE LENGTH	51.69 cm	CORE/RUN	3/2
CORE DIAMETER	5.044 cm	DISPLACEMENT	Dirt W-OIL
DEAD VOL'S: U	2.5 cc	CORE TEMPERATURE	200.0 F
D	3.0 cc	OUTLET TEMPERATURE	76.0 F
SEPARATOR OUTLET	81.41 cm	WATER VISCOSITY	.303 cp
BUBBLE VELOCITY	11.99 cm/sec	OIL VISCOSITY	3.64 cp
ABSOLUTE PERM	6.900 darcirs	VISCOSITY RATIO	12.00
INIT SAT - WATER	10.4 %	UATER DENSITY RATIO	1.0361
FINAL SAT - OIL	16.0 %	OIL DENSITY RATIO	1.0564

	TIME	SEPARATOR HEIGHT	SEPARATOR CALIB	D-VOL INJ	D-P	FLOWRATE CHART AVG	CHART @t	CHART CAL	cc min	PVi	Ret	Inj
	(min)	(cm)	(cc/cm)	(cc)	(psi)							
ST		20.35										
0	0.00	20.00	4.97	0.0	7.60	.499	.499	42.8	21.3	0.000	.000	1.00
1	4.20	39.00	4.97	92.8	5.68	.541	.542	42.8	23.2	.241	.245	1.45
BT	7.54				4.00		.546	42.8	23.4	.438	.438	2.08
2	8.42	57.58	4.97	92.9	3.60	.544	.545	42.8	23.3	.489	.485	2.31
3	12.62	64.40	4.99	92.8	2.68	.548	.549	42.1	23.1	.734	.573	3.07
4	16.73	66.60	4.99	92.6	2.23	.550	.550	42.5	23.4	.977	.601	3.73
5	20.97	68.00	4.99	95.0	1.95	.550	.549	42.3	23.2	1.226	.619	4.24
6	25.15	69.20	4.99	94.6	1.75	.549	.549	42.7	23.5	1.474	.635	4.77
7	29.35	70.08	4.99	93.9	1.62	.547	.545	42.4	23.1	1.719	.645	5.08
8	33.60	70.75	4.99	95.4	1.53	.544	.543	42.8	23.2	1.969	.655	5.41
9	37.85	71.48	4.99	94.9	1.45	.542	.542	42.7	23.2	2.218	.664	5.68
10	42.00	72.00	4.99	93.3	1.40	.541	.540	43.1	23.3	2.462	.672	5.92
11	46.23	72.50	4.99	94.5	1.35	.540	.540	42.9	23.1	2.710	.678	6.10
12	50.40	72.95	4.99	93.2	1.30	.539	.539	43.0	23.2	2.954	.684	6.35
13	54.65	73.38	4.99	95.4	1.25	.538	,536	43.2	23.2	3.203	.689	6.60
14	58.88	73.65	4.99	95.0	1.21	.537	.538	43.3	23.3	3.452	.694	6.86
15	63.13	73.95	4.99	95.6	1.20	.536	.536	43.5	23.3	3.702	.698	6.92
16	84.86	75.00	4.99	484.0	-.00	.531	.526	43.6	22.9	4.969	.712	-.00
17	107.62	75.80	4.99	506.0	-.00	.523	.520	43.9	22.8	6.294	.722	-.00
18	129.52	76.32	4.99	483.0	-.00	.520	.517	43.9	22.7	7.558	.729	-.00
19	151.68	76.80	4.99	487.0	-.00	.514	.510	44.3	22.6	8.832	.736	-.00
20	155.97	76.80	0.00	94.0	-.00	.510	.508	44.6	22.6	9.078	.736	-.00

CURVE FITS	C0	C1	c2	%E-MAX	%E-AVG
Recovery	6.0167E-01	8.9859E-02	-1.3138E-02	.2	.1
Inj. X Pore Vol. Inj.	1.3269E+00	1.6093E+00	-1.1187E-01	1.7	.6

	PVi	R-ACT	R-CALC	R-%E	I*P-ACT	I*P-CALC	I*P-%E	Sw	Krw	Kro	Kw/Ko
								.104	0.000	.938	0.008
BT		.438	.542		.91	1.35					
3	.734	.573	.573	.0	2.25	2.27	.6	.579	.125	.231	.541
4	.977	.601	.600	.2	3.64	3.63	.4	.613	.163	.200	.816
5	1.226	.619	.619	.1	5.20	5.21	.1	.639	.198	.176	1.125
6	1.474	.635	.635	.0	7.03	6.92	1.7	.659	.228	.156	1.457
7	1.719	.645	.647	.2	8.73	8.73	.0	.675	.255	.141	1.811
8	1.969	.655	.657	.2	10.65	10.66	.1	.688	.280	.127	2.194
9	2.218	.664	.665	.1	12.61	12.65	.3	.700	.302	.116	2.597
10	2.462	.672	.672	.e	14.57	14.68	.7	.710	.322	.107	3.016
11	2.710	.678	.678	.0	16.54	16.78	1.4	.719	.341	.098	3.462
12	2.954	.684	.684	.1	18.76	18.69	.7	.726	.358	.091	3.924
13	3.283	.689	.688	.1	21.15	21.09	.3	.733	,374	.085	4.419
14	3.452	.694	,693	.1	23.67	23.32	1.5	.740	.390	.079	4.935
15	3.782	.698	.697	.1	25.61	25.58	.1	.745	.404	.074	5.478
16	4.969	.712	.712	.0	-.00	-.00	-.0	.768	-.000	-.000	8.590
17	6.294	.722	.723	.0	-.00	-.00	-.0	.785	-.000	-.000	12.544
18	7.558	.729	.730	.1	-.00	-.00	-.0	.797	-.000	-.000	17.067
19	8.832	.736	.735	.1	-.00	-.00	-.0	.806	-.000	-.000	22.475
20	9.078	.736	.736	.1	-.00	-.00	-.0	.808	-.000	-.000	23.628

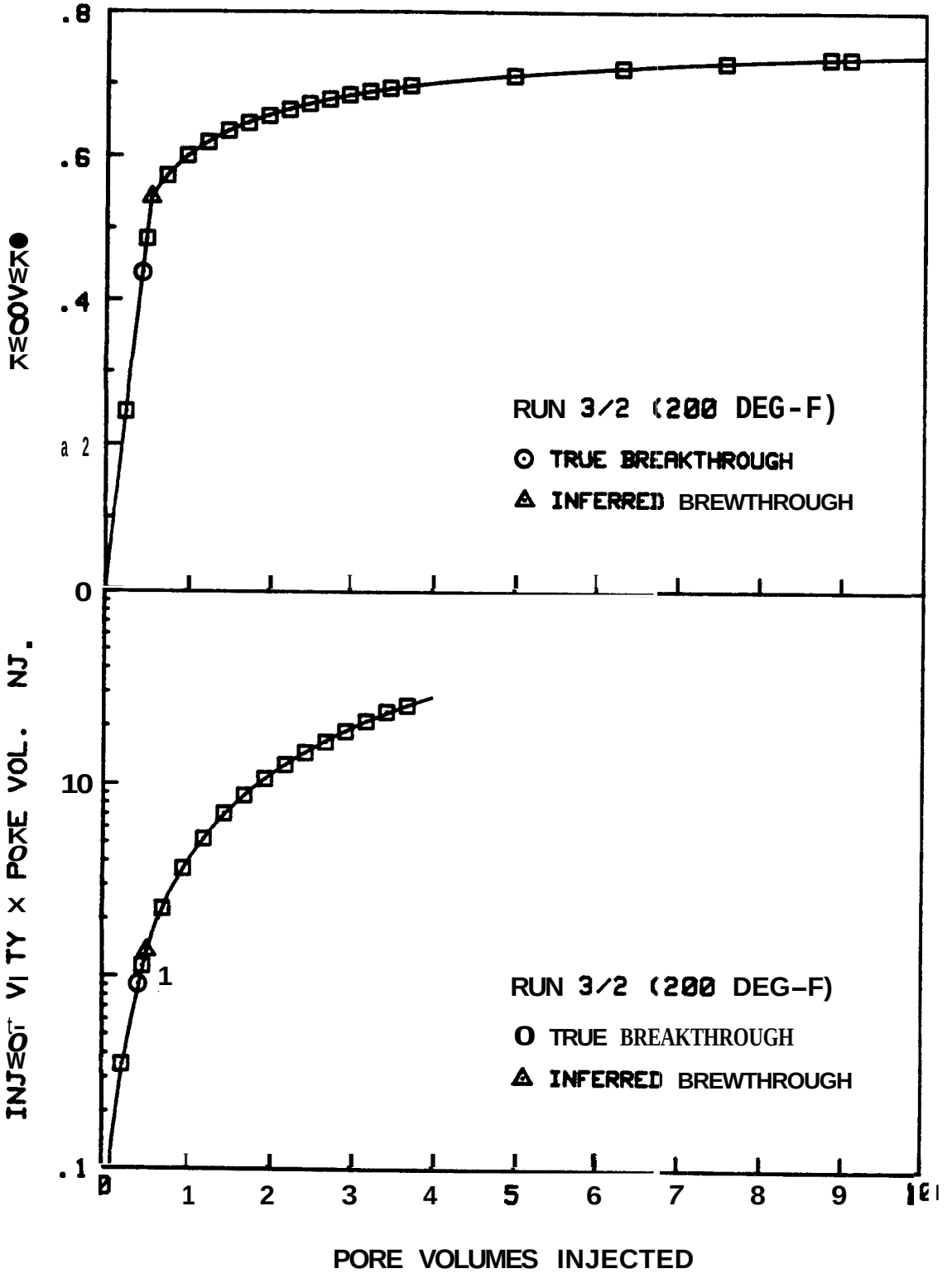

Figure 5.15 Recovery and Injectivity x Pore Volumes Injected vs. Pore Volumes Injected — Run 3/2

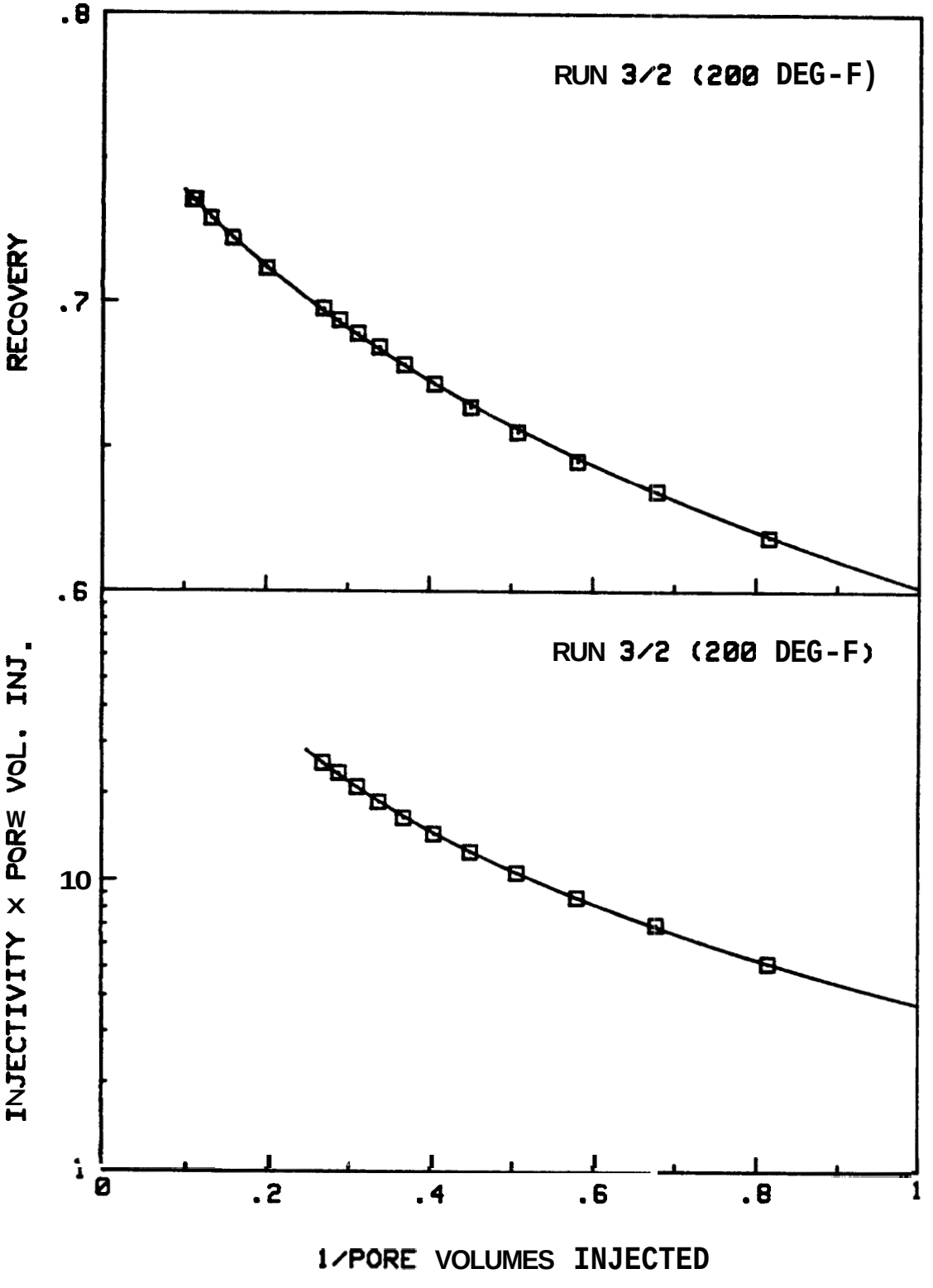

Fig. J.16 Recovery and Injectivity x Pore Volumes Injected vs. 1/Pore Volumes Injected — Run 3/2

Table J.21 Water Displacement Calculations -- Run 3/3

DISPLACEMENT EXPERIMENT CALCULATIONS

PORE VOLUME	395.9 cc	DATE	12/18/82
CORE LENGTH	51.69 cm	CORE/RUN	3/3
CORE DIAMETER	5.044 cm	DISPLRCEMENT	Dist U-OIL
DEAD VOL'S: U	2.5 cc	CORE TEMPERATURE	294.0 F
D	3.0 cc	OUTLET TEMPERATURE	75.0 F
SEPRRATOR OUTLET	81.41 cm	UATER VISCOSITY	.188 cp
BUBBLE VELOCITY	10.00 cm/sec	OIL VISCOSITY	1.67 cp
ABSOLUTE PERM	6.900 darcirs	VISCOSITY RATIO	8.89
INIT SAT - UATER	9.7 %	UATER DENSITY RATIO	1.0838
FINAL SAT - OIL	17.0 %	OIL DENSITY RATIO	1.1017

	TIME	SEPRRRTOR HEIGHT	SEPRRRTOR CALIB	D-VOL INJ	D-P	FLOWRRTE CHRRT AVC	CHRRT @t	CHRRT CRL	cc/min	PVi	Rec	Inj
	(min)	(cm)	(cc/cm)	(cc)	(psi)							
ST		14.80										
0	0.00	14.35	5.01	0.0	3.20	.506	.506	43.2	21.8	0.000	.000	1.00
1	4.35	33.58	5.01	94.7	2.88	.546	.548	43.2	23.6	.257	.260	1.24
2	8.72	52.50	4.93	93.9	1.84	.549	.550	43.2	23.7	.518	.514	1.89
BT	9.12				1.67		.550	43.2	23.8	.543	.543	2.08
3	13.80	59.90	5.05	110.6	1.40	.549	.547	43.2	23.6	.823	.613	2.47
4	18.33	61.80	5.05	97.5	1.25	.547	.547	42.7	23.3	1.090	.639	2.74
5	22.73	63.10	5.05	95.1	1.14	.545	.545	43.0	23.5	1.351	.657	3.03
6	27.20	64.00	5.05	96.0	1.04	.543	.541	42.9	23.2	1.614	.669	3.27
7	31.53	64.70	5.05	93.1	.96	.541	.540	43.1	23.3	1.869	.679	3.55
8	35.97	65.40	5.05	96.0	.91	.540	.540	43.5	23.5	2.132	.689	3.80
9	40.48	65.80	5.05	96.0	.86	.540	.540	43.5	23.5	2.395	.694	4.02
10	44.72	66.40	5.05	93.5	.81	.539	.537	43.6	23.4	2.651	.703	4.23
11	49.05	66.70	5.05	93.8	.77	.538	.538	43.6	23.5	2.908	.707	4.47
12	53.43	66.90	5.05	94.8	.75	.538	.538	43.6	23.4	3.167	.710	4.61
13	57.75	67.20	5.05	94.8	.72	.538	.536	43.9	23.5	3.425	.714	4.79
14	62.05	67.40	5.05	92.9	.70	.537	.537	43.6	23.4	3.679	.717	4.90
15	66.42	67.50	5.05	94.2	.69	.536	.535	43.6	23.3	3.937	.718	4.96
16	88.55	67.80	5.05	475.0	.61	.532	.528	43.7	23.1	5.237	.722	5.59
17	110.62	68.30	5.05	474.0	-.00	.524	.521	44.4	23.1	6.535	,729	-.00
18	132.50	68.50	5.05	468.0	-.00	.519	.520	44.7	23.2	7.816	.732	-.00
19	136.87	68.55	5.05	94.3	-.00	.519	.519	45.1	23.4	8.075	,733	-.00

CURVE FITS	c0	C1	c2	%E-MAX	%E-AVG
Recovery	6.3043E-01	9.3498E-02	-2.1530E-02	.5	.1
Inj. X Pore Vol. Inj.	9.4706E-01	1.5573E+00	-5.1715E-02	1.6	.7

	PVi	R-ACT	R-CALC	R-%E	I*P-ACT	I*P-CALC	I*P-%E	Sw	Krw	Kro	Kw/Ko
								.097	0.008	1.045	0.000
BT		,543	.571		1.13	1.06					
4	1.090	.639	,638	.1	2.98	2.95	1.2	.646	.188	.150	1.255
5	1.351	.657	.657	.0	4.09	4.10	.2	.673	.220	.124	1.774
6	1.614	.669	.670	.1	5.28	5.37	1.6	.694	.248	.104	2.378
7	1.869	.679	.680	.2	6.64	6.69	.8	.711	.272	.089	3.045
8	2.132	.689	.689	.0	8.11	8.14	.4	.725	.295	.077	3.825
9	2.395	.694	.696	.2	9.64	9.66	.2	.737	.315	.067	4.707
10	2.651	.703	.701	.3	11.22	11.20	.2	.747	.334	.059	5.675
11	2.908	.707	.706	.2	12.99	12.81	1.4	.755	.352	.052	6.768
12	3.167	.710	.710	.0	14.61	14.49	.e	.763	.369	.046	8.011
13	3.425	.714	.713	.2	16.40	16.21	1.1	.769	.384	.041	9.401
14	3.679	.717	.716	.2	18.04	17.96	.5	.775	.399	.036	10.951
15	3.937	.718	.718	.0	19.52	19.77	1.3	.781	.413	.032	12.727
16	5.237	.722	,726	.5	29.29	29.48	.7	.801	.475	.018	26.425
17	6.535	.729	.730	.1	-.00	-.00	-.0	.814	-.000	-.000	57.921
18	7.816	.732	.732	.1	-.00	-.00	-.0	.824	-.000	-.000	177.244
19	8.075	.733	.732	.2	-.00	-.00	-.0	.825	-.000	-.000	255.160

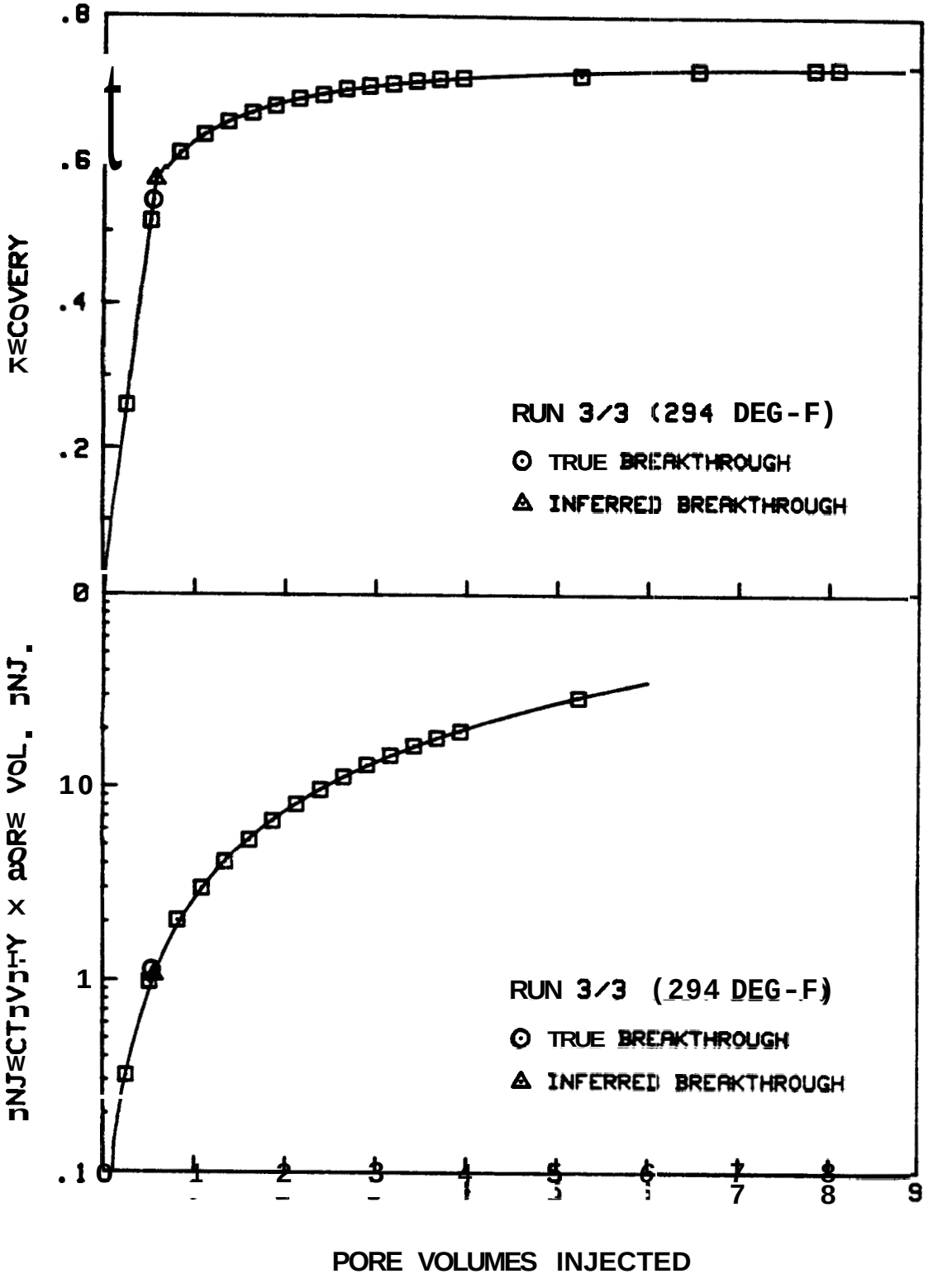

Figure 5.17 Recovery and Injectivity x Pore Volumes Injected vs. Pore Volumes Injected -- Run 3/3

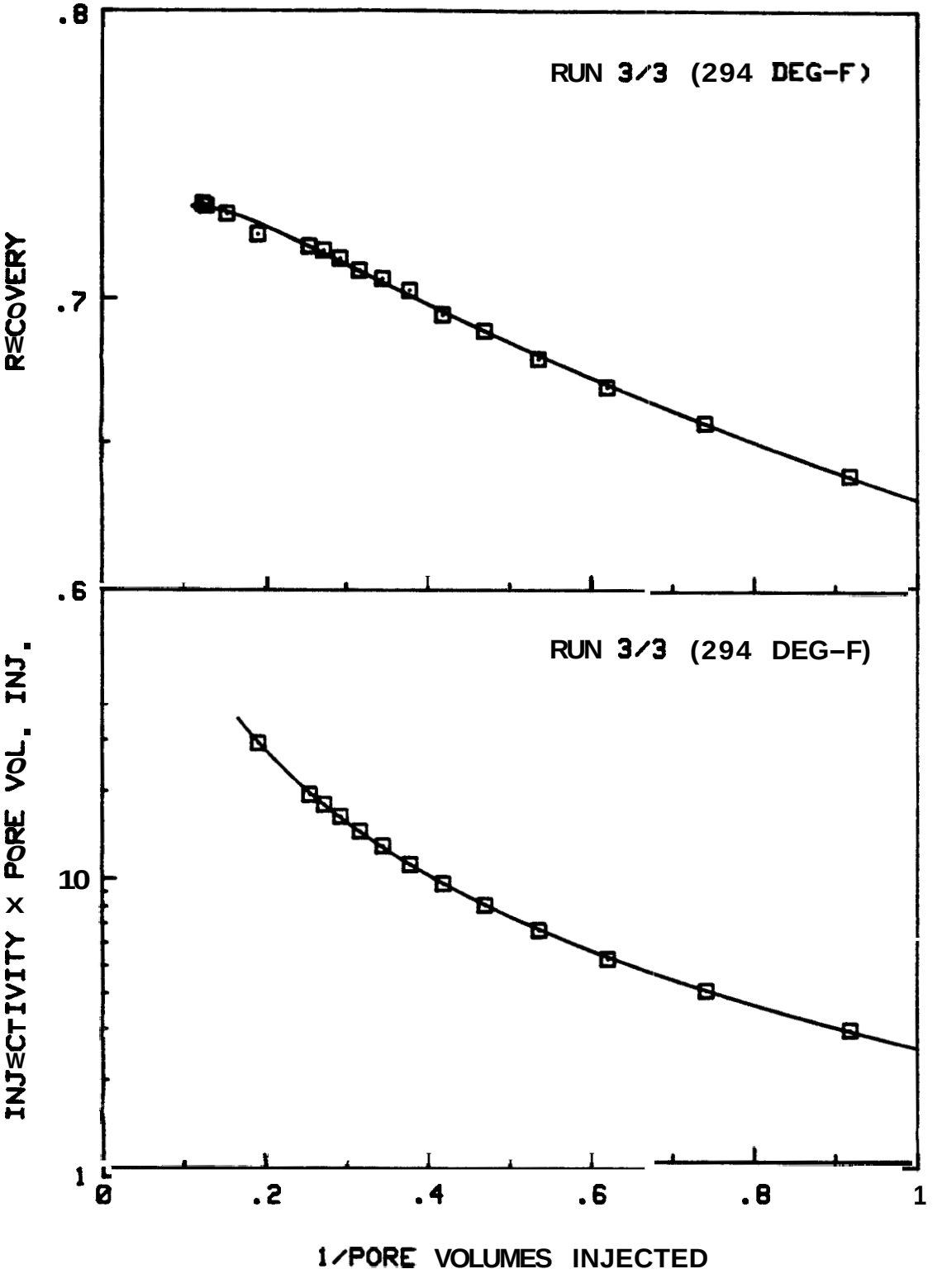

Fig. 5.18 Recovery and Injectivity x Pore Volumes Injected vs. 1/Pore Volumes Injected — Run 3/3

Table 5.22 Water Displacement Calculations -- Run 3/4

DISPLACEMENT EXPERIMENT CALCULATIONS

PORE VOLUME	395.9 cc	DATE	12/16/82
CORE LENGTH	51.69 cm	CORE/RUN	3/4
CORE DIAMETER	5.844 cm	DISPLACEMENT	Dirt W-OIL
DEAD VOL'S: U	2.5 cc	CORE TEMPERATURE	72.0 F
D	3.8 cc	OUTLET TEMPERATURE	72.0 F
SEPARATOR OUTLET	81.41 cm	WATER VISCOSITY	.953 cp
BUBBLE VELOCITY	9.32 cm/sec	OIL VISCOSITY	28.37 cp
ABSOLUTE PERM	6.900 darcies	VISCOSITY RATIO	29.77
INIT SAT - MATER	18.2 %	UATER DENSITY RATIO	1.0000
FINAL SAT - OIL	20.6 %	OIL DENSITY RATIO	1.0000

	TIME	SEPARATOR HEIGHT	CRLIB	D-VOL INJ	D-P	FLOWRATE CHART AVG	@t	CAL	cc min	PVi	Rec	Inj
	(min)	(cm)	(cc/cm)	(cc)	(psi)							
ST		13.00										
0	0.00	12.60	4.95	0.0	54.90	.436	.436	36.8	16.0	0.800	.000	1.00
1	4.87	31.00	4.95	92.0	41.60	.512	.522	36.8	19.2	.226	.222	1.58
BT	5.35				36-00		.527	36.6'	19.4	.250	.250	1.84
2	9.63	47.00	4.95	94.0	21.08	.536	.550	36.8	20.2	.464	.417	3.30
3	14.20	52.70	4.91	93.5	13.10	.553	.555	37.0	20.5	.700	.484	5.37
4	18.68	55.00	4.89	92.9	10.95	.556	.555	37.3	20.7	.934	.512	6.46
5	23.13	56.70	4.89	92.0	9.63	.553	.552	37.4	20.6	1.167	.532	7.33
6	27.55	58.00	4.89	91.9	8.75	.551	.550	37.8	20.8	1.399	.548	8.12
7	32.02	59.20	4.89	92.9	8.05	.549	.548	37.9	20.8	1.633	.563	8.83
8	36.62	60.10	4.89	95.8	7.55	.547	.546	38.1	20.8	1.875	.574	9.42
9	41.22	60.95	4.89	96.0	7.00	.544	.541	38.4	20.8	2.118	.584	10.15
10	45.77	61.70	4.89	94.4	6.68	.541	.540	38.3	20.7	2.356	.594	10.61
11	50.27	62.40	4.89	93.5	6.38	.540	.539	38.5	20.7	2.593	.602	11.13
12	54.72	62.90	4.89	93.0	6.13	.538	.537	38.8	20.9	2.827	.608	11.65
13	59.20	63.50	4.89	93.8	5.90	.536	.535	39.0	20.9	3.064	.616	12.11
14	63.77	64.00	4.89	94.8	5.70	.534	.531	38.9	20.6	3.304	.622	12.39
15	68.45	64.50	4.89	98.0	5.55	.532	.532	39.3	20.9	3.551	.628	12.90
16	91.92	66.38	4.89	496.0	4.93	.529	.526	39.5	20.8	4.789	.650	14.41
17	113.92	67.60	4.89	457.0	4.48	.523	.520	39.7	20.7	5.943	.666	15.78
18	161.03	69.50	4.89	977.8	3.98	.516	.512	40.2	20.6	8.411	.690	18.06
19	165.73	69.68	4.89	97.1	3.85	.512	.510	40.4	20.6	8.656	.692	18.29

CURVE FITS	C0	C1	C2	%E-MAX	%E-AVG
Recovery	5.1797E-01	9.3893E-02	-6.1020E-03	.1	.1
Inj. X Pore Vol. Inj.	1.9026E+00	1.5874E+00	-5.7940E-02	1.2	.4

	PVi	R-ACT	R-CALC	R-%E	I*P-ACT	I*P-CALC	I*P-%E	SW	Krw	Kro	Kw/Ko
								.102	0.000	.761	0.000
BT		.250	.436		.46	1.72					
3	.700	.484	.484	.1	3.76	3.77	.5	.487	.073	.354	.206
4	.934	.512	.512	.0	6.84	6.02	.4	.519	.093	.312	.298
5	1.167	.532	,532	.0	8.56	8.55	.1	.542	.110	.280	.392
6	1.399	,548	,549	.1	11.36	11.35	.2	.561	.125	.256	.490
7	1.633	.563	.563	.1	14.42	14.41	.I	.577	.139	.236	.591
8	1.e75	.574	.575	.1	17.67	17.78	.6	.590	.153	.219	.697
9	2.118	.584	.585	.1	21.49	21.35	.6	.602	.165	.205	.806
10	2.356	.594	.594	.1	25.00	25.04	.2	.613	.176	.192	.915
11	2.593	.602	.602	.1	28.84	28.85	.0	.622	.187	.182	1.025
12	2.827	.608	.609	.1	32.93	32.78	.4	.630	.196	.173	1.136
13	3.664	.616	.615	.1	37.12	36.88	.7	.637	.206	.165	1.249
14	3.304	.622	.621	.1	40.95	41.14	.5	.644	.214	.157	1.366
15	3.551	.628	.627	.1	45.83	45.66	.4	.651	.223	.150	1.487
16	4.789	.650	.650	.0	69.83	69.89	1.2	.677	.261	.123	2.118
17	5.943	.666	.666	.1	93.78	94.42	.7	.696	.291	.106	2.734
18	8.411	,690	.690	.1	151.87	151.46	.3	.724	.341	.083	4.127
19	8.656	.692	,692	.0	158.36	157.40	.6	.727	.345	.081	4.270

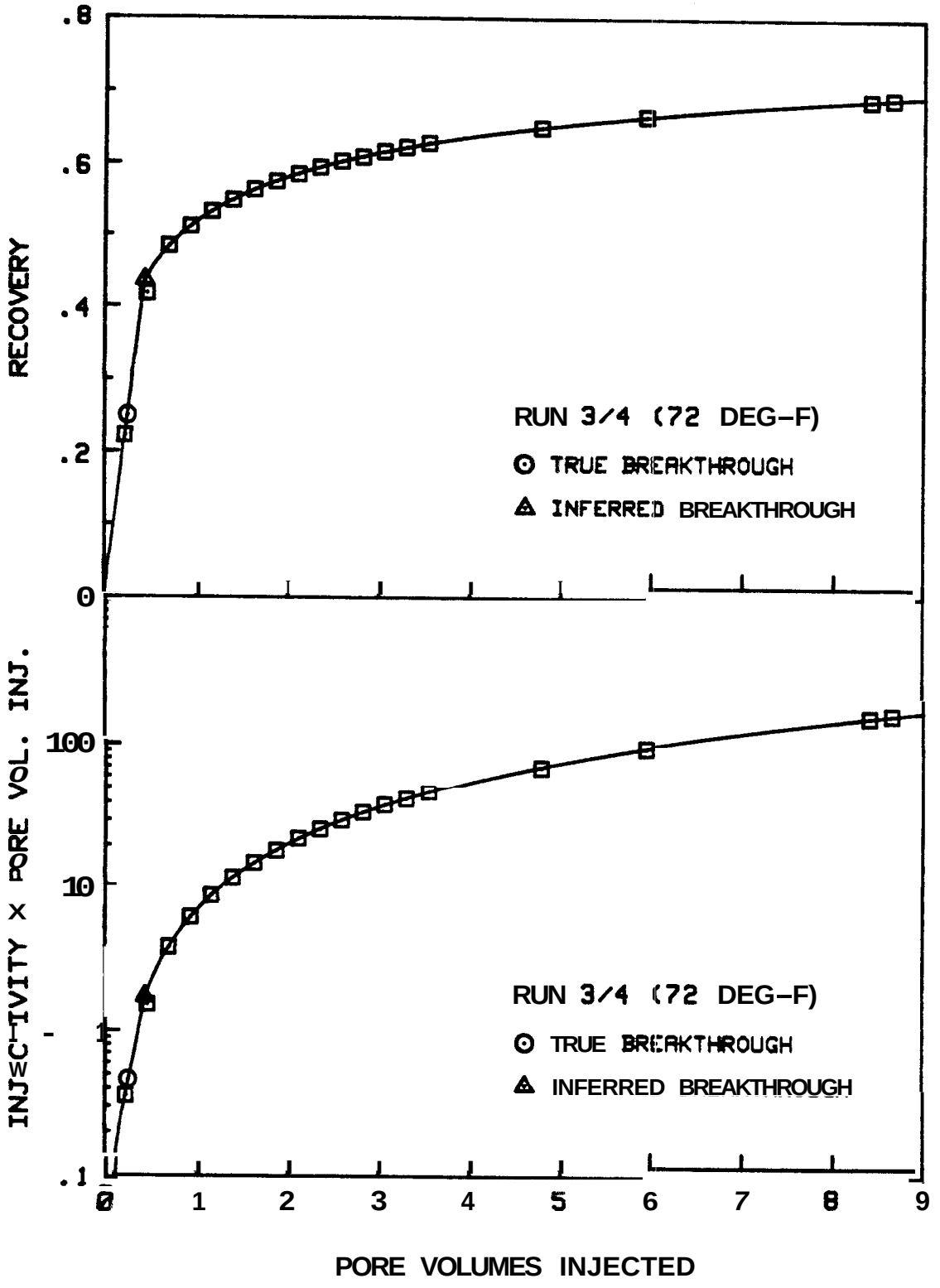

Figure J.19 Recovery and Injectivity x Pore Volumes Injected vs. Pore Volumes Injected — Run *3/4*

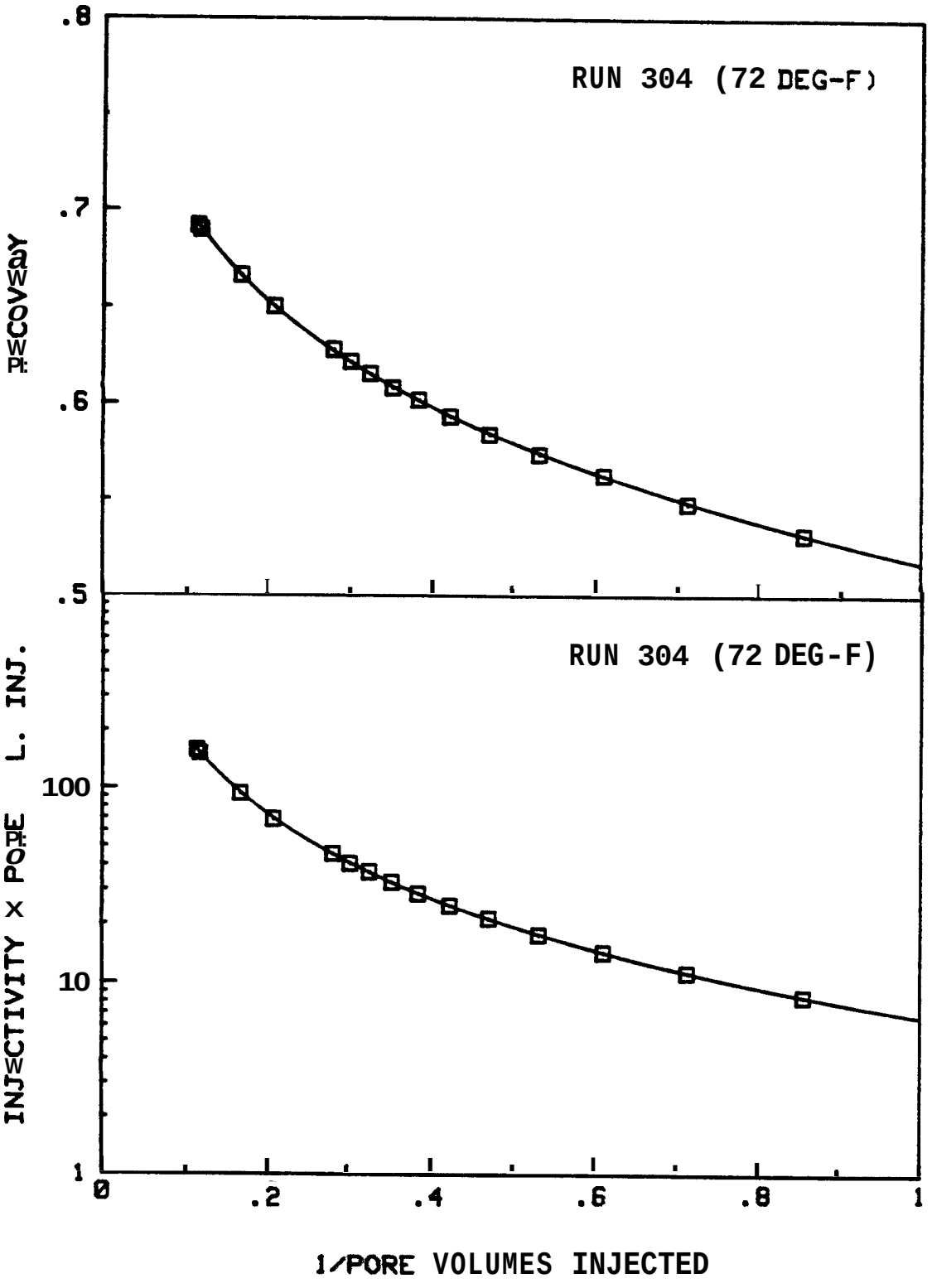

Fig. 5.20 Recovery and Injectivity x Pore Volumes Injected vs. 1/Pore Volumes Injected — Run *3/4*

Table 5.23 Water Displacement Calculations — Run 4/1

DISPLACEMENT EXPERIMENT CALCULATIONS

PORE VOLUME	391.4 cc	DATE	12/28/82
CORE LENGTH	51.60 cm	CORE/RUN	4/1
CORE DIAMETER	5.044 cm	DISPLACEMENT	Dirt W-OIL
DEAD VOL'S: U	2.5 cc	CORE TEMPERATURE	70.0 F
D	3.0 cc	OUTLET TEMPERATURE	69.0 F
SEPARATOR OUTLET	81.40 cm	WATER VISCOSITY	.979 cp
BUBBLE VELOCITY	11.44 cm/sec	OIL VISCOSITY	29.81 cp
ABSOLUTE PERM	6.750 darcies	VISCOSITY RATIO	30.45
INIT SAT - WATER	9.4 %	WATER DENSITY RATIO	1.0002
FINAL SAT - OIL	20.0 %	OIL DENSITY RRTIO	1.0004

	TINE	SEPARATOR HEIGHT	SEPARATOR CALIB	D-VOL INJ	D-P	FLOWRATE CHRRT AVG	CHRRT @t	CHRRT CAL	cc/min	.PVi	Rec	Inj
	(min)	(cm)	(cc/cm)	(cc)	(psi)							
ST		8.10										
0	8.00	7.70	5.00	0.0	70.20	.497	.497	36.7	18.2	0.000	.000	1.00
1	4.13	26.60	5.00	94.8	49.80	.612	.630	36.7	23.1	.236	.233	1.79
BT	4.33				43.70		.634	36.7	23.2	.248	.248	2.05
2	8.03	46.70	4.89	92.9	28.80	.650	.659	36.7	24.2	.473	.405	3.23
3	11.80	47.70	4.90	93.0	17.80	.668	.672	37.0	24.8	.711	.489	5.38
4	15.67	49.90	4.95	96.0	14.80	.673	.673	36.9	24.8	.956	.515	6.46
5	19.43	51.60	4.95	93.7	13.05	.673	.672	37.0	24.8	1.196	.536	7.33
6	23.17	52.90	4.95	93.4	11.85	.673	.676	37.2	25.1	1.434	.553	8.17
7	26.93	54.16	4.95	93.9	10.85	.676	.674	36.9	24.9	1.674	.568	8.83
8	30.63	55.00	4.95	92.1	16.13	.672	.671	37.0	24.9	1.910	.579	9.45
9	34.48	55.85	4.95	95.6	9.50	.672	.670	37.8	24.8	2.154	.590	10.84
10	38.23	56.60	4.95	93.9	8.98	.670	.669	37.4	25.0	2.394	.599	10.73
11	42.1%	57.30	4.95	96.2	8.50	.668	.667	37.3	24.8	2.640	.608	11.26
12	45.95	57195	4.95	95.9	8.13	.665	.663	37.5	24.8	2.885	.616	11.77
13	49.85	58.45	4.95	96.2	7.78	.662	.660	37.3	24.6	3.131	,622	12.18
14	53.68	59.00	4.95	95.2	7.50	.660	.660	37.6	24.8	3.374	.629	12.76
15	57.48	59.40	4.95	95.0	7.28	.660	.660	37.9	25.0	3.617	.634	13.23
16	61.37	59.80	4.95	96.9	7.03	.659	.658	37.9	24.9	3.864	.639	13.66
17	81.15	61.55	4.95	484.0	5.33	.647	.610	37.8	23.1	5.101	.661	15.51
18	102.08	62.80	4.95	475.0	5.05	.600	.590	37.8	22.3	6.315	.677	17.03
19	123.45	63.70	4.95	467.6	4.55	.574	.567	38.1	21.6	'7.508	.689	18.28
20	164.87	64.95	4.95	890.0	4.10	.565	.562	38.0	21.4	'9.783	.704	20.09
21	169.12	65.10	4.95	92.0	4.10	.562	.561	38.5	21.6	10.018	.706	20.31

CURVE FITS	c0	C1	C2	%E-MAX	%E-AVG
Recovery	5.2009E-01	9.7210E-02	-6.9023E-03	.5	.2
Inj. X Pore Vol. Inj.	1.8884E+00	1.5937E+00	-4.5257E-02	1.1	.4

	PVi	R-ACT	R-CALC	R-%E	I*P-ACT	I*P-CALC	I*P-%E	Sw	Krw	Kro	Kw/Ko
								.094	0.800	.725	0.000
BT		.248	.434		.51	1.69					
3	.711	.489	.486	.5	3.82	3.82	.2	.478	.067	.343	.196
4	.956	.515	.516	.1	6.18	6.15	.5	.512	.086	.299	.288
5	1.196	.536	,537	.2	8.77	6.78	.8	.537	.102	.267	.382
6	1.434	.553	.554	.3	11.72	11.68	.4	.556	.116	.243	.478
7	1.674	.568	.568	.1	14.78	14.85	.4	.572	.129	.224	.577
8	1.910	.579	.580	.2	18.06	18.18	.7	.586	.141	.208	,678
9	2.154	.590	.591	.2	21.63	21.86	1.1	.598	.152	,194	.784
10	2.394	.599	.600	.1	25.69	25.67	.1	.609	.162	.t83	.890
11	2.640	.608	.608	.0	29.73	29.75	.1	.618	.172	.172	1.001
12	2.885	.616	.615	.1	33.96	33.99	.1	.627	.182	.163	1.114
13	3.131	.622	.622	.1	38.13	38.41	.7	.635	.191	.155	1.22%
14	3.374	.629	.628	.2	43.05	42.43	.3	.642	.199	.148	1.345
15	3.617	.634	.634	.1	47.86	47.58	.6	.648	.207	.142	1.462
16	3,864	.639	.639	.1	52.18	52.46	.6	.654	.215	.136	1.583
17	5.101	.661	.660	.2	79.13	78.65	.6	.679	.250	.113	2.209
18	6.315	.677	.676	.2	107.52	106.88	.6	.698	.279	.098	2.856
19	7.508	.689	.688	.1	137.29	136.63	.5	.713	.304	,086	3.521
20	9.783	.704	.706	.2	196.53	197.85	.7	.734	.345	.071	4.854
21	10.818	.706	.707	.2	203.45	204.47	.5	.736	.348	.070	4.997

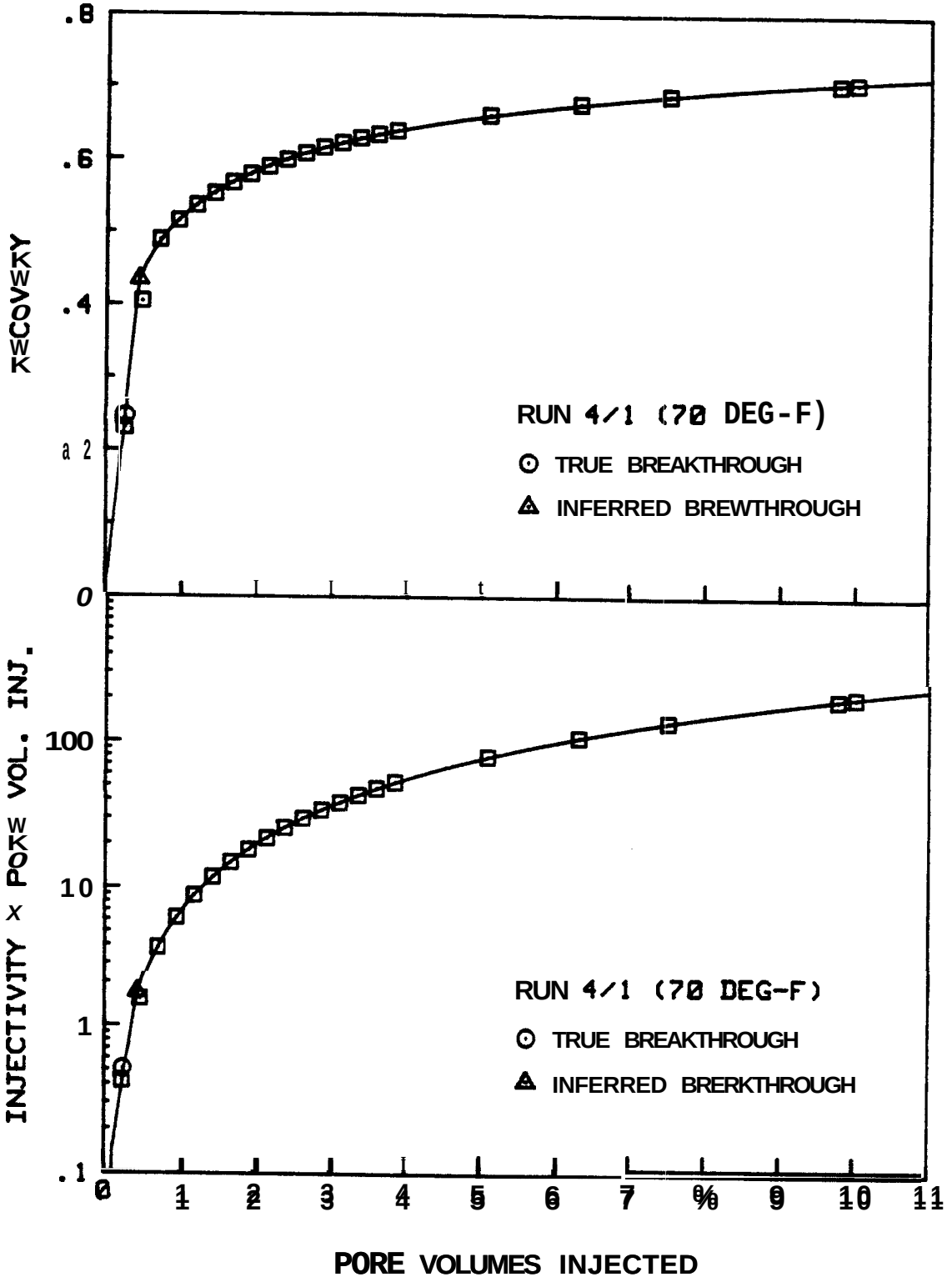

Figure 5.21 Recovery and Injectivity x Pore Volumes Injected vs. Pore Volumes Injected -- Run 4/1

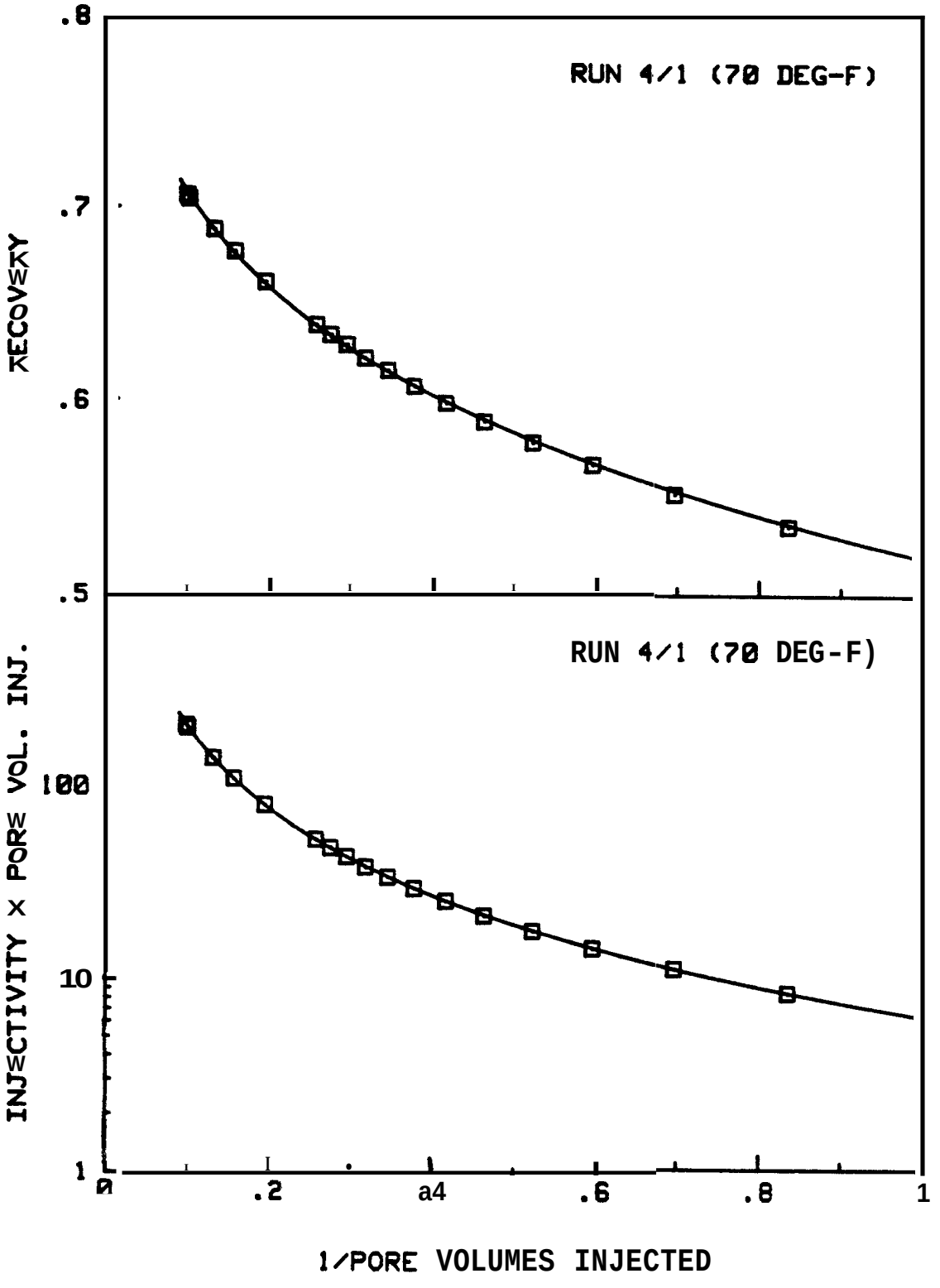

Fig. 5.22 Recovery and Injectivity x Pore Volumes Injected vs. 1/Pore Volumes Injected -- Run 4/1

Table J.24 Water Displacement Calculations -- Run 4/2

DISPLACEMENT EXPERIMENT CALCULATIONS

PORE VOLUME	391.4 cc	DATE	12/21/82
CORE LENGTH	51.60 cm	CORE/RUN	4/2
CORE DIAMETER	5.844 cm	DSSPLRCEWEWT	Dist W-OIL
DEAD VOL'S: U	2.5 cc	CORE TEWPERATURE	292.0 F
D	3.0 cc	OUTLET TEMPERATURE	70.0 F
SEPARATOR OUTLET	81.40 cm	UATER VISCOSITY	.189 cp
BUBBLE VELOCITY	11.66 cm/sec	OIL VISCOSITY	1.69 cp
ABSOLUTE PERM	6.758 darcies	VISCOSITY RATIO	8.93
INIT SAT - UATER	10.9 %	UATER DENSITY RATIO	1.0835
FINAL SAT - OIL	19.5 %	OIL DENSITY RATIO	1.1032

	TIME	SEPARATOR HEIGHT	SEPARATOR CALIB	D-VOL INJ	D-P	FLOWRATE CHART AVG	CHART @t	CHART CAL	cc min	PVi	Rec	Inj
	(min)	(cm)	(cc/cm)	(cc)	(psi)							
ST		15.70										
Ø	0.00	15.30	5.00	0.0	4.00	.573	.573	40.3	23.1	8.000	.000	1.00
1	4.10	34.00	5.80	92.5	3.48	.611	.621	40.3	25.0	.254	.256	1.25
2	8.17	53.00	4.94	92.6	2.24	.623	.628	40.3	25.3	.515	.515	1.96
BT	8.32				2.06		.630	40.2	25.4	.525	.525	2.19
3	12.12	59.50	4.92	92.0	1.78	.631	.632	40.2	25.4	.772	.601	2.48
4	16.15	61.30	4.92	93.9	1.59	.630	.629	40.1	25.2	1.032	.624	2.76
5	20.25	62.65	4.92	95.7	1.45	.628	.628	40.3	25.3	1.297	.643	3.02
6	24.25	63.60	4.92	93.8	1.36	.626	.623	40.6	25.3	1.557	.656	3.22
7	28.33	64.50	4.92	94.0	1.31	.622	.621	40.1	24.9	1.818	.668	3.29
8	32.35	65.10	4.92	93.2	1.29	.621	.620	40.5	25.1	2.076	.676	3.38
9	36.47	65.66	4.92	95.6	-.00	.618	.616	40.5	24.9	2.339	.683	-.00
10	40.48	66.00	4.92	93.0	-.00	.614	.612	40.9	25.0	2.596	.689	-.00
11	44.85	66.50	4.92	101.6	-.00	.611	.610	41.3	25.2	2.878	.696	-.00

CURVE FITS	c0	c1	c2	%E-MAX	%E-AVG
Recovery	6.2140E-01	8.6211E-02	-1.5507E-02	.1	.1
Inj. X Pore Vol. Inj.	9.9800E-01	1.4920E+00	-2.6387E-01	.6	.3

	~~PVi~~	~~R-ACT~~	R-CALC	~~R-%E~~	~~I*P-ACT~~	~~I*P-CALC~~	~~I*P-%E~~	Sw	Krw	Kro	Kw/Ko
								.109	0.000	.915	0.000
BT		.525	.568		1.15	1.07					
4	1.032	.624	.624	.0	2.84	2.84	.0	.648	.175	.141	1.244
5	1.297	.643	.643	.0	3.92	3.93	.2	.674	.215	.123	1.747
6	1.557	.656	.657	.1	5.02	4.99	.6	.693	.249	.108	2.293
7	1.818	.668	.667	.1	5.99	6.02	.6	.709	.278	.096	2.895
8	2.076	.676	.676	.0	7.02	7.01	.2	.722	.303	.085	3.544
9	2.339	.683	.683	.0	-.00	-.00	-.0	.733	-.000	-.000	4.262
18	2.596	.689	.690	.1	-.00	-.00	-.0	.742	-.000	-.000	5.822
AI	2.878	.696	.695	.1	-.00	-.00	-.0	.751	-.000	-.000	5.918

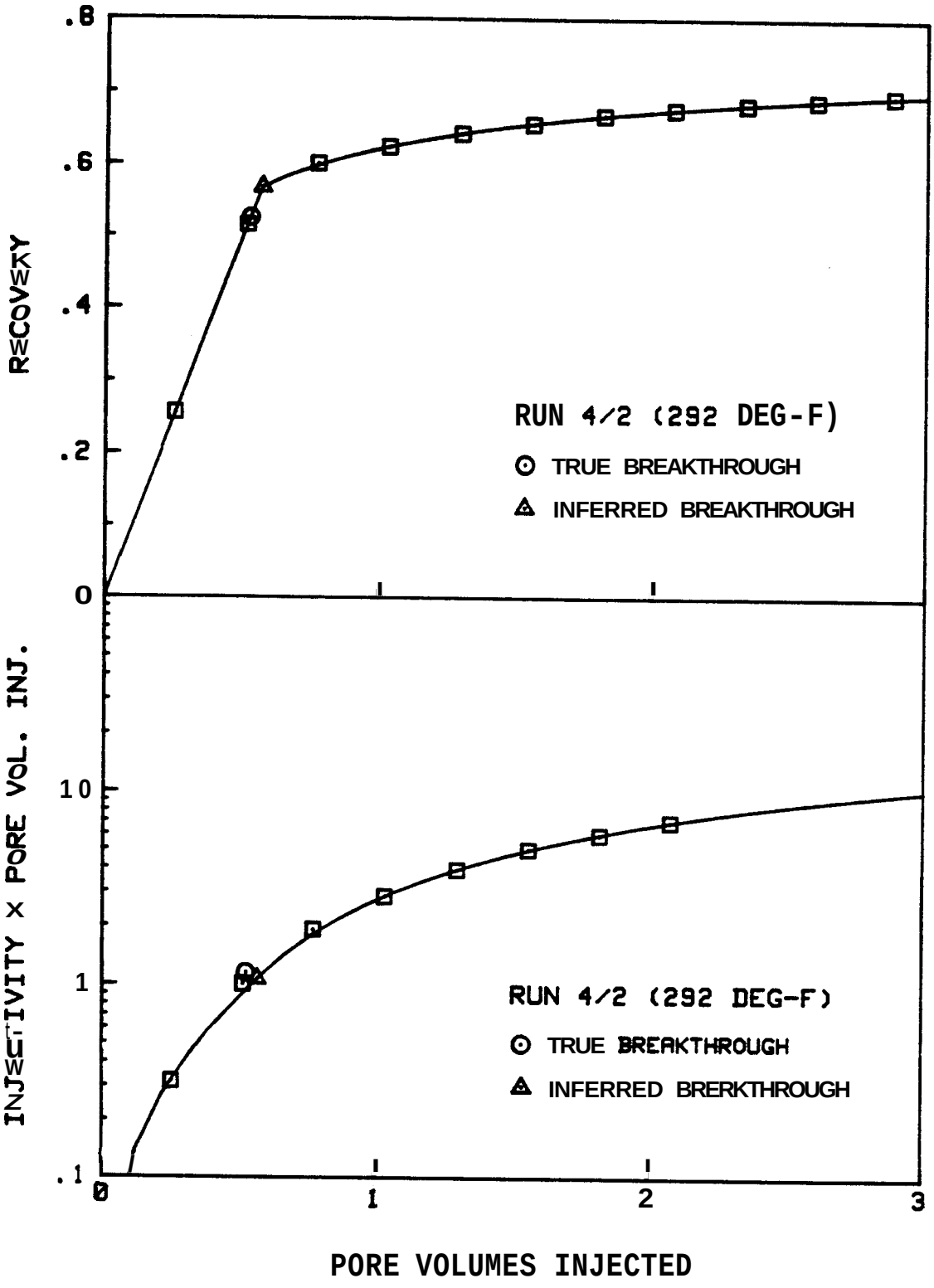

Figure 5.23 Recovery and Injectivity x Pore Volumes Injected vs. Pore Volumes Injected -- Run *4/2*

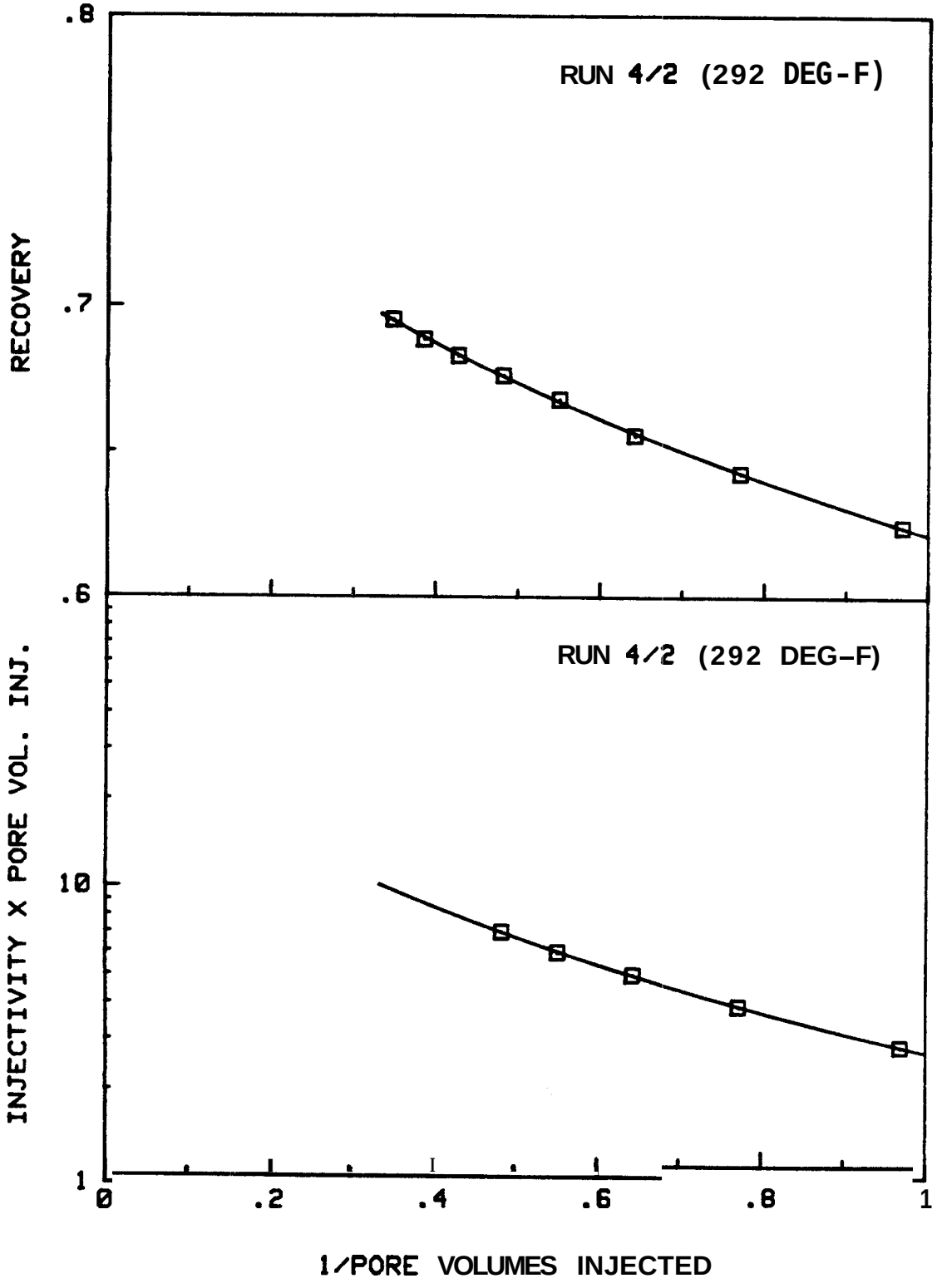

Fig. *5.24* Recovery and Injectivity x Pore Volumes Injected vs. 1/Pore Volumes Injected — Run *4/2*